Investigating the role of the extracellular calcium-sensing receptor, CaSR, in the pathogenesis of asthma using surrogate disease models

by

Ping Huang

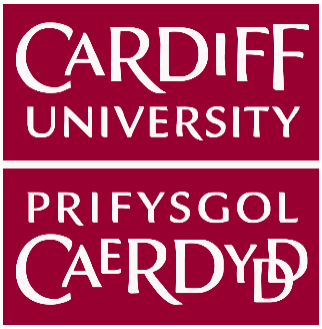

Thesis submitted for the degree of Doctor of Philosophy

School of Biosciences

Cardiff University

2024

Acknowledgements

I am extremely grateful to Professor Daniela Riccardi, Professor Paul J. Kemp, Professor Ying Sun, Professor Christopher J. Corrigan, Professor Kenneth J. Broadley, Dr. Polina L. Yarova, Dr., Martin W. Schepelmann, Prof. Emma J. Kidd and Dr. William R. Ford for all of the help and support they have given me throughout my PhD studies. Without their help I would not be able to finish my PhD. I would also thank Drs Richard T. Bruce, Kasope L. Wolffs, Bethan Mansfield, David Evans, Jess Bahena, Kimberley Marie Jones, Grazia Battaglino, Benji Bryant, Siân Lewis, Shuang Peng, Tanya Tsugorka and Elen Wynne Jones for their friendly help in my experiments and office work and for making my time enjoyable both in the lab and office. I also thank Dr. Rupert Ecker and his group from TissueGnostics for all the help and support for image analysis.

Many thanks to the “CaSR Biomedicine” Marie Curie Training Network for the discussion and communication about science and life aspects during our several meetings, including Professor Enikö Kallay and her then PhD students, Drs Luca Iamartino and Taha Elajnaf from Medical University of Vienna, Dr. Carmen de Torres Gomez-Pallete and her then PhD student, Dr Eliana Goncalves Alvez from Fundació Sant Joan de Deu, Professor Hans Beäuner-Osborne and his then PhD student, Dr Iris Mos from University of Copenhagen, Dr. Fadil Hannan and his then PhD student, Dr Mie Kronborg Olesen, from University of Liverpool, Dr. Donald T Ward and his PhD then student, Patricia Pacios Centeno from University of Manchester, Professor Maria Luisa Brandi and her PhD student, Dr Preeti Sharma from Universita’ di Firenze, Professor Rajesh V Thakker and his then PhD student, Dr Anna Glück from University of Oxford, Dr. Romuald Mentaverri and his then PhD student Souvik Das from Univeristé de Picardie, Professor Frank J Bruggeman and his then PhD student, Dr Sergei Chavez Abiega from Stichting Vu, Professor András Dinnyés and his then PhD student, Dr Maria Lo Giudice from Biotalentum, Dr. Luisa Pugliese and her then PhD student Wolfgang Schlattl from S.A.F.AN. as well as the PhD student Amirreza Mahbod from TissueGnostics. Also, many thanks to Professor Wei Wang and

the students Qiong Huang, Xiaonan Du, Yiran Yang, Yan Li, Chenduo Li and the technicians Ze Lv and Jie Liu from Capital Medical University for their help when I did my experiment in China.

I would also thank my friends Xindong Chen, Xiaobo Wang, Bin Guo, Min Chen, Xiuyuan Lu, Yang Jiao, Jingjing Xue, Xie Tian, Kuthala Vellem, Elisabeta Dominte and Ugis Patmalnieks for their help and happy time with them during my life in Cardiff.

I would send my biggest thanks to my supervisor Prof. Daniela Riccardi for her patient and unending support. I had some difficulties with my thesis writing due to the very severe COVID-2019 and my mother's health issues, and as a result, I had issues with my health. After undergoing 2 major abdominal surgeries, I also developed some mental problems. It was my supervisor who always told me if you need any help, feel free to send an e-mail to ask me. When I finish part of my writing, she always gave me affirmation without hesitation. I would never have been able to complete my thesis without her encouragement and support. I am so grateful to her for her support to my study and my life.

Finally, I am indebted to Marie Curie ITN scholarship for the financial support and thank my family for all of the encouragement and support!

CONTENTS

List of Tables

List of Figures

SUMMARY

Asthma is a prevalent chronic respiratory inflammatory disease, affecting over 300 million people worldwide. There is no curable treatment for asthma. The most common existing combination therapies, inhaled corticosteroids (ICS) and bronchodilators, can only control the symptoms without addressing the underlying cause of asthma and present significant side effects. In addition, asthma is still poorly controlled in many patients even when taking systemic corticosteroids, for instance, in subjects affected by steroid-resistant asthma. Despite the existing unmet medical need, new small-molecule drugs have not been introduced for asthma treatment for the last four decades. The development of biologics in recent years targeting Immunoglobulin E (IgE) or asthma-related cytokines interleukin-4 (IL-4), IL-5 and IL-13, represents potentially novel and effective treatments for asthma. However, biologics are only effective in a subset of patients, due to the difficulty in identifying the targetable patients, and their cost limits for the usages. So, there is a need for the development of more effective, cheaper, small-molecule drugs for asthma, particularly for severe, steroid-resistant asthma management and prevention. During my PhD, I set out to further elucidate the pathogenesis of asthma, and to search potential drugs for asthma patients, especially for severe, steroid-resistant asthmatics, who have limited available treatment options to control their disease.

My laboratory has previously shown the widespread expression of calcium-sensing receptor (CaSR), a G-Protein-coupled receptor (GPCR), in human and mouse airways, and its involvement in asthma pathogenesis (Yarova et al, 2015). Our group has also shown that administration of its negative allosteric modulators of the CaSR (CaSR NAMs, also termed calcilytics), delivered to the lung via inhalation, can reduce both airway hyperresponsiveness (AHR) and airway inflammation in murine asthma surrogates, suggesting that inhaled calcilytics may represent a potential therapeutic for asthma. So the aims of my PhD were: 1. To select the best available calcilytic amongst those initially developed for a different use for asthma treatment in an inhaled form; 2. To compare the efficacy of inhaled calcilytic with the current standard-of-care (SoC), inhaled fluticasone

propionate (FP), and 3. To test the efficacy of inhaled calcilytic in a classic Th2 asthma model induced by ovalbumin (OVA) and alarmin-driven asthma model induced by IL-33, which may contribute to the pathogenesis of severe, steroid-resistant asthma.

The key findings from my PhD studies are as follows:

- Inhaled calcilytic reduced acetylcholine (ACh)-induced airway contraction *ex vivo* in naïve animals in both prophylactic and therapeutic settings.

- Inhaled calcilytic significantly inhibited total leucocyte infiltration and eosinophil infiltration in the BALF in a magnitude similar to that achieved by FP inhalation in a murine asthma model of allergic asthma *in vivo*. In addition, calcilytic can reduce the mean goblet cell number in the airways, while FP can't.

- Inhaled calcilytic reduces airway inflammation, airway hyperresponsiveness and some aspects of remodelling in both IgE- and alarmin-driven asthma models *in vivo*.

ABBREVIATIONS

α -SMA = α -smooth muscle actin

ACh = Acetylcholine

ADH = autosomal dominant hypocalcaemia

ADRB2 =β2-adrenoreceptor

AERD = Aspirin Exacerbated Respiratory Disease

AHR = Airways hyperresponsiveness

$Al(OH)_3$ = Aluminium hydroxide

ALOX5 = arachidonate 5-lipoxygenase

ANOVA = Analysis of Variance

AP-1 = activator protein-1

AUC = area under the curve

BALF = Bronchoalveolar Lavage Fluid

BSA = Bovine Serum Albumin

Ca^{2+} = calcium ion

CaSR = Calcium-Sensing Receptor

CD = cluster of differentiation

c-KIT = CD117/stem cell growth factor receptor/tyrosine-protein kinase

COA = certificate of analysis

COPD = Chronic obstructive pulmonary disease

CRC = Concentration-Response Curve

CRTH2 = Chemoattractant receptor-homologous molecule expressed on T helper type 2 cells

CT = Calcitonin

CTGF = connective tissue growth factor

CXCR = chemokine receptor

CysLTR1 = cysteinyl leukotriene receptor 1

C_{max} = maximal concentrations

CVD = cardiovascular disease

DMSO = Dimethyl Sulfoxide

DNA = DeoxyriboNucleic Acid

DP2 = Prostaglandin D2 receptor 2

DPP4 = Dipeptidyl peptidase 4

ELISA = Enzyme-Linked Immunosorbent Assay

EMA = European Medicines Agency

EtOH = Ethanol

EOA = early-onset atopic

FDA = Food and Drug Administration

FeNO = Fraction of exhaled nitric oxide

FEV_1 = Forced expiratory volume in the first second

FHH = Familial Hypocalciuric Hypercalcaemia

FP = Fluticasone Propionate

FW = formula weight

GATA-3 = GATA Binding Protein 3

GC = Glucocorticoid

GCR = Glucocorticoid receptor

GINA = Global Initiative for Asthma

GM-CSF = Granulocyte Macrophage Colony Stimulating Factor

GPCR = G Protein - Coupled Receptor

GR = glucocorticoid receptor

GRE = glucocorticoid response elements

HE = Haematoxylin & Eosin staining

HEK = Human Embryonic Kidney

HPT = hyperparathyroidism

IC_{50} = half maximal inhibitory concentration

IC_{80} = 80% maximal inhibitory concentration

ICAM-1 = intercellular cell adhesion molecule 1

ICS = Inhaled Corticosteroids

IgE = Immunoglobulin E

IL = Interleukin

IL-1 RA = interleukin-1 receptor antagonist

ILC2 = Type 2 innate lymphoid cell

IP = Intraperitoneal Injection

Iκ B1 = NF-κB inhibitor protein 1

JAK = Janus Kinase

KCl = Potassium Chloride

KO = knock out

LABA = Long-acting Beta Agonist

LAMA = Long-acting muscarinic antagonist

LOA = Late-onset asthma

LONA = late-onset, nonatopic asthma

LPS = Lipopolysaccharide

LTE4 = leukotriene E4

LTRA = leukotriene receptor antagonists

MA = Mixed allergen

MAP = mitogen-activated protein

MAPK = mitogen-activated protein Kinase

MCh = Methacholine

MW = molecular weight

NaCl = Sodium chloride

Na_2HPO_4 = Dibasic sodium phosphate

NaH_2PO_4 = Sodium dihydrogen phosphate

NaOH = Sodium hydroxide

NAM = negative allosteric modulator

NF-κB = nuclear factor kappa B

NICE = National Institute for Health and Care Excellence

NK = natural killer

OVA = Ovalbumin

PAS = Periodic Acid-Schiff

PBS = Phosphate Buffered Saline

PDGFRA = Platelet-derived growth factor receptor alpha

PDGFRB = Platelet-derived growth factor receptor Beta

PDE4 = phosphodiesterase 4

Penh = enhanced pause

PHPT = primary hyperparathyroidism

PI_3K = Phosphoinositide 3-kinase

PKA = Protein kinase

PTH = Parathyroid Hormone

SABA = Short-acting beta-agonist

SAMA = Short-acting muscarinic antagonist

SMC = smooth muscle cell

SoC = Standard of Care

SRA = Steroid-Resistant Asthma

ST2 = Suppression of tumorigenicity 2

$t_{1/2}$ = time to 50% maximal concentration

TGF-β = transforming growth factor beta

Th = T helper cells

Th2 = T helper cell type 2

T_{max} = time to maximal concentration

TNF α = tumour necrosis factor alpha

Treg = regulatory T cell

TSLP = Thymic stromal lymphopoietin

Tyk2 = Tyrosine kinase 2

ULABAs = Ultra-long-acting beta-agonists

ULAMAs = ultra-long-acting muscarinic antagonists

VCAM-1 = vascular cell adhesion molecule-1

WBP = whole-body plethysmography

γδ T cells = gamma delta T cells

Chapter I General Introduction

1.1 Asthma

Asthma is the most prevalent chronic pulmonary disease and over 300 million people are affected worldwide (Anderson et al. 2007). In the UK, more than 8 million people have been diagnosed with asthma according to The National Institute for Health and Care Excellence (NICE 2023). The prevalence of asthma has been increasing since around the 1950s globally due to the rate of urbanisation, and now it appears to have plateaued since the mid-1990s in developed countries (Lundbäck 1998; Kwong et al. 2001; Anderson et al. 2004; Braun-Fahrländer et al. 2004; Devenny et al. 2004; Robertson et al. 2004; Toelle et al. 2004; Zöllner et al. 2005; Anderson et al. 2007; Ma et al. 2009; Wennergren 2011). However, it is still steadily rising in countries and regions undergoing rapid urbanization as well as in middle- and low-level-income countries (Anderson et al., 2007; Moorman et al., 2007) . Asthma has significant direct and indirect economic burden to the patients and their family members due to its chronic nature, including hospital visits, medications, and clinical tests, as well as costs related to absence from work (Masoli et al. 2004; Nunes et al. 2017). Inhaled corticosteroids (ICS) and bronchodilators such as long-acting beta-agonists (LABA) are the most effective asthma treatments and are used stepwise recommended by the Global Initiative for Asthma (GINA) (Global Initiative for Asthma 2023). However, patients with severe, steroid-resistant asthma (SRA) have very poor or no response even at high doses of inhaled or even of systemic corticosteroids (Yim and Koumbourlis 2012) . They are of special interest because though severe, steroid-resistant asthma affects only 3% (Hekking et al. 2015) to 10% (Chung et al. 2014) of the population of adults with asthma, their healthcare cost is estimated to account for more than 60% of the total costs associated with treating asthma (Sadatsafavi et al. 2010) . Asthma-associated costs are even higher than those for most other chronic diseases, such as stroke, chronic obstructive pulmonary disease (COPD), or type 2 diabetes (T2DM) (O'Neill et al. 2015).

Asthma is also a heterogeneous disease, with patients showing various phenotypes and different severities, thus making it more intractable (Kim et al.

2009). The typical asthma symptoms include chest tightness, shortness of breath, wheezing, and a persistent cough (Global Initiative for Asthma 2023). The severity of the asthma symptoms varies widely from patient to patient and even from one episode to the next, and they can display only one symptom or any combination of these symptoms which can be episodic or persistent (Morosco and Kiley 2007). It has been known that numerous mediators and cytokines are involved in the development of asthma, such as Th2 cytokines interleukin-4 (IL-4), IL-13, IL-9, and IL-5, that typically regulate allergic inflammation (Lambrecht et al. 2019). IL-4 is the major cytokine promoting IgE and IgG1 synthesis by B cells (Moon et al. 1989; Cohn et al. 1998). IL-13 is involved in mucus production, airway hyperresponsiveness, and airway remodelling (Lambrecht et al. 2019). IL-5 is the major cytokine affecting the growth, differentiation, recruitment, activation, and survival of eosinophils (Lambrecht et al. 2019). IL-9 can promote mast cell survival, bronchial hyperresponsiveness (BHR), mucus cell metaplasia, and airway remodelling as well (Figure 1) (Renauld 2001). Th1 and Th17 cytokines, more prevalent in severe asthma than in mild to moderate asthma also have recently been found to be involved in the development of asthma (Lambrecht et al. 2019).

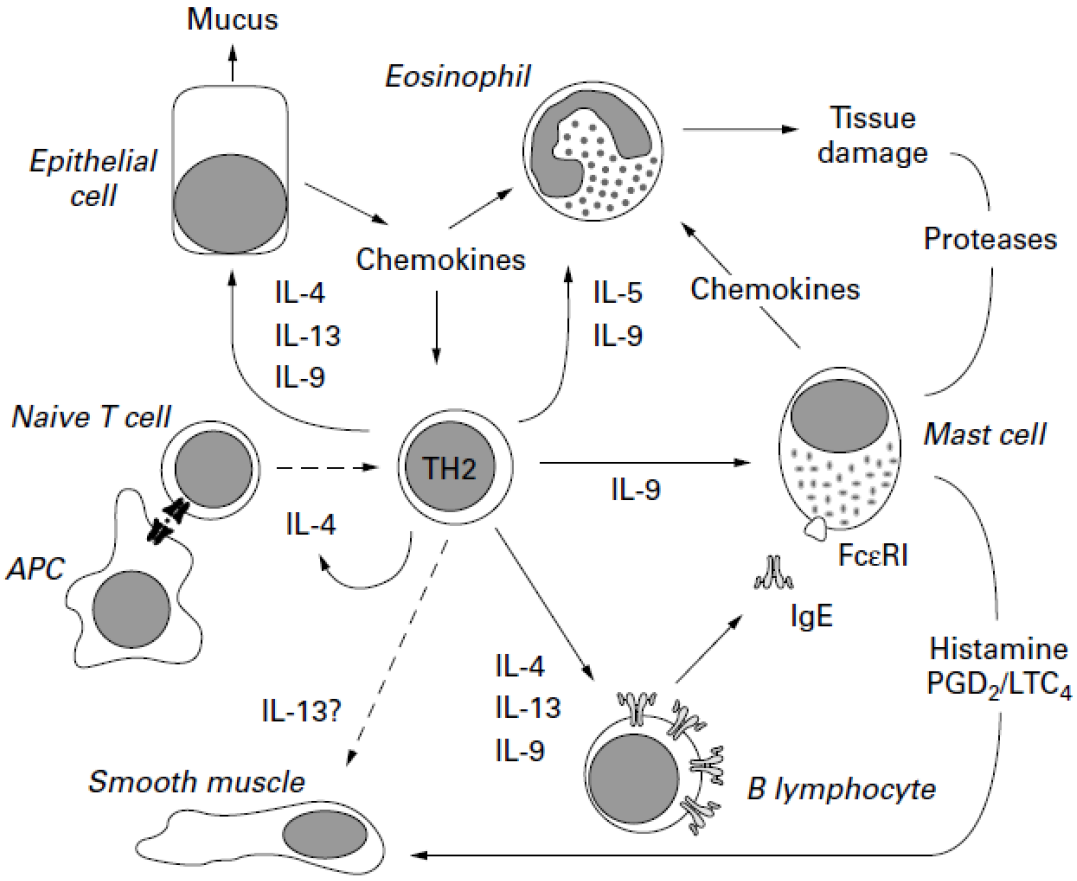

Figure 1. Role of T helper type 2 (Th2) cytokines in allergic asthma.
IL-13 induces airway hyperresponsiveness (AHR), promotes mucus production by goblet cells, and stimulates airway smooth muscle hyperplasia and hypertrophy, leading to airway remodelling. IL-5 plays a very important role in the pathophysiology of eosinophilic inflammation in asthma, it can stimulate the survival, differentiation, maturation, and activation of eosinophils. IL-4 stimulates B cells to produce immunoglobulin E (IgE) antibodies and promotes the differentiation of naïve T cells into Th2 cells, amplifying the Th2 response. IL-9 promotes the proliferation and survival of mast cells; and enhances the production of mucus by goblet cells. Image taken from Renauld (2001).

1.2 Different phenotypes and endotypes of asthma

While the term "asthma" has been used historically to describe all individuals experiencing a group of bronchial hyperresponsiveness, airway lability, and variable chest symptoms with reversible expiratory airflow limitation, significant heterogeneity exists among affected patients (Fitzpatrick et al.

2020). The characterization of heterogeneity has promoted the concept “phenotype” of asthma (i.e., groups of patients sharing common clinical characteristics), which has been used since the early 1940s (Fitzpatrick et al. 2020). The first phenotypes were described by Rackemann, which classified asthma into “intrinsic” (non-allergic) and “extrinsic” (allergic) asthma (Rackemann 1940). The author reported that individuals with “extrinsic” asthma typically developed asthma during their early life and typically with an allergic predisposition, whereas those with “intrinsic” asthma often had a late asthma onset after the age of 40 years and tended to have less allergic predisposition (Rackemann 1940; Rackemann 1947; Virchow 2000). However, more recent studies found that levels of Th2 cytokines were similar in extrinsic and intrinsic asthma, and treatment with inhaled corticosteroids appears to be effective for most mild to moderate asthmatics, leading to the distinctions between extrinsic and intrinsic asthma lost favour (Humbert et al. 1996a; Humbert et al. 1996b). More recently, Wenzel et al described 2 inflammatory subtypes (eosinophil (+) and eosinophil (-)) in severe, corticosteroid-dependent asthma patients based on the degree of eosinophilia (Wenzel et al. 1999). However, a major limitation of this approach is that it is based on a single variable, so the categories can’t distinguish the groups, and many characteristics overlap between groups (Kuruvilla et al. 2019). In contrast, the newer approaches have employed more systematic methodology-cluster analyses to integrate the impact of multiple interacting components in large cohorts to delineate and forecast clinical phenotypes as well as molecular mechanisms of asthma (Moore et al. 2010; Shaw et al. 2015). While variations in clusters have been observed, a consensus has emerged regarding specific subsets, notably the identification of two major groups: T2-“high ” and T2-“low” asthma groups (Kuruvilla et al. 2019; Fitzpatrick et al. 2020). T2-“low” asthma patients tend to have a later age of onset, higher medication requirements, and significant symptomatology when compared to T2-high asthmatics (Kuruvilla et al. 2019; Fitzpatrick et al. 2020; McIntyre and Viswanathan 2023).

1.2.1 Asthma phenotypes

Based on the cellular profile as well as other demographic characteristics, asthma can be divided into several phenotypes. According to GINA 2023 strategy document, several phenotypes of asthma have been identified to optimize the disease treatment due to its heterogeneous nature, based on its clinical features, onset time, atopic status as well as the cellular profile (Bel 2004; Moore et al. 2010; Peters 2014). T2 high phenotypes are typically characterized by allergic sensitisation, eosinophilia, and early age of onset compared to those of the T2 low phenotypes (McIntyre and Viswanathan 2023). A detailed description of each phenotype is provided in the following section (Table 1).

Table 1. Phenotypes and endotypes of asthma: Differences between T2-high and T2-low asthma

Endotype	Phenotype	Biomarkers	Clinical Characteristics
T2 high	Allergic	Blood/sputum eosinophil count, allergic sensitization (IgE), high total IgE, high FeNO, periostin, DPP4, plasma galectin-3	Early onset, steroid responsive
	Late-Onset	Blood/ sputum eosinophil count, high FeNO, periostin, DPP4, plasma galectin-3	Steroid refractory, may have CRSwNP
	AERD	Blood/sputum eosinophil count, urinary LTE4, periostin, DPP4, plasma galectin-3	Adult onset
T2 low	Non-allergic	Sputum neutrophil count	Adult onset
	Smokers	Sputum neutrophil count	Older adults
	Obesity-related	Serum IL-6	Female sex
	Very late onset	Sputum neutrophil count	>50-65 at onset

Asthma has been classified into two different endotypes (T2 high and T2 low) based on the inflammatory process caused by helper T cells. This table summarizes the endotypes and associated phenotypes of asthma and the key differences between T2-high and T2-low asthma. T2-high asthma is characterized by a predominant type 2 (T2) immune response, whereas T2-low asthma lacks a predominant T2 immune response. Patients with T2-high asthma may exhibit eosinophilic inflammation, whereas T2-low asthma may involve neutrophilic inflammation or a paucigranulocytic phenotype. Additionally, patients with T2-low asthma may show less response to corticosteroid treatment. AERD, Aspirin Exacerbated Respiratory Disease; CRSwNP, chronic rhinosinusitis with nasal polyps; DPP4, Dipeptidyl peptidase 4; FeNO, Fraction of exhaled nitric oxide; IL-6, Interleukin-6; IgE, Immunoglobulin E; LTE4, leukotriene E4; T2, T helper cell type 2. Adapted from McIntyre and Viswanathan (2023).

1.2.1.1 Allergic asthma

Allergic asthma is the most common phenotype among all asthmatic patients (Romanet-Manent et al. 2002), it accounts for ~50-60% of the total asthmatic population and it is the most easily recognized asthma phenotype through examination with increased eosinophils in the induced sputum and blood as well as high levels of Immunoglobulin E (IgE) in blood in patients with this asthma phenotype (Romanet-Manent et al. 2002; Schatz and Rosenwasser 2014). The first onset of this phenotype typically starts in childhood, and is associated with an allergic diathesis of the patient and/or his/her family (Global Initiative for Asthma 2023). The incidence of allergic diseases including allergic rhinoconjunctivitis and atopic dermatitis are commonly increased in patients with allergic asthma (Mullane 2011). It is well known that allergic asthma is triggered by specific allergens. Patients who present with this asthma phenotype usually respond well to the existing treatment methods, such as ICS, short and long-acting beta2-agonist (SABA, LABA), leukotriene receptor antagonists (LTRA) and IgE antibodies (Romanet-Manent et al. 2002; Schatz and Rosenwasser 2014).

1.2.1.2 Non-allergic asthma

Though the majority of patients present with allergic symptoms, some patients with asthma do not show typical allergic symptoms, having normal or low serum total IgE levels (Romanet-Manent et al. 2002). This type of asthma is estimated to occur in 10% to 33% of individuals (Romanet-Manent et al. 2002; Novak and Bieber 2003). The incidence of allergic diseases such as nasal polyposis, rhinosinusitis, and gastroesophageal reflux disease are commonly increased in patients with non-allergic asthma (Humbert et al. 1999; Romanet-Manent et al. 2002; Kanani et al. 2005; Peters 2014). The cellular profile in the sputum, bronchoalveolar lavage fluid (BALF) and blood of these patients have higher neutrophils counts, lower eosinophils count (Zoratti et al. 2014), more remodelling (Paganin et al. 1996) and lower IgE level than those of allergic asthmatic patients (Romanet-Manent et al. 2002; Peters 2014). Non-allergic asthma phenotype appears to be more severe, more common in female adult patients who tend to respond less well to the existing treatment methods than that of allergic asthmatic patients (Kitch et al. 2000; Romanet-

Manent et al. 2002; Abraham et al. 2003; Kanani et al. 2005; Leynaert et al. 2012; Amelink et al. 2013; Schatz and Rosenwasser 2014; Gonzalez-Uribe et al. 2023). Currently, little is known about the pathophysiology of non-allergic asthma which may be triggered by a wide range of factors, including viruses, pollutants, smoking, and other nonspecific stimuli (Peters 2014). However, there is a drop in age-adjusted risk of asthma in postmenopausal compared to premenopausal women, suggesting that asthma improves after menopause, possibly associated with levels of sex hormones (Zemp et al. 2012; Zein and Erzurum 2015; Fuseini and Newcomb 2017; Chowdhury et al. 2021).

1.2.1.3 Late-onset asthma (LOA)

The vast majority of asthmatic patients have their first onset during childhood, however, some adults, particularly women, present with asthma symptoms during adulthood for the first time (Global Initiative for Asthma 2023). The incidence of this asthma phenotype is increasing because of the aging of the population, and albeit the reason is still unclear, it may be related to the age-related declines in immune function, pulmonary structure and function as well as obesity in this population (Hirano and Matsunaga 2018) . Patients with LOA tend to be non-allergic, non-atopic status, and often have worse lung function, worse response to ICS, or require higher doses to control their symptoms (Miranda et al. 2004). Bauer et al reported that the incidence of asthma in elderly people (≥ 65 years old) was up to 0.1% per year (Bauer et al. 1997). Furthermore, in patients with LOA, there are some additional risk factors, such as elderly, poor inhaler technique, polymedication, multiple comorbidities, limited mobility and staying home alone, as well as psychological status (dementia, depression, etc.) (Ilmarinen et al. 2016; Susan Mayor 2016), making LOA difficult to treat. In addition, a paper also reported patients with LOA are at higher risk of developing cardiovascular disease (CVD) (Tattersall et al. 2016).

1.2.1.4 Asthma with fixed airflow limitation

A proportion of asthmatic patients develop airway wall remodelling after longer disease duration despite optimal pharmacologic treatment that causes persistent or incompletely reversible airflow limitation that may be the main reason for difficult-to-treat & severe asthma (Global Initiative for Asthma 2023). Patients with this asthma phenotype tend to be older, and have more frequent exacerbations (Contoli et al. 2010), which increases asthma-related mortality (Panizza et al. 2006), and difficulties to be treated (Hansen et al. 1999). The causes of this asthma phenotype are unknown, but may be related to the structural changes of airways (i.e., airway remodelling), including the airway smooth muscle hyperplasia, subepithelial fibrosis, angiogenesis, mucous gland hyperplasia as well as goblet cell hyperplasia and airway wall thickening (James and Wenzel 2007). Such changes cause airway narrowing that develop over many years, particularly in patients with severe disease.

1.2.1.5 Asthma with obesity

Obesity increases the incidence and severity and consequently affects the clinical manifestations of asthma. Although the reasons remain incompletely understood, it has been suggested that obesity may affect asthma by changing the normal structure of the respiratory tract or the function of the immune system (Quinto et al. 2011; Bates et al. 2017). Some obese patients have very severe respiratory symptoms of asthma, but have less eosinophilic airway inflammation (Lambrecht et al. 2019; Miethe et al. 2020). This phenotype is composed of two distinct groups, early-onset atopic (EOA) asthma and late-onset, nonatopic asthma (LONA), the former is complicated by the co-existence of obesity and the symptoms do not remit when the patients lose their weight, the latter likely has asthma developing due to obesity and consequently has symptoms resolved when they lose weight (Dixon et al. 2011; Bates et al. 2017).

1.3 The pathophysiology and inflammatory pathways of asthma

As previously mentioned, asthma is a heterogeneous disease characterized by airway hyperresponsiveness, chronic airway inflammation, as well as variable airflow obstruction (Calhoun and Chupp 2022). The pathogenesis of asthma is not yet entirely clear; however, the pathophysiology of asthma involves a complex interplay of genetic, environmental, immunological, and inflammatory factors (including massive cytokine production and inflammatory cell infiltration), as well as structural changes such as goblet cell hyperplasia, excess mucus production, collagen deposition, airway smooth muscle hyperplasia and hypertrophy. These events together lead to airway inflammation and remodelling, bronchial hyperresponsiveness, and ultimately, symptoms like wheezing, shortness of breath, chest tightness, and coughing (Figure 2) (Morosco and Kiley 2007; Calhoun and Chupp 2022).

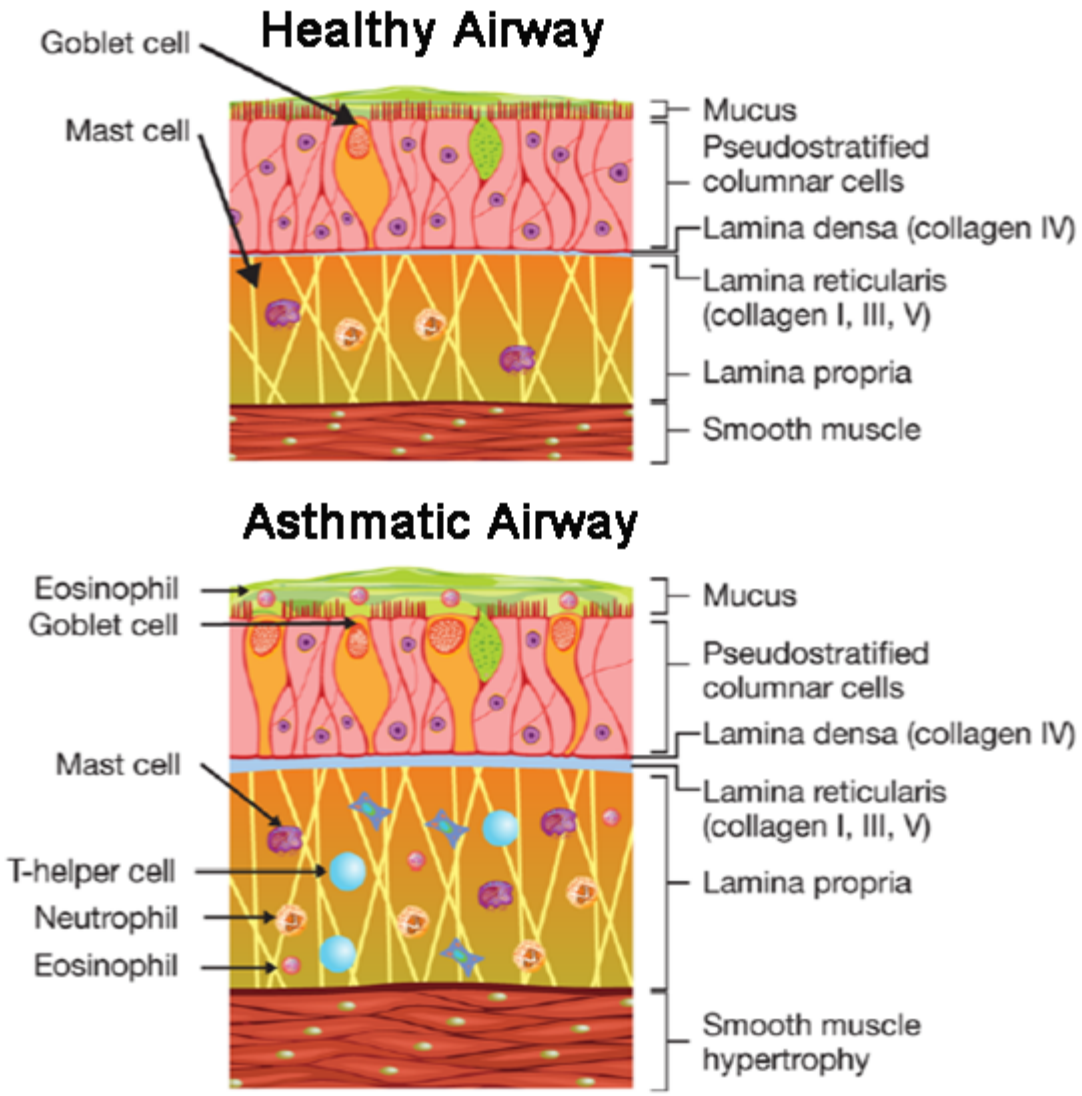

Figure 2. Comparison of cross-section and histology of airways in a healthy subject and asthmatic patient.

The asthmatic airway has significant goblet cell hyperplasia, excess mucus production, collagen deposition, airway smooth muscle hyperplasia and hypertrophy as well as massive cytokine production and inflammatory cell infiltration, compared to the airway of the normal person. Image taken from Calhoun and Chupp (2022).

It has been known that inflammation plays a pivotal role in the pathophysiology of asthma, although it is heterogeneous and involves a cascade of immunological responses, which can be primarily classified into

two types: type 2 (T2)- and non-type 2 (non-T2, also called T2 low) inflammations (McIntyre and Viswanathan 2023).

1.3.1 Type 2 (or T2 high) Inflammation

Type 2 inflammation is most commonly initiated by the adaptive immune system upon exposure to environmental triggers like allergens through the actions of thymic stromal lymphopoietin (TSLP), which stimulates naïve T-helper cells to differentiate into type 2 (Th2) cells, resulting in the production of Th2 cytokines IL-5, IL-4, and IL-13. In addition, TSLP can also act on innate lymphoid cells type 2 (ILC2s) to generate similar cytokines to Th2 cells (Halim et al. 2012; Lund et al. 2013; Israel and Reddel 2017; Kuo et al. 2017). IL-4, IL-5, and IL-13 play key roles in promoting eosinophilic inflammation, mucus production, airway hyperresponsiveness, and airway remodelling (Kuo et al. 2017; Lambrecht et al. 2019). These cytokines, particularly IL-4 and IL-13, also promote IgE production, thereby resulting in mast cell activation and degranulation as well as the release of inflammatory mediators like histamine and prostaglandin D2 (PGD2) (Lambrecht et al. 2019). Type 2 inflammation is typically associated with allergic sensitization, elevated levels of IgE, and a Th2-dominated immune inflammation (McIntyre and Viswanathan 2023). Triggering factors for type 2 inflammation include exposure to allergens, viral infections, and environmental pollutants (Israel and Reddel 2017).

1.3.2 Non-Type 2 (or T2 low) Inflammation

A subset of asthma patients exhibit non-T2 inflammation characterized by the activation of innate immune pathways and present with neutrophilic predominant inflammation, which is likely driven by T-helper type 1 (Th1) and type 17 cells (Th17) (Ray and Kolls 2017). Non-T2 asthma can manifest with inflammatory pathways distinct from those characterized by type 2 (T2) inflammation and have poorer response to steroids and short-acting bronchodilators (Fitzpatrick et al. 2020). To this end, understanding the inflammatory pathways and pathophysiology of asthma is essential for developing novel therapeutic targets aimed at modulating specific components of the immune response and achieving better control of asthma symptoms and exacerbations (Israel and Reddel 2017). The inflammatory

pathways that may be involved in type 2 and non-type 2 inflammation as well as the biomarkers involved in each pathway and various therapeutic agents targeting different biomarkers are summarized in Figure 3 (Calhoun and Chupp 2022).

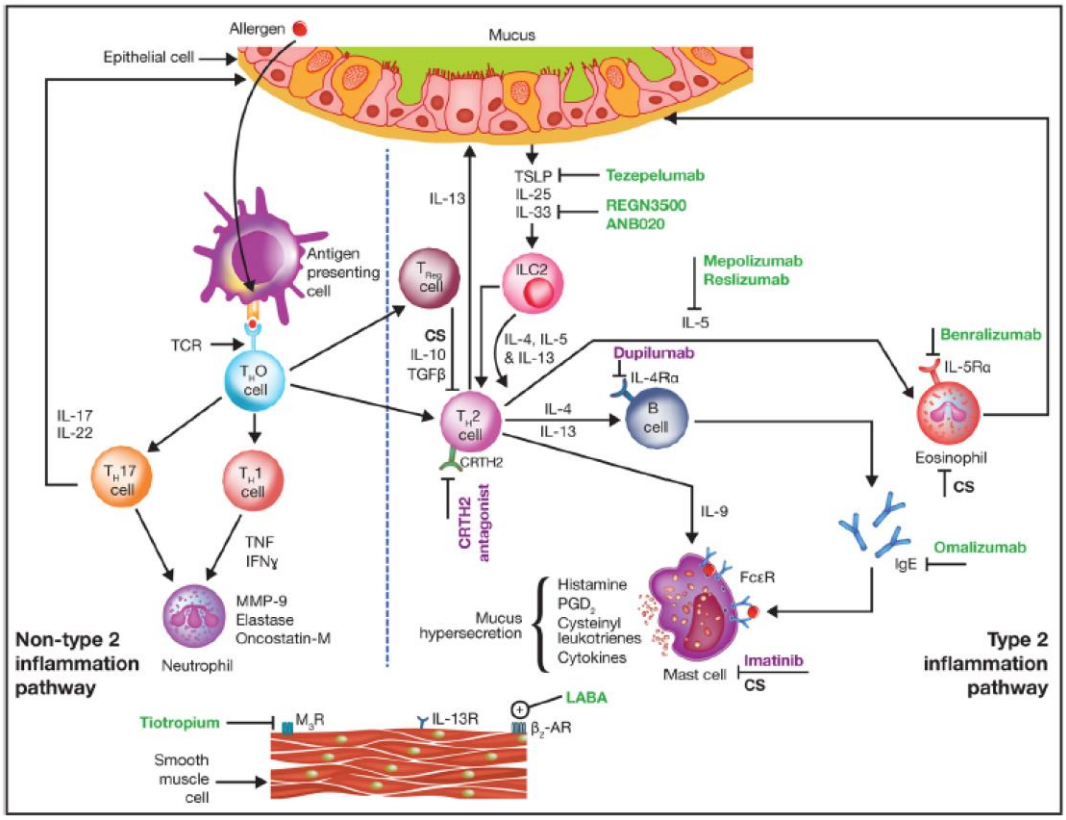

Figure 3. The inflammatory and immunologic pathways involved in asthma.

The figure displays the T2 and non-T2 inflammatory pathways in asthma, the biomarkers involved, and the mechanism of action of various therapeutic agents. Type 2 inflammation is typically initiated by the response of adaptive immune system upon exposure to allergens, triggered by thymic stromal lymphopoietin (TSLP), which stimulates the differentiation of type 2 T-helper (Th2) cells and innate lymphoid cells type 2 (ILC2), prompting the production of type 2 cytokines interleukin (IL) 4, IL-5, and IL-13, facilitated by activation of the GATA3 transcription factor. The resulting cytokines prompt IgE production via IL-4 and mast cell activation as well as the activation and recruitment of eosinophils via IL-5 and IL-13, leading to airway hyperresponsiveness, remodelling and increased mucus production. Mast cells can produce various mediators and cytokines, including IL-3, IL-4, IL-5, and IL-9 which are involved

in airway smooth-muscle contraction, eosinophil infiltration, remodelling, and amplification of the inflammatory cascade, as well as prostaglandin D2 (PGD2), which activates eosinophils and other cells through its CRTH2 receptor. The above process can also be activated by environmental triggers, like respiratory viruses, irritants and pollutants through the production of IL-33 and IL-25 by the innate immune system to stimulate ILC2 and Th2 cells to produce the above cytokines involved in this process. The production of cytokines upon exposure to the above agents can trigger non-type 2 pathways as well, involving Type 17 helper T (Th17) cells and Type 1 helper (Th1) cells, leading to neutrophilic inflammation. β_2-AR, β_2-adrenergic receptor; CS, corticosteroids; CRTH2, chemoattractant receptor-homologous molecule expressed on Th2 cells; FcεR, Fcε receptor; IFNγ, interferon gamma; IgE, immunoglobulin E; IL, interleukin; ILC2, innate lymphoid cell type 2; LABA, long-acting β_2-agonist; MMP-9, matrix metallopeptidase 9; M_3R, muscarinic receptor type 3; PGD2, prostaglandin D2; TCR, T-cell receptor; TGF-β, transforming growth factor beta; Th2, type 2 helper; TNF, tumour necrosis factor; TSLP, thymic stromal lymphopoietin. Image taken from Calhoun and Chupp (2022).

1.4 Existing and pipeline treatment of asthma

Current standard treatments for asthma include small molecules such as ICS and beta-agonists, both SABA and LABA, long-acting muscarinic antagonists (LAMA) as well as some symptomatic treatments, such as drugs targeting eosinophils (such as anti-IL-5 or anti-IL-5R), theophylline, IgE antibody, anti-IL-4R, anti-TSLP, and leukotriene receptor antagonists, even in some patients with severe asthma oral corticosteroids are being used. Since the pathogenesis of asthma was not very well defined, only two classes of drugs, the anti-leukotrienes and anti-IgE antibodies, have been approved in the last 30 years despite the need for new therapeutics, and a huge research effort (Mullane 2011) before the approval of targeting biologics. According to the stepwise asthma treatment strategy for adults and adolescents recommended by GINA 2023 guideline, the management of asthma involves a systematic approach to managing asthma symptoms and exacerbations based on their severity and control level, from as-needed low-dose ICS plus formoterol in step 1 to medium-dose maintenance ICS plus formoterol in step 4, to high-dose maintenance ICS plus formoterol plus add-on treatment with LAMA or biologics in step 5 (Figure 4). Overall, the GINA 2023 guideline emphasizes the importance of individualized treatment based on asthma severity and control, with regular assessment and adjustment of therapy to achieve optimal asthma management and improve patient outcomes (Global Initiative for Asthma 2023).

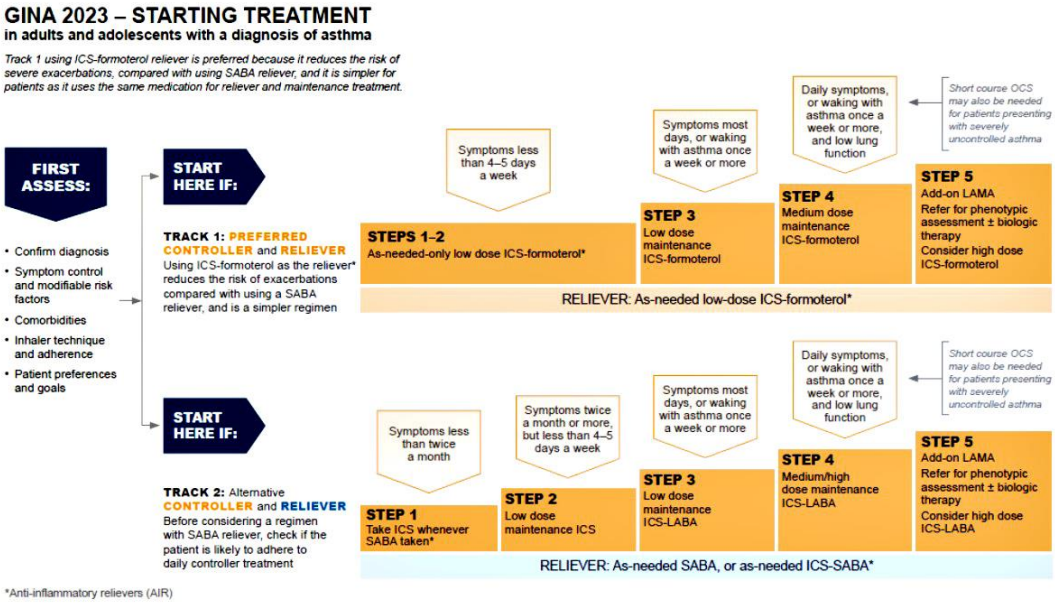

Figure 4.The stepwise asthma treatment strategy for adults and adolescents recommended by GINA 2023.

The GINA 2023 guideline recommends a stepwise and personalized asthma management strategy according to the diagnosis, symptom control, exacerbations, side effects and patient satisfaction. The selection of ICS-formoterol as the preferred reliever is because it reduces the risk of exacerbations compared with using a SABA reliever, and is a simpler regimen. If a patient doesn't present with symptoms twice a month or more, as-needed only low-dose ICS-formoterol outlined in TRACK 1 or low-dose ICS whenever SABA is taken outlined in TRACK 2 is recommended as the preferred approach. If a patient presents with symptoms twice a month or more, as-needed only low-dose ICS-formoterol outlined in TRACK 1 or low-dose ICS + as-needed SABA (or ICS-SABA) outlined in TRACK 2 is recommended as the preferred approach. If a patient has symptoms most days, or wakes at night once a week or more, low-dose ICS-formoterol maintenance and reliever (MART) outlined in TRACK 1 or low-dose ICS-LABA + as-needed SABA (or ICS-SABA) outlined in TRACK 2 is recommended as the preferred approach. If a patient has daily symptoms, waking at night once a week or more, medium-dose ICS-formoterol maintenance and reliever in TRACK 1 or medium/high-dose ICS-LABA + as-needed SABA (or ICS-SABA) in TRACK 2 is recommended as the preferred approach. ICS, inhaled corticosteroid; LABA, long-acting beta$_2$-agonist;

LAMA, long-acting muscarinic antagonist; LTRA, leukotriene receptor antagonist; OCS, oral corticosteroid; SABA, short-acting beta$_2$-agonist. Image taken from GINA 2023 guideline (Global Initiative for Asthma 2023).

1.4.1 Inhaled corticosteroid (ICS)

Inhaled corticosteroid comprises the backbone of asthma therapy and represents the gold-standard anti-inflammatory therapy for asthma treatment (Hansel 2004; Paggiaro and Bacci 2011). ICS can reduce the number of inflammatory cells, including lymphocytes, eosinophils, mast cells, macrophages, dendritic cells, and structural cells (such as endothelial cells, epithelial cells, and smooth muscle cells), in asthmatic airways (Barnes 2010a) (Figure 5). The main mechanism of action of ICS is to activate the glucocorticoid receptor (GR) which then migrates to the cell nucleus and regulates inflammatory gene transcription, thus inhibiting inflammatory response and reducing inflammatory damage, thereby reducing airway hyperresponsiveness, improving respiratory function, alleviating symptoms, and preventing further deterioration of symptoms. ICS binds to GR and regulates the release of inflammation-related factors through the following two major pathways: (1) Binding to glucocorticoid response elements (GRE) which are located in the promoter of the structural genes or the upstream and thus increase the transcription of these genes, such as interleukin-1 receptor antagonist (IL-1 RA), IL-10, etc.; (2) Inhibition of transcription factors; ICS reduces the up-regulation of the transcription of multiple inflammatory factors by inhibiting nuclear factor kappa-B (NF-κB) and activator protein-1 (AP-1) and other transcription factors, thereby reducing the synthesis of pro-inflammatory factors. Similarly, ICS can down-regulate the gene expression of multiple inflammatory mediators such as IL-1, IL-3, IL-5, vascular cell adhesion molecule-1 (VCAM-1), tumour necrosis factor α (TNFα), and intercellular adhesion molecule-1 (ICAM-1), E-selectin and granulocyte-macrophage colony-stimulating factor (GM-CSF), but can increase the gene expression of a variety of protective mediators, such as NF-κB inhibitor protein 1 (Iκ B1), IL-10, IL-12 and IL-1RA (Payne and Adcock 2001; Barnes 2011; Sibila et al. 2015) (Figure 6).

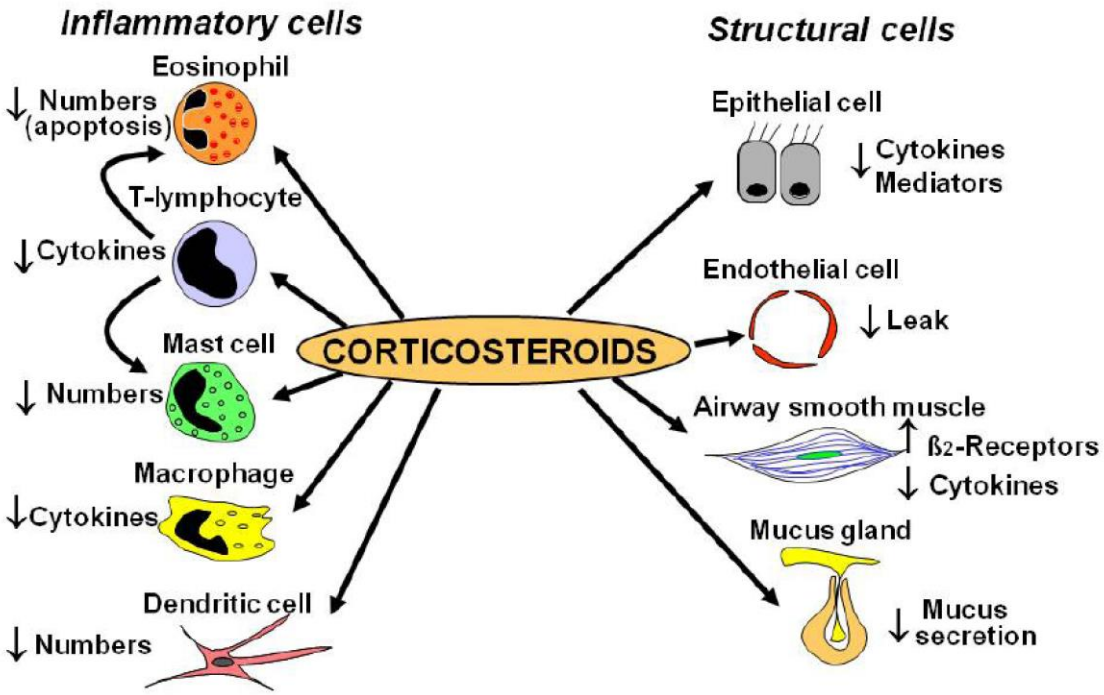

Figure 5. Cellular effects of corticosteroids.

Inhaled corticosteroid can inhibit the production of chemotactic mediators and adhesion molecules, thereby inhibiting the recruitment of inflammatory cells into the airway. They also suppress the activity of inflammatory cells involved in the pathogenesis of asthma, such as eosinophils, mast cells, lymphocytes, macrophages and dendritic cells. Image taken from Barnes (2010).

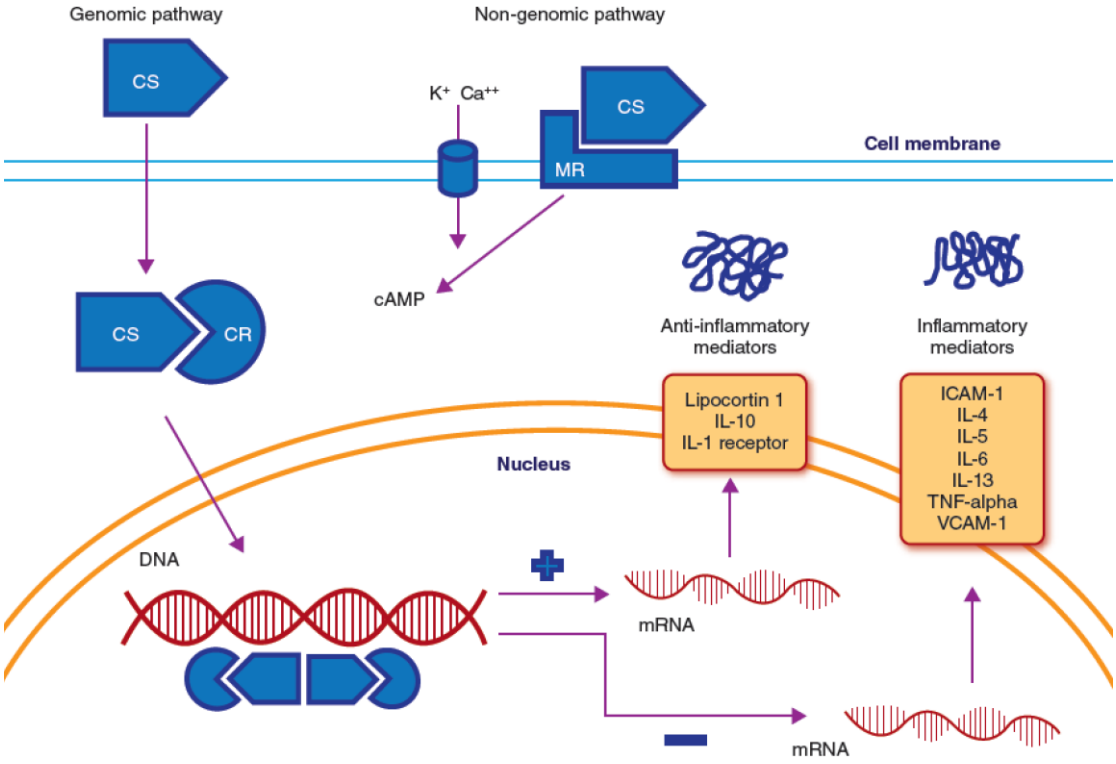

Figure 6. Cellular mechanism of action of corticosteroids in the inhibition of inflammation.

Corticosteroids work through genomic and nongenomic pathways such as transactivation, and transrepression: (i) transactivation: increases anti-inflammatory mediators such as lipocortin 1, IL-10 and IL-1 receptor, (ii) transrepression: decreases inflammatory mediators such as TNF-alpha, IL-4, -5, -6, and -13, ICAM -1, VCAM-1, and (iii) increase anti-inflammatory messengers through membrane-associated receptors. Ca^{++}, calcium ions; CR, corticosteroid receptor; CS, corticosteroids; cAMP, adenosine monophosphate; DNA, Deoxyribonucleic acid; ICAM, intercellular adhesion molecule; IL, interleukin; K^{+}, potassium ions; MR, membrane receptor; mRNA, Messenger RNA; TNF, tumour necrosis factor; VCAM, vascular cell adhesion molecule. Image taken from Sibila et al. (2015).

There are several ICSs that are now available in the clinical setting, such as hydrocortisone, beclomethasone, budesonide, fluticasone propionate, flunisolide and triamcinolone (Figure 7) (Barnes 2010a). However, they are all associated with long-term side effects due to the transactivation and binding of the glucocorticoid receptors to DNA, such as osteoporosis, which is one of

the well-known adverse effects of long-term administration of glucocorticoids (Van Staa et al. 2002). In a study conducted by Israel et al., the authors reported that ICS treatment was associated with a dose-dependent reduction in bone density among premenopausal women with asthma (Israel et al. 2001)Click or tap here to enter text.. In a study conducted by Adinoff and Hollister, they reported that long-term steroid treatment is associated with decreased bone density and increased prevalence of fractures in patients with asthma (Adinoff and Hollister 1983). In addition, long-term usage of glucocorticoid is associated with poor compliance, which may contribute to difficulty in controlling asthma (Barnes 2010c; Barnes 2011). So, the recent research is focusing on the development of new molecules with low risk of side effects which is associated with fewer systemic side effects (Nave 2009).

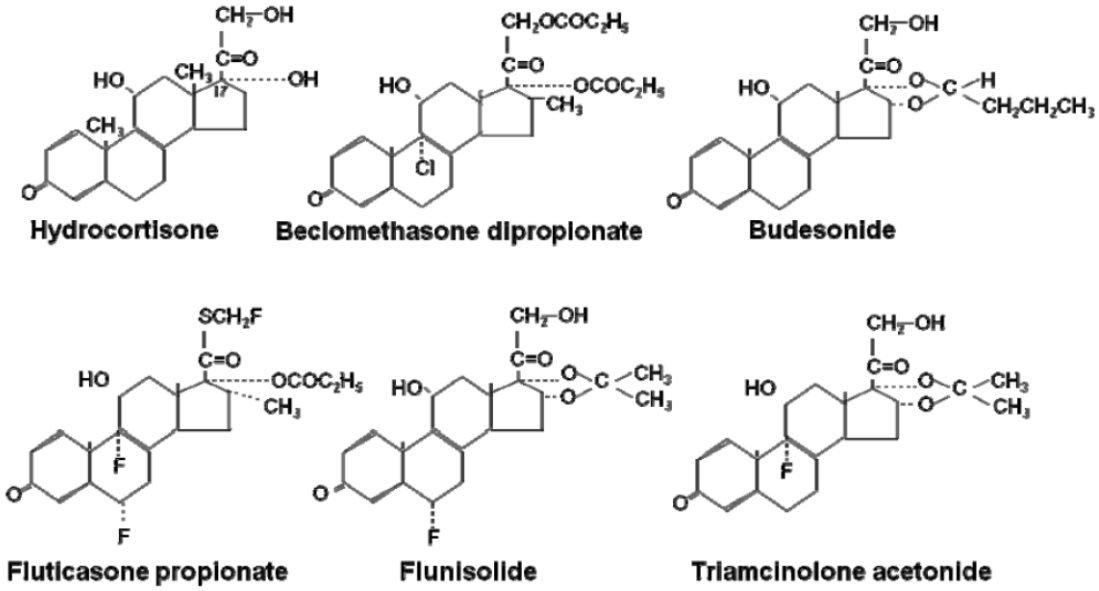

Figure 7. Chemical structures of inhaled Corticosteroids.

This figure elucidates the chemical structure of hydrocortisone, beclomethasone, budesonide, fluticasone propionate, flunisolide and triamcinolone. All these drugs share a common basic structure known as the corticosteroid backbone, which consists of three six-membered rings (A, B, and C rings) and one five-membered ring (D ring) fused together. The differences in their substitution groups contribute to differences in their

potency, bioavailability, metabolism, glucocorticoid receptor binding affinity, duration of action, and side effect profiles. Image taken from Barnes (2010).

1.4.2 Bronchodilators

Bronchodilators can be divided into short- and long-acting bronchodilators depending on their onset time, including beta-agonists or muscarinic antagonists (SABA or SAMA, LABA or LAMA). The commonly used bronchodilators are beta-agonists, of which salbutamol, formoterol and salmeterol are the most common drugs in the clinical setting. The understanding of the mechanism of action of this class of drugs is currently not uniform. However, the main function of bronchodilators in the airway is to activate adenylate cyclase (AC), thereby promoting the production of cyclic adenosine monophosphate (cAMP) from adenosine triphosphate (ATP), thus decreasing the concentration of intracellular Ca^{2+} ($[Ca^{2+}]_i$) or Ca^{2+} sensitivity, resulting in significant airway relaxation (Figure 8) (Endou et al. 2004; Oguma et al. 2006; Mahn et al. 2010; Billington and Hall 2012; Billington et al. 2013). Beta2-agonists can also inhibit the aggregation of inflammatory cells and release inflammatory mediators, reduce plasma exudation, improve sensory nerve response (Barnes 1999). This is of great significance for reducing the damage of airway inflammation and preventing deterioration. These agents can be used as an add-on treatment with ICS or even rescue treatment in patients with severe asthma because they are highly effective at relieving airway constriction and obstruction. However, the safety of the agents is also a matter of debate. The major adverse effects of Beta2-agonists include skeletal muscle tremor, tachycardia, cardiac arrhythmias, reduction in the arterial oxygen pressure (PaO_2) and various metabolic effects, mediated by β-adrenoceptor stimulation (Lulich et al. 1986).

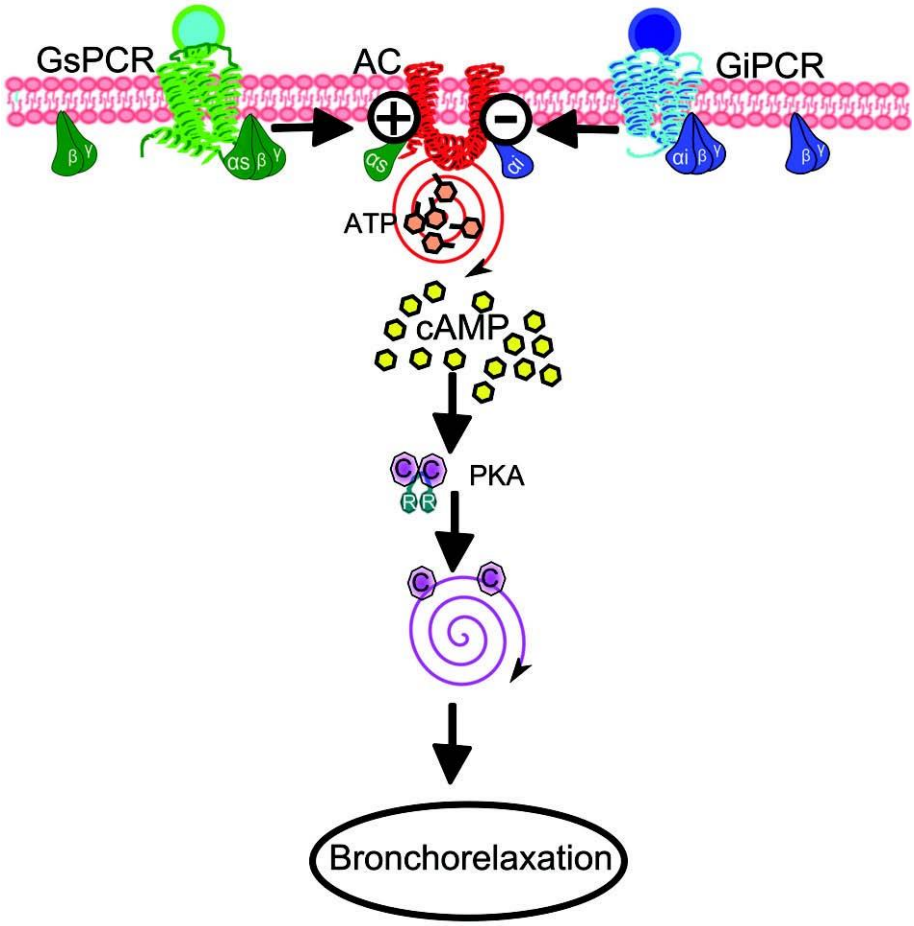

Figure 8. Proposed model of bronchorelaxation.

The binding of agonist to a Gs-protein coupled receptor (GsPCR), such as the Beta$_2$-adrenoceptor, or a Gi-protein coupled receptor (GiPCR), such as the muscarinic M2 acetylcholine receptor results in a conformational change, leading to the dissociation of the Gα subunit. While the Gαi-protein inhibits AC, the Gαs-protein stimulates adenylate cyclase (AC), inducing it to produce cyclic adenosine monophosphate (cAMP) from adenosine triphosphate (ATP). The resulting increase in cAMP slows or abolishes Ca^{2+} oscillations via binding to protein kinase A (PKA). In addition, cAMP/PKA also decreases Ca^{2+} sensitivity. Either a decrease in intracellular free ionized Ca^{2+} ($[Ca^{2+}]_i$) or Ca^{2+} sensitivity or both can result in bronchorelaxation. AC, adenylyl cyclase; ATP, adenosine triphosphate; cAMP, cyclic adenosine monophosphate;

$[Ca^{2+}]_i$, intracellular free ionized Ca^{2+}; PKA, protein kinase A. Image taken from Billington and Hall (2012).

The addition of inhaled β2-agonists to ICS is recommended by the treatment guideline as regular treatment and can provide optimal asthma control in most patients (Global Initiative for Asthma 2023). (Figure 4). Though corticosteroids and bronchodilators are effective in the majority of patients, it is appreciated that 30-40% of asthmatics have a poor response to these treatments, and in 10% this likely contributes to the presence of severe asthma (American Thoracic Society 2000; Wenzel and Busse 2007). The poor asthma control in this population is because of the poor understanding of the underlying disease mechanisms. In addition, these treatments are nonspecific anti-inflammatory drugs and thus pose the risk of systemic side effects. These considerations have led to a search for novel or improved therapies for asthma. Many new treatments are in development, which are specific, targeting a specific mediator or receptor, and might be effective in specific asthma phenotypes. A summary of the currently approved and under development treatments for asthma can be found in the below Table 2.

Table 2. Currently approved and under development treatments for asthma

	Target	Drug name	Molecule type	status	Company
Biologicals	IgE	Omalizumab	Antibody	FDA/EMA	Novartis
		Ligelizumab/QGE031	Antibody	Under development	Novartis
		Quilizumab	Antibody	Under development	Genentech
		MEDI4212	Antibody	Under development	MedImmune LLC
		FB825	Antibody	Under development	Oneness Biotech
	IL-5	Mepolizumab	Antibody	FDA/EMA	GSK
		Reslizumab	Antibody	FDA/EMA	Teva
		Benralizumab	Antibody	FDA/EMA	AstraZeneca
		Depemokimab	Antibody	Under development	GSK
	IL-4	Pascolizumab	Antibody	Under development	GSK
		VAK694	Antibody	Under development	Novartis
	IL-4/IL-13	Dupilumab	Antibody	FDA/EMA	Regeneron/ Sanofi
		Pitrakinra	Recombinant IL-4 variant	Under development	Aerovance
		AMG317	Antibody	Under development	Amgen
		QBX258(VAK-94/QAX-576)	Antibody	Under development	Novartis

	IL-13	CNTO 5825	Antibody	Under development	Janssen Biotech
		Anrukinzumab	Antibody	Under development	Wyeth
		GSK679586	Antibody	Under development	GSK
		IMA-026	Antibody	Under development	Pfizer
	IL-25	ABM125	Antibody	Under development	Abeome
	Tryptase tetramers	MTPS9579A	Antibody	Under development	Roche/Genentech
	TSLP	Tezepelumab	Antibody	FDA	AstraZeneca /Amgen
		CSJ117	Antibody	Under development	Novartis
		ASP7266	Antibody	Under development	Upstream Bio
	IL-33	REGN3500	Antibody	Under development	Regeneron and Sanofi
		Tozorakimab/MEDI3506	Antibody	Under development	AstraZeneca
		Itepekimab	Antibody	Under development	Regeneron/ Sanofi
		Astegolimab	Antibody	Under development	Hoffmann-La Roche
	TSLP/IL-13	Zweimab	Antibody	Under development	Boehringer Ingelheim
		Doppelmab	Antibody	Under development	Boehringer Ingelheim
	IL-13/IL-17	BITS7201A	Antibody	Under development	Genentech

	TNFα	Infliximab	Antibody	Under development	MSD
		Etanercept	TNFR:Fc	Under development	Sobi
		Infliximab	Antibody	Under development	MSD
		Golimumab	Antibody	Under development	Centocor
	IL-9	Enokizumab	Antibody	Under development	AstraZeneca /MedImmune
	IL-6	Tocilizumab	Antibody	Under development	Roche
	IL-1	Anakinra	Antibody	Under development	Sobi
	C5	Eculizumab	Antibody	Under development	Alexion
Small molecule drugs	IL-4Rα	AIR645	Antisense oligo	Under development	Altair
	CXCR2 (CXC chemokine receptor 2)	Navarixin/MK-7123	Antagonist	Under development	Merck Sharp & Dohme LLC
		AZD5069	Antagonist	Under development	AstraZeneca
	CCR3 (eotaxin receptor)	GW766944	Inhibitor	Under development	Glaxo
	CXCR1/2	SCH527123	Antagonist	Under development	MSD
	Reactive aldehyde species (RASP)	ADX-629	Inhibitor	Under development	Aldeyra
LTRAs	CysLTR1	Montelukast	Antagonist	FDA	Merck
		Zafirlukast	Antagonist	FDA/EMA	AstraZeneca

		Pranlukast	Antagonist	Approved in Japan	Ono Pharmaceuticals
	CRTH2/DP2(PGD2 receptor)	Timapiprant/OC000459	Antagonist	Under development	Chiesi
		Setipiprant	Antagonist	Under development	Actelion
	Muscarinic receptors	Umeclidinium	Antagonist	Under development	GSK
		Glycopyrronium	Antagonist	Under development	Max Health Ltd
SABAs	ADRB2	Fenoterol	Agonist	FDA/EMA	Boehringer Ingelheim
		Levalbuterol	Agonist	FDA/EMA	Sunovion
		Salbutamol (Albuterol)	Agonist	FDA/EMA	GSK
LABAs		Formoterol	Agonist	FDA/EMA	Dey, L.P
		Salmeterol	Agonist	FDA/EMA	GSK
ULABAs		Indacaterol	Agonist	FDA/EMA	Novartis
		Vilanterol	Agonist	FDA/EMA	GSK
ULAMAs		Tiotropium	Antagonist	FDA/EMA	Boehringer Ingelheim
ICS	GR	Beclomethasone dipropionate	Agonist	FDA/EMA	Teva
		Budesonide	Agonist	FDA/EMA	AstraZeneca
		Ciclesonide	Agonist	FDA/EMA	Nycomed
		Fluticasone propionate/furoate	Agonist	FDA/EMA	Teva
		Triamcinolone acetonide	Agonist	Under development	Kos
	GR	Betamethasone	Agonist	FDA/EMA	Teva

Systemic CS		Deflazacort	Agonist	FDA/EMA	Marathon
		Hydrocortisone	Agonist	FDA/EMA	Pharmacia & Upjohn
		Methylprednisolone	Agonist	FDA/EMA	Pfizer
		Prednisone	Agonist	FDA/EMA	Shionogi Pharma, Inc.
	PI3K/p110δ	Nemiralisib/GSK2269557	Inhibitor	Under development	GSK
	pan-JAK(JAK1,2,3 and Tyk2)	VR588	Inhibitor	Under development	Vectura
	GATA-3	SB010	DNAzyme	Under development	Sterna biologicals GmbH & Co. KG
	Mast cell stabilizer	Nedocromil	Inhibitor	Under development	Pfizer
	c-KIT, PDGFRA and PDGFRB	Imatinib	Inhibitor	Under development	Novartis
	PDE4	Ibudilast	Inhibitor	Approved in Japan	Kyorin
	PDE3/4	RPL554	Inhibitor	Under development	Verona
	5-lipoxygenase/ALOX5	Zileuton	Inhibitor	FDA	Chiesi

ADRB2, β2-adrenoreceptor; ALOX5, arachidonate 5-lipoxygenase; CS, Corticosteroids; c-KIT, CD117/stem cell growth factor receptor/tyrosine-protein kinase; CRTH2, Chemoattractant receptor homologous molecule expressed on T2 cells; CXCR2, interleukin 8 receptor; CysLTR1, cysteinyl leukotriene receptor 1; DP2, Prostaglandin D2 receptor 2; EMA, European Medicines Agency; FDA, Food and Drug Administration; GATA-3, GATA binding protein 3; GR, Glucocorticoid receptor; ICS, Inhaled Corticosteroids;

IgE, Immunoglobulin E; IL, Interleukin; IL-4Rα, interleukin 4 receptor α chain; JAK, Janus kinase; LABAs, Long-Acting Beta Agonists; LTRAs, leukotriene receptor antagonists; p110δ, PI3K catalytic subunit delta; PDE, phosphodiesterase; PDGFRA, platelet-derived growth factor receptor alpha; PDGFRB, platelet-derived growth factor receptor beta; PI3K, phosphoinositide 3-kinase; SABAs, Short-acting beta-agonists; TSLP, Thymic stromal lymphopoietin; Tyk2, Tyrosine kinase 2; ULABAs, Ultra-long-acting beta-agonists; ULAMAs, ultra-long-acting muscarinic agonists. Adapted from Roth-Walter et al. (2019).

1.4.3 Approved biologic therapies

As the understanding of the pathophysiology of asthma has improved over the past decade, the management of asthma is now shifting toward a personalized treatment strategy (McGregor et al. 2019). When developing personalized treatment strategy for a patient with asthma, doctors should take into account both patient-specific characteristics as well as the underlying endotype, rather than solely relying on disease severity (McGregor et al. 2019). As mentioned above, there are two specific endotypes, T2-high and T2-low, that are defined based on their distinct inflammatory characteristics, such as the expression of IL-4, IL-5, and IL-13. Based on this concept, it is important to distinguish the endotypes when considering biologic therapy. Up till now, the majority of the biologic therapies that have been approved or under development for asthma target inflammatory mediators that have been found to increase predominantly in patients with T2-high or eosinophilic asthma and shown promising results specifically (Castro et al. 2011; Castro et al. 2014; Normansell et al. 2014; Ortega et al. 2014; Wenzel et al. 2016). Nowadays, there are six biologics, omalizumab (anti-IgE), benralizumab (anti-IL5R), mepolizumab and reslizumab (anti-IL5), dupilumab (anti-IL4 receptor α) and Tezepelumab (anti-TSLP), which have been approved as add-on treatment by subcutaneous (SC) injection for moderate to severe asthma with T2-high phenotype (Global Initiative for Asthma 2023).

1.4.3.1 Anti-IgE antibodies

IgE was the first therapeutic target biologic being used for the treatment of asthma. Studies using recombinant humanized monoclonal anti-IgE antibodies have demonstrated efficacy in allergic asthma to reduce asthma exacerbations and responses to inhaled allergen, including moderate-to-severe allergic asthma (Boulet et al. 1997; Fahy et al. 1997; Fahy et al. 1999; Milgrom et al. 1999; Busse et al. 2001; Milgrom et al. 2001; Solèr et al. 2001; Vignola et al. 2004; Van Rensen et al. 2009; Busse et al. 2011; Corren et al. 2011b; Hanania et al. 2011). However, due to the costs of anti-IgE antibodies, the route of administration (SC) and frequency of administration (1-2 times per month), and also the unpredictability in patients' responses, usages of anti-IgE antibodies were limited (Fajt and Wenzel 2014). Anti-IgE antibody omalizumab, a recombinant humanised IgG1 monoclonal antibody, has been approved as an add-on treatment by SC injection for allergic asthma (Global Initiative for Asthma 2023). Omalizumab binds to the Fc part of free IgE to form complexes with free IgE, preventing the binding of IgE to FcƐR1 receptors, thus blocking the interaction between IgE and effector cells (Thomson and Chaudhuri 2011). Omalizumab has been shown to reduce serum concentrations of free IgE and eosinophilic airway inflammation; however, effects on airway wall structural remodelling and airway hyperresponsiveness are less clear (Milgrom et al. 1999). In a meta-analysis of RCTs in severe allergic asthma, omalizumab decreased severe exacerbations, and improved quality of life (Agache et al. 2020). The adverse effects associated with omalizumab include injection site reactions and anaphylaxis (Normansell et al. 2014).

1.4.3.2 Anti-IL-5 antibodies

IL-5 is a type 2 cytokine that is responsible for the maturation, proliferation, activation, and migration of eosinophils (Pelaia et al. 2019). Since most of the allergic asthmatics present with eosinophilia, monoclonal antibodies targeting IL-5, the cytokine play an important role in this process, may be effective in this population. Studies targeting anti-IL-5 have shown efficacy in reducing asthma exacerbations (Haldar et al. 2009) , blood and sputum eosinophils (Leckie et al. 2000; Flood-Page et al. 2003; Flood-Page et al. 2007), improving lung function and asthma control (Castro et al., 2011),however,

there were less or even no effects on the tissue eosinophils and fraction of exhaled nitric oxide (FeNO) (Haldar et al. 2009). There were also some effects on asthma quality of life and airway wall thickening, but with no effect on the other asthma-associated outcomes, such as the forced expiratory volume in one second (FEV_1), symptom scores, daily β-agonist use and airway hyperresponsiveness (Leckie et al. 2000; Flood-Page et al. 2003; Flood-Page et al. 2007). Additionally, a recent study from Oxford University showed the priming and activation of eosinophils in severe eosinophilic asthma are reversed by mepolizumab (Luo et al. 2024). Anti-IL5 antibodies mepolizumab and reslizumab as well as anti-IL5R antibody benralizumab have been approved as add-on treatment by SC injection for eosinophilic asthma (Global Initiative for Asthma 2023). Mepolizumab and reslizumab have been shown to reduce serum eosinophils through binding to IL-5 and interfering with its ligation to the IL-5 receptor on eosinophils and basophils (Farne et al. 2017). Benralizumab has also been shown to be effective in reducing serum eosinophil counts through binding to IL-5 receptor alpha subunit to inhibit its activation, leading to apoptosis of eosinophils (Busse et al. 2010; Castro et al. 2014).

1.4.3.3 Anti-IL-4/13 antibodies

Among the cytokines that contribute to the pathogenesis of asthma, IL-4 and IL-13 are two important cytokines involved in the production of IgE, mucus hypersecretion, airway hyperresponsiveness, and airway inflammation (Grünig et al. 1998; Wills-Karp et al. 1998; Webb et al. 2000; Izuhara et al. 2002; Bloemen et al. 2007). IL-4 and IL-13 share many biological functions because they can both function through IL-4 receptor α chain (IL-4Rα) (Rolling et al., 1996), so drugs targeting a single cytokine or the IL-4Rα to affect the downstream signals for both cytokines are being developed (Corren et al. 2009; Wenzel et al. 2013). Results of studies using these drugs showed some effect on IgE production, FEV_1 improvement, reduction in β-agonist use and FeNO levels, but without effects on any other asthma outcomes, and the effects seem to be more obvious in mild, atopic asthmatics with significant blood eosinophilia (Chibana et al. 2008; Corren et al. 2010; Corren et al. 2011a; Gauvreau et al. 2011; Slager et al. 2012; Piper et al. 2013). An anti-

IL4 receptor α antibody dupilumab has been approved as an add-on treatment by SC injection for eosinophilic asthma (Global Initiative for Asthma 2023), which is a fully humanized monoclonal antibody binding to IL-4 receptor alpha, therefore blocking both IL-4 and IL-13 signalling (Ricciardolo et al. 2021). In a meta-analysis of RCTs in patients with uncontrolled severe asthma, anti-IL4Rα reduced severe exacerbations and improved quality of life, symptom control and lung function (Agache et al. 2020). Potential predictors of asthma response to dupilumab include higher blood eosinophils and higher FeNO (Castro et al. 2018).

1.4.3.4 Anti-TSLP antibodies

Thymic stromal lymphopoietin (TSLP) is primarily released by bronchial epithelial cells after epithelial cell damage in response to various triggers such as allergens, viruses, bacteria, pollutants, and smoke during the initial stages of inflammatory pathways in asthma (Comeau and Ziegler 2010; Gauvreau et al. 2020a). TSLP plays a crucial role in stimulating Th2 cells as well as ILC2s to produce Th2 cytokines, including IL-4, IL-5 and IL-13, which are integral to both innate and adaptive immune responses in asthma (Kitajima et al. 2011; Gauvreau et al. 2020a). Given its involvement in the initiation and persistence of inflammatory pathways in asthma, targeting TSLP has the potential to be a promising treatment for treating inflammation in asthma (Comeau and Ziegler 2010; Gauvreau et al. 2020a). Tezepelumab, a human monoclonal antibody (IgG2λ) that can bind to TSLP, has been approved as an add-on treatment by SC injection for severe asthma (Global Initiative for Asthma 2023). Results of recently published phase 2 and 3 studies showed that tezepelumab reduced severe exacerbations, and improved lung function, symptom control and quality of life (Corren et al. 2017; Menzies-Gow et al. 2021). Potential predictors of asthma response to anti-TSLP include higher blood eosinophils and higher FeNO levels (Menzies-Gow et al. 2021).

Since the above biologics target a single mediator or receptor, they might be effective in some patients with specific asthma phenotypes; further studies on this topic are necessary to find the asthma phenotype and endotype that may respond to these biologic therapies. Considering they are unlikely to have a

major clinical impact in non-phenotypic asthmatics, recent studies have focused on finding new therapeutic targets for asthma. In addition, considering the administration route of subcutaneous injection, the cost of these biologics is high and associated with notable side effects such as injection site reactions and anaphylaxis, thus limiting their use in asthma patients (Global Initiative for Asthma 2023). Considering all these together, studies finding new innovative and creative small molecule drugs remain significantly attractive to researchers.

1.5 The role of interlukin-33 in asthma pathogenesis

Airway epithelial cells can secrete various cytokines to participate in the immune response and regulation of asthma after being stimulated by allergens or pathogenic microorganisms, including IL-33 which attracted the researchers to develop the new drug targeting it. IL-33 was first identified in 2005 as a new member of the IL-1 cytokine superfamily, which is a potent initiator of T helper type 2 polarization, and can activate mast cells, lymphocytes, eosinophils and other cells to produce Th2 cytokines, thus play an important role in inflammation, infection, and autoimmune diseases (Schmitz et al. 2005). After the epithelial barrier injury, IL-33 is released and binds to its receptor suppression of tumorigenicity 2 (ST2) in a number of cells that express ST2, such as ILC2 cells, subgroup of Th2 cells, eosinophils, mast cells, etc. IL-33 induces NF-κB phosphorylation and MAPK activation and Th2 cytokine production, eosinophilia, and increases levels of serum IgA and IgE after binding with $ST2^{+}$ cells, thus participating in the process of allergic diseases (Schmitz et al. 2005). Previously, IL-33 was found to be highly expressed in the serum, sputum and lung tissues of asthma patients, among which IL-33 expression in severe asthma patients increases more significantly (Préfontaine et al. 2009; Liew et al. 2010; Lloyd 2010). In addition, IL-33 can promote the synthesis of collagen by fibroblasts of children with severe steroid-resistant asthma (SRA), indicating that IL-33 also plays a role in airway remodelling (Olin and Wechsler 2014).

Ovalbumin (OVA) induced asthma model is a classic animal model of allergic asthma, in which airway hyperresponsiveness, eosinophil infiltration, airway

remodelling as well as other common human asthma pathological changes can be recapitulated in the mouse (Yu and Chen 2018). In a study conducted by Yan Li, the authors directly compared the pathological changes in murine models of asthma induced with OVA and IL-33, indicating that as compared to OVA, IL-33 induced a later, more severe asthma phenotype as well as more neutrophilic inflammation (Li et al. 2015), which is like events observed in the later onset of asthmatics. There are also other studies showing that bronchial epithelial cells, vascular endothelial cells, and human lung fibroblasts all express IL-33R (ST2) (Brown et al. 1993; Yagami et al. 2010; Fujita et al. 2012). Therefore, these observations indicate that IL-33 may be involved in asthma airway remodelling by acting on the above structural cells.

1.6 G protein-coupled receptors as novel drug targets for asthma

G protein-coupled receptors (GPCRs) are a class of cell surface membrane receptors involved in many cellular signal transduction processes (Wendell et al. 2020). GPCRs consist of an extracellular N-terminus, seven transmembrane alpha-helices (TM-1 to TM-7), which are linked via three extracellular (EL-1 to EL-3) and three intracellular loops (IL-1 to IL-3), and an intracellular C-terminus (Figure 9) (Gacasan et al. 2017). Upon binding of an activating ligand to the receptor's extracellular domain, GPCRs undergo conformational changes, resulting in the activation of intracellular signaling pathways through heterotrimeric G proteins (Tuteja 2009). It has been known that GPCRs play a crucial role in most cellular responses to different triggers, including hormones, neurotransmitters, and other environmental factors, thus constitute the largest family of drug targets in humans (Rosenbaum et al. 2009; Katritch et al. 2013; Fasciani et al. 2022).

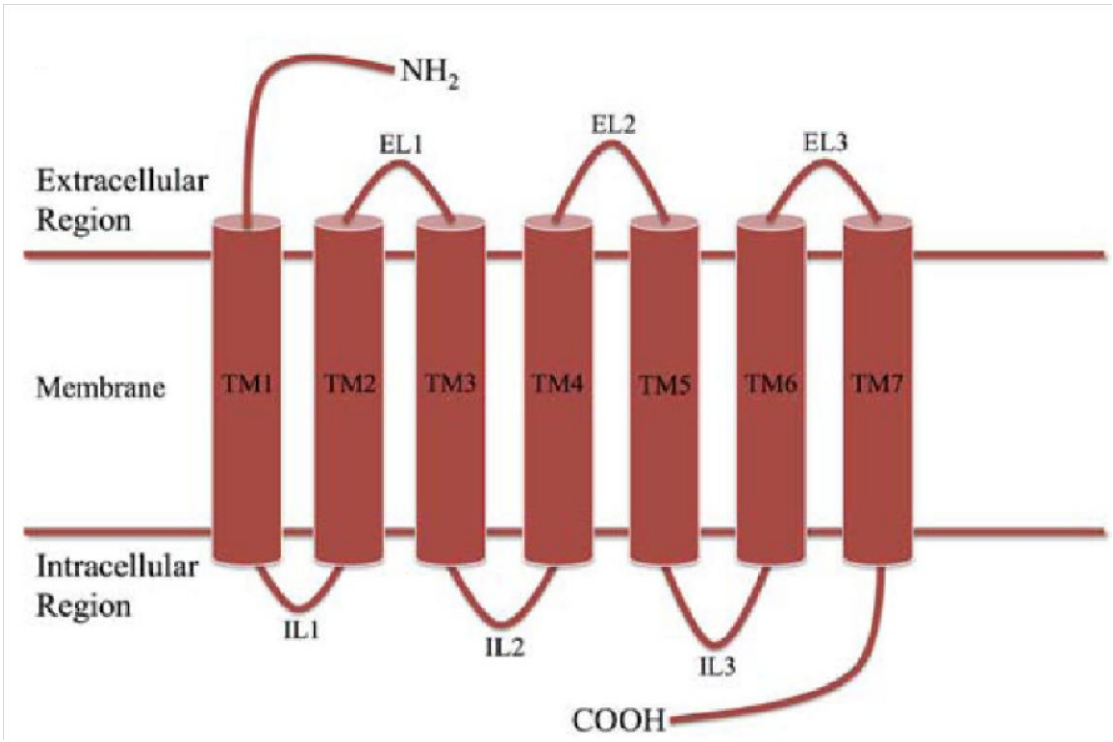

Figure 9. Schematic of the classical G protein-coupled receptor. GPCRs consist of an extracellular N-terminus, a transmembrane part (seven alpha-helices (TM-1 to TM-7), connected by three extracellular (EL-1 to EL-3) and three intracellular loops (IL-1 to IL-3) and an intracellular C-terminus. Image taken from Gacasan et al. (2017)

GPCRs have emerged as novel drug targets for asthma due to their pivotal role in mediating airway inflammation and bronchoconstriction, key pathological features of the disease. These receptors are expressed on diverse cell types involved in the pathogenesis of asthma, such as airway smooth muscle cells, immune cells (including mast cells, eosinophils, and T cells), and epithelial cells (Wendell et al. 2020). For example, GPCRs on airway smooth muscle cells play a prominent role in regulating bronchoconstriction, while GPCRs on immune cells can modulate inflammation and immune responses. Additionally, GPCRs expressed on epithelial cells can influence mucus production and airway remodelling (Billington and Penn 2003; Patel et al. 2020). Several current medications have been used for the treatment of asthma through targeting GPCRs, including the β2-adrenergic receptor (LABA, SABA), leukotriene receptors (montelukast, pranlukast and zafirlukast) and muscarinic acetylcholine

receptors (SAMA, LAMA) (Global Initiative for Asthma 2023). By modulating GPCR activity, these drugs aim to mitigate airway inflammation, bronchoconstriction, and other pathological processes associated with asthma, ultimately providing more effective and personalized treatment options for patients. Furthermore, the therapeutic potential of targeting GPCRs in asthma is under investigation, including prostaglandin D2 receptors, histamine receptors, chemokine receptors, and adenosine receptors (Wendell et al.,2020). Recently, our group has identified the extracellular Calcium-Sensing Receptor (CaSR) as a novel potential drug target for asthma (Yarova et al. 2015).

1.7 The extracellular Calcium-Sensing Receptor

The calcium-sensing receptor is a member of the C family of GPCR, which in humans is 1,078 amino acids long (Brown et al. 1993; Garrettt et al. 1995). It was first identified in bovine parathyroid glands by Brown et al in 1993 (Brown et al. 1993), since then, it enhanced our understanding of the pivotal role of extracellular free ionised calcium ($[Ca^{2+}]_o$) homeostasis in health and disease (Pollak et al. 1993; Pollak et al. 1994a; Pollak et al. 1994b; Pearce et al. 1995; Brown and Macleod 2001; Thakker 2004; RV 2012). Genetic mutations in the *CASR* gene in humans are associated with diseases such as familial hypocalciuric hypercalcaemia (FHH), hyperparathyroidism (HPT) and autosomal dominant hypocalcaemia (ADH) (Brown et al. 1993; Brown et al. 1995; Chikatsu et al. 2003; Miyashiro et al. 2004; Waller et al. 2004).
The CaSR is widely expressed in tissues involved in extracellular calcium homeostasis, including thyroid, parathyroid, kidney, intestine, and bone (Brown and Macleod 2001). Studies have shown that the main CaSR function is in extracellular calcium ion homeostasis through the regulation of parathyroid hormone (PTH) release (Brown et al. 1993; Riccardi and Brown 2010). When the extracellular free ionised calcium concentration increases, CaSR is activated, which then leads to an inhibition of PTH release (Brown et al. 1993; Conigrave and Ward 2013; Conigrave 2016). Patients with FHH and HPT have reduced sensitivity to $[Ca^{2+}]_o$ due to CaSR inactivating mutations leading to loss of function, while patients with ADH have increased sensitivity to extracellular calcium due to CaSR activating mutations (Chibana et al.

2008; Slager et al. 2012; Piper et al. 2013). CaSR expression was first identified and is of greatest expression in the parathyroid glands as a regulator of PTH secretion, but the CaSR is also found in the other key organs that participate in calcium homeostasis:calcitonin-secreting C-cells of the thyroid gland, kidney, gut and bone (Brown and Macleod 2001). In addition, CaSR is also expressed in various organs that are not generally considered to be involved in extracellular calcium metabolism, such as the brain, pancreas, pituitary, bone marrow, skin, breast, testis, placenta, heart and vascular smooth muscle (Riccardi et al. 1995; Cheng et al. 1998; Cheng et al. 1999; Wonneberger et al. 2000; Tennakoon et al. 2016; Hannan et al. 2018; Das et al. 2020; Ranieri et al. 2023). It has also been shown that the CaSR plays roles outside divalent mineral ion homeostasis, and involves in the regulation of cell differentiation, proliferation, chemotaxis, apoptosis, gene expression, aging, etc (Lin et al. 1998; Brown and Macleod 2001; Ba and Friedman 2004; Brown 2007). The primary physiological ligand of CaSR is free ionised extracellular calcium ($Ca^{2+}{}_{o}$), however, CaSR can also be activated by many other molecules with a lower affinity, such as other divalent cations Mg^{2+}, Ba^{2+}, Mn^{2+}, Ni^{2+}, Sr^{2+} and trivalent cations La^{3+} and Gd^{3+}, polyamines and L-amino acids (Brown and Macleod 2001).

CaSR exerts its effects by activating multiple signaling pathways, including Gαq/11, Gαi/o, Gα12/13 and Gαs (Figure 11). The primary signaling pathway associated with CaSR is its coupling to Gαq/11, which stimulates phospholipase C (PLC)-β to hydrolyze phosphatidylinositol 4,5-bisphosphate, generating the second messengers inositol trisphosphate (IP_3) and diacylglycerol (DAG) (Brown et al. 1993; Chang et al. 1998). CaSR activation of Gαi/o proteins suppresses adenylate cyclase activity, leading to a reduction in intracellular cAMP levels (Chang et al. 1998; Kifor et al. 2001). Additionally, in certain cell types, CaSR has been reported to couple with Gα12/13 proteins, leading to the activation of the Rho family of GTPases, which are pivotal in cytoskeletal reorganization and cell motility(Huang et al. 2004). CaSR coupling to Gαs leads to an increase in intracellular cAMP levels, which activates protein kinase A (PKA) and promotes the release of parathyroid hormone-related protein (PTHrP) in both immortalized and malignant breast cells, as well as in the AtT-20 pituitary-derived cell line (Mamillapalli et al.

2008; Mamillapalli and Wysolmerski 2010). In addition to the pathways mentioned above, CaSR can also activate the mitogen-activated protein kinase (MAPK) pathway through various G protein-dependent and -independent mechanisms. This activation leads to the phosphorylation of key proteins involved in cell proliferation, differentiation, and survival (Brown et al. 1993). Furthermore, CaSR has been shown to influence the regulation of ion channels and transporters, particularly in the kidneys and parathyroid glands, thereby contributing to calcium homeostasis (Chang et al. 1998; Kifor et al. 2001). The downstream pathways of CASR are illustrated in Figure 10.

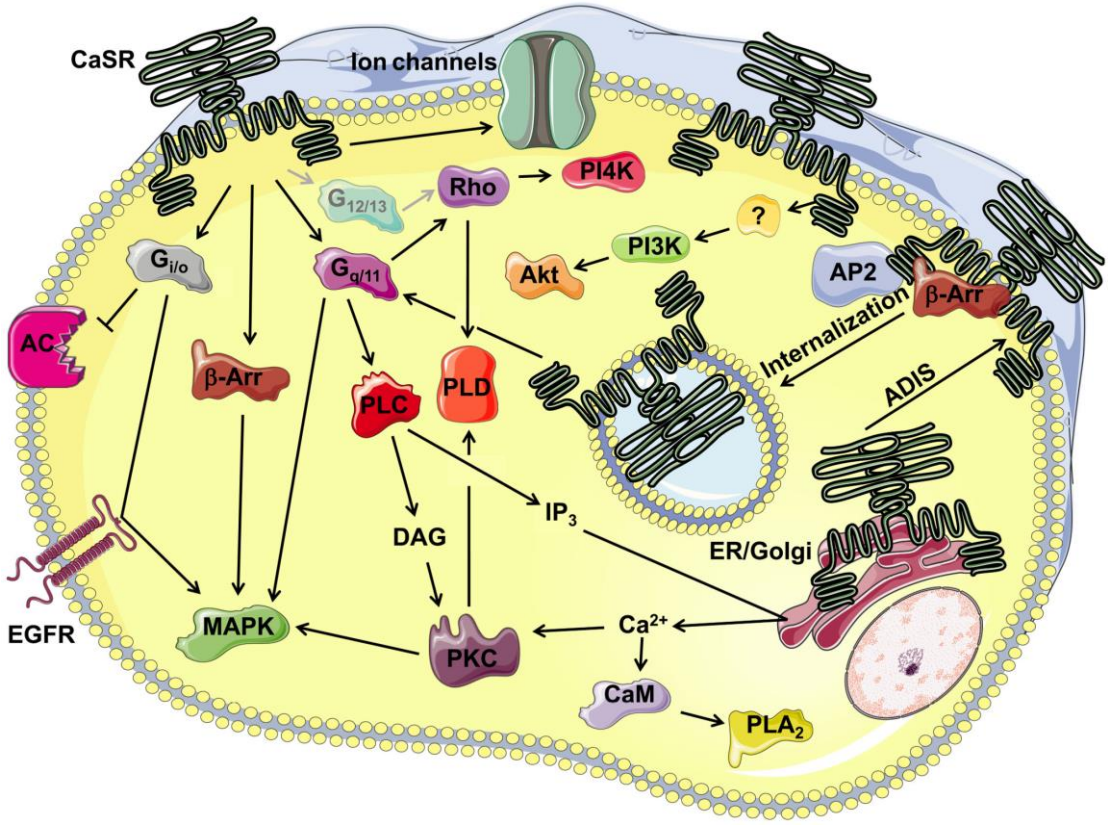

Figure 10. CaSR downstream pathways.

The CaSR activates a variety of signaling pathways. In many cell types, CaSR primarily signals through G-protein alpha subunits Gαq/11, which stimulate phospholipase C (PLC), leading to an increase in intracellular calcium levels and the activation of mitogen-activated protein kinase (MAPK). It also couples with G-protein alpha subunits Gαi/o to inhibit adenylate cyclase (AC), resulting in a reduction in cyclic adenosine monophosphate (cAMP) levels. Additionally, the Gα12/13 pathway involves the activation of Rho GTPases, which regulate cytoskeletal dynamics and cell movement, as well as the activation of

phosphatidylinositol 4-kinase (PI4K), which plays a key role in regulating membrane trafficking and various signaling processes. AC, adenylate cyclase; ADIS, agonist-driven insertional signaling; AP2, adaptor-related protein complex-2; β-Arr, β-Arrestin; CaM, calmodulin; DAG, diacylglycerol; EGFR, epidermal growth factor receptor; ER, endoplasmic reticulum; IP_3, inositol 1,4,5-trisphosphate; MAPK, mitogen-activated protein kinase; PI3K, phosphatidylinositol 3-kinase; PI4K, phosphatidylinositol 4-kinase; PLC, phospholipase C; PLA_2, phospholipase A_2; PLD, phospholipase D; PKC, protein kinase C. Image taken from Leach et al (2020).

1.7.1 CaSR-based therapeutics

Due to its broad expression across various tissues and cells involved in extracellular calcium homeostasis and associated disorders, the development of CaSR-based therapeutics has been widely studied and successfully applied in clinical settings to manage disorders related to mineral ion metabolism, characterized by changes in CaSR expression or function. CaSR-based therapeutics include positive allosteric modulators (“calcimimetics”) (Nemeth et al. 1998) and negative allosteric modulators (“calcilytics”) (Gowen et al. 2000). The positive allosteric modulators of CaSR can restore the function of CaSR and several studies demonstrated the efficacy of calcimimetics in treating secondary hyperparathyroidism in patients receiving hemodialysis during end-stage kidney disease (Antonsen et al. 1998; Goodman et al. 2002; Block et al. 2004; Ohashi et al. 2004). The CaSR agonist, cinacalcet hydrochloride, stimulates the function of CaSR in an allosteric manner and has been approved for many years for the treatment of secondary hyperparathyroidism and hypercalcaemia in patients with parathyroid cancer. Goodman et al (Goodman 2001)and Peacock et al (Peacock et al. 2005) reported cinacalcet hydrochloride also shows efficacy in primary hyperparathyroidism (PHTP), and is recommended by hyperparathyroidism (primary) NICE guideline to be considered for patients with primary hyperparathyroidism whose albumin-adjusted serum calcium level is 2.85 mmol/L or above with symptoms of hypercalcaemia or 3.0 mmol/L or above even without symptoms of hypercalcaemia if surgery has been unsuccessful, is unsuitable or has been declined (Jawaid and Rajesh

2020). The second and third-generation calcimimetics e.g. etelcalcetide, evocalcet have demonstrated efficacy in reducing PTH levels as well as phosphorus and calcium levels within a relatively short time period in several studies (Block et al. 2017; Akizawa et al. 2018; Fukagawa et al. 2018; Jena Patel and Mary Barna Bridgeman 2018; Pereira et al. 2018; Akizawa et al. 2020) and thus received their approval for dialysis patients with secondary hyperparathyroidism recently.

In addition, previous studies showed that CaSR can promote the proliferation and differentiation of osteoblasts (Dvorak et al. 2004; Yamaguchi and Sugimoto 2007) and osteoclast apoptosis (Mentaverri et al. 2006), thus promoteing bone remodelling in bone microenvironments, supporting the CaSR agonist strontium ranelate being used in postmenopausal osteoporotic women (Doublier et al. 2013). Due to their ability to evoke short, sharp changes in plasma PTH, a known bone anabolic stimulus, the negative allosteric modulators of CaSR (CaSR NAMs), also known as calcilytics, have been initially developed as potential novel therapeutic agents for age-related osteoporosis and their clinical utility was being assessed in clinical trials, but their development in treating this condition has been suspended due to lack of efficacy (Gowen et al. 2000; Ward and Riccardi 2012; Nemeth and Goodman 2016) (Figure 11, Table 3). Recently JTT305 (Encaleret) is being repurposed for the treatment of autosomal dominant hypocalcemia type 1 (ADH1) due to activating mutations in the CASR gene. A Phase 2 clinical trial (ClinicalTrials.gov number, NCT04581629) in 13 participants with ADH1 concluded that encaleret restored blood and urine calcium levels, increased mean blood levels of intact PTH, magnesium, and 1,25-dihydroxyvitamin D, decreased phosphorus levels and tubular reabsorption of phosphate, thus restored physiologic mineral homeostasis (Gafni et al. 2023). A Phase 3 study (ClinicalTrials.gov number, NCT05680818) compared Encaleret to standard-of-care in ADH1 subjects is ongoing.

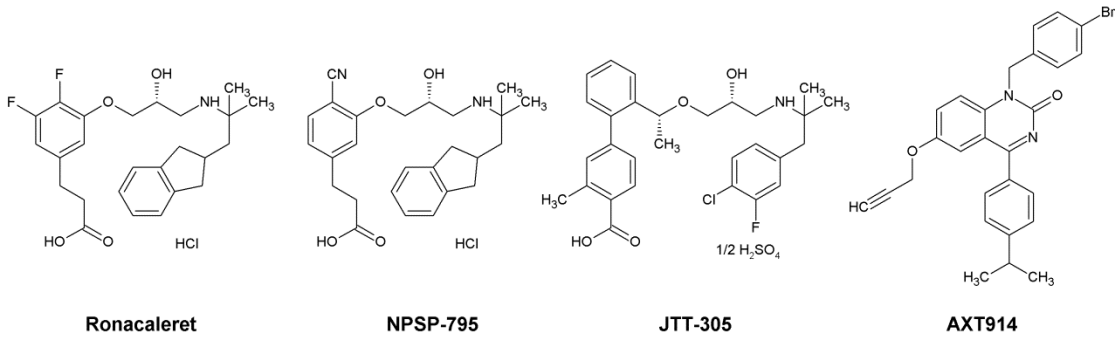

Figure 11. Structures of calcilytics with known human safety and tolerability.

NPSP-795, Ronacaleret, and JTT-305 are amino alcohols that all derived from the same amino-alcohol lead structure SB-222338. Ronacaleret and NPSP-795 were codeveloped by NPS Pharmaceuticals with GlaxoSmithKline, with Ronacaleret derived from a modification of the aromatic substitution group of NPSP-795, with improvement of oral exposure. JTT-305 was codeveloped by Japan Tobacco in collaboration with Merk Sharp& Dohme (MSD), with the introduction of methyl group ortho to the COOH unit improved in vivo potency. Novartis first developed 2 quinazolin-2-one derivatives ATF936 and AXT914 to be tested in clinical trials which are associated with good bioavailability and exposure levels. However, AXT914 was finally selected in future development of a market formulation based on its superior solubility properties in microemulsion preconcentrates. Image taken from Widler (2011).

Table 3. Potential calcilytics to be repurposed as inhaled drugs for asthma which previously developed for systemic use in ADH1 and osteoporosis tested in clinal trials.

Code	MW (g/mol)	Company	Development stage
NPSP-795/SB-423562 (amino-alcohol) NPSP790/ SB-423557 (ester pro-drug) NPSP-795/SHP635 (amino-alcohol)	436.5	NPS/GSK (osteoporosis) NPS (ADH1)	Phase I (Kumar et al. 2010)(n=28; i.v.; 2 study sessions, seven days apart) (n=50; oral; > 2 study sessions, seven days apart) Phase II (Roberts et al. 2019) (n=7; 17 days; i.v.)
Ronacaleret/SB-751689 (amino-alcohol)	447.5	GSK (osteoporosis)	Phase II (Caltabiano et al. 2013) (n=569; 12 months; oral)
JTT-305/MK-5442; Encaleret (amino alcohol)	514	Japan Tobacco/Merck (osteoporosis)	Phase II (Cosman et al. 2016)(n=526; 12 months; oral)
AXT914 (quinazolin-2-one)	487.4	Novartis (osteoporosis)	Phase II (John et al. 2014) (n=105; 4 weeks; oral)
ATF936 (quinazolin-2-one)	482.6	Novartis (osteoporosis)	Phase I (John et al. 2011) (n=14; 7 weeks; oral)

Details of the compound code, molecular weight (MW), developing company as well as the details of the clinical trials, including number of patients, stages

of development, route of administration and duration of the trials. i.v.,intravenous, Adapted from Yarova et al. (2021).

1.7.2 The role of CaSR in asthma pathogenesis

Since the CaSR can be activated by various polycations and polycation precursors known to be released by inflammatory cells, including those involved in the inflammatory infiltration of the airways in asthma (Kurosawa et al. 1992; Maarsingh et al. 2008), previously we demonstrated for the first time that the CaSR can be activated by substances produced by neutrophils and eosinophils, such as arginine metabolites, spermine, spermidine, and the eosinophil-derived cationic proteins (Yarova et al. 2015). Also, our laboratory has previously demonstrated that the CaSR is present in human and mouse airway epithelium, smooth muscle and inflammatory cells involved in the development of inflammation of the airways in asthma such as T lymphocytes, eosinophils, and that its expression increased during asthma (Yarova et al. 2015). In addition, unpublished data from my colleague Mansfield showed that the CaSR is present in monocytes, dendritic cells, macrophages and ILC2 (manuscript in progress). We have also shown that activation of CaSR in the airways drives airway hyperresponsiveness, inflammation and remodelling, which are the major characteristics of asthma (Yarova et al. 2015; Yarova et al. 2021). Using in vivo murine models of asthma, we were also able to show that all of these effects could be prevented by inhaled calcilytic (Yarova et al. 2015). In addition, in a lipopolysaccharide (LPS)-induced COPD-like animal model, a model for steroid-resistant inflammatory lung disease, inhalation of the calcilytic, NPS98636 for nine days commencing after the fifth LPS exposure significantly reduced LPS-induced total leukocyte counts, as well as neutrophil, eosinophil, and lymphocyte infiltration into airways and interstitial wall thickening of LPS-treated animals (Yarova et al. 2016).

1.8 Hypothesis

Based on the previous results published by us and others, i.e., 1) the CaSR is expressed in airways cells, which increases during asthma, 2) the inhaled calcilytic can inhibit steroid-resistant inflammation in LPS-induced COPD-like animal model and 3) IL-33 contributes to the pathogenesis of severe, steroid-

resistant asthma with a predominantly neutrophilic inflammatory profile compared to the eosinophilic inflammation of mild or allergic asthma (Préfontaine et al. 2009; Liew et al. 2010; Lloyd 2010), I hypothesized that the application of inhaled calcilytic is effective in both allergic asthma and IL33-driven asthma. To test this hypothesis, I selected the best available calcilytic inhalators amongst those that have been previously tested in patients for osteoporosis, and then went on to test its effects against the current standard of care, fluticasone propionate, in a Th2/IgE asthma model; subsequently, I went to the laboratory of Prof Ying at CMU to set up two parallel models of OVA and IL-33-induced asthma to compare the efficacy of inhaled calcilytic in these two models.

1.9 Thesis aims and objectives

The overall aims of my thesis are as follows:

1) To select the best available calcilytic suitable for inhalation;
2) To test inhaled calcilytic against current standard-of-care (SoC);
3) To test efficacy in both OVA- and IL-33-induced asthma models.

Chapter II Methods

2.1 Materials and Equipment

The following list is a summary table of reagents, equipment, software and their manufacturers I used during my PhD studies.

REAGENT	MANUFACTURER
Congo red stain	Beijing Solarbio Technology Co Ltd, Beijing, China
Red Blood Cell Lysis Buffer	Beijing Solarbio Technology Co Ltd, Beijing, China
Haematoxylin Solution, Harris Modified	Sigma-Aldrich, Missouri, United States
Eosin1	Sigma-Aldrich, Missouri, United States
Hematoxylin2	Zhongshan Golden Bridge Biotechnology Co., Ltd, Beijing, China
Eosin2	Zhongshan Golden Bridge Biotechnology Co., Ltd, Beijing, China
Masson stain	Nanjing Mindit Biochemistry Co Ltd, Nanjing, China
AB-PAS stain	Beijing Yi Li Fine Chemistry Co Ltd, Beijing, China
Paraffin with low melting point	Beijing Chemical Reagent Co., Ltd, Beijing, China
Paraffin with high melting point	Beijing Chemical Reagent Co., Ltd, Beijing, China
Ethanol	Beijing Chemical Co., Ltd, Beijing, China
Paraformaldehyde	Beijing Chemical Reagent Co., Ltd, Beijing, China

Pentobarbital sodium	Sigma-Aldrich, Missouri, United States
Ovalbumin (Experiment in China)	Sigma-Aldrich, Missouri, United States
Aluminium hydroxide	Sigma-Aldrich, Missouri, United States
Methacholine	Sigma-Aldrich, Missouri, United States
Mouse IL-33 Recombinant Protein	R&D Systems, Minneapolis MN, USA
Mouse IL-5 ELISA kit	Invitrogen, Carlsbad, CA, USA
Mouse IL-13 ELISA kit	Invitrogen, Carlsbad, CA, USA
Mouse IL-6 ELISA kit	Invitrogen, Carlsbad, CA, USA
Mouse TNF-α ELISA kit	Invitrogen, Carlsbad, CA, USA
Gibco™ PBS, pH 7.4, 500 mL	Thermo Fisher Scientific, Paisley, UK
Phosphate Buffer, PBS	HyClone Laboratories, logan, UT, USA
NaH_2PO_4	Sinopharm Chemical Reagent Co., Ltd, Beijing, China
Na_2HPO_4	Sinopharm Chemical Reagent Co., Ltd, Beijing, China
Citrate	Zhongshan Golden Bridge Biotechnology Co., Ltd, Beijing, China
Tris	Ameresco, Framingham, Massachusetts, USA
Triton X-100	Beijing Solarbio Technology Co Ltd, Beijing, China
Neutral Balsam	Zhongshan Golden Bridge Biotechnology Co., Ltd, Beijing, China

Dimethylbenzene	Sinopharm Chemical Reagent Co., Ltd, Beijing, China
Protease inhibitor cocktail	Roche Diagnostics GmbH, Mannheim, Germany
Glycine	Sigma-Aldrich, Beijing, China
NaOH	Sinopharm Chemical Reagent Co., Ltd, Beijing, China
NaCl	Sinopharm Chemical Reagent Co., Ltd, Beijing, China
Methacholine 1	Sigma, Poole, UK
Methacholine 2	Sigma-Aldrich, Beijing, China
Fluticasone propionate	Sigma, Poole, UK
Leishman's solution	Fisher Scientific UK, Loughborough, UK
NPS 2143 hydrochloride	Sigma, Poole, UK
0.9% Sodium chloride solution	Sigma, Poole, UK
TWEEN 80	Sigma, Poole, UK
Ovalbumin	VWR International, Leicestershire, UK

EQUIPMENT	**MANUFACTURER**
Capillary Blood Collection Tube	Fisher Scientific UK, Loughborough, UK
Polypropylene 100 Place Slide Box	Fisher Scientific UK, Loughborough, UK
Fiberboard Storage Boxes	Thermo Fisher Scientific, Paisley, UK
Adventurer balance	Ohaus, New Jersey, United States
Bright Line Counting Chamber	CellPath, Powys, United Kingdom

Micropipette	Eppendorf AG, Hamburg, Germany
Multipette	Eppendorf AG, Hamburg, Germany
Freezer	Thermo Fisher Scientific, Waltham, MA, USA
HYC-360 Fridge	Qingdao Haier Company Limited, Qingdao, China
Forma 700 Series Ultra Low Temperature Upright Freezer	Thermo Fisher Scientific, Waltham, MA, USA
MDF-U50V Fridge	SANYO, Osaka, Japan
Clean Bench	Tianjin Taisite Instrument Co., Ltd, Tianjin, China
1300 SERIES A2 Biosecurity cabinet	Thermo Fisher Scientific, Waltham, MA, USA
Inverted Microscope	Nikon, Tokyo, Japan
Optical microscope	Nikon, Tokyo, Japan
FlexiVent small animal ventilator system	Scireq Inc., Montreal, Canada
EnSpire Multimode Plate Reader	Perkin Elmer, Waltham, MA, USA
3K-15 Centrifuge	Sigma-Aldrich, Beijing, China
MicroCL21 mini Microcentrifuge	Thermo Fisher Scientific, Waltham, MA, USA
MicroCL17R mini Microcentrifuge	Thermo Fisher Scientific, Waltham, MA, USA
Spectrafuge Mini Microcentrifuge	Labnet International, Edison, New Jersey, USA
C3i Centrifuge	Thermo Fisher Scientific, Waltham, MA, USA
CL31R Centrifuge	Thermo Fisher Scientific, Waltham, MA, USA
1-16K Centrifuge	Sigma-Aldrich, Beijing, China

C2500-230 Microcentrifuge	Labnet International, Edison, New Jersey, USA
Centrifuge 5810 R Centrifuge	Eppendorf AG, Hamburg, Germany
ALLEGRA X-15R Centrifuge	Beckman Coulter,Inc., Brea, CA, USA
Millli-Q water-purification system	Millipore, Billerica, Massachusetts, USA
4 ℃ Constant temperature medicine cabinet	Panasonic, Osaka, Japan
LEICA TP1020 tissue processor	Leica, Wetzlar, Germany
LEICA EG 1150 H/C Tissue Embedding System	Leica, Wetzlar, Germany
Fully Automated IHC and ISH Staining System	Leica, Wetzlar, Germany
LEICA RM 2255 Fully Automated Rotary Microtome	Leica, Wetzlar, Germany
HI1210 Water bath for paraffin sections	Leica, Wetzlar, Germany
HI1220 Flattening table for clinical histopathology	Leica, Wetzlar, Germany
HW.SY11-KP1 Intelligent constant temperature water bath	Beijing Changfeng Instrument Company, Beijing, China
VORTEX-GENIE 2	Scientific Industries, Inc., New York, USA
TL2010S High-throughput tissue grinder	DHS Life Science & Technology Co., Ltd, Beijing, China
TC20 Automated Cell Counter	Bio-Rad Laboratories Co., Ltd, Hercules, California, USA
Ice-making Machine	SANYO, Osaka, Japan
HI4221 pH meter	Hanna Instruments, Limena, Italy
SH-5 Heating magnetic stirrer	Beijing Jinbeide Industry and Trade

	Co., Ltd, Beijing, China
ESJ120-4 Electronic balance	Longteng Electronic Co.Ltd, Shenyang, China
WD-9405B Shaker	Beijing Liuyi Instrument Factory, Beijing, China
S2020-P4-B Digital Microtube and Microplate Shaker	Labnet International, Edison, New Jersey, USA
S2025-XL-B-230V Shaker	Labnet International, Edison, New Jersey, USA
Unimax 1010 DT Shaker	Heidolph Instruments GmbH & Co. KG Schwabach, Germany
4344 Thermo Shaker	Thermo Fisher Scientific, Waltham, MA, USA
Handheld tissue homogenizer	Sigma-Aldrich, Beijing, China
Whole-body plethysmography (WBP)	Buxco Research Systems, DSI, St Paul, MN, USA

SOFTWARE	**COMPANY**
GraphPad Prism 8	GraphPad Software, San Diego, CA, USA
Microsoft Excel 2010	Microsoft Corporation, Redmond, Wash, USA
TissueFAXS	TissueGnostics, Vienna, Austria

2.2 Methods

A general principle of the methodological approaches used throughout my PhD study is described below, while the detailed methods for each experiment can be found in the corresponding chapter.

2.2.1 Ex Vivo experiments:

Determining efficacy and safety of calcilytics in the airways: Measurements of airway tension in mouse trachea using wire myography (WM).

In order to be safe and suitable for inhaled delivery, first of all, I needed to determine whether calcilytics might evoke airway contraction under experimental conditions mimicking physiological conditions. Therefore, I used WM to test the airway tension induced by bronchoconstrictor acetylcholine (ACh) before and after treatment with calcilytics to rule out if calcilytics can induce airway contraction, and also to see if calcilytics have any preventive or therapeutic effect on the trachea contraction, in the presence of medium containing physiological $[Ca^{2+}]_o$ (i.e., 1 mM).

2.2.1.1 Wire Myography

Wire myography (WM) is widely used in the field of vascular biology and pharmacology to measure the contractile and relaxation properties of blood vessels. This technique allows researchers to investigate the physiological and pathophysiological mechanisms regulating vascular tone and reactivity (Spiers and Padmanabhan 2005). In addition to vascular biology, it is also utilized in respiratory research to assess airway tension and responsiveness in isolated segments of airway smooth muscle. By measuring the contractile force generated by airway smooth muscle in response to stimuli, researchers can gain insights into the pathogenesis of airway diseases such as asthma and COPD. The image of the wire myograph system and a brief overview of the measurement flowchart can be found in the below Figure 12. Briefly, tracheae were isolated from normal male BALB/c mice (5 weeks) and mounted on the chamber; tracheae tensions induced by ACh were measured via the steel wire across the tracheae. Tracheae were placed in ice-cold Krebs buffer, a physiological buffer solution used to maintain the pH, osmolarity, and ion concentration of tissues (Krebs and Henseleit 1932),

bubbled with 5%CO_2/ 95%O_2 throughout the whole experiment. A diagram demonstrating the steps of mounting the trachea and wiring the jaws can be found in Figure 13.

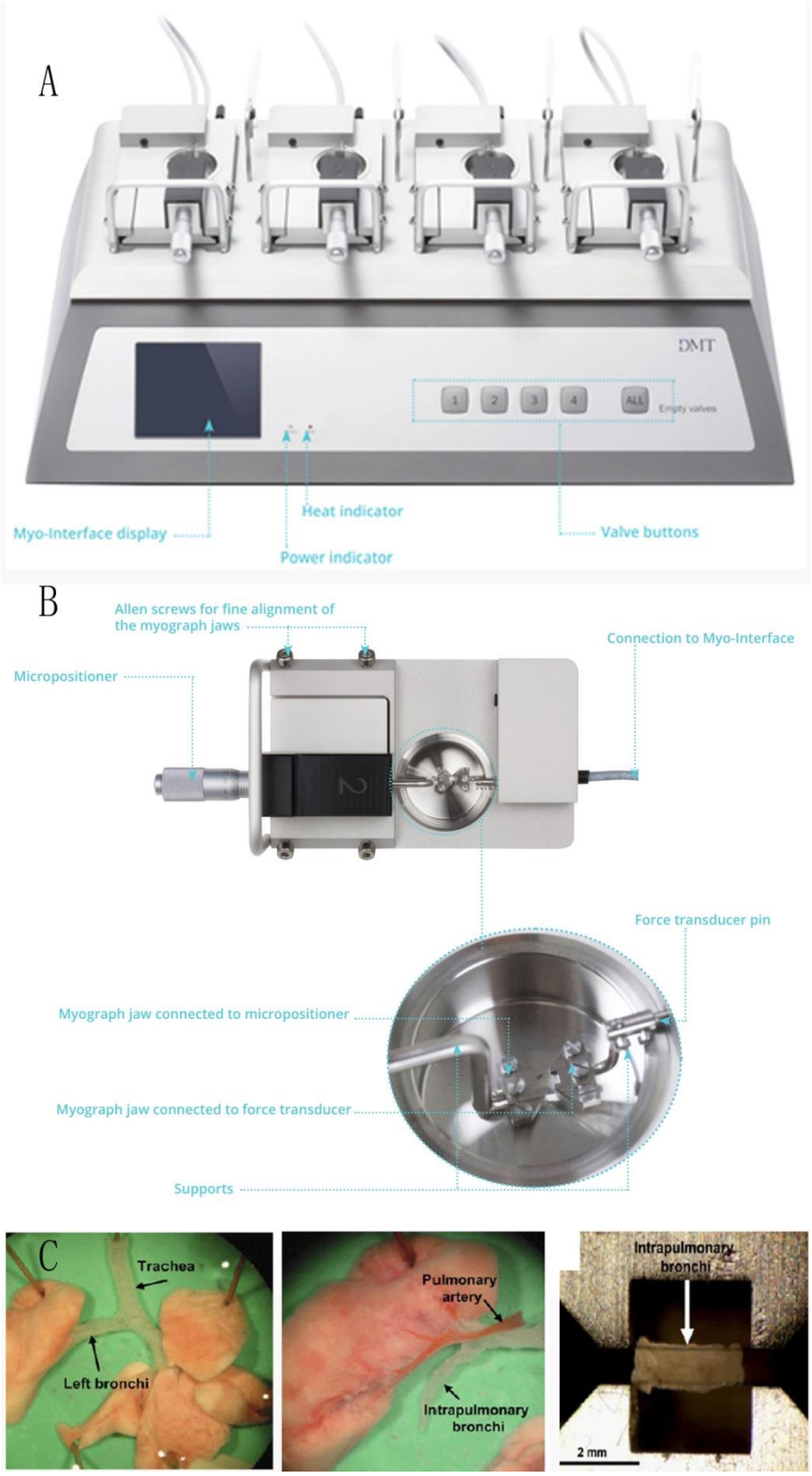

Figure 12 Multi-Wire Myograph System

A. Interface Front Panel of Multi Wire Myograph System; B. Multi Wire Myograph Unit; C. Schematic Diagram of Measurements of Airway Tension in

Mouse Trachea. For the measurements of airway tension in mouse trachea, tracheae were isolated first from animals and carefully dissected under a microscope to ensure they are intact and free of surrounding connective tissue and blood vessels and cut into small segments to suit the size of the myograph jaw. Then, tracheae were mounted using steel wire (40 µm in diameter). Each piece of the trachea was gradually stretched in a stepwise manner until a passive isometric tension of about 5 mN was achieved. After that, the tension of the trachea will be measured after the addition of acetylcholine (ACh) before and after treatment with calcilytics. The Images of the Wire Myograph System are adapted from: https://www.dmt.dk/guides.html.

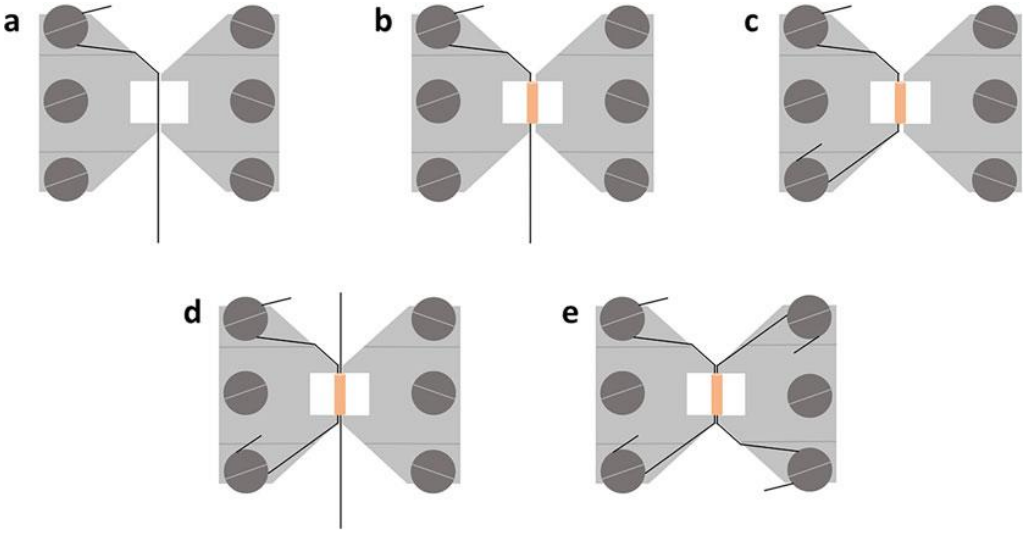

Figure 13. Mounting trachea and wire.

Step-by-step diagram to demonstrate how to mount the trachea and wire the jaws (a-e). The orange rectangle represents the trachea. Images adapted from Griffiths and Madhani (2022).

2.2.1.1.1 Prophylactic experiments.

I first conducted the prophylactic experiments to rule out whether calcilytics can induce airway contraction, and to see whether calcilytics have any preventive effects on trachea contraction (Figure 14A). A concentration-response curve to increasing concentrations of ACh (1 nM - 3 µM) was constructed before the addition of vehicle (dimethyl sulfoxide (DMSO), 0.001% w/v) or the four calcilytics (NPSP-795, Ronacaleret, JTT-305 and AXT 914, 100 nM) or the positive control calcilytics, NPS 2143 (100 nM) and

NPS89636 (300 nM) to serve as the baseline. Another concentration-response curve to ACh was constructed after the addition of the vehicle or the above compounds. Each data point was normalized to the percentage of contraction relative to the maximum contraction evoked by Ach.

2.2.1.1.2 Therapeutic experiments.

Therapeutic experiments were also carried out on mouse tracheae half-maximally contracted with Ach to investigate the therapeutic effects of calcilytics on the existing trachea contraction (Figure 14B). A concentration-response curve to increasing concentrations of ACh (1 nM - 3 μM) was constructed to generate the maximum contraction level. 20 nM Ach was selected as the half-maximum contraction level and added first to evoke a stable trachea contraction before increasing concentrations of calcilytics (1 nM - 30 μM) or DMSO (vehicle) were added. Each data point was normalized to the percentage of contraction relative to the contraction evoked by the 20 nM ACh before the treatment, and concentration-response curves for each calcilytic were generated.

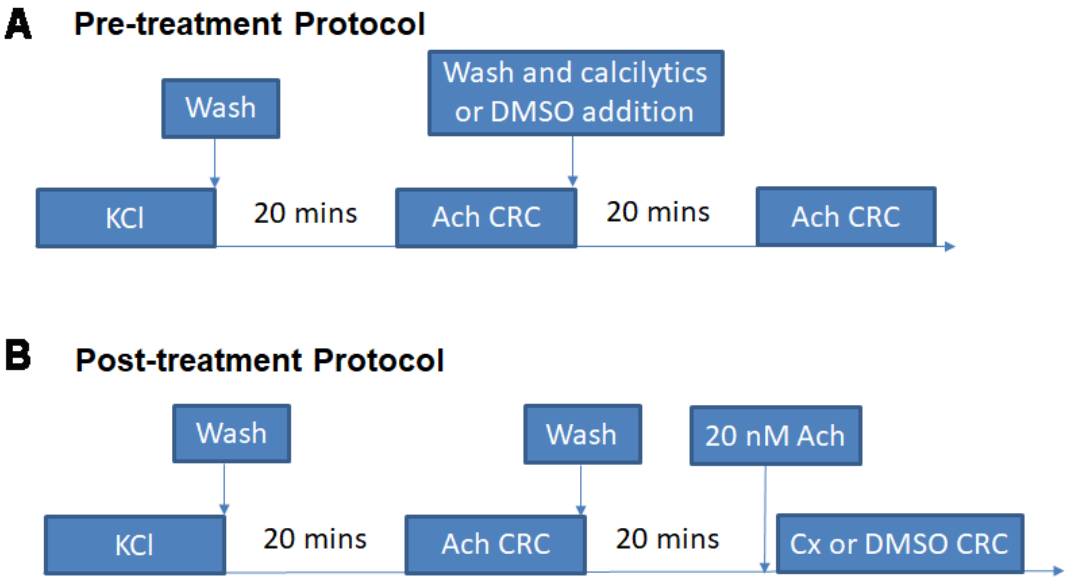

Figure 14. Prophylactic (A, pre-treatment) and therapeutic (B, post-treatment) Protocol in Wire Myography experiments.

Tracheae were first examined for viability using high concentrations of KCl (40 mM and 80 mM). For the prophylactic experiments, tracheal contraction was evoked by increasing concentrations of ACh (1 nM - 3 µM) to serve as the baseline after 3 washes with Krebs' buffer (1 min each) and left to equilibrate for 20 min. After tracheae were treated with DMSO (vehicle control, 0.001%) or different types of calcilytics (NPSP-795, Ronacaleret, JTT-305 and AXT 914, 100 nM) or with the positive control calcilytics that we previously used, NPS 2143 (100 nM) and NPS89636 (300 nM), tracheal contraction was evoked again by increasing concentrations of ACh. For the therapeutic experiments, tracheae were pre-contracted with 20 nM ACh (sufficient to generate approximately 50% of the maximal contraction to ACh) to serve as baseline levels. After contraction stabilized, increasing concentrations of the different calcilytics (1 nM - 30 µM) or DMSO (corresponding concentrations relative to the concentrations of calcilytics) were added to measure the contraction and then to calculate the percentage of contraction relative to the baseline. KCl = potassium chloride; ACh = acetylcholine; CRC = concentration-response curve; DMSO = Dimethyl Sulphoxide.

For all prophylactic and therapeutic experiments, tracheae were all first checked for viability as demonstrated by their contraction to 40 mM and 80 mM KCl. For each experiment, at least 5 replicate measurements were carried out.

2.2.2 In vivo experiments to compare the effects of inhaled calcilytic against the current standard-of-care, fluticasone propionate (FP).

NPSP-795 was selected for further investigation in the in vivo experiments since it showed good efficacies in both prophylactic and therapeutic experiments. After the wire myography experiments, I conducted a head-to-head comparison of inhaled calcilytic with FP, the recommended first-line asthma treatment (Chipps et al. 2020).

2.2.2.1 Animals

These studies were carried out in the UK and conformed to the regulations of the Animals (Scientific Procedures) Act 1986, under valid Home Office project licence (PPL 30/3032) and personal licence (PIL IE/0EE40CD). Five-week old BALB/c male/female mice (20-25g) were purchased from Charles River and housed at Cardiff University. They were housed under a constant temperature of 20°C±2°C and twelve hours light/dark cycle, with room humidity maintained at 50%. The cages were enriched with plastic pipes and wood strips, with food and water given ad libitum. All animals were housed for 2 weeks before any procedures were conducted for environmental accommodation.

2.2.2.2 Acute asthma model

This part of work was conducted by my colleague Polina L. Yarova in parallel with my wire myography experiments, so she used the control calcilytic, NPS89636 that she used in her previous experiments. Animals were sensitized with ovalbumin (OVA, VWR International Ltd) from chicken eggs according to the following protocol: mice were sensitized through intraperitoneal (i.p.) injection of 250 µL 0.2 mg/mL OVA (50 µg /mouse) and 10% (50 mg/mouse) aluminium hydroxide in phosphate buffered solution (PBS) on days 0 and 5, respectively. Fourteen days after the last injection, mice were challenged by inhalation of a 0.5% OVA aerosol for one hour, twice daily, 4 hours apart (Figure 15). NPS89636 (3 µM, dissolved in 0.3% DMSO in

PBS), FP (0.5 mg/day, dissolved in 25% DMSO, 50% EtOH in PBS), or respective vehicles treatment was performed at 1 hour prior to the first OVA challenge and 4 hours post the last OVA challenge. AHR data were taken 24 hours after the last OVA inhalation challenge.

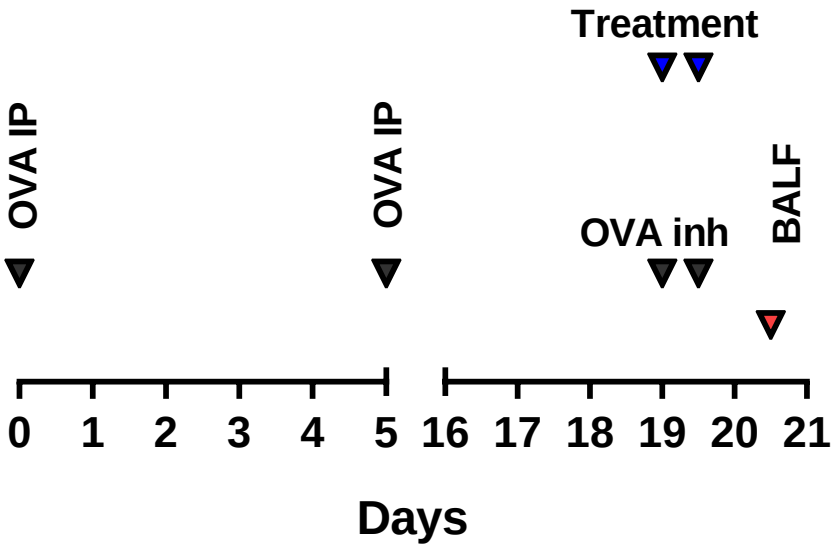

Figure 15. Protocol for shorter-term (prophylactic) OVA-induced murine model of allergic asthma.

BALB/c male mice (5 weeks) were sensitized on days 0 and 5 by i.p. injection. Fourteen days after the last injection, mice were challenged by 2 inhalations of OVA, 4 h apart. Calcilytic, FP or respective vehicle treatments were given at 1 hour prior to the first OVA challenge and 4 hours post the last OVA challenge. Bronchoalveolar lavage fluid (BALF) samples were collected after 24 hours. N = 4-6 animals per experimental group. i.p. injection: 250 ul 0.2 mg/mL OVA (50 µg /mouse) + 10% (50 mg/mouse) aluminium hydroxide in phosphate buffered solution (PBS). Inhalation: 20 mL 5 mg/mL OVA aerosol for one hour. Treatment: Calcilytic: 3 µM, dissolved in 0.3% DMSO in PBS, 10 mL, FP: 0.5 mg/day, dissolved in 25% DMSO, 50% EtOH in PBS, 10 mL.

2.2.2.3 Longer-term asthma model

Animals were sensitized on days 0 and 10 by i.p. injection of 250 µL 0.2 mg/mL OVA (50 µg /mouse) and 10% (50 mg/mouse) aluminium hydroxide in PBS. After the sensitization, mice were challenged by inhalation of a 0.5% OVA aerosol for one hour from day 21, and the OVA challenges continued

every other day for 11 days (Figure 16). From day 26, twice daily calcilytic (6 μM NPSP-795), the current standard-of-care fluticasone propionate FP (0.5 mg/day) or vehicle (0.3% dimethyl sulfoxide (DMSO) +0.01% Tween-80) treatments were performed at 1 hour prior to the OVA challenge and 8 hours after the previous one. Airway hyperresponsiveness data were taken 24 hours after the last OVA inhalation challenge.

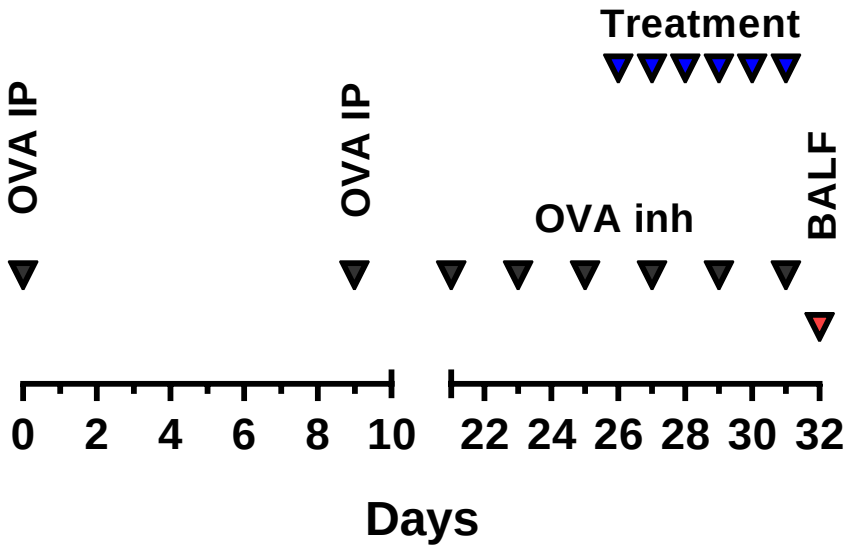

Figure 16. Protocol for longer-term therapeutic OVA-induced murine model of allergic asthma.

BALB/c male mice (5 weeks) were sensitized on days 0 and 10 by i.p. injection. After the sensitization, mice were challenged by inhalation of a 0.5% OVA aerosol for one hour from day 21, and the OVA challenges continued every other day for 11 days. From day 26, twice daily calcilytic, FP or respective vehicle treatments were given 1 hour prior to the OVA challenge and 8 hours after the previous one. Bronchoalveolar lavage fluid (BALF) and airway hyperresponsiveness (AHR) data were collected at the end of experiment. N = 4-6 animals per experimental group. i.p. injection: 250 μL 0.2 mg/mL OVA (50 μg /mouse) + 10% (50 mg/mouse) aluminium hydroxide in PBS. Treatment: Calcilytic: 6 μM NPSP-795, 10 ml, 30 min, FP:0.5 mg/day, 10 ml, 30 min, vehicle: 0.3% dimethyl sulfoxide (DMSO) +0.01% Tween-80.

2.2.2.4 Measuring lung function by non-invasive technique, whole-body plethysmography

Throughout all studies conducted at Cardiff University, a non-invasive method, whole-body plethysmography (WBP) (Buxco Research Systems, DSI, St Paul, MN, USA), was employed to measure the lung function of all animals. Whole-body plethysmography is a technique used to measure respiratory function in laboratory animals without anesthesia or restraint. Whole-body plethysmography can be conducted in unrestrained, conscious mice, and the mice are allowed to move freely around the airtight chamber which can minimize the stress on the animal and the effects of traumatic tracheotomy and anesthesia, improve animal welfare and produce results at the physiological conditions. It involves placing the animal in a sealed chamber and measuring changes in chamber pressure resulting from breathing movements. A sensitive pressure transducer is connected to the chamber to measure pressure changes inside the chamber (Hamelmann et al. 1997). Before the measurements, animals were trained twice in the chamber, allowing them to acclimatize to the environment in the chamber to minimize the effects of measurement variability.

Enhanced pause (Penh) is a dimensionless parameter related to airway resistance (Lomask 2006) derived from whole-body plethysmography measurements in rodents. It is commonly used as an index of airway obstruction or bronchoconstriction in experimental studies involving small animals, particularly mice and rats. The concept of Penh was introduced by Hamelmann et al. in 1997 as a non-invasive method to assess airway responsiveness and bronchoconstriction in allergic mice (Hamelmann et al. 1997). Penh is calculated based on changes in pressure within a sealed chamber as the animal breathes. Higher Penh values indicate increased airway resistance and bronchoconstriction, while lower values suggest reduced airway resistance and improved lung function. Although the physiological data provided by a Penh-based approach differ from those using the forced oscillation technique of the FlexiVent system, the non-invasive approach allowed for longitudinal measurements of baseline and chronic drug effects in the same animals. Also, previous studies have shown that Penh is a good indication of airway obstruction (Hamelmann et al. 1997; Yarova et al.

2015). A schematic diagram of the whole-body plethysmography system is shown in Figure 17.

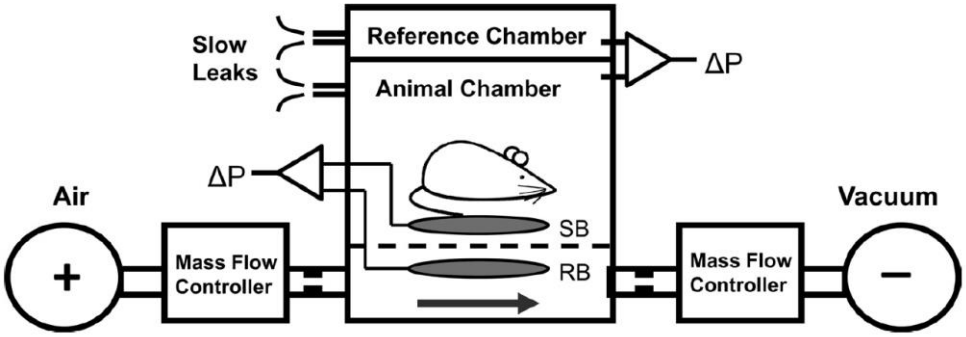

Figure 17. Schematic diagram of the whole-body plethysmograph.

For the whole-body plethysmography system, mice can freely move in the chamber while Penh is being measured, which can reduce environmental and irritant effects on animals. Positive and negative pressure sources are connected in tandem with mass flow controllers and high-resistance elements to establish a consistent bias flow through the animal chamber. A reference chamber is utilized to eliminate background noise from the pressure signal. Both chambers slowly leak to equalize pressure with the atmospheric pressure. The sensor bladder (SB) detected the mechanical pressure fluctuations changes caused by mouse breathing, while the reference bladder (RB) signal facilitates the elimination of unwanted chamber pressure interference through the use of a differential pressure transducer. +, Pressurized air source; -, vacuum source; narrowed tubes, high resistance elements; →, bias flow; -----, platform; ΔP, differential pressure transducer. Image taken from Hernandez et al. (2012)**.**

2.2.2.5 Blood collection

Following the measurement of non-invasive lung function, animals were killed by intraperitoneal injection of overdose sodium pentobarbital (Euthatal, 400 mg/kg body weight). Blood samples were collected via cardiac puncture and stored at 4 ℃ overnight. Serum was obtained next day by centrifugation at 2,000 g for 5 minutes and stored at -80 ℃ for further analysis.

2.2.2.6 Bronchoalveolar lavage fluid (BALF) collection and analysis

To quantify the degree of inflammatory cell infiltration, I collected bronchoalveolar lavage fluid (BALF) using PBS to lavage the lung and then counted the number of cells infiltrated in the BALF as a measurement of inflammatory cell infiltration in the lung. After blood collection, BALF was collected via a tube inserted into the small incision in mice trachea using 3 washes of 1 mL PBS to rinse the lung (this yields at least 2.5 mL of BALF + PBS). The BALF was centrifuged at 1500 rpm at 4℃ for 15 minutes to collect the supernatant. Cell pellets were resuspended in 0.3 mL PBS and the number of total cells was counted using a hemocytometer (CellPath, Powys, United Kingdom) at x20 magnification.

2.2.2.7 BALF differential cell counts with Leishman's staining protocol

Cytospin slides were prepared using 100 µL BALF under centrifugation for 7 minutes at 110 G using a Shandon Cytospin (ThermoFisher Scientific, Hemel Hempstead, UK). The slides were subsequently air dried and then stained with 0.15% Leishman's solution (Fisher Scientific UK, Loughborough, UK) in 100% methanol for 6 minutes and washed twice in dd$H_2$0. Once slides were dried overnight, at least 300 cells were counted under a light microscope at x100 magnification to count the different types of inflammatory cells that typically present in asthma, including eosinophils, neutrophils, lymphocytes and macrophages (Gude et al., 1982).Macrophages are the most common and largest cells in BALF in normal mice, they can be easily found under Leishman's staining because of their larger size. Eosinophils are very common in the OVA-induced animals which are smaller than macrophages, measuring 10-14 µm in diameter and showing red/brown stained granules in the cytoplasm under Leishman's staining. Lymphocytes are mononuclear cells whose diameter can vary depending on their activation, and that can be divided into small (6-8 µm), medium (8-10 µm) and large (10 µm or more), of which the small lymphocytes are most common and show a dark blue large spherical nucleus and a small light blue cytoplasm in the Leishman's staining. Neutrophils are the rarest cells in BALF, with morphology and diameter (9-12 µm) similar to eosinophils and without red/brown stained granules in the cytoplasm compared to eosinophils, instead showing light purple-stained

granules (Figure 18). The different types of inflammatory cells for Leishman's staining were calculated as the percentage in 300 total cells and then multiplied by the total cell counts, which was determined as described above.

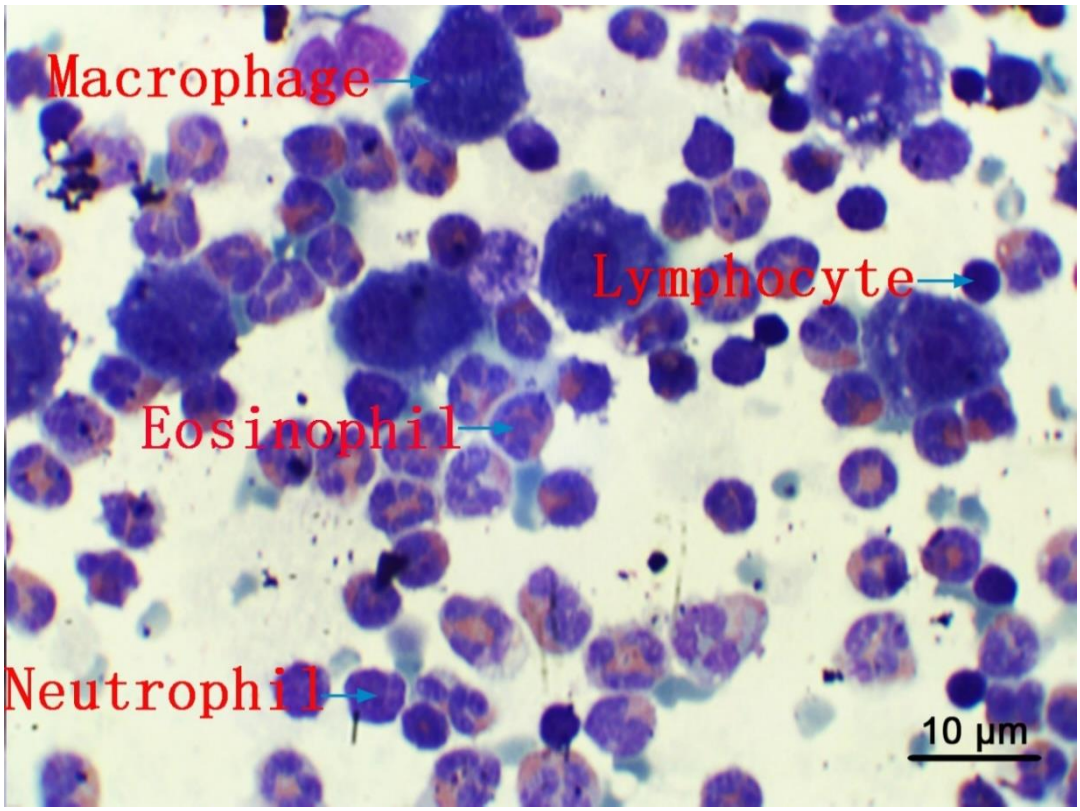

Figure 18. Photograph of the four subtypes of leukocytes, eosinophils, neutrophils, lymphocytes and macrophages stained with Leishman's staining.

The largest mononuclear cells are macrophages. The medium-sized cells full of red/brown stained granules in the cytoplasm are eosinophils. Another type of medium-size cell which is a little smaller than eosinophil without red/brown stained granules instead of light purple stained granules in the cytoplasm are neutrophils. The smallest cells with dark blue large spherical nucleus and small light blue cytoplasm are lymphocytes(Gude et al. 1982).

2.2.3 Development of parallel therapeutic models of allergic and alarmin-driven asthma

Allergic asthma and alarmin-driven asthma represent distinct mechanisms of airway inflammation. Allergic asthma is primarily triggered by exposure to allergens, including pollen, dust mites, animal dander, and certain foods, while alarmin-driven asthma is triggered by the release of alarmins (such as TSLP,

IL-25, and IL-33), which are released by damaged or stressed cells in response to various insults such as respiratory viruses, pollutants, or tissue injury. Allergic asthma primarily involves an adaptive immune response mediated by IgE antibodies, while alarmin-driven asthma primarily involves an innate immune response mediated by ILC2s, which in turn promote IgE-independent type 2 inflammation.

Once I had identified the best calcilytic based on my airway contractility I went on to determine the therapeutic effects of one of the four clinically tested calcilytics, NPSP-795, delivered by inhalation, in murine asthma models of T2 vs non-T2 asthma. To this end, I visited Prof. Sun Ying's laboratory. These studies were carried out in China, in the laboratory of Capital Medical University (CCMU), which also allowed me to conduct invasive lung function measurements using the FlexiVent small animal ventilator system (Scireq Inc., Montreal, Canada).

2.2.3.1 Animals

In this part of the work, I used female BALB/c mice (6-8-weeks). All mice were obtained from Vital River Laboratories (Beijing, China) and housed in the pathogen-free mouse facility, with environmental enrichment and ad libitum access to food and water.

2.2.3.2 Th2/IgE- and alarmin-driven asthma models

Female BALB/c mice (6-8 weeks, around 20 g body weight) were randomly assigned to each experimental group. Animals in the Th2/IgE-driven asthma model were first sensitized with two IP injections of OVA (Sigma-Aldrich, Missouri, United States, 100 µg emulsified in $AL[OH]_3$/dose) or saline on day-17 and day-5, and then for both models, animals were intranasally given OVA (50 µg/mouse) or saline and IL-33 (Mouse IL-33 Recombinant Protein, R&D Systems, Minneapolis MN, USA, 30 ng in 50 µL saline) or saline for 6 days. From the second day, NPSP-795 (200 µg/mouse in 50 µL vehicle) or vehicle (0.6% DMSO in saline) were given twice daily, 2h before OVA/ IL-33 administration (Figure 19 and Figure 20).

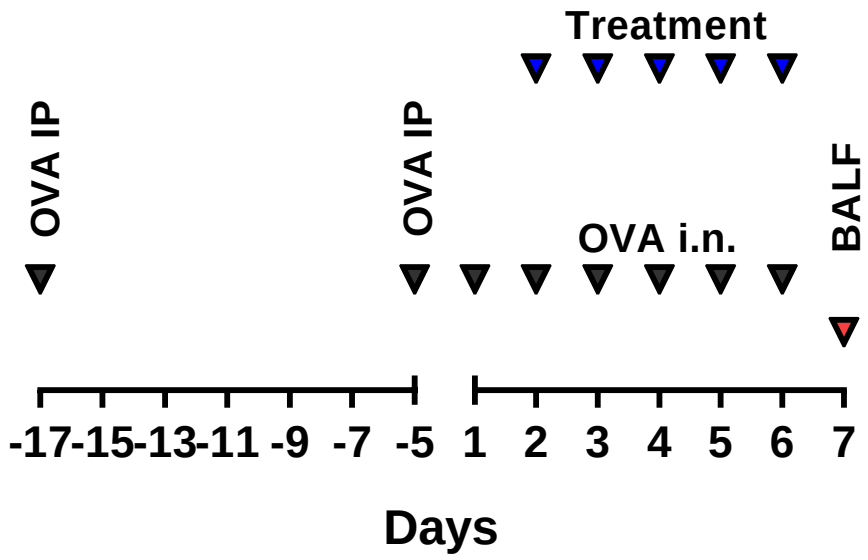

Figure 19. Protocol for OVA-induced murine model of asthma

Treatments: Female BALB/c mice (6-8 weeks) were sensitized by i.p. injection of 100 µg OVA (OVA group and OVA + NPSP-795 group) or saline (Vehicle group) in $Al(OH)_3$ in 200 µL on days -17 and -5. After sensitisation, animals were intranasally given OVA (50 µg/mouse in 50 µL saline, OVA group and OVA + NPSP-795 group) or saline (Vehicle group) from day 1 to day 6 for 6 days. From day 2, NPSP-795 (200 µg/mouse in 50 µL vehicle, OVA + NPSP-795 group) or vehicle (0.6% DMSO in saline, OVA group and Vehicle group) were given twice daily, with the evening dosing given 2h before OVA administration. N = 6-7 animals per experimental group.

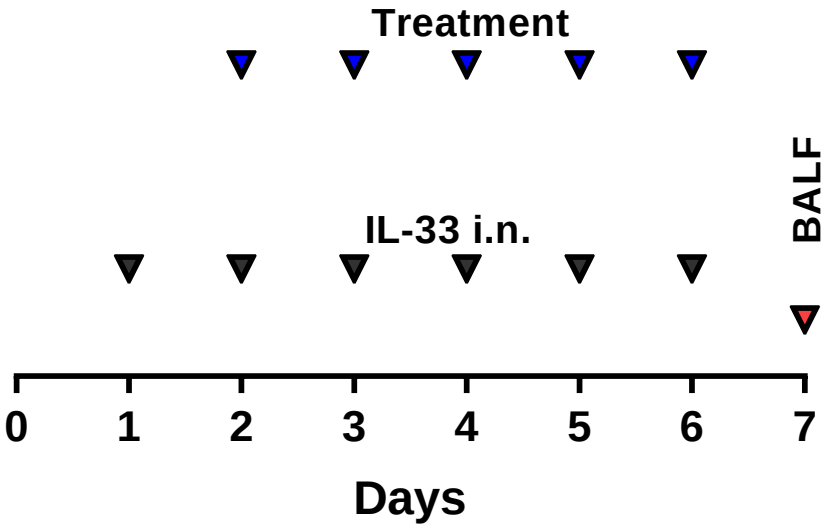

Figure 20. Protocol for alarmin (IL-33)-induced murine model of asthma. Treatments: Female BALB/c mice (6-8 weeks) were given IL-33 intranasally (30 ng/mouse in 50 µL saline, IL-33 group and IL-33+ NPSP-795 group) or saline (Vehicle group) from day 1 to day 6 for 6 days. From day 2, NPSP-795 (200 µg/mouse in 50 µL vehicle, IL-33 + NPSP-795 group) or vehicle (0.6% DMSO in saline, IL-33 group and Vehicle group) were given twice daily, with the evening dosing given 2h before IL-33 administration. N = 8 animals per experimental group.

2.2.3.3 Invasive lung function measurements by FlexiVent system

For the animal work I conducted in China, I used an invasive method, the FlexiVent system (Scireq Inc., Montreal, QC, Canada), to measure lung function. The FlexiVent system is widely used in small animal respiratory research, such as mice and rats, for assessing lung function and mechanics. The invasive animal lung function measurements measured by the FlexiVent system have very high accuracy, surpassing the non-invasive methods (SCIREQ 2024), though it is not a good choice for longitudinal study comparisons since animals undergo terminal anaesthesia for these experiments (Ahookhosh et al. 2023). Briefly, mouse lung function was measured in response to increased concentrations of methacholine (MCh, 0, 6, 12, 24 and 48 mg/ml) for animals treated with or without inhaled calcilytic (NPSP-795). A schematic diagram of the FlexiVent system is shown in Figure

21. The key respiratory function parameters related to asthma measured by FlexiVent, and their indications, are as below:

- Respiratory Resistance (Rrs): Rrs measures the overall resistance to airflow within the respiratory system, including central and peripheral airways. Increased Rrs indicates airway obstruction, bronchoconstriction, or changes in airway caliber. Monitoring Rrs helps assess the degree of airway resistance and the presence of airflow limitation, which are common features of respiratory diseases like asthma and chronic obstructive pulmonary disease (COPD).
- Respiratory System Compliance (Crs): Crs represents the ability of the respiratory system to expand and accommodate changes in lung volume for a given pressure change during breathing. Crs measures lung distensibility and elasticity, reflecting the extent of ease how the lungs can be inflated and deflated. Higher Crs values indicate greater lung compliance, meaning the lungs can stretch more easily, while lower Crs values suggest decreased compliance and increased stiffness or resistance to expansion. Changes in Crs can occur due to various factors, including lung diseases such as emphysema, fibrosis, or acute respiratory distress syndrome (ARDS).
- Respiratory Elastance (Ers): Ers measures the stiffness or elasticity of the respiratory system, representing the inverse of compliance. Increased Ers suggests reduced lung compliance and increased lung stiffness, which can occur due to factors like fibrosis, inflammation, or decreased surfactant production. Monitoring Ers helps assess lung tissue properties and how easily the lungs expand and contract during breathing.
- Central Airway Resistance (Rn): Rn specifically measures the resistance in the central airways, which includes larger conducting airways. Increased Rn may indicate narrowing or obstruction in the larger airways, such as the trachea and bronchi. Monitoring Rn

helps evaluate the patency and function of the central airways, which play a crucial role in regulating airflow and gas exchange.

- Tissue Elastance (H): H represents the viscoelastic properties of the lung tissue, reflecting the energy dissipation during lung inflation and deflation. Changes in H can indicate alterations in lung tissue mechanics, such as tissue remodelling, fibrosis, or inflammation. Monitoring H provides insights into the dynamic behavior of lung tissue and its response to mechanical forces.
- Tissue Damping (G): G measures the resistance to airflow caused by energy dissipation within the lung tissue during breathing. Increased G suggests increased resistance to airflow within the lung parenchyma, which can occur due to factors like tissue stiffness, inflammation, or mucus accumulation. Monitoring G helps assess the energy dissipation properties of lung tissue and its contribution to overall lung function.

Overall, the parameters measured by FlexiVent provide valuable insights for diagnosing asthma, assessing disease severity, and evaluating the effectiveness of asthma treatments, including bronchodilators and anti-inflammatory medications.

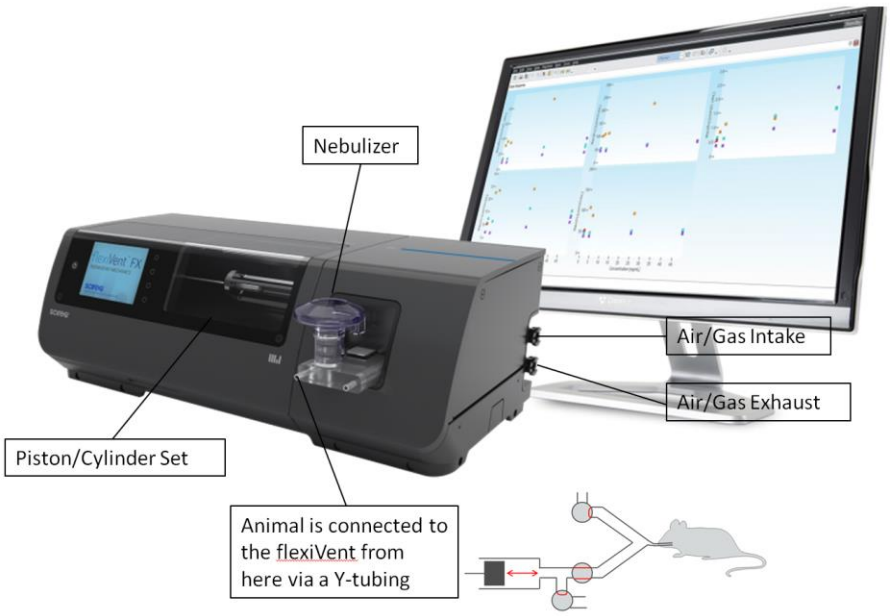

Figure 21. A schematic diagram of the FlexiVent system.

The FlexiVent system can directly measure lung function with high accuracy, and is thus regarded as the gold standard for in vivo small animal lung function measurements. The diagram is taken from the FlexiVent FX User Manual download from the SCIREQ company website (https://www.scireq.com/downloads/).

2.2.3.4 Blood collection

After the animal was euthanized, blood samples were collected to measure the concentration of Ca^{2+} for animals treated with or without inhaled calcilytic as an indication for systemic "overspill" effects of inhaled calcilytic, given the role of the CaSR in extracellular free ionised calcium homeostasis. Briefly, blood samples were collected from the retro-orbital venous plexus by removing the eyeball after AHR measurement. Sera were obtained by centrifuging the samples at 2,300 g at 4℃ for 20 minutes. Samples were stored overnight at 4℃.

2.2.3.5 BALF collection

For this part of the work, I also collected the BALF to measure the inflammatory cell infiltration into the lungs. Lungs from each animal were lavaged with 2 x 0.8 ml (3 times for each lavage to collect the infiltrated inflammatory cells as much as possible) of pre-cooled sterile PBS buffer to

yield at least 1.2ml BALF. The collected samples of BALF were centrifuged at 300 g at 4℃ for 10 minutes to collect the supernatants pending analysis of cytokine concentrations into the BALF. The remaining cell pellets were processed to count for total and differential cell counts.

2.2.3.6 Differential cell counts

For the differential cell counts from the animal work conducted in China, I used Congo red staining to identify the 4 cell types since this was the standard staining in the laboratory. In Congo red stained slides, macrophages appear as the largest cells with abundant cytoplasm and irregularly shaped nuclei with a diameter of 15-20 μm. Eosinophils typically have bilobed nuclei and exhibit red-stained granules in the cytoplasm. Eosinophils are slightly smaller than macrophages, with a diameter ranging from 10-14 μm. Neutrophils have multilobed nuclei (usually 2-5 lobes) with a diameter around 9-12 μm. Lymphocytes typically have different sizes from small (6-8 μm), medium (8-10 μm) and large (10 μm or more), but most of them appear as the smallest ones with a round blue large spherical nucleus and minimal cytoplasm (Figure 22) (Gude et al. 1982). 300 total cells were counted and the percentage of the 4 different types of cells were calculated. Absolute inflammatory cell count was calculated as the cell percentage multiplied by the total cell counts.

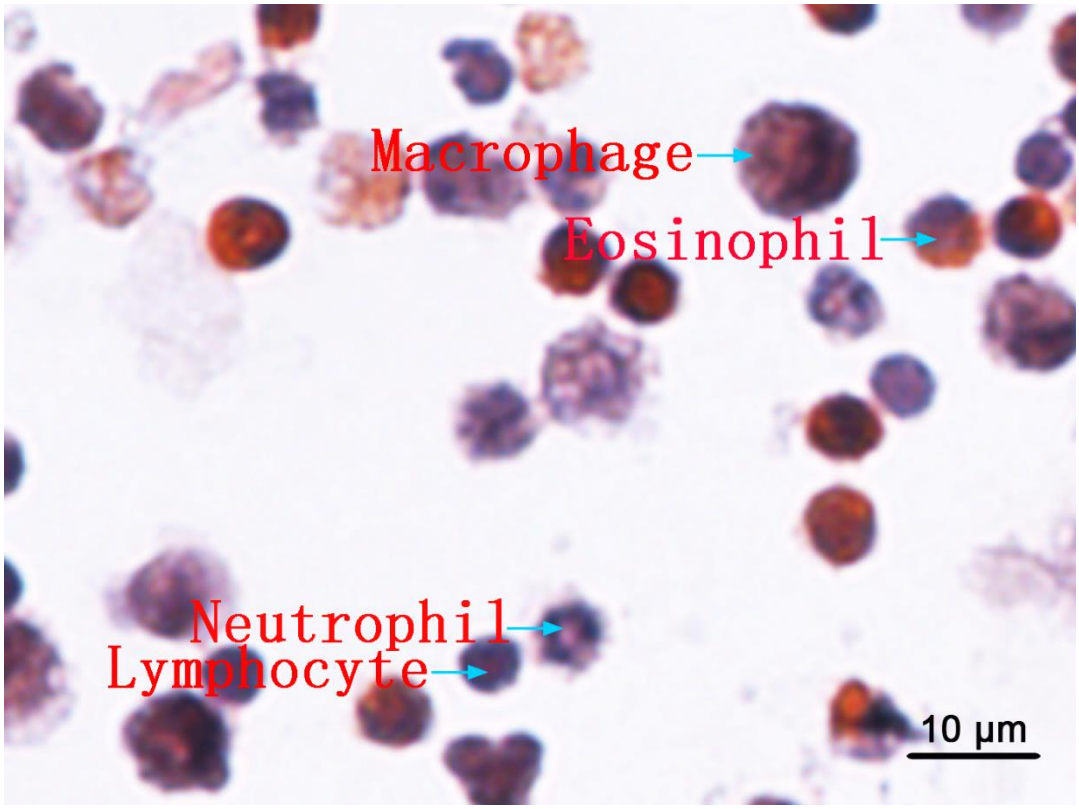

Figure 22. Exemplar photograph of Congo red staining used to identify the four subtypes of leukocytes, eosinophils, neutrophils, lymphocytes and macrophages.

The largest mononucleated cell is the macrophage. There are two medium-size cells, one with red-stained granules in the cytoplasm is an eosinophil, and the other one without red-stained granules in the cytoplasm is a neutrophil. The smallest cell with a dark-blue large spherical nucleus and little light blue cytoplasm is a lymphocyte(Gude et al. 1982).

2.2.3.7 Tissue collection

To see the pathological changes in lung tissue, the left lungs were collected and fixed with 10% neutral-buffered formalin for 24h. The next day, fixed lungs were paraffin-embedded. The blocks were cut into 4-µm thick sections and processed for histological staining. Formalin-fixed paraffin-embedded (FFPE) tissue processing is a standard method used to prepare tissue samples for histological staining. This process is essential for preserving tissue structure and optimizing microscopic examination. The protocol for a formalin-fixed paraffin-embedded procedure is as follows:

2.2.4 Preparation Protocol for Formalin-Fixed Paraffin-Embedded Lung Tissue

1. Lung tissue was fixed with approximately 2ml 10% formalin for 24 hours at room temperature.
2. The fixed lungs were horizontally cut into 3 pieces to show the different types of airways. Then the 3 pieces of lungs were placed in embedding cassettes.
3. Processed for paraffin embedding schedule as follows:

70% Ethanol	1 hour
80% Ethanol	1 hour
95% Ethanol	2 x 1 hour
100% Ethanol	2 x 1 hour
Xylene	2 x 40 minutes
Paraffin wax (60 ºC)	2 x 2 hours

4. Embed tissues into paraffin blocks.
5. Before cutting, the blocks were cooled in the fridge at about 4 ºC for a while to make them easy to cut.
6. Paraffin blocks were trimmed as necessary and cut at 4 µm.
7. Each paraffin ribbon was placed in a water bath at about 40 ºC.
8. Mounted sections onto slides and labeled as appropriate.

Sections were allowed to dry at 36 ºC for about 30 minutes and then baked in a 60 ºC oven overnight.

2.2.5 Histological staining

2.2.5.1 Haematoxylin & eosin (H&E) staining

Haematoxylin and eosin (H&E) staining is the most widely used histological staining technique in both clinical pathology and research laboratories. It involves staining tissue sections with two dyes: haematoxylin and eosin. Nuclei are stained as blue or purple by haematoxylin, while cytoplasm and extracellular matrix are stained as pink or red by eosin. H&E is widely used for the visualization of tissue architecture, cell morphology, and abnormalities, making it invaluable in the diagnosis of various diseases and conditions, as well as in research studies aimed at understanding tissue structure and function. The detailed staining procedures for lung tissue are as follows:

- Placed the slides in an oven preset at 60℃ for 2 hours.
- Deparaffinization and hydration steps

Xylene	2 x 10 minutes
100 % EtOH	2 x 5 minutes
95 % EtOH	5 minutes
70 % EtOH	5 minutes
50% EtOH	5 minutes
30% EtOH	5 minutes
Distilled Water	5 minutes

- Stained with haematoxylin for 3.5 minutes, and washed with running tap water.
- Stained with 1% Alcohol acid for 2 seconds, and washed with running tap water.
- Stained with eosin for 10 seconds, and washed with running tap water.
- Dehydration

95% EtOH	2 minutes
100 % EtOH	2 x 5 minutes
Xylene	2 x 10 minutes

- Mounted using neutral balsam and covered with a coverslip.

2.2.5.2 Congo red staining for lung tissue slides

Congo red staining is primarily used to identify and visualize amyloid deposits in tissues. However, eosinophils can be stained as orange-red colour clearly with Congo red. So, it is also used to identify eosinophils and used in the BALF differential cell counts. The detailed staining procedures for lung tissue are as follows:

- Placed the slides in an oven preset at 60℃ for 2 hours.
- Deparaffinization and hydration

Xylene	2 x 10 minutes
100 % EtOH	2 x 5 minutes
95 % EtOH	5 minutes
70 % EtOH	5 minutes
50% EtOH	5 minutes
30% EtOH	5 minutes
Distilled Water	5 minutes

- Stained with haematoxylin for 3.5 minutes, and washed with running tap water.
- Stained with 1% Alcohol acid for 2 seconds, and washed with running tap water.
- Stained with Congo red for 40 minutes, and washed with running tap water.
- Dehydration

95% EtOH	2 minutes
100 % EtOH	2 x 5 minutes
Xylene	2 x 10 minutes

- Mounted using neutral balsam and covered with a coverslip.

2.2.5.3 Congo red staining for differential BALF cell counts

As mentioned above, since eosinophils can be stained orange-red colour clearly with Congo red, it is also used in the BALF differential cell counts. The detailed staining procedures for BALF slides are as follows:

- Hydration: placed the slides in Distilled Water for 5 minutes.
- Stained with haematoxylin for 3.5 minutes, and washed with running tap

water.

- Stained with 1% Alcohol acid for 2 seconds, and washed with running tap water.
- Stained with Congo red for 40 minutes, and washed with running tap water.
- Dehydration

95% EtOH	2 minutes
100 % EtOH	2 x 5 minutes
Xylene	2 x 10 minutes

- Mounted using neutral balsam and covered with a coverslip.

2.2.5.4 Masson’s trichrome staining of lung tissue

Masson's trichrome staining is a histological staining technique that is widely used to differentiate connective tissues, particularly collagen, on tissue sections. It involves staining tissue sections with three different dyes, nuclei are stained as blue or dark blue by haematoxylin, cytoplasm are stained as red or pink by acid fuchsin or fuchsine acid, collagen fibers are stained as blue-green by aniline blue or light green. By staining tissues with these three dyes, Masson's trichrome staining allows for the visualization and differentiation of collagen fibers, muscle fibers, and cell nuclei, aiding in the histological examination of tissues, particularly in studies related to fibrosis, scarring, and structural changes in tissues. The detailed staining procedures for lung tissue are as follows:

- Placed the slides in an oven preset at 60℃ for 2 hours.
- Deparaffinization and hydration

Xylene	2 x 10 minutes
100 % EtOH	2 x 5 minutes
95 % EtOH	5 minutes
70 % EtOH	5 minutes
50% EtOH	5 minutes
30% EtOH	5 minutes
Distilled Water	5 minutes

- Placed the slides in 25% potassium dichromate solution overnight, and

then washed with running tap water.

- Mixed equal parts of Weigert's Iron Haematoxylin A and B solution and the slides were stained for 5 minutes, and then washed with running tap water.
- Stained with 1% Alcohol acid for 2 seconds, and washed with running tap water.
- Stained with Lichunhong-acid fuchsin solution for 5 minutes, and washed with distilled water.
- Differentiated the sections in the phosphomolybdic acid solution for 8 minutes without wash.
- Directly transferred the slides to aniline blue solution and stained for 5 minutes. Rinsed in distilled water briefly, differentiated in 1% acetic acid solution for 1 minute, and then washed with distilled water.
- Dehydration

95% EtOH	2 minutes
100 % EtOH	2 x 5 minutes
Xylene	2 x 10 minutes

- Mounted using neutral balsam and covered with a coverslip.

2.2.5.5 AB-PAS staining of lung tissue

Periodic acid-Schiff (PAS) staining is also a widely used histological staining technique to identify carbohydrate-containing structures in tissues, including glycogen, mucins, glycoproteins, and basement membranes. The PAS stain is particularly useful in diagnosing various diseases and conditions involving these substances. It is most commonly used to detect glycogen deposits in the liver and muscle tissues. In respiratory tracts, PAS staining can highlight mucus-secreting cells and glands. Carbohydrate-containing structures are stained as magenta/bright pink by Schiff reagent after oxidation by periodic acid. Other tissue components are stained as blue or dark blue by haematoxylin, providing contrast to the magenta-stained structures. The detailed staining procedures for lung tissue are as follows:

- Placed the slides in an oven preset at 60℃ for 2 hours.
- Deparaffinization and hydration

Xylene	2 x 10 minutes

100 % EtOH	2 x 5 minutes
95 % EtOH	5 minutes
70 % EtOH	5 minutes
50% EtOH	5 minutes
30% EtOH	5 minutes
Distilled Water	5 minutes

- The slides were stained with Alcian solution for 5 minutes, and then washed with running tap water.
- Oxidization in the periodic acid solution for 15 minutes, washed with running tap water, and then rinsed in distilled water.
- The slides were stained with Schiff reagent for 20 minutes (protected from light during this step), and then washed with running tap water.
- Dehydration

95% EtOH	2 minutes
100 % EtOH	2 x 5 minutes
Xylene	2 x 10 minutes

- Mounted using neutral balsam and covered with a coverslip.

2.2.6 Measurements of cytokine concentrations in the lung tissue

The measurements of cytokine concentrations in the lung tissue were conducted by Enzyme-Linked Immunosorbent Assay (ELISA) that is widely used for detecting and quantifying specific proteins, peptides, antibodies, hormones, and other molecules in biological samples due to its simplicity, versatility, sensitivity, and specificity, developed by Engvall and Perlman in 1971 (Engvall and Perlmann 1971). There are four types of ELISA methods: direct ELISA, indirect ELISA, sandwich ELISA, and Competitive ELISA (Figure 23). For my experiments, I used a sandwich ELISA to measure cytokine concentrations: briefly, 1. Capture antibodies were coated on the plate; 2. Blocking solutions were added; 3. Samples and standards were added; 4. Detection antibodies were added; 5. Avidin-HRP solutions were added; 6.TMB substrates were added; 7. Stop solutions were added to stop the reaction; 8. The plates were read at 450 nm.

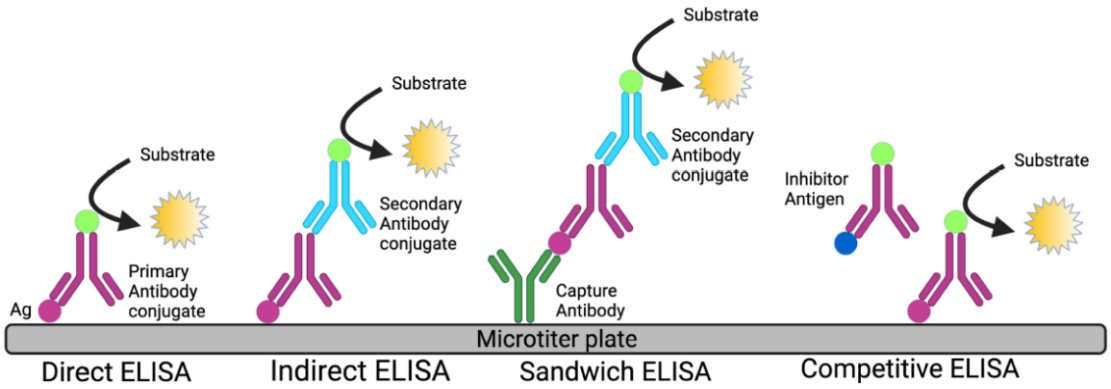

Figure 23. Four major types of ELISA assays and their principles. In a direct ELISA, the antigen of interest is immobilized directly onto the surface of a microplate well. In an indirect ELISA, the main difference compared to direct ELISA is it uses an unlabeled primary antibody and a labeled secondary antibody, amplifying the signal to detect the target molecule indirectly. In a sandwich ELISA, the capture antibody is immobilized onto the surface of the microplate well, and the antigen in the sample and standards bind to the capture antibody. Competitive ELISA is used to measure the concentration of an antigen in a sample by competition between the antigen in the sample and a labeled antigen (often a synthetic antigen or antigen conjugate) for binding to a limited amount of specific antibody immobilized onto the microplate well (Hayrapetyan et al. 2023). Image taken from Lengfeld et al. (2021).

The right lung tissue was stored at -80℃ on the sampling day and homogenized on the next day using homogenizer (Wuhan Servicebio Technology Co., Ltd, Wuhan, China, 2,000 rpm). Supernatants of the homogenized lung tissue were collected and stored at -80℃ until analysis. Asthma-associated cytokines IL-5, IL-13, IL-6 and TNF α (tumour necrosis factor-alpha), were measured in the supernatants of homogenized lung tissue and quantified using commercial ELISA kits (eBioscience, San Diego, CA, USA), according to the manufacturer's instructions. A typical ELISA protocol is described below, with IL-6 as an example.

1. Corning Costar 9018 ELISA plates were first coated with capture antibody (100 µL/well) in 1X Coating Buffer (diluted according to certificate of analysis (COA)). The plates must be sealed and incubated overnight at 2-8°C.
2. The wells were aspirated and washed for 3 x 2 minutes with 300 µL/well Wash Buffer the next day. The plates were placed on absorbent paper to remove any residual buffer.
3. One part of 5X ELISA/ELISPOT Diluent and 4 parts of DI water were mixed to prepare the working Diluent. The wells were blocked with 200 µL/well of 1X ELISA/ELISPOT Diluent and incubated for 1 hour at room temperature.
4. Lyophilized standards were reconstituted according to Certificate of Analysis (C of A) using DI water. Wait for 15 minutes with gentle agitation prior to diluting further.
5. The reconstituted standards were diluted according to C of A using 1X ELISA/ELISPOT Diluent to prepare the top standard concentration. 100 µL/well of top standard concentration was added to the appropriate wells, and two-fold serial dilutions of the top standards were made to generate 8 standard curve data points. 100 µL/well samples were added to the appropriate wells. Two well of 100 µL/well of 1X ELISA/ELISPOT Diluent only were included to serve as plate blanks. The plates must be sealed and incubated at room temperature for 2 hours.
6. Follow the aspirate/wash process as in step 2 for a total of 3-5 washes.
7. 100 µL/well of detection antibody in 1X ELISA/ELISPOT Diluent (diluted according to C of A) was added. The plates must be sealed and incubated at room temperature for 1 hour.
8. Follow the aspirate/wash process as in step 2 for a total of 3-5 washes.
9. 100 µL/well of Avidin-HRP in 1X ELISA/ELISPOT Diluent (diluted according to C of A) was added. The plates must be sealed and incubated at room temperature for 30 minutes.
10. Follow the aspirate/wash process as in step 2 for a total of 5-7 washes.
11. 100 µL/well of 1X TMB Solution was added to each well. The plates must be sealed and incubated at room temperature for 15 minutes.
12. 50 µL Stop Solution was added to terminate the reaction in each well.
13. The plates were read at 450 nm.

2.2.7 Measurements of serum Ca^{2+} levels

Blood samples were collected from the retro-orbital venous plexus after lung function measurements, and serum samples were collected by centrifuge at 1000 g, 4 ℃ for 20 minutes on the second day and stored at -80℃ until used. The measurements of Ca^{2+} level in serum were conducted by the Biochemstry laboratory within the University of Wales Hospital.

2.2.8 Quantification of the histochemical staining slides using TissueFAXS image analysis software StrataQuest

To know the degree of the effects of inhaled calcilytic on asthma symptoms, I use the TissueFAXS image analysis software StrataQuest (TissueGnostics, Vienna, Austria) to quantify the degree of the inflammatory cell infiltration, eosinophilia, mucus overproduction, collagen deposition in H-E-, Congo red-, PAS- and Masson's trichrome- staining slides. Briefly, an area of interest was selected, and the total area was counted by pre-defined rules; the area of the colour of interest (Masson's trichrome- staining, Figure 24) or the number of cells of interest (H-E-, Congo red- and PAS-staining, Figure 25) were counted to calculate the percent of colour in the total area or the number of interested cells per 10000 μm^2 area. Generally, 4 pictures per animal were counted.

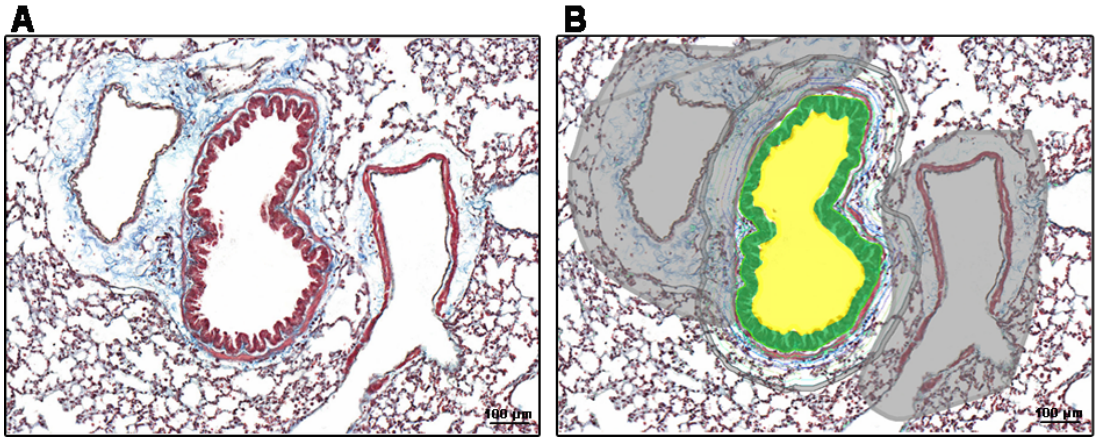

Figure 24. Graphical representation of the Masson's trichrome-stained slides used to determine peribronchial collagen in StrataQuest.

(A) Masson's trichrome-staining of airway regions. (B) Airways were identified by drawing the airway lumen with yellow and the airway epithelium with green. Grey area is the area to exclusion. StataQuest (TissueGnostics, AT) was then programmed to analyse the percentage of positively stained blue pixels in the different parts around the peribronchial area, with 7 peribronchial rings extending away from the airway epithelium in increments of 30 µm. Scale bar = 100 µm.

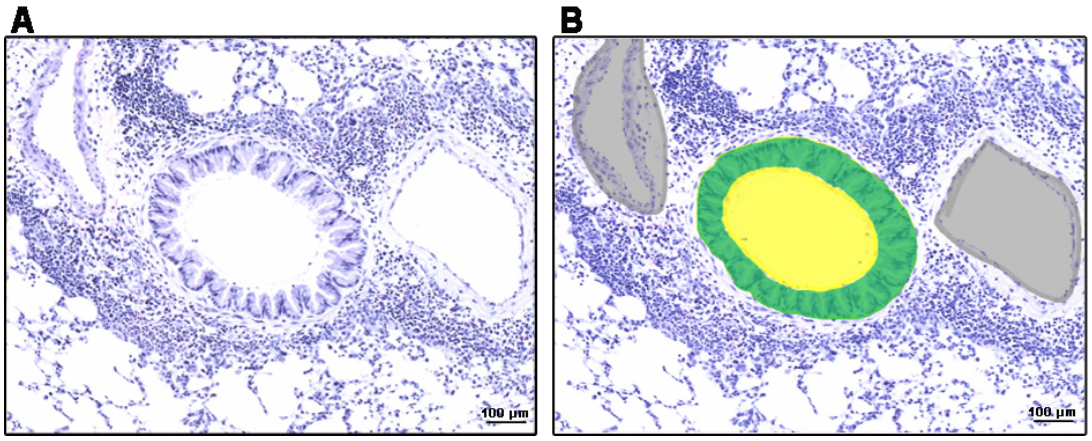

Figure 25. Graphical representation of the H&E-stained slides used to determine peribronchial inflammation in StrataQuest.

(A) H&E staining of airway regions. (B) Airways were identified by drawing the airway lumen with yellow and the airway epithelium with green. Grey area is the area to exclusion. StataQuest was then programmed to analyse the

number of positively stained cells per 10000 μm^2 area tissue to quantify the peribronchial inflammation. Scale bar = 100 μm.

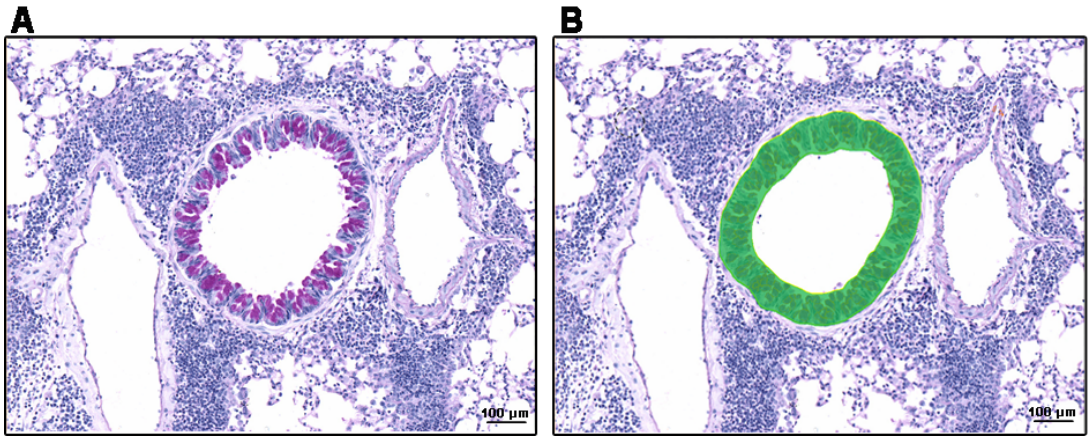

Figure 26. Graphical representation of the PAS-stained slides used to determine mucus production in StrataQuest.

(A) PAS staining of airway regions. (B) Airways were identified by drawing the airway epithelium with green. StataQuest was then programmed to analyse the number of positively stained cells per 10000 μm^2 area airway to quantify the mucus production. Scale bar = 100 μm.

2.2.9 Preparation of solutions used in studies

500 μg/ml OVA in aluminium hydroxide solution

Take 1 mg OVA and dissolve in 1 ml saline, then add 1 ml $AL(OH)_3$ and mix.

10% formalin fixative (pH 7.0)

Take 100 ml 40% formaldehyde, 4.0 g KH_2PO_4, 6.5 g Na_2HPO_4, and dissolve in 900 ml distilled water to make a 10% formalin fixative.

1% Triton X-100 protease inhibitor (PI) solution preparation for the lung tissue homogenate.

Take 1 tablet protease inhibitor cocktail (Roche, Basel, Switzerland) dissolve it in 1 ml distilled water, add 9 ml PBS to dilute it, and then add 100 μL Triton X-100 and vortex to mix completely.

3 % H_2O_2 solution preparation

Use Distilled Water to dilute 30 % H_2O_2 solution.

Preparation of 0.3% Triton X-100

Add 0.3 ml Triton X-100 to 100 ml 0.01M PBS and vortex to mix thoroughly.

Antibody dilution fluid preparation

Dissolve 1% BSA and 3% goat serum in filter-sterilised PBS, pH7.4.

10 X Phosphate Buffered Saline (PBS) preparation

For 1 litre 10 X PBS, add the following in Milli-Q water

Na_2HPO_4 (dibasic anhydrous)	12 g
NaH_2PO_4 (monobasic anhydrous)	2.0 g
NaCl (sodium chloride)	85.0 g

Mix and adjust the pH to 6.75. Dilute to make 1 X PBS, and adjust the pH to 7.4 when using.

PBST wash buffer for ELISA

Add 0.25 mL Tween-20 to 500 mL PBS and mix thoroughly.

ELISA stop solution

Add 10 mL concentrated sulphuric acid to 170 mL distilled water and mix thoroughly.

Glycine buffer (pH 10.0), Congo red staining solution

Glycine	0.225 g
sodium chloride	0.1215 g
sodium hydroxide	0.16 g

Mix and stir to completely dissolve in 100 ml of distilled water. Then take 1 g of Congo red powder and dissolve it in a mixed solution of 100 ml of glycine buffer and 100 ml of ethanol to make a 0.5% Congo red staining solution.

1% HCl alcohol

For a 100 mL solution, carefully add 1 mL of concentrated (37%) HCl to 99 mL of ethanol (70%) while stirring, and mix well. This solution is used for decolorization and differentiation of stained slides.

4 mM hydrochloric acid

Dissolve 100 µL concentrated hydrochloric acid in 301.4 ml saline and mix well.

4% Sodium pentobarbital solution (pH 7.5)

Accurately weigh 0.4 g sodium pentobarbital and add to a tube with 10 ml saline, mix until it is completely dissolved.

0 mg/ml, 6 mg/ml, 12 mg/ml, 24 mg/ml, 48 mg/ml Methacholine solution for airway hyperresponsiveness measurement

Label 5 tubes with 0, 6, 12, 24, 48. Accurately weigh 96 mg MCh and add to the tube labelled with 48, which contains 2 ml saline to make a 48 mg/ml concentration solution, then dilute in sequence to make 24, 12, 6 and 0 mg/ml concentration solution.

2.2.10 Statistical Analysis

For the sample size calculation, I followed the resource equation approach as recommended by (Arifin and Zahiruddin 2017), and the formula is: n = DF/k + 1 for the one-way ANOVA. Using this method, the acceptable range of the degrees of freedom (DF) for the error term in an ANOVA is in the range of 10 to 20 (Festing and Altman 2002; Festing 2006; Mead et al. 2009). The minimum and maximum numbers of animals in each group can be calculated by replaced the DF in the formulas with the minimum (10) and the maximum (20) as follow:

Minimum n = 10/k + 1

Maximum n = 20/k + 1

Where k = number of groups, and n = number of animals in each group.

For my experiment, k = 3, hence in this case, minimum n = 10/3 + 1 = 4.3, maximum n = 20/3 + 1 = 7.7. The minimum and maximum are rounded up and down to 5 and 7, respectively, to keep the DF for each group within the limit (DF = k(n – 1), e.g., DF = 12 for n = 5, and DF = 18 for n = 7). Considering that 10% of animal may die during an experiment, n = 6/7 for OVA experiment and n = 8/9 for IL-33 experiment were chosen.

Data were analysed using the Prism 9.0 software package (GraphPad Inc.). All data were plotted as mean ± SEM. One-way ANOVA (with Bonferroni post hoc analysis) or unpaired t test were used to test the differences between groups after the Shapiro-Wilk's test for normality. P-values < 0.05 were considered significant.

Chapter III Selecting the best available calcilytic

3.1 Introduction

Because of the involvement of CaSR in the regulation of physiological processes that may play a critical role in the process of inflammation and proliferation, our lab previously tested the role of the CaSR in the development of asthma (Yarova et al., 2015, 2016), and the possibility of using calcilytics to alter disease onset and progression. Firstly, we have demonstrated that the CaSR is expressed in both human and mouse airways and its expression increases during asthma (Yarova et al., 2015). Furthermore, calcilytics, delivered topically to the lung, abrogate airway hyperresponsiveness and inflammation in a mixed allergen (MA) -sensitized and in a triple allergen (Aspergillus, Alternaria, house dust mite)-sensitised murine asthma models (Yarova et al., 2015). We have also demonstrated that, in a lipopolysaccharide (LPS) - induced model of steroid-resistant inflammatory lung disease in Guinea pigs, nebulised calcilytics reduce inflammation and interstitial wall thickening in the lungs of these animals (Yarova et al., 2016).

CaSR antagonists, calcilytics, were initially developed for osteoporosis, but their development has been discontinued owing to a lack of efficacy for this indication (Ward & Riccardi, 2012; GINA). There are two main classes of calcilytics (Widler 2011), which have been previously tested in the clinical trials via the systemic route: 1) amino alcohols (SB-423557, Ronacaleret, JTT-305, NPSP-795/SB-423562); 2) quinazolin-2-one (AXT914 and ATF936) (Table 3). SB-423562 has a very low systemic exposure due to poor intestinal absorption and/or first-pass hepatic extraction after oral administration. SB-423557 is the prodrug of SB-423562, with improved absorption and increased bioavailability after oral administration. AXT914 and ATF936 are two quinazolin-2-one derivatives that Novartis developed for testing in clinical trials, which showed almost identical dose-dependent exposure levels in healthy male volunteers. However, AXT914 was finally selected to be tested in the later phase of development due to its superior solubility properties in microemulsion preconcentrates, enabling substantially higher drug loading of

the emulsions (Widler 2011). In the previous experiment, our lab demonstrated that calcilytic can abrogate airway hyperresponsiveness and inflammation, a generic calcilytic NPS89636 was used, the one didn't-test in the clinical trials (Yarova et al., 2015). So, in the first part of my PhD studies, I wanted to select the best available calcilytic previously tested in clinal trials which could be suitable for repurposing for inhalation. To this end, I compared the effects of calcilytics previously tested in humans, namely NPSP-795, Ronacaleret, JTT-305 and AXT 914, on acetylcholine (ACh)-induced airway contraction in naïve mouse tracheae *ex vivo*, with the scope to identify the best calcilytic for repurposing in asthma using wire myography. In my experiments, the candidate calcilytics were custom-synthetized by Signature Discovery (Durham, United Kingdom), and the control calcilytic, NPS2143, was purchased from Tocris (Tocris Bioscience, Bristol, United Kingdom).

3.2 Aims And Objectives

To further explore the possibility of repurposing existing calcilytics, delivered topically to the lung, as a novel asthma drug in humans, the aim of this chapter was to select the best calcilytic amongst those previously tested in humans via the systemic route (i.e., NPSP-795, Ronacaleret, JTT-305 and AXT 914) for testing in preclinical *in vivo* asthma models. The purpose of this part of my work was to carry out wire myography on isolated airways in which contraction was induced by ACh in naïve mouse tracheae *ex vivo* in order to compare the bronchoconstricting and bronchodilatory properties of the selected calcilytics.

3.3 Materials and Methods

To select the best calcilytic for further clinical development, I tested the bronchodilatory properties of calcilytics *ex vivo* by wire myography by determining the effects of different concentrations of clinical-grade calcilytics on airway contraction evoked by the acetylcholine (ACh), in tracheae isolated from male Balb/C mice.

3.3.1 Wire Myography

For this part of the work, I tested the effects of calcilytics both prophylactically and therapeutically. For both settings, tracheae were isolated, processed and mounted on a wire myography machine as detailed in the Methods section 2.2.1.1. The contraction of the trachea was induced by the bronchoconstrictor acetylcholine and the effect of the four candidate calcilytics (NPSP-795, Ronacaleret, JTT-305 and AXT 914, 100 nM) or the positive control calcilytics, NPS 2143 (100 nM) and NPS89636 (300 nM) were tested in the pre-treatment (Figure 14A) and post-treatment (Figure 14B) settings. For the prophylactic experiments, I aimed to rule out the possibility of causing trachea constriction by calcilytics, and to check if they had any preventive effects on trachea constriction. So, calcilytics were added before evoking tracheal contractions by increasing concentrations of ACh (1 nM - 3 μM) (Figure 14A in Methods section 2.2.1.1.1). For the therapeutic experiments, trachea constriction was induced by half-maximum effects of Ach (20 nM) before increasing concentrations of calcilytics (1 nM - 30 μM) or DMSO (vehicle) were added, to investigate their effects on pre-existing partial trachea constriction. The generated averaged data points for each experiment were then fitted as contraction with logarithm dose (% contraction v.s. log dose, % contraction as Y axis, log dose as X axis, ACh dose for the pre-treatment experiments, dose of different calcilytics for the post-treatment experiments) to generate concentration-response curves (Microsoft Excel 2010, Microsoft Corporation, Redmond, Washington; GraphPad Prism 7, San Diego, CA).

3.3.2 Materials

Clinically tested calcilytics, the quinazolin-2-one, AXT914, and the amino alcohols, JTT-305, NPSP-795 and Ronacaleret, were custom-synthetized by Sygnature Discovery Ltd. NPS89636 was a gift from NPS Pharmaceuticals Inc. NPS2143 was purchased from Tocris. All other chemicals from this part of work were purchased from Sigma-Aldrich (Merck), unless otherwise specified.

3.4 Results

3.4.1 Prophylactic effects of calcilytics on ACh-induced airway contraction *ex vivo* in naïve animals

As shown in Figure 27, pharmacologically relevant concentrations of NPSP-795 and AXT-914 evoke a rightward shift in the ACh dose-response curve with statistically significant effects albeit with differences in the modes and magnitude for the relaxation, suggesting that NPSP-795 and AXT-914 have prophylactic effects in preventing trachea constriction induced by ACh. By comparing the ACh dose-response curve obtained in the presence of the calcilytic vs that observed in control (DMSO) conditions, I found that: the ACh dose-response curve in the presence of prophylactic administration of NPSP-795 exhibits a rightward shift from the DMSO (control) group at concentrations as low as 100 nM, which becomes statistically significant at 300 nM until the highest dosage tested 3 μM. However, prophylactic administration of AXT-914, though the ACh dose-response curve also exhibits a rightward shift at 100 nM, this difference only became statistically significant at the highest concentration tested, 3 μM. Though Ronacaleret, and the control calcilytics NPS2143 and NPS89636 evoked a rightward shift in the ACh dose-response curve, this effect was not significantly different from that seen in the DMSO control group (Figure 27).

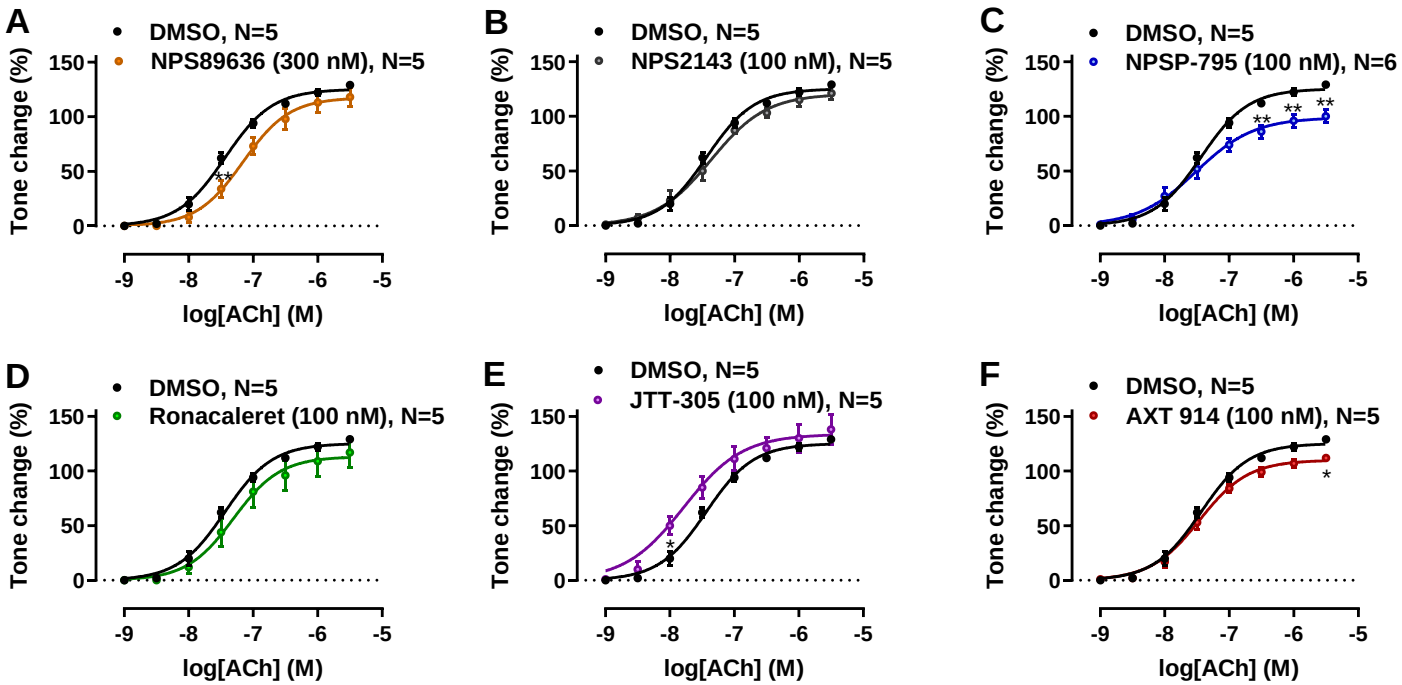

Figure 27. Prophylactic effects of calcilytics on acetylcholine-induced trachea contraction.

Trachea contraction was evoked by increasing concentrations of acetylcholine (Ach, 1 nM - 3 μM) to serve as the baseline levels, after which tracheae were treated with DMSO (0.001%, control) or calcilytics (100 nM), then the percentage of contraction relative to the contraction evoked by the ACh alone was measured. NPSP-795 and AXT 914 significantly reduced bronchial constriction. Results are from 5 or 6 independent experiments. Data are presented as Mean ± SEM. P-values are from unpaired t test, *: $p < 0.05$, **: $p < 0.01$.

3.4.2 Therapeutic effects of calcilytics in acetylcholine (ACh)-induced airway contraction *ex vivo* in naïve animals

To test the ability of calcilytics to affect pre-contracted airways, 20 nM ACh was added first to evoke a trachea contraction and after stability was achieved, different concentrations of calcilytics were added to investigate whether calcilytics evoked further constriction, or relaxation, of half-maximally pre-contracted mouse tracheae (Figure 14B in Methods section 2.2.1.1.2). 5 calcilytics, including three repurposing calcilytics Ronacaleret, NPSP-795 and JTT-305 and the control calcilytics NPS2143 and NPS89636, evoked a statistically significant airway relaxation compared to the DMSO control. In contrast, AXT 914 didn't show any effect on airway contraction. NPS2143, NPS89636, NPSP-795, Ronacaleret, and JTT-305 are all amino alcohols with similar structures, while AXT 914 is a quinazolin-2-one with different structure. The mode and magnitude of relaxation effects of NPS89636, NPSP-795 and Ronacaleret were comparable, and they all demonstrated to evoke relaxation from concentrations of 10 μM. NPS2143 and JTT-305 also had comparable relaxation effects mode and magnitude, with the effect onset at the highest dosage tested 30 μM (Figure 28).

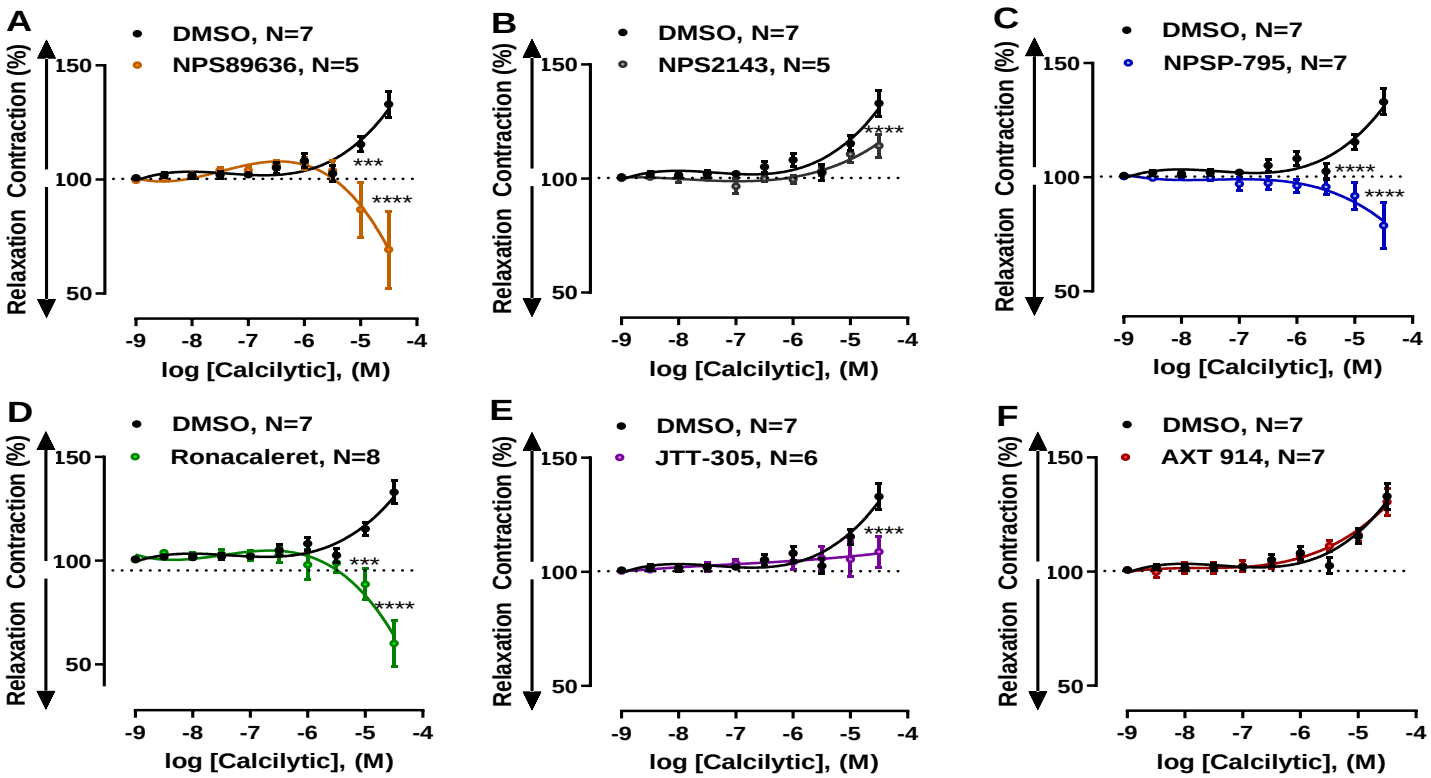

Figure 28. Therapeutic effects of calcilytics on acetylcholine-induced trachea contraction.
Measurements of trachea contraction were carried out in the presence of different concentrations of calcilytics (1 nM - 30 µM) in naïve mouse trachea half-maximally pre-constricted with the bronchoconstrictor acetylcholine (ACh, 20 nM). NPSP-795, Ronacaleret, JTT-305 and the control calcilytics (NPS2143 and NPS89636) significantly reduced bronchoconstriction compared with the DMSO vehicle control, while AXT 914 did not. Results are from 5-8 independent experiments. Data are presented as Mean ± SEM. P-values are from unpaired t test, **: $p < 0.01$, ***: $p < 0.001$, ****: $p < 0.0001$.

3.5 Discussion

In this chapter, I tested, for the first time, the prophylactic and therapeutic effects of the four calcilytics previously clinically tested in osteoporosis trials on ACh-induced airway contraction ex vivo in naïve mouse trachea to identify the best available calcilytic for repurposing as a novel asthma drug. In mouse trachea, all the tested amino alcohol calcilytics evoked reductions in ACh-induced tracheal contraction to some degree when applied therapeutically, showing different modes and magnitude of relaxation, while quinazolin-2-one calcilytic AXT 914 didn't show any effects. The control calcilytic NPS89636 and two repurposing calcilytics, NPSP-795 and Ronacaleret exhibited comparable great effects, with effects onset from the concentration of 10 μM. NPS2143 and JTT-305 demonstrated comparable effects, with effects onset from the concentration of 30 μM. In contrast, only two calcilytics, NPSP-795 and AXT 914 attenuated ACh-induced tracheal contraction when applied prophylactically at concentrations known to selectively inhibit the CaSR. For the therapeutic treatments, the Ach dose-response curve in the NPSP-795 group seems to have a rightward shift from the DMSO-treated group earlier (100 nM) than the AXT-914 group (3 μM). In contrast, Ronacaleret, JTT-305, NPS2143 and NPS89636 didn't show a significant effect when compared to the DMSO control group. NPS2143, Ronacaleret, JTT-305 and NPSP-795 belong to the same structural class amino alcohols and with similar structures, however, their effects on tracheal contraction were significantly different in both prophylactic and therapeutic settings; in the prophylactic setting, NPSP-795 showed significant inhibition of the airway contraction, however Ronacaleret and JTT-305 didn't show any effect; in the therapeutic setting, though the 3 calcilytics evoked relaxation, Ronacaleret and NPSP-795 induced a similar and much earlier and greater relaxation than JTT-305. The reason for the differential effect of different calcilytics may be related to their distribution in tissue, or the differential affinity for the receptor. NPS2143 is the early-developed amino alcohol, while Ronacaleret, NPSP-795 and JTT-305 are later-developed amino alcohols with improved selectivity profiles compared with NPS2143 (Widler 2011). They also have different half-life, volume of distribution and oral bioavailability when applied systemically. However, aside from receptor affinity, the bioavailability was related to

intestinal absorption and/or first-pass hepatic extraction when applied systemically (Widler 2011). Their effects when applied locally haven't been investigated before my study; however, a group from Australia published in 2023 that they compared the effects of CaSR NAMs on MCh-induced airway contraction with the standard of care, salbutamol (Diao et al. 2023). In that study, the authors reported that by using the mouse precision-cut lung slices, they were able to demonstrate that CaSR NAMs reverse MCh-induced airway contraction to a similar extent with salbutamol. In addition, the authors showed that the bronchodilator effects of CaSR NAMs are maintained under conditions mimicking a severe asthma attack when β2-adrenergic receptor desensitization while salbutamol shows no efficacy. Furthermore, some CaSR NAMs also show preventive effects after overnight treatment on MCh-induced airway contraction while formoterol has no effects. Taken together, these data highly support the bronchodilator properties of NAMs and their preventive effect on bronchoconstriction in asthma.

I conducted this experiment using Krebs' solution containing 1 mM Ca^{2+} to mimic physiologic conditions, while my colleague Polina Yarova also carried out parallel experiments in Krebs' solution containing 2 mM Ca^{2+} to mimic proinflammatory conditions (Yarova et al. 2021). In the proinflammatory conditions, CaSR NAMs were able to relax precontracted tracheae even more effectively than those of the physiologic conditions. All CaSR NAMs tested were able to relax precontracted tracheae, even the one that didn't show an effect under physiologic conditions, AXT-914 (Yarova et al. 2021). Since these data showed that CaSR NAMs may have greater effects in proinflammatory conditions, these data further support the repurpose of CaSR NAMs in pulmonary inflammatory diseases, such as COPD and asthma.

Airway hyperresponsiveness is the most important feature of asthma, contributing to airway narrowing and obstruction. Airway hyperresponsiveness in asthma is associated with increased ASM contractile function, the mechanisms of which have not been fully elaborated but may be related to the elevation of $[Ca^{2+}]_i$ concentration and Ca^{2+} sensitivity (Camoretti-Mercado and Lockey 2021). CaSR located on the plasma membrane detects changes in

extracellular calcium levels and modulates cellular responses accordingly. Activation of these receptors can regulate calcium entry and release, contributing to overall $[Ca^{2+}]_i$ homeostasis (Riccardi et al. 2022).

Bronchial challenge tests have been long used to measure BHR using bronchoconstrictive stimuli to rule out or confirm a diagnosis of asthma (Sterk et al. 1993; Cockcroft 2010). The most common stimulus utilized in bronchial challenge testing is methacholine, a direct-acting agent that mimics the neurotransmitter acetylcholine and functions as an agonist of muscarinic M3 receptors on ASM cells (Sterk et al. 1993). However, its specificity is poor since healthy subjects and subjects with other diseases such as COPD also respond to the stimulus, with less sensitivity than asthmatic (Lexmond et al. 2018). This is because instead of directly measuring BHR, bronchial challenge test actually measures airway obstruction, which comprises of bronchial smooth muscle hyperresponsiveness, submucosal inflammation, excessive mucus production and airway remodelling (Corrigan 2020). Airways inflammation and remodelling make the airways narrow, and excessive mucus production may critically obstruct the airways, which all exert very great influences on the resistance to airflow aside from bronchial hyperresponsiveness (Corrigan 2020). This is why inhaled corticosteroids were said to reduce bronchial hyperresponsiveness whereas they do not: they simply increase the internal diameter of the airways by reducing inflammatory cellular infiltration and edema, which results in a reduction of airway resistance (Corrigan 2020). One of the advantages of my experiments is that I used wire myography to directly test the airway tension without the confounding effects of airflow resistance resulting from airway inflammation and remodelling. My results clearly demonstrate that calcilytics exhibit bronchodilator properties.

Although existing bronchodilators temporarily alleviate bronchospasm caused by bronchial smooth muscle hyperresponsiveness, there is no therapy that directly and efficiently targets smooth muscle hyperresponsiveness. There isn't a specific drug designed solely to prevent bronchial hyperresponsiveness to date. Thus, asthmatics who have bronchial hyperresponsiveness but with mild symptoms also have a high risk of death due to a lack of preventive treatment or radical treatment of bronchial hyperresponsiveness (Corrigan 2020). If the observed effects of the calcilytics on tracheal contraction and relaxation in my experiments translate to humans, they support the beneficial prophylactic and therapeutic use of calcilytics as bronchodilators in asthma patients, i.e. prevent the onset of bronchial hyperresponsiveness and to relax constricted airways in ICU settings.

Based on these observations, and additional data concerning PK/PD and formulation studies (Yarova et al. 2021), I selected NPSP-795 as the best calcilytic to carry out my future experiments, along with the control calcilytic, NPS89636.

Chapter IV Testing the effects of inhaled calcilytic against the current standard of care, fluticasone propionate, in a Th2/IgE asthma model

4.1 Introduction

Since asthma is a heterogeneous group of disorders, the causative factors and key components can vary, leading to their different susceptibility to different treatments. According to GINA 2023(Global Initiative for Asthma 2023), the treatment of asthma follows a stepwise approach, of which corticosteroids and beta 2-agonists are the standard-of-care that have been used to treat asthma for more than 40 years. However, they do not work for all patients, 5%-25% amongst asthmatic patients who have more severe disease typically have poor response to high doses of or even with oral steroid treatment (Rhen and Cidlowski 2005; Barnes 2010b), and represent the severe, steroid-resistant asthma.

Though steroid-resistant asthma is only seen in a small percentage of patients, it accounts for significant healthcare costs, which leaves steroid-resistant asthma as an area of unmet medical need (Serra-Batlles et al. 1998). In addition, inhaled steroids and beta-agonists are associated with significant side effects (Barnes and Woolcock 1998; Huscher et al. 2009), of which voice problems and cough are the most common local side effects resulting from oropharyngeal and laryngeal deposition of inhaled drugs (Williamson et al. 1995; Leach 1998; Global Initiative for Asthma 2023). Also, patients taking ICS/OCS have an increased risk of pneumonia and osteoporosis, which are dose-dependent (Israel et al. 2001; Kim 2019; Chalitsios et al. 2021; Global Initiative for Asthma 2023).

In contrast to the significant health and economic burden of asthma, very few classes of safe and effective therapies have been introduced to the market during the last decades because of a poor understanding of the underlying disease mechanisms, such as leukotriene receptor antagonists such as zafirlukast, montelukast and zileuton, as well as anti-IgE monoclonal antibody omalizumab (Mullane 2011; Chini et al. 2014). Also, anti-IL5 monoclonal antibody Mepolizumab (Nucala®), Reslizumab (Cinqair®) and Benralizumab (Fasenra®), anti-IL4R monoclonal antibody Dupilumab (Dupixent®) as well as

anti-TSLP monoclonal antibody Tezepelumab (Tezspire®) have been approved recently by FDA for treatment of severe asthmatics (Matera et al. 2019). Although there is a pipeline of these innovative new treatments for asthma, they have been shown to be effective only in a specific sub-type of asthma (McGregor et al. 2019).

In our previous studies, we have shown that calcilytics, delivered topically to the lung, can abrogate airway hyperresponsiveness and inflammation in an allergic asthma model and also decrease steroid-resistant neutrophilic inflammation and airway remodelling in an LPS-induced COPD-like animal model (Yarova et al. 2015; Yarova et al. 2016). In this case, in the current study, I aimed to compare the effects of the inhaled calcilytic with the standard of care, inhaled FP, in two different protocols of Th2/IgE asthma (shorter-term and longer-term) induced by OVA *in vivo*.

4.2 AIMS AND OBJECTIVES

4.2.1 AIMS

The aim of this chapter was to compare the effects of inhaled calcilytic against the current SOC, FP, in murine asthma models *in vivo*.

4.2.2 OBJECTIVES

1) To test the effects of inhaled calcilytic against FP in a shorter-term, prophylactic murine OVA-induced asthma model *in vivo*;
2) To select the best vehicle that could be used to dissolve both calcilytic and FP;
3) To compare the effects of inhaled calcilytic against the current SOC, FP, in a longer-term, therapeutic murine OVA-induced asthma model *in vivo*.

4.3 Materials and Methods

4.3.1 Animals

As described in Methods section 2.2.2.1, 5 weeks BALB/c male/female mice (20-25g) were used in the experiments which I conducted in UK. They were purchased from Charles River and housed at Cardiff University for 2 weeks before any procedures were conducted for environmental accommodation.

The housing conditions are as described in Methods section 2.2.2.1. There was an additional one-week acclimatisation and training for the animals before the start of the experiment.

4.3.2 Acute asthma model

The schematic diagram of the protocol is shown in Figure 15 in Methods section 2.2.2.2. Briefly, on days 0 and 5, animals were sensitized and challenged by 2 inhalations of OVA fourteen days later. Calcilytic or FP treatments were given at 1 hour prior to the first OVA challenge and 4 hours post the last OVA challenge.

4.3.3 Longer-term asthma model.

Animals for the longer-term asthma model were sensitized and challenged as described in Figure 16 in Methods section 2.2.2.3. Briefly, on days 0 and 10, animals were sensitized and challenged every other day from day 21 for a total of 6 inhalations. Calcilytic or FP treatments were given twice daily from day 26.

4.3.4 BALF collection and analysis

Following the measurement of non-invasive lung function, BALF was collected as described in Methods section 2.2.2.6 to determine total and differential inflammatory cell infiltration.

4.3.5 BALF differential cell counts with Leishman's staining protocol

BALF cells were spun onto slides using Cytospin centrifugation. After this, the slides were air-dried, and stained with 0.15% Leishman's solution to count differential cell counts. At least 300 cells were counted and 4 different cell types, eosinophils, neutrophils, lymphocytes and macrophages, were counted according to the method described in the above Methods section 2.2.2.7.

4.4 Results

4.4.1 Comparison of the effect of inhaled calcilytic NPS89636 to inhaled FP on inflammatory cell infiltration in BALF in acute murine asthma model.

In order to compare the ability of inhaled calcilytics to suppress acute airway inflammation with that of the current standard of care, inhaled FP, I employed a short-term OVA-sensitized, OVA-challenged murine asthma model where animals were challenged twice in one day before the BALF collection (Figure 15). The results from the BALF total cell counts and differential cell counts demonstrated that inhaled calcilytic (3 μM NPS89636) significantly inhibited total leucocyte infiltration in the BALF in a magnitude that is similar to that one achieved by FP inhalation (0.5 mg/day). Moreover, the calcilytic was able to suppress eosinophil infiltration in the BALF significantly (Figure 29).

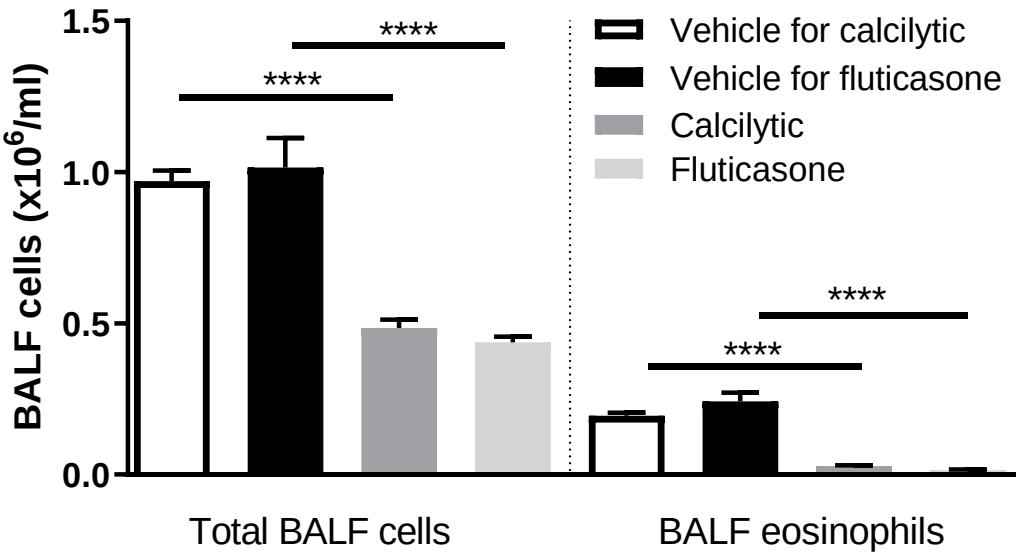

Figure 29. Effect of NPS89636 and fluticasone propionate (FP) on Bronchoalveolar lavage fluid (BALF) leucocyte cell count in the short-term asthma model.

This work was conducted by my colleague Polina Yarova. BALB/c male mice (5 weeks) were sensitized on days 0 and 5 by an i.p. injection of 250 µL 0.2 mg/mL OVA (50 µg /mouse) and 10% (50 mg/mouse) aluminium hydroxide in phosphate buffered solution (PBS). Fourteen days after the last injection, mice were challenged by inhalation of a 20 mL 5 mg/mL OVA aerosol for one hour twice on the same day, 4 h apart (Figure 15). Calcilytic (NPS89636, 3 µM, dissolved in 0.3% DMSO in PBS, 10 mL), FP (0.5 mg/day, dissolved in 25% DMSO, 50% EtOH in PBS, 10 mL), or respective vehicle treatment is at 1 hour prior to the first OVA challenge and 4 hours post the last OVA challenge. Bronchoalveolar lavage fluid (BALF) samples were collected at the end of the experiment. Inhaled calcilytic significantly inhibited total leucocyte infiltration and eosinophil infiltration in a magnitude similar to FP in the BALF. N=4-6 animals per experimental group. Data are presented as Mean ± SEM. P-values are from one-way ANOVA with Bonferroni's *post hoc* test, ****: $p<0.0001$.

In conclusion, in this short-term asthma model, I was able to determine that inhaled NPS89636 inhibits inflammatory cell infiltration in the BALF, with an effect comparable to that of inhaled FP. However, in this model, I used

different vehicles for calcilytic and FP, which may partly affect the comparison. So, in the next step, I aimed to use the same vehicle for both drugs.

4.4.2 Vehicle optimization

Since inhaled calcilytic showed an inhibitory effect similar to inhaled FP in the OVA-induced asthma, as a further development, I wanted to compare the therapeutic effect of inhaled calcilytic to that of inhaled FP in a longer-term asthma model. In order to make a better comparison, I set out to find the optimal vehicle for these two agents that did not cause significant airway irritancy by dissolving them in different vehicles, and by determining the effects of nebulized drugs on airway obstruction (by plethysmography), and by measuring airway inflammation (by measuring BALF cell infiltration). First of all, a stock solution was prepared in DMSO at a concentration of 12 mM. On the day of measurement, the stock solution was diluted in the corresponding vehicle to the desired working concentration.

1. 25% DMSO + 50% ethanol + 25% Saline

To find the optimal vehicle that works for both calcilytic and FP, initially, I used the vehicle that we used in our previous experiment for calcilytic, 25% DMSO + 50% ethanol + 25% PBS. However, FP did not completely dissolve in this vehicle, as shown in the Figure below (Figure 30).

Figure 30. Solubility test of 0.5 mg FP in 1 mL of 25% DMSO, 50% ethanol, and 25% PBS.

FP did not completely dissolve in 25% DMSO + 50% ethanol + 25% PBS, with a lot of precipitate in the solution.

2. 30% ethanol + 70% Saline

I then tried 30% ethanol as a vehicle since that has been used previously to dissolve FP (Escotte et al. 2002). My results showed that, while FP dissolved completely in this vehicle, it precipitated in the nebulizer after the nebulization. This is likely to be due to the fact that ethanol volatilized faster than nebulized saline during the nebulization, leaving only saline being nebulized at the later phase, while given its hydrophobic nature, FP cannot be dissolved in aqueous saline solutions.

3. 1% DMSO + 0.1% Tween 80

I next tried 1% DMSO + 0.1% Tween 80, because Tween 80 can be used to increase the solubility of the drugs, because it has been previously used to dissolve FP (Patterson et al. 2012) and also because it has been used to dissolve human drugs (such as FP spray) (*Pirinase Allergy 0.05% Nasal Spray - Summary of Product Characteristics (SmPC)* 2023). The result of the dissolution test showed that FP completely dissolved in this vehicle, yielding a clear, colorless liquid (Figure 31). However, when I then measured the total number of BALF cell infiltration in the vehicle group, I found that its administration resulted in an increase in inflammatory cell infiltration, though this increase was not statistically significant (Figure 32). Analysis of whole-body plethysmography showed that the change of Penh after the challenge with the vehicle relative to before the challenge (∆Penh) increased compared to the naïve animals, indicating some irritancy effect of this vehicle (Figure 33).

Figure 31. Solubility test of 0.5 mg FP in 1 mL of 1% DMSO and 0.1% Tween 80.

FP completely dissolved in 1% DMSO + 0.1% Tween 80.

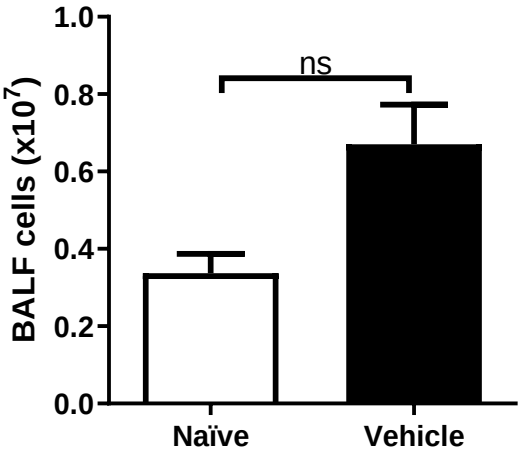

Figure 32. Total cell counts of the naïve and vehicle-treated BALB/c male mice

Male BALB/c mice (5 weeks) were divided into naïve control and vehicle groups. Animals in the naïve control group are naïve BALB/c male mice without treatment. Animals in the vehicle group were challenged with vehicle (1% DMSO + 0.1% Tween 80) twice daily for 6 days. N=4-6 animals per experimental group. Data are presented as Mean ± SEM. P-values are from unpaired t-test, ns: not-significant. The total cells in the vehicle group

increased compared to that of the naïve animals, but the difference did not reach significance.

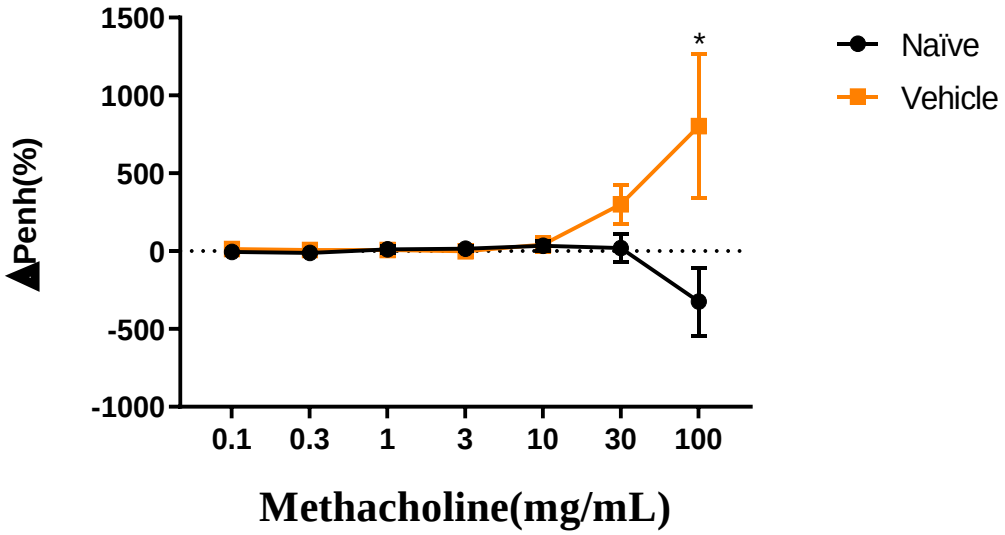

Figure 33. ΔPenh of the naïve and vehicle-treated BALB/c male mice measured by plethysmography

Male BALB/c mice (5 weeks) were divided into naïve control and vehicle groups. Animals in the naïve control group are naïve mice without treatment. Animals in the vehicle group were challenged with vehicle (1% DMSO + 0.1% Tween 80) twice daily for 6 days. N=4-6 animals per experimental group. Data are presented as Mean ± SEM. P-values are from unpaired t-test for each points, *: $p < 0.05$. ΔPenh significantly increased in the vehicle group compared to that measured for the naïve animals.

4. 0.3% DMSO + 0.01% Tween 80

Finally, I further decreased the concentrations of DMSO and Tween 80 to 0.3% and 0.01%, respectively. The result of the dissolution test also showed that FP completely dissolved in this vehicle, resulting in a clear, colorless liquid (Figure 34). The total BALF cells infiltration and whole-body plethysmography showed no significant effects of the vehicle, indicating there was no induction of airway irritancy when this vehicle was used (Figure 35 and Figure 36). As NPSP-795 also fully dissolved in this vehicle, I used it for

both FP and NPSP-795 in my future studies aimed at testing the effects of inhaled NPSP-795 in an *in vivo* therapeutic asthma model.

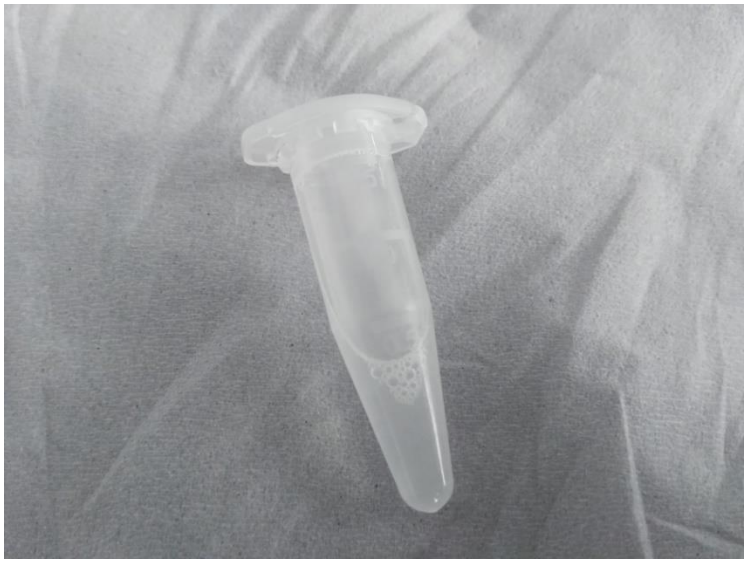

Figure 34. Solubility test of 0.5 mg FP in 1 mL of 0.3% DMSO and 0.01% Tween 80.

FP completely dissolved in 0.3% DMSO + 0.01% Tween 80 PBS solution.

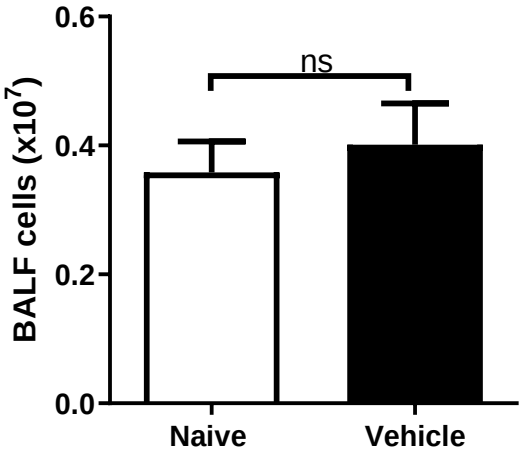

Figure 35. Total cell counts of the naïve and vehicle-treated male BALB/c mice

Male BALB/c mice (5 weeks) were divided into naïve control and vehicle groups. Animals in the naïve control group are naïve mice without treatment. Animals in the vehicle group were challenged with vehicle (0.3% DMSO + 0.01% Tween 80 PBS solution) twice daily for 6 days. N=4-6 animals per experimental group. Data are presented as Mean ± SEM. P-values are from

unpaired t-test, ns: not-significant. There is no statistical difference in the total cells infiltrated into the BALF in the vehicle group compared to the naïve animals.

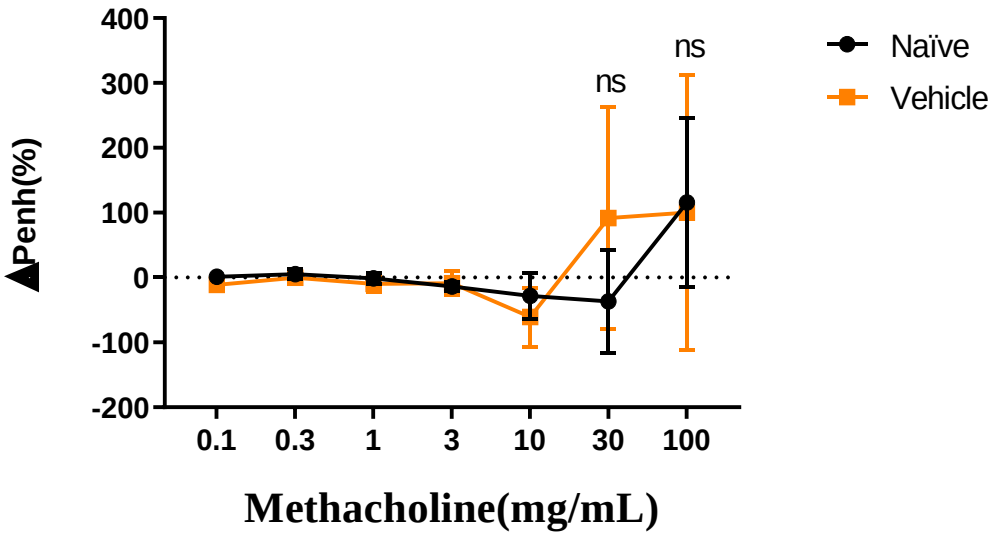

Figure 36. ΔPenh of the naïve and vehicle-treated male BALB/c mice measured by plethysmography

Male BALB/c mice (5 weeks) were divided into naïve and vehicle groups. Animals in the vehicle group were challenged with vehicle (0.3% DMSO + 0.01% Tween 80 PBS solution) twice daily for 6 days. N=4-6 animals per experimental group. Data are presented as Mean ± SEM. P-values are from unpaired t-test for each point, ns: not-significant. There is no difference in ΔPenh in the vehicle group compared to the naïve animals.

4.4.3 Comparison of the effect of inhaled calcilytic and inhaled FP on inflammatory cell infiltration in BALF in a longer-term murine asthma model.

Once I had identified a suitable vehicle that allowed me to dissolve both FP and the calcilytic NPSP-795, I went on to investigate how well the inhaled calcilytic performs in comparison to the current standard of care, inhaled FP, at suppressing airway inflammation. To this end, I employed a previously established OVA-sensitized OVA-challenged murine asthma model where animals were challenged every other day for twelve days to achieve a strong and robust inflammation (Figure 16). Aerosolised calcilytic inhalation (6 μM NPSP-795) was able to significantly suppress total leucocyte infiltration and eosinophil infiltration in a magnitude similar to the one achieved by FP

inhalation (0.5 mg/day)

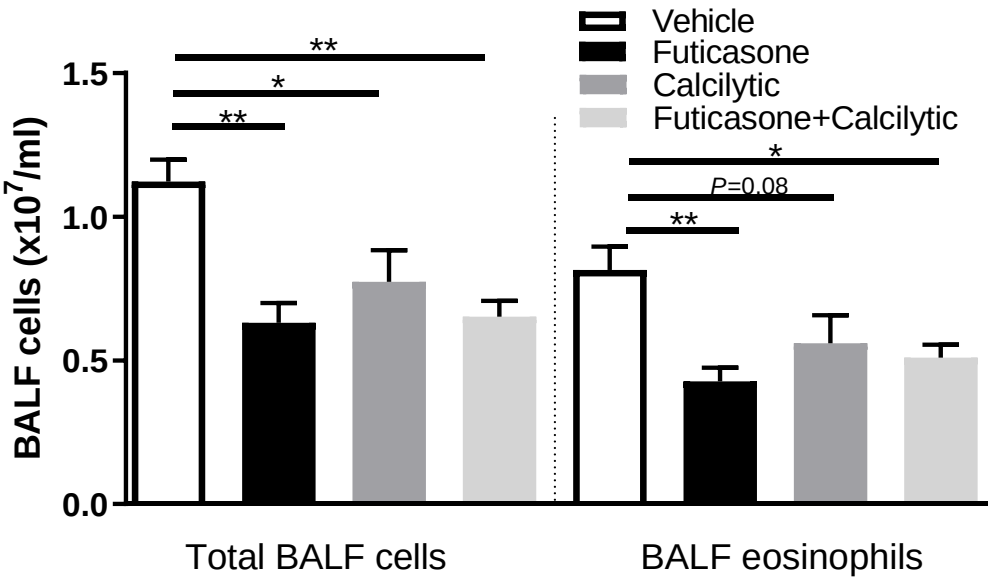

(

Figure 37). Combined treatment with both calcilytic and FP resulted in an effect that was similar to the one produced by each of the compounds individually

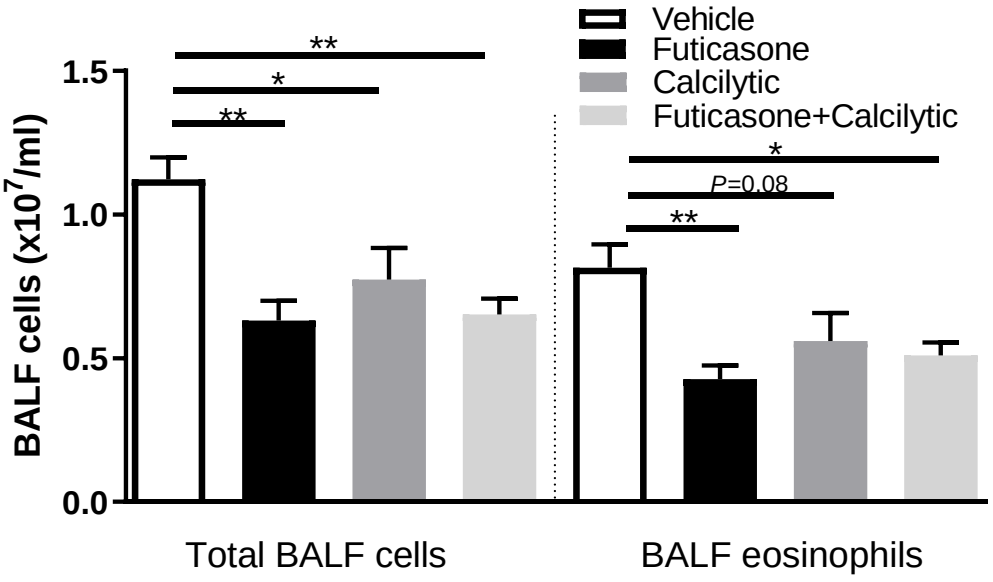

(

Figure 37), showing there were no additive effects of calcilytic and ICS.

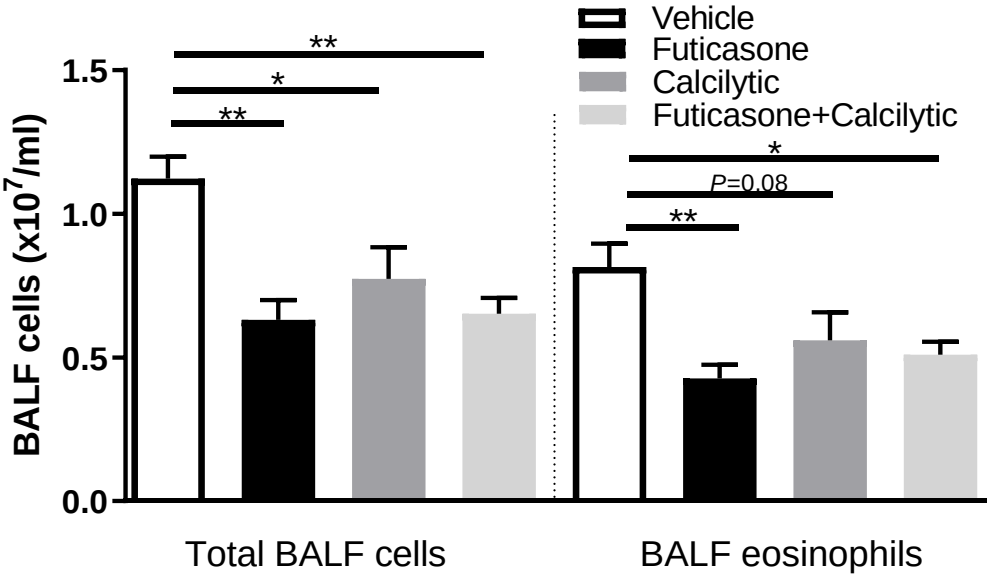

Figure 37. BALF leucocyte cell count from male BALB/c mice in the longer-term asthma model.

Male BALB/c mice (5 weeks) were sensitized on days 0 and 10 by i.p. injection of 250 µL 0.2 mg/mL OVA (50 µg /mouse) and 10% (50 mg/mouse) aluminium hydroxide in PBS. After the sensitization, mice were challenged by inhalation of a 0.5% OVA aerosol for one hour from day 21, and the OVA challenges continued every other day for 11 days. From day 26, twice daily calcilytics (6 µM NPSP-795, 10 ml, 30 min), FP (0.5 mg/day, 10 ml, 30 min) or vehicle (0.3% dimethyl sulfoxide (DMSO) +0.01% Tween-80) treatments were performed at 1 hour prior to the OVA challenge and 8 hours after the previous one. Inhaled NPSP-795 and FP (0.5 mg/day) both significantly suppress total leucocyte infiltration and eosinophil infiltration to a comparable magnitude, with no additive effect of calcilytic and steroid. N=4-6 animals per experimental group. Data are presented as Mean ± SEM. P-values are from one-way ANOVA with Bonferroni's *post hoc* test, *: $p<0.05$, **: $p<0.01$.

4.4.4 Comparison of the effect of inhaled calcilytic to the inhaled FP on goblet cell hyperplasia in a longer-term murine asthma model.

After I found that inhaled calcilytic was able to inhibit total cell infiltration and eosinophil infiltration in BALF, I compared their effect on goblet cell hyperplasia. This work was conducted by my colleague Richard Bruce using StrataQuest image analysis software. Quantitative image analysis revealed

that inhaled NPSP-795 reduced goblet cell hyperplasia as demonstrated by a reduction of the mean goblet cell number in the airways, whereas inhaled FP did not show any effects (Figure 38B).

A

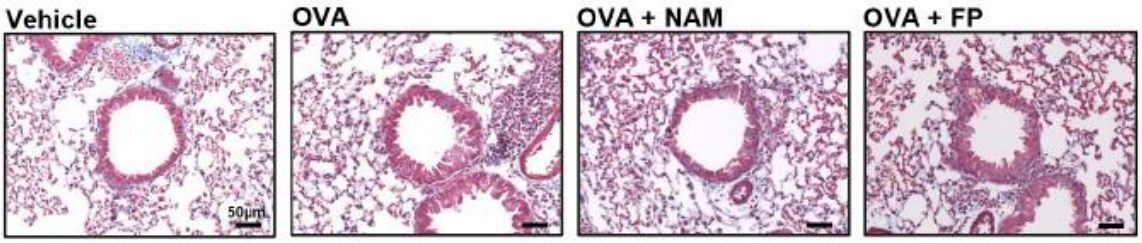

B

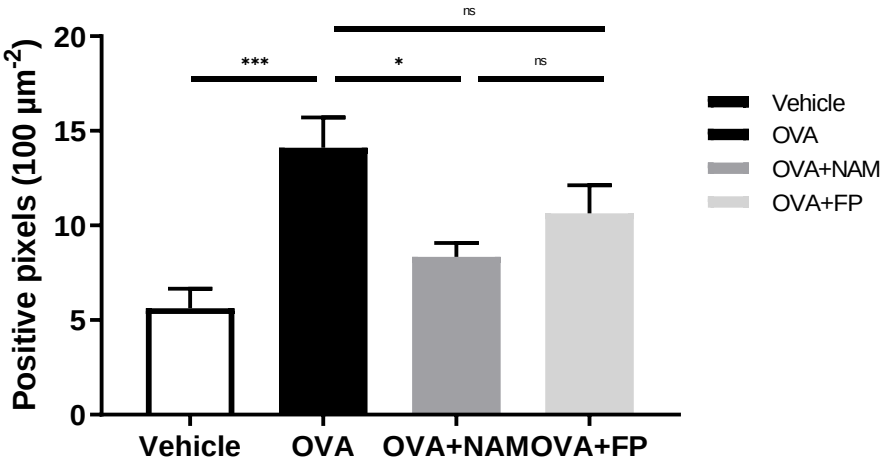

Figure 38 (A) Representative images of Masson's trichrome-stained slides and (B) The effects of inhaled NPSP-795 or FP on goblet cells. The effects of inhaled NPSP-795 (6 µM) or FP (0.5 mg/day) on goblet cells were quantified using StrataQuest image analysis software conducted by my colleague Richard Bruce. Briefly, regions of interest were manually drawn, and the percentage of positive goblet cells was calculated. N = 6 animals per experimental group. Data are presented as Mean ± SEM. P-values are from one-way ANOVA with Holm-Sidak's post hoc test. ns: not-significant, *: P<0.05, ***: p < 0.001.

4.5 Discussion

The most common treatment of asthma is bronchodilators, β-adrenoceptor agonists, and anti-inflammatory corticosteroids, or in some severe patients require therapy with the combination of them (Global Initiative for Asthma 2023). However, all of them raise safety concerns, compliance issues and are ineffective even when used in combination in some patients (Kim et al. 2009; Sadatsafavi et al. 2010; O'Neill et al. 2015). Therefore, a safe and effective single treatment that has effect on both inflammation and AHR would be highly advantageous (Page and Cazzola 2014). In one of our previous papers, we have already demonstrated that inhaled calcilytics have the potential to abolish AHR in a safe and steroid-independent fashion (Yarova et al. 2015). So, in this study, I compared the therapeutic effect of inhaled calcilytic with the current SOC, inhaled corticosteroid in the OVA-induced asthma model.

FP is the most common corticosteroid used in clinical, however it is poorly soluble in common solvents. From the previous study, the common solvents and route of administration used in the animal models are saline:dimethyl sulfoxide (DMSO):ethanol (40:30:30) by aerosol (Evans et al. 2012), DMSO in saline and administered intranasally (Kimura et al. 2013), DMSO in PBS and intratracheal treatment (Wakahara et al. 2008), Tween-20 in PBS and through intranasal (i.n.) administration (Ravanetti et al. 2017), Tween-80 in sterile saline via nebulization (Patterson et al. 2012). However, I tried DMSO:ethanol in saline, DMSO in PBS, Tween-20 in PBS, and Tween-80 in sterile saline, which all failed to dissolve the drug, or evoked airway irritancy. Instead, I found that Tween-80 in sterile saline with DMSO is the best vehicle, with good solubility and low toxicity. So, I used 0.3% DMSO + 0.01% Tween 80 as the vehicle to dissolve both FP and calcilytic for our further studies.

Inflammatory cells and eosinophil infiltration are the major characteristics of asthma (Hamid et al. 2003), so in my study, I measured the total cell and eosinophil counts in BALF. Both inhaled calcilytic and steroid reduced the inflammatory cells and eosinophil infiltration; however, there were no additive effects of calcilytic and steroid. In addition, inhaled calcilytic can reduce goblet cell hyperplasia, while inhaled FP did not, suggesting that they might show greater efficacy than steroids, thereby representing a novel, first-in-class

asthma treatment. These findings align with a previously published study indicating that CaSR NAMs reduce mucus production in human epithelial cells stimulated by tobacco smoke (Lee et al. 2017a). This suggests that long-term use of inhaled CaSR NAMs could potentially protect airway integrity and mitigate irreversible airway obstruction caused by remodelling.

Overall, my results indicate that treatment with inhaled calcilytic exerts comparable efficacy to that of inhaled steroid FP in suppressing airway inflammation and superior efficacy to that of inhaled steroid FP in reducing goblet cell hyperplasia in an asthma model. Thus, this approach could empower disease management for asthmatics worldwide whilst avoiding regular steroid exposure.

Chapter V Testing the efficacy of inhaled calcilytic in OVA and IL-33-induced asthma models.

5.1 Introduction

Although the majority of asthmatics respond well to steroid therapies, approximately 30% of severe asthmatics are steroid-refractory (Rhen and Cidlowski 2005; Barnes 2010b; Chung et al. 2014). Also, steroid-resistant asthma (SRA) occurs in ~10% of the total asthmatic population, but it accounts for up to 90% of the total asthma healthcare costs, which costs over $8 billion/ year in Europe, USA, and Australia combined (Shaw et al. 2007; WHO. 2024). Thus, effective treatments for severe, steroid-resistant asthma are urgently required. Recently, several biologics including reslizumab, mepolizumab, benralizumab and omalizumab have been approved for the treatment of moderate-to-severe asthma and found to improve lung function in patients with severe asthma (Busse et al. 2013; Hanania et al. 2013; Bel et al. 2014; Gauvreau et al. 2014; Humbert et al. 2014; Ortega et al. 2014; Brightling et al. 2015; Castro et al. 2015; Krug et al. 2015; Bjermer et al. 2016; Bleecker et al. 2016; Corren et al. 2016; FitzGerald et al. 2016; Wenzel et al. 2016; Saco et al. 2017; *CINQAIR® (reslizumab) Injection – About CINQAIR* 2020; *NUCALA® (mepolizumab) prescribing information* 2023; *XOLAIR® (omalizumab) prescribing information* 2024). However, unlike other medications for asthma, most biologics are currently administered as a subcutaneous injection or as an intravenous infusion which is not easy for patients to use. In addition, biologics are more expensive compared to other medications for asthma. Therefore, the development of new therapies offering both convenience and lower costs are needed.

IL-33 is an epithelial-derived cytokine, first discovered in 2005 (Schmitz et al. 2005), which is released after cell injury or infection, so it functions as an alarmin to alert the innate immune system (Pichery et al. 2012). After being discovered, IL-33 has been found to be expressed in a variety of organs in human, including lung tissue, skin, lymph nodes, spleen, kidney, heart, stomach and pancreas(Schmitz et al. 2005; Liew et al. 2010). IL-33 is mainly expressed in fibroblasts, smooth muscle cells, and epithelial cells as well as some inflammatory cells, including endothelial cells, macrophages and dendritic cells (Moussion et al. 2008; Préfontaine et al. 2010; Pichery et al.

2012; Nabe 2014). IL-33 is released after epithelial barrier injury to induce NF-κB phosphorylation and MAPK activation and TH2 cytokine production, eosinophilia, and increased levels of serum IgA and IgE after binding with its ligand ST2 in cells that express ST2 (Schmitz et al. 2005). In asthma patients, IL-33 is highly expressed in the serum, sputum and lung tissue, especially those from severe asthmatics, where IL-33 expression increases significantly (Préfontaine et al. 2009). IL-33 can promote collagen synthesis by fibroblasts in children with severe steroid-resistant asthma, indicating that IL-33 also plays a role in airway remodelling (Olin and Wechsler 2014). In addition, accumulating data show that levels of IL-33 are increased in asthma patients compared to the control group, especially in patients with severe asthma, suggesting that IL-33 may be an inflammatory marker of severe and steroid-resistant asthma (Préfontaine et al. 2009; Israel and Reddel 2017).
Because of the important role of IL-33 in severe and steroid-resistant asthma, Li Yan et al. compared OVA and IL-33-induce asthma mouse models at different time points and found that, compared to OVA-induced asthma, IL-33 induced a later and more persistent lung neutrophilic infiltration (Li et al. 2015). It is well established that steroid-resistant asthma is associated with an increased number of neutrophils that is non-allergic (Alam et al. 2017) although the exact pathogenesis is still not clear. Our previous studies showed that inhaled calcilytics can suppress both neutrophilic and eosinophilic inflammation induced by LPS and OVA (Yarova et al. 2015; Yarova et al. 2016). Thus, I hypothesized that inhaled calcilytics can attenuate airway inflammation and airway remodelling in Th2/IgE- and alarmin (IL-33)-driven asthma murine models *in vivo*.

5.2 AIMS AND OBJECTIVES

5.2.1 AIMS

The aim of this chapter was to test the effects of inhaled calcilytics in Th2/IgE- and IL33-driven asthma models *in vivo*.

5.2.2 OBJECTIVES

1) To develop parallel, therapeutic Th2/IgE- and IL33-driven murine asthma models *in vivo*;

2) To compare the effects of inhaled calcilytic NPSP-795 in the above two models, with specific emphasis on airway hyperresponsiveness, airway inflammation, eosinophilia, mucus production and collagen deposition;
3) To determine the systemic effects of topically delivered NPSP-795 by measuring serum Ca^{2+} levels in animals exposed to intranasal instillations of this calcilytic.

5.3 Materials and Methods

5.3.1 Animals

This part of work was conducted in a pathogen-free mouse facility from the Department of Laboratory Animal Sciences, Capital Medical University, Beijing, China under constant temperature and light cycles. All animal experiments were conducted following protocols and regulations approved by the Institutional Animal Care and Use Committee at Capital Medical University (Licence number: SYXK (Jing) 2018-0002). Female BALB/c mice (6-8 weeks) were purchased from Vital River Laboratories (Beijing, China), housed in groups of 5 in each cage, with *ad libitum* access to certified pelleted commercial laboratory diet and water, with enrichment devices provided in the cages.

5.3.2 Th2/IgE-driven asthma model

5.3.2.1 Sensitisation

Mice were randomly assigned into different groups and sensitized first by an intraperitoneal injection of OVA (Sigma-Aldrich, Missouri, United States, 100 μg emulsified in $AL[OH]_3$/dose)/ saline on day-17 and day-5.

5.3.2.2 Ovalbumin Challenges

As described in

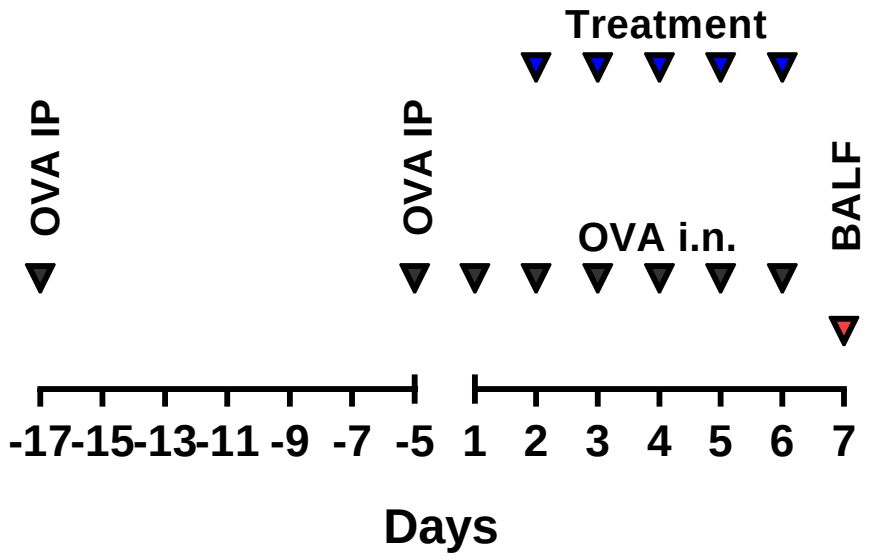

Figure 19, animals were intranasally given OVA (50 µg/mouse) or saline from day 1 to day 6 for 6 days after the initial sensitisation. From day 2, NPSP-795 (200 µg/mouse in 50 µL vehicle) or vehicle (0.3% DMSO in saline) were given twice daily, 2h before OVA administration.

5.3.3 Alarmin-driven asthma model

For the alarmin-driven asthma model, sensitisation is not needed because IL-33 can induce asthma symptoms independently of IgE production (Saikumar Jayalatha et al. 2021). Animals were given IL-33 intranasally (Mouse IL-33 Recombinant Protein, R&D Systems, Minneapolis MN, USA, 30 ng/mouse in 50 µL saline) or saline from day 1 to day 6 for 6 days. From day 2, NPSP-795 (200 µg/mouse in 50 µL vehicle) or vehicle (0.6% DMSO in saline) were given twice daily, 2h before IL-33 administration. The details of the administration protocol can be found in

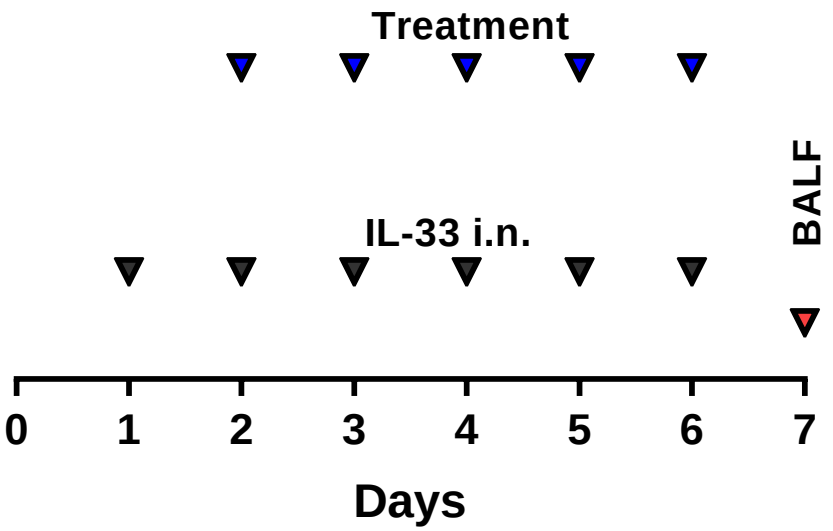

Figure 20 in Methods section 2.2.3.2.

5.3.4 Invasive lung function measurements

On Day 7, mice were anesthetized by intraperitoneal injection of 80 mg/kg body weight phenobarbital sodium (Sigma-Aldrich, Missouri, United States), tracheostomized and ventilated through the tracheal intubation in the supine position then tested as follows: (1) mechanical ventilation with 21% O_2, a respiratory rate of 150 breaths/min, a positive end-expiratory pressure (PEEP)

of 2 cmH_2O, and a tidal volume of 10 ml/kg; (2) block the exhalation to increase the intrapulmonary pressure to 30 cmH_2O and continue for 5 s to open the atelectatic part of lung tissue when the mouse breathes smoothly to make sure all the animals are at the same baseline level; (3) After 2 minutes, when the PEEP is 2 cmH_20, the single compartment model (SnapShot-150) and the constant phase model (Prime-8) were used to measure the respiratory function parameters respiratory resistance (Rrs), central airway resistance (Rn), respiratory elastance (Ers), tissue elastance (H) and tissue damping(G). Concentrations of 0, 6, 12, 24 and 48 mg/ml methacholine (Sigma-Aldrich, Missouri, United States) were delivered via a nebulizer.

5.3.5 Blood collection and process

Following the measurement of airway hyperresponsiveness, blood samples were collected from the retro-orbital venous plexus. The blood was then stored overnight at 4℃, after which it was centrifuged at 2,300 g at 4℃ for 20 minutes to collect the serum. The serum was stored at -80 ℃ until use for analysis of free ionised Ca^{2+} concentrations.

5.3.6 BALF collection and process

After blood collection, BALF samples were collected by injection of 2 x 0.8 ml pre-cooled sterile PBS buffer through tracheal intubation and each lung was lavaged 3 times to yield at least 1.2ml BALF. The collected BALF samples were centrifuged at 300 g for 10 minutes at 4℃, and the resulting supernatants were collected and stored at -80°C until cytokine detection. 200 µL red blood cell lysis buffer (Beijing Solarbio Technology Co Ltd, Beijing, China) was added to the remaining cell pellets, mixed and kept at room temperature for 4 minutes to remove the red blood cell contamination, after that 1 ml PBS was added, and centrifuged at 300 g for 10 minutes at 4℃ to remove the supernatants. The cell pellets were resuspended with 1 ml PBS and the number of total cells were counted using a hemocytometer (CellPath, Powys, United Kingdom) under the microscope (Nikon, Tokyo, Japan) using x20 magnification.

5.3.7 Differential cell counts

After measurements of total cell counts, cytospins were prepared from 100 µL of cell suspension, dried and fixed with 4% paraformaldehyde for 10-20 minutes. The slides were stained with Congo red staining (Beijing Solarbio Technology Co Ltd, Beijing, China) to count the differential cells (eosinophils, lymphocytes, neutrophils and macrophages) as described previously (E et al. 2012). At least 300 total cells were counted for each slide.

5.3.8 Tissue collection

Lung tissue was collected after all the experiments were done and fixed with 10% neutral formalin for 24h. On the next day, the lungs were paraffin-embedded and prepared for sectioning (nominal 4-µm thickness). The right lung tissue was homogenized and stored at -80 ℃ until analysis.

5.3.9 Preparation of lung tissue homogenate

The weight of the right lung was weighed and recorded using an electronic balance (Adventurer Analytical Balance, New Jersey, United States). The appropriate volume of tissue homogenate solution containing protease inhibitor was added according to the weight of the lung tissue. Tissue homogenate was then obtained using a tissue homogenizer (Wuhan Servicebio Technology Co., Ltd, Wuhan, China) by 10 working cycles with working for 40s and intermittent for 10s. The resulting homogenate was centrifuged at 13200 g for 10 minutes at 4 ° C. The supernatant was stored at -80 ℃ until analysis.

5.3.10 Histological staining and quantification

The 4-µm thickness slides were stained with haematoxylin and eosin (Sigma-Aldrich, Missouri, United States), Congo red, periodic acid-Schiff (PAS) (Beijing Yi Li Fine Chemicals Co Ltd, Beijing, China) and Masson’s trichrome (MT) blue (Nanjing Mindit Biochemistry Co Ltd, Nanjing, China) staining to examine inflammatory cellular and eosinophil infiltration into the lung tissue, mucus productions and collagen deposition in the lung peribronchial and perivascular regions, respectively. Stained slides were scanned via the Olympus BX40 slide scanner system (Olympus Corporation, Shinjuku, Tokyo,

Japan) at ×20 magnification and then quantified objectively using TissueFAXS image analysis software StrataQuest (TissueGnostics, Vienna, Austria) as described in Figure 24 and Figure 25.

5.3.11 Quantitative image analysis method for Masson's trichrome-stained slides using StrataQuest

I used Masson's trichrome-staining to quantify collagen deposition. First, I drew the airway lumen with yellow and the airway epithelium with green to identify the airway. Then I drew 7 peribronchial rings extending away from the airway epithelium in increments of 30 µm. The area of stained collagen in each ring and the total area (µm^2) of each ring were automatically calculated by the software. Then, the percentage of collagen area in the total ring area was calculated as the readout. A detailed explanatory figure can be found in Figure 24 in Methods section 2.2.2.1.

5.3.12 Quantitative image analysis method for H&E and Congo-stained slides using StrataQuest

As with Masson's trichrome-stained slides, I first identified the airway by drawing the airway lumen with yellow and the airway epithelium with green. The number of total cells (with H&E Staining) or positive stained cells (with Congo Red Staining) around the peribronchial region and the total area (µm^2) of tissue was automatically calculated by the software. Then, the number of cells per 10000 µm^2 area tissue was calculated as the readout. A detailed explanatory figure can be found in Figure 25 in Methods section 2.2.2.1.

5.3.13 Quantitative image analysis method for PAS-stained slides using StrataQuest

For the PAS-stained slides, the airways were identified by drawing the airway epithelium with green. The number of positive stained cells (PAS Staining) on the airway and the total area (µm^2) of airway were automatically calculated by the software. Then the number of positive cells per 10000 µm^2 area tissue was calculated as the readout. Figure 24

5.4 Results

5.4.1 Effect of inhaled NPSP-795 on BALF inflammatory cell infiltration in Th2/IgE- and alarmin-driven asthma models

To investigate the effect of inhaled NPSP-795 on the asthma symptoms evoked in these two asthma models, I first looked at the effect of inhaled NPSP-795 on inflammation, one of the major characteristics of asthma by measuring inflammatory cell infiltration into the BALF. Figure 39 shows that the total cell count dramatically increased in the OVA group. The cell population was mainly composed of eosinophils in this asthma model. Inflammatory cell infiltration into the BALF was significantly reduced by inhaled calcilytic in the OVA-induced model. Inflammation was not differentially affected in the IL-33 model (Figure 39 and Figure 40). For the differential cell counts, calcilytic significantly reduced eosinophil, neutrophil and lymphocyte infiltration induced by OVA and partially reduced eosinophil and neutrophil infiltration induced by IL-33 (Figure 39 and Figure 40).

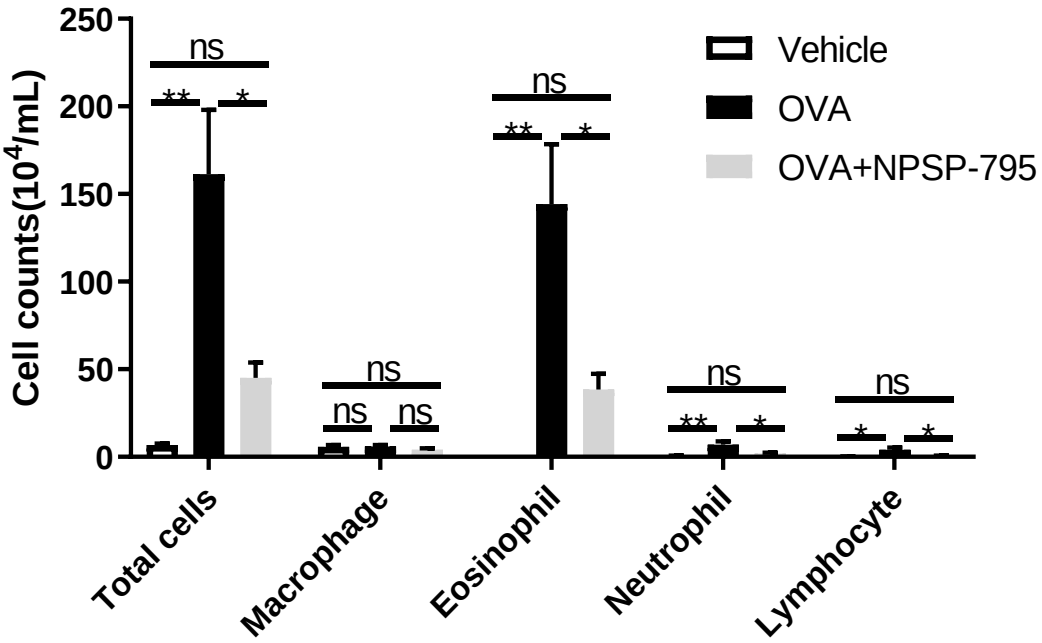

Figure 39. Effect of inhaled NPSP-795 on total cell and differential cell infiltration into the lung in the OVA-induced asthma model.

Female BALB/c mice (6-8 weeks) were sensitized by intraperitoneal injection of 100 µg OVA (OVA group and OVA + NPSP-795 group) or saline (Vehicle group) in $Al(OH)_3$ in 200 µL on days -17 and -5. After sensitisation, animals

were intranasally given OVA (50 μg/mouse in 50 μL saline, OVA group and OVA + NPSP-795 group) or saline (Vehicle group) from day 1 to day 6 for 6 days. From day 2, NPSP-795 (200 μg/mouse in 50 μL vehicle, OVA + NPSP-795 group) or vehicle (0.6% DMSO in saline, OVA group and Vehicle group) were given twice daily, with the evening dosing was given 2h before OVA administration. On day 7, Following the measurement of airway hyperresponsiveness and blood collection, BALF samples were collected and centrifuged at 300 g for 10 min at 4℃ to count the total cells using a hemocytometer under the microscope and the differential cells (eosinophils, lymphocytes, neutrophils and macrophages) using Congo red staining. At least 300 total cells were counted. Inflammatory cell infiltration into the BALF was significantly reduced by calcilytic in the OVA-induce model. For the differential cell counts, calcilytic significantly reduced eosinophil, neutrophil and lymphocyte infiltration induced by OVA. N= 6-7 animals per experimental group. Data are presented as Mean ± SEM. P-values are from one-way ANOVA with Bonferroni's post hoc test. ns: not-significant, *: P<0.05, **: P<0.01.

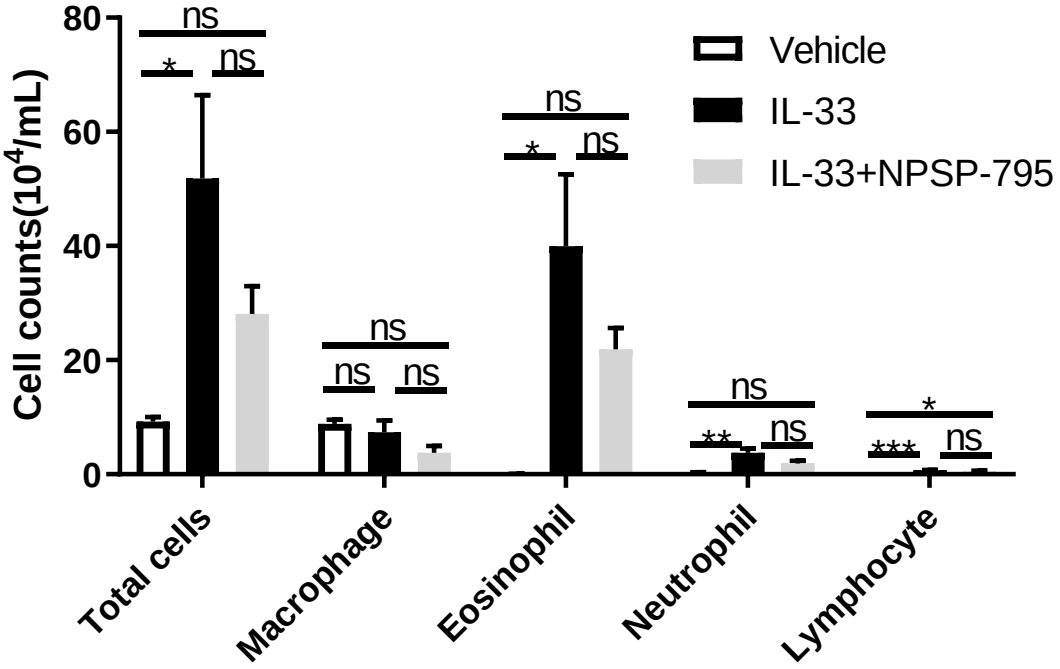

Figure 40. Effect of inhaled NPSP-795 on total cell infiltration into the lung in the IL-33-induced asthma model

Female BALB/c mice (6-8 weeks) were given IL-33 intranasally (30 ng/mouse in 50 µL saline, IL-33 group and IL-33+ NPSP-795 group) or saline (Vehicle group) from day 1 to day 6 for 6 days. From day 2, NPSP-795 (200 µg/mouse in 50 µL vehicle, IL-33 + NPSP-795 group) or vehicle (0.6% DMSO in saline, IL-33 group and Vehicle group) were given twice daily, with the evening dosing was given 2h before IL-33 administration. On day 7, Following the measurement of airway hyperresponsiveness and blood collection, BALF samples were collected and centrifuged at 300 g for 10 min at 4℃ to count the total cells using a hemocytometer under the microscope and the differential cells (eosinophils, lymphocytes, neutrophils and macrophages) using Congo red staining. At least 300 total cells were counted. There is a decreasing trend for total cell, eosinophil and neutrophil infiltration after inhaled NPSP-795 treatment; however, the reduction had no statistical significance. N= 8-9 animals per experimental group. Data are presented as Mean ± SEM. P-values are from one-way ANOVA with Bonferroni's *post hoc* test. ns: not-significant, *: $P<0.05$, **: $P<0.01$, ***: $p < 0.001$.

5.4.2 Effect of inhaled NPSP-795 on airway hyperresponsiveness in Th2/IgE- and IL33-driven asthma models

Airway hyperresponsiveness is a main feature of asthma, which is present in the majority of patients with asthma (Meurs et al. 2008). The presence of AHR is useful to assist in the clinical diagnosis of asthma in individuals presenting with symptoms and signs suggestive of asthma (Brannan and Lougheed 2012). In the present study, airway resistance induced by increasing concentrations of MCh was detected by the invasive approach using the FlexiVent system. In the OVA-sensitized and challenged mice, the respiratory resistance, respiratory elastance, tissue damping and tissue elastance all significantly increased, while central airway resistance didn't change significantly. However, only the respiratory resistance and elastance were significantly reduced by inhaled NPSP-795, while the other parameters were not significantly affected (Figure 41). In the IL-33 asthma model, there was increased respiratory resistance, respiratory elastance, tissue damping and tissue elastance, and all of these parameters were significantly reduced by inhaled NPSP-795 (Figure 42).

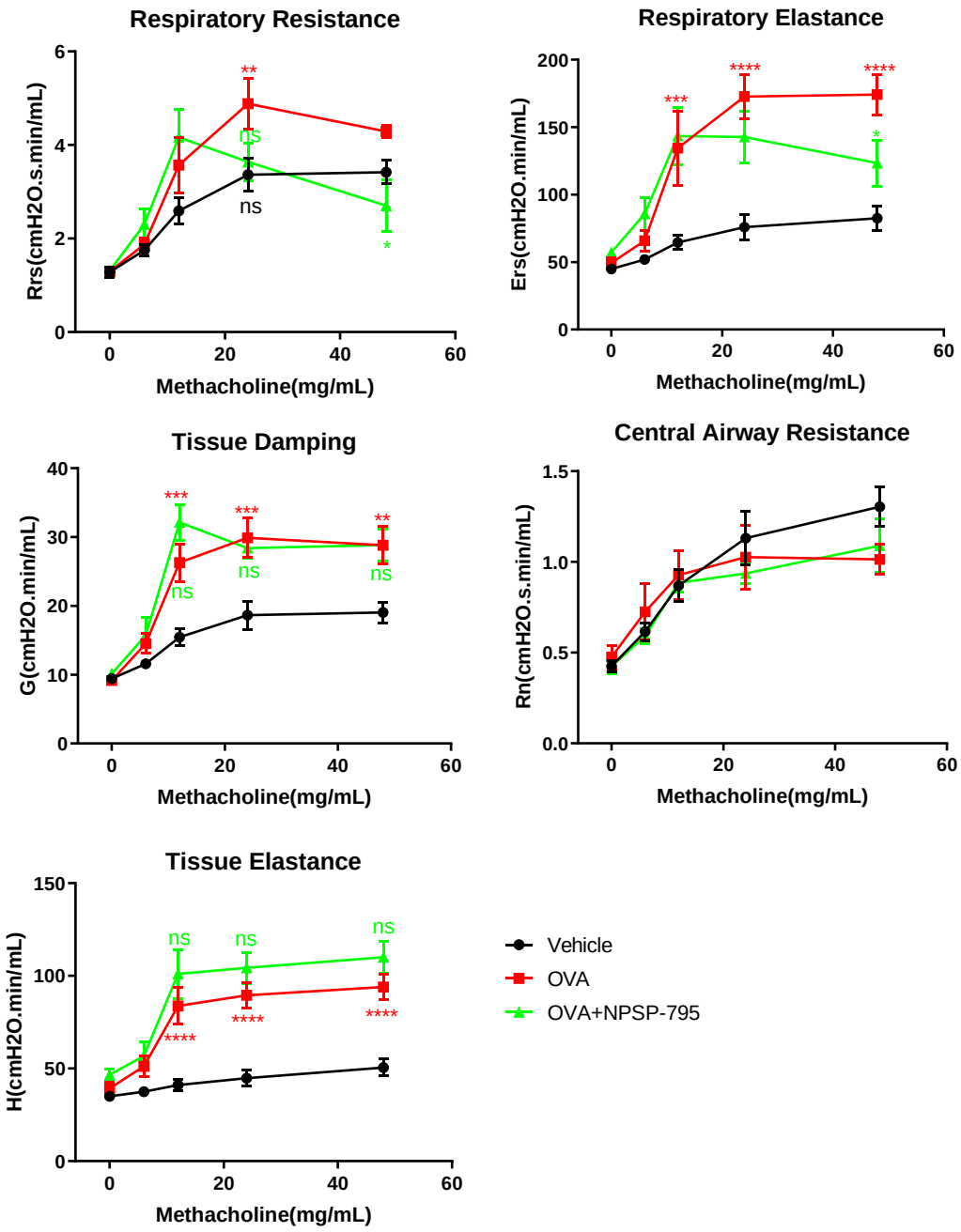

Figure 41. Effect of inhaled NPSP-795 on airway hyperresponsiveness in the OVA-induced asthma model.

Female BALB/c mice (6-8 weeks) were sensitized by intraperitoneal injection of 100 µg OVA (OVA group and OVA + NPSP-795 group) or saline (Vehicle group) in $Al(OH)_3$ in 200 µL on days -17 and -5. After sensitisation, animals were intranasally given OVA (50 µg/mouse in 50 µL saline, OVA group and OVA + NPSP-795 group) or saline (Vehicle group) from day 1 to day 6 for 6 days. From day 2, NPSP-795 (200 µg/mouse in 50 µL vehicle, OVA + NPSP-

795 group) or vehicle (0.6% DMSO in saline, OVA group and Vehicle group) were given twice daily, with the evening dosing was given 2h before OVA administration. On day 7, mice were anesthetized by intraperitoneal injection of 80 mg/kg body weight phenobarbital sodium, tracheostomized and ventilated through the tracheal intubation in the supine position to measure the respiratory function parameters respiratory resistance (Rrs), central airway resistance (Rn), respiratory elastance (Ers), tissue elastance (H) and tissue damping(G) (SCIREQ 2024) by applying concentrations of 0, 6, 12, 24 and 48 mg/ml MCh to see the effect on the airway hyperresponsiveness (AHR). AHR was significantly reduced by calcilytic in the OVA-induced asthma model. N= 6-7 animals per experimental group. Data are presented as Mean ± SEM. P-values are from one-way ANOVA with Bonferroni's *post hoc* test, **: P<0.01, ***: p < 0.001, ****: P<0.0001, "red *" represents Vehicle v.s. OVA, "green *" represents OVA v.s. OVA+NPSP-795. "black*" represents OVA+NPSP-795 v.s. Vehicle.

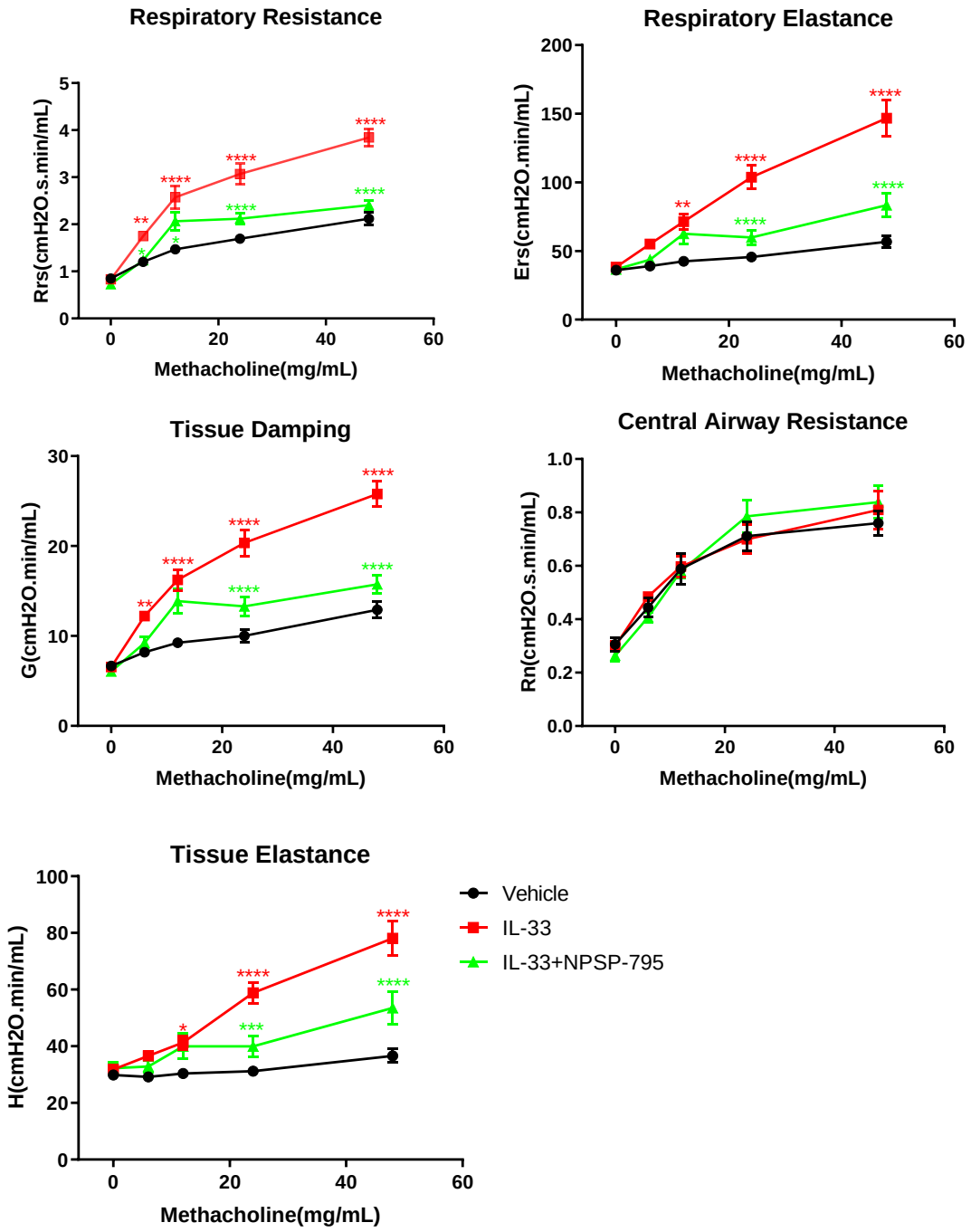

Figure 42. Effect of inhaled NPSP-795 on airway hyperresponsiveness in IL-33-induced asthma model.

Female BALB/c mice (6-8 weeks) were given IL-33 intranasally (30 ng/mouse in 50 µL saline, IL-33 group and IL-33+ NPSP-795 group) or saline (Vehicle group) from day 1 to day 6 for 6 days. From day 2, NPSP-795 (200 µg/mouse in 50 µL vehicle, IL-33 + NPSP-795 group) or vehicle (0.6% DMSO in saline, IL-33 group and Vehicle group) were given twice daily, with the evening

dosing was given 2h before IL-33 administration. On day 7, mice were anesthetized by intraperitoneal injection of 80 mg/kg body weight phenobarbital sodium, tracheostomized and ventilated through the tracheal intubation in the supine position to measure the respiratory function parameters Rrs, Rn, Ers, H and G by applying concentrations of 0, 6, 12, 24 and 48 mg/ml methacholine to see the effect on the airway hyperresponsiveness (AHR). Airway hyperresponsiveness was significantly reduced by inhaled calcilytic in IL-33-induced asthma model. N= 8 animals per experimental group. Data are presented as Mean ± SEM. P-values are from one-way ANOVA with Bonferroni's *post hoc* test, **: P<0.01, ***: p < 0.001, ****: P<0.0001, "red *" represents Vehicle v.s. IL-33, "green *" represents IL-33 v.s. IL33 +NPSP-795. "black*" represents IL-33 +NPSP-795 v.s. Vehicle.

5.4.3 Effect of inhaled NPSP-795 on cytokines in lung homogenate and BALF in Th2/IgE- and alarmin-driven asthma models

To further investigate the effect of inhaled NPSP-795 on inflammation, I next looked at the levels of cytokines that are typically involved in asthma pathogenesis, specifically IL-5, IL-13, IL-6 and TNF-α, in lung homogenate and in the BALF. In the OVA-induced asthma model, IL-5, IL-13 and IL-6 were all significantly increased in both lung homogenate and BALF (Figure 43). Albeit the above cytokines are all decreased in both lung homogenate and BALF by the inhaled NPSP-795, only the reduction in IL-6 in BALF reached statistical significance. However, the levels of IL-5, IL-13 and IL-6 between the vehicle and inhaled NPSP-795 group in both lung homogenate and BALF didn't show significant differences. In the IL-33-induced asthma model, IL-5, IL-13, IL-6 and TNF-α were all significantly increased in lung homogenate in the IL-33 group, while only IL-5 significantly increased in BALF. Among the increased levels of cytokines, only IL-5 showed a significant decrease in the inhaled NPSP-795 group (Figure 44).

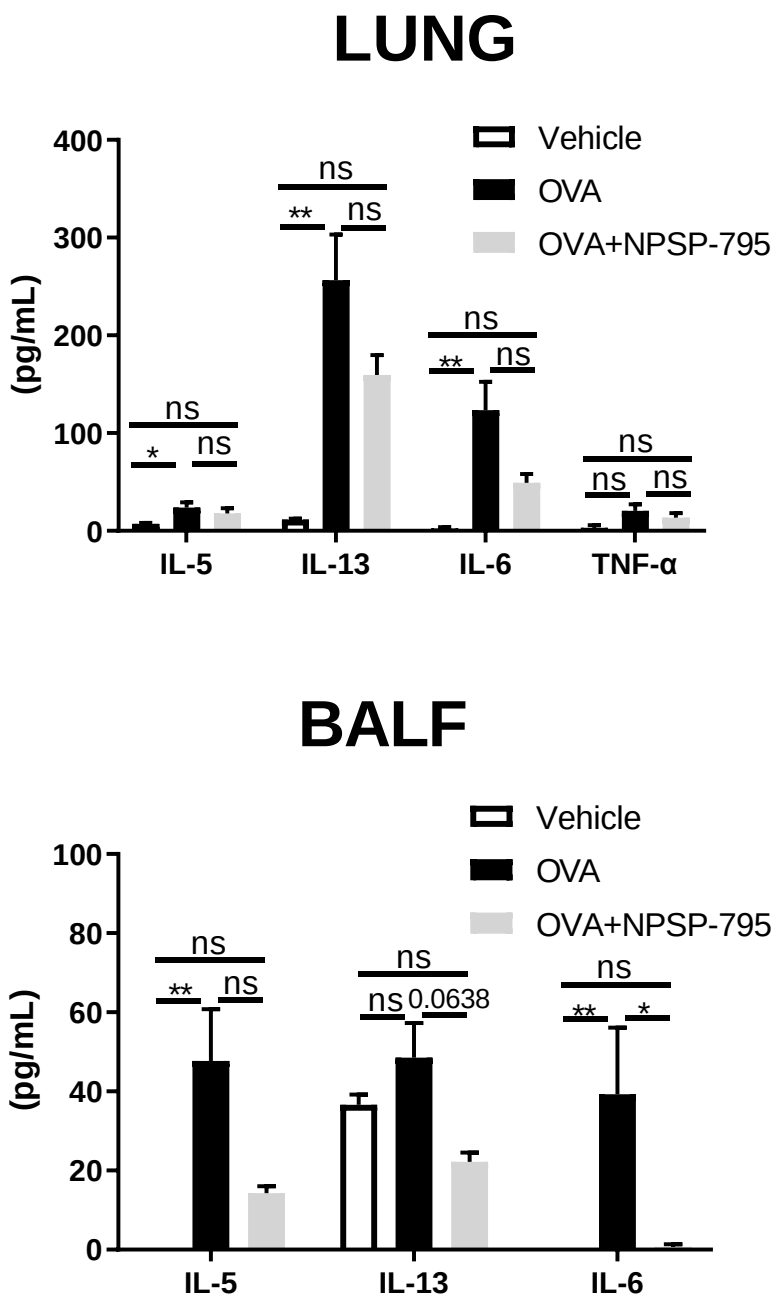

Figure 43. Effects of inhaled calcilytics on Th2 cytokines in the OVA-induced asthma model.

Female BALB/c mice (6-8 weeks) were sensitized by intraperitoneal injection of 100 µg OVA (OVA group and OVA + NPSP-795 group) or saline (Vehicle group) in $Al(OH)_3$ in 200 µL on days -17 and -5. After sensitisation, animals were intranasally given OVA (50 µg/mouse in 50 µL saline, OVA group and OVA + NPSP-795 group) or saline (Vehicle group) from day 1 to day 6 for 6 days. From day 2, NPSP-795 (200 µg/mouse in 50 µL vehicle, OVA + NPSP-

795 group) or vehicle (0.6% DMSO in saline, OVA group and Vehicle group) were given twice daily, with the evening dosing given 2h before OVA administration. On day 7, the right lung and BALF were collected and processed to analyze the level of Th2 cytokines. IL-13 and IL-5 as well as IL-6 and TNF-α (proinflammatory cytokines) in the OVA-induced asthma model in lung homogenate (left-panel) and BALF (right-panel). NPSP-795 significantly reduced IL-5, IL-13 and IL-6, but not TNF-α in the OVA model. N = 5-8 animals per experimental group. Data are presented as Mean ± SEM. P-values are from Kruskal-Wallis test with Dunn's multiple comparisons test. ns: not-significant, *: $p < 0.05$, **: $p < 0.01$.

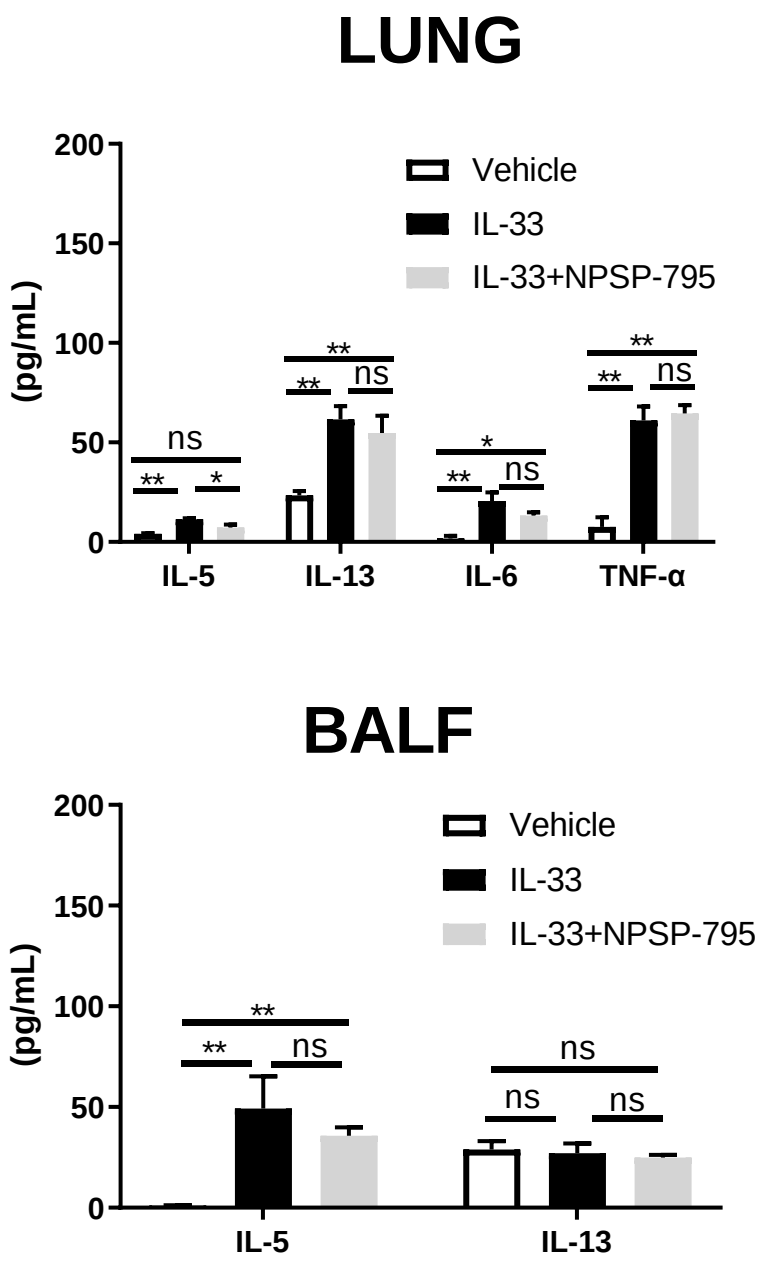

Figure 44. Effects of inhaled calcilytics on Th2 cytokines in IL-33-induced asthma model.

Female BALB/c mice (6-8 weeks) were given IL-33 intranasally (30 ng/mouse in 50 µL saline, IL-33 group and IL-33+ NPSP-795 group) or saline (Vehicle group) from day 1 to day 6 for 6 days. From day 2, NPSP-795 (200 µg/mouse in 50 µL vehicle, IL-33 + NPSP-795 group) or vehicle (0.6% DMSO in saline, IL-33 group and Vehicle group) were given twice daily, with the evening dosing given 2h before IL-33 administration. On day 7, the right lung and BALF were collected and processed to analyze the level of Th2 cytokines. IL-

13 and IL-5 as well as IL-6 and TNF-α (proinflammatory cytokines) in the IL-33-induced asthma model in lung homogenate (left-panel) and BALF (right-panel). NPSP-795 significantly reduced IL-5, but not IL-13, IL-6 and TNF-α in the IL-33 model. N = 5-7 animals per experimental group. Data are presented as Mean ± SEM. P-values are from Kruskal-Wallis test with Dunn's multiple comparisons test. ns: not-significant, *: $p < 0.05$, **: $p < 0.01$.

5.4.4 Effect of inhaled NPSP-795 on immune cells infiltration in lung tissue in Th2/IgE- and alarmin-driven asthma models

I further investigated the effect of inhaled NPSP-795 on inflammatory cell infiltration in lung by H&E staining. I used the TissueFAXS software (TissueGnostics, Vienna), to quantify total cell number around the peribronchial and perivascular regions per 10000 μm^2 area to quantify the degree of inflammation. Briefly, Airways were identified by drawing the airway lumen with yellow and airway epithelium with green on H&E-stained slides. The number of total cells around the peribronchial and perivascular regions and the number per 10000 μm^2 area tissue were automatically calculated by StataQuest. In the OVA-induced asthma model, there is dramatically increased cell infiltration around the peribronchial and perivascular regions in lung tissue in the OVA group. However, these increased cell infiltrations were significantly decreased by inhaled NPSP-795 (Figure 45). In the IL-33-induced asthma model, there is also significantly increased cell infiltration in lung tissue in the IL-33 group, which was significantly decreased by inhaled NPSP-795 (Figure 46).

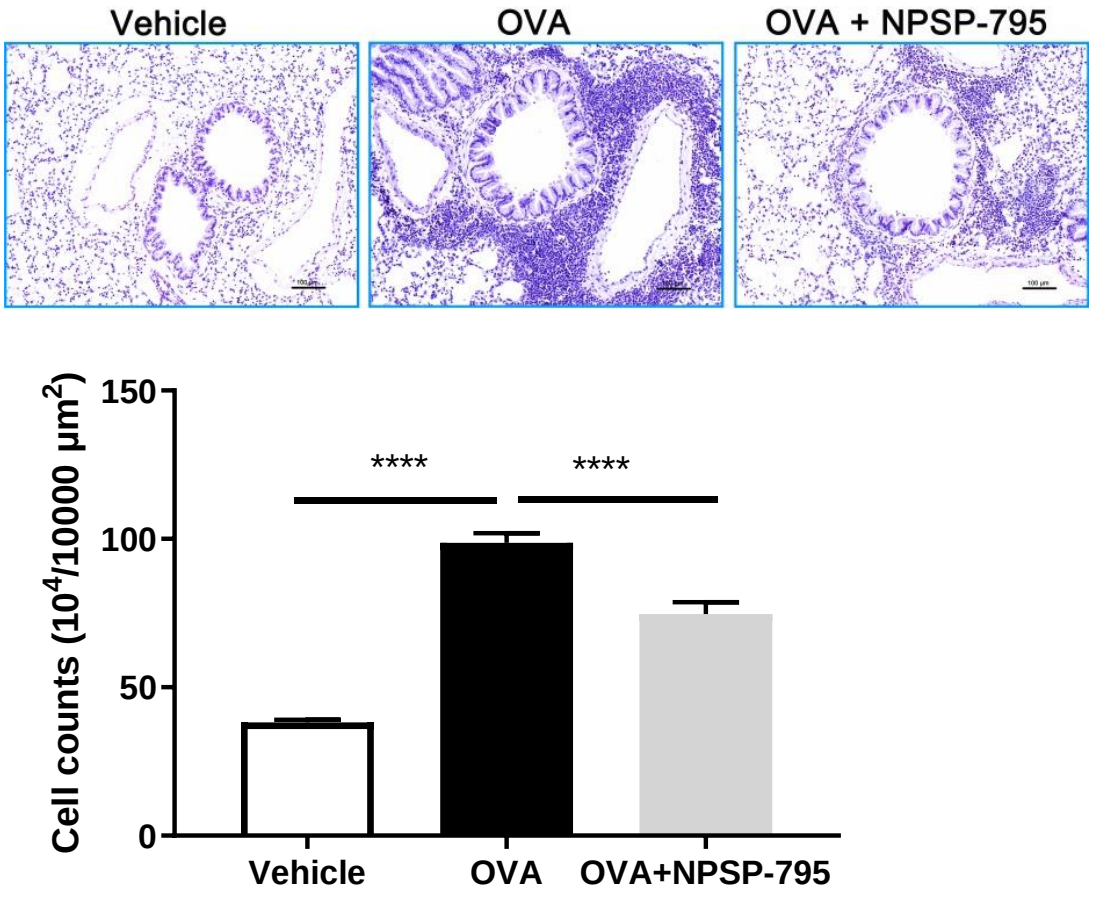

Figure 45. H & E staining in the OVA-induced asthma model.

Female BALB/c mice (6-8 weeks) were sensitized by intraperitoneal injection of 100 µg OVA (OVA group and OVA + NPSP-795 group) or saline (Vehicle group) in $Al(OH)_3$ in 200 µL on days -17 and -5. After sensitisation, animals were intranasally given OVA (50 µg/mouse in 50 µL saline, OVA group and OVA + NPSP-795 group) or saline (Vehicle group) from day 1 to day 6 for 6 days. From day 2, NPSP-795 (200 µg/mouse in 50 µL vehicle, OVA + NPSP-795 group) or vehicle (0.6% DMSO in saline, OVA group and Vehicle group) were given twice daily, with the evening dosing was given 2h before OVA administration. On day 7, the left lung tissues were collected. Haematoxylin and eosin staining was conducted after the lung tissues were fixed and paraffin-embedded. The number of total cells around the airway area per 10000 μm^2 area was calculated using the TissueFAXS image analysis software StrataQuest on the scanned H&E-stained slides. Briefly, the airways were identified by drawing the airway lumen with yellow and the airway epithelium with green. The number of total cells around the peribronchial

region per 10000 μm^2 area tissue was automatically calculated by the software. The top panel is the representative photograph of HE staining, and the right panel is quantitative data quantified using the TissueFAXS image analysis software StrataQuest. Inflammatory cell infiltration around the airway and perivascular area in lung tissue was significantly reduced in the OVA + NPSP-795 group compared to the OVA group in the OVA-induced asthma model. Data are expressed as the cell counts in 10000 μm^2 lung tissue. N = 36-42 slides per experimental group. Data are presented as Mean ± SEM. P values are from one-way ANOVA with Bonferroni's post-hoc test. ns: not-significant, ****: $p < 0.0001$. Scale bar: 100 μm.

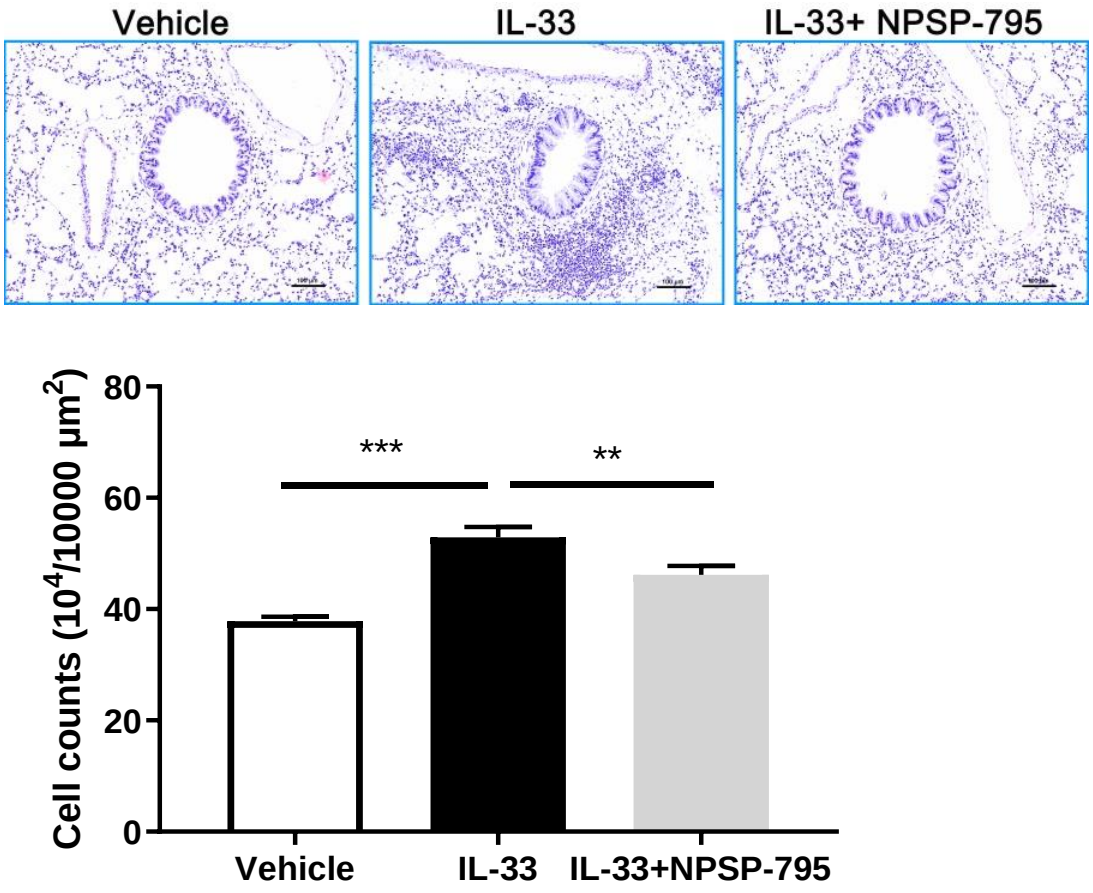

Figure 46. H & E staining in IL-33-induced asthma model.

Female BALB/c mice (6-8 weeks) were given IL-33 intranasally (30 ng/mouse in 50 μL saline, IL-33 group and IL-33+ NPSP-795 group) or saline (Vehicle group) from day 1 to day 6 for 6 days. From day 2, NPSP-795 (200 μg/mouse in 50 μL vehicle, IL-33 + NPSP-795 group) or vehicle (0.6% DMSO in saline, IL-33 group and Vehicle group) were given twice daily, with the evening dosing was given 2h before IL-33 administration. On day 7, the left lung tissues were collected. Haematoxylin and eosin staining was conducted after the lung tissues were fixed and paraffin-embedded. As described above, the number of total cells around the airway area per 10000 μm^2 area was calculated using the TissueFAXS image analysis software StrataQuest on the scanned H&E-stained slides. The top panel is the representative photograph of HE staining, and the lower panel is quantitative data quantified using the TissueFAXS image analysis software StrataQuest. Inflammatory cell infiltration around the airway and perivascular area in lung tissue was significantly reduced in the IL-33 + NPSP-795 group compared to the IL-33

group in the IL-33-induced asthma model. Data are expressed as the cell counts in 10000 μm^2 lung tissue. N = 48-54 slides per experimental group. Data are presented as Mean ± SEM. P values are from one-way ANOVA with Bonferroni's post-hoc test. ns: not-significant, **: $p < 0.01$, ***: $p < 0.001$. Scale bar: 100 µm.

5.4.5 Effect of inhaled calcilytic on lung tissue eosinophilia in Th2/IgE- and alarmin-driven asthma models

Patients with asthma often exhibit airway eosinophilia, so I next compared the counts of eosinophils around the peribronchial and perivascular regions per 10000 μm^2 area before and after the administration of inhaled calcilytic in lung tissue in both models using Congo red staining. The number of eosinophils per 10000 μm^2 lung tissue was also determined using the TissueFAXS software StrataQuest (TissueGnostics, Vienna) on Congo red-stained slides according to the procedure similar to total cell infiltration. In the OVA-induced asthma model, the number of eosinophils around the peribronchial and perivascular regions dramatically increased in the OVA group. However, the administration of inhaled NPSP-795 reversed the increase of eosinophils induced by OVA (Figure 47). The same effect was seen in the IL-33-induced asthma model, where IL-33 increased the counts of eosinophils and these were reversed by inhaled NPSP-795 (Figure 48).

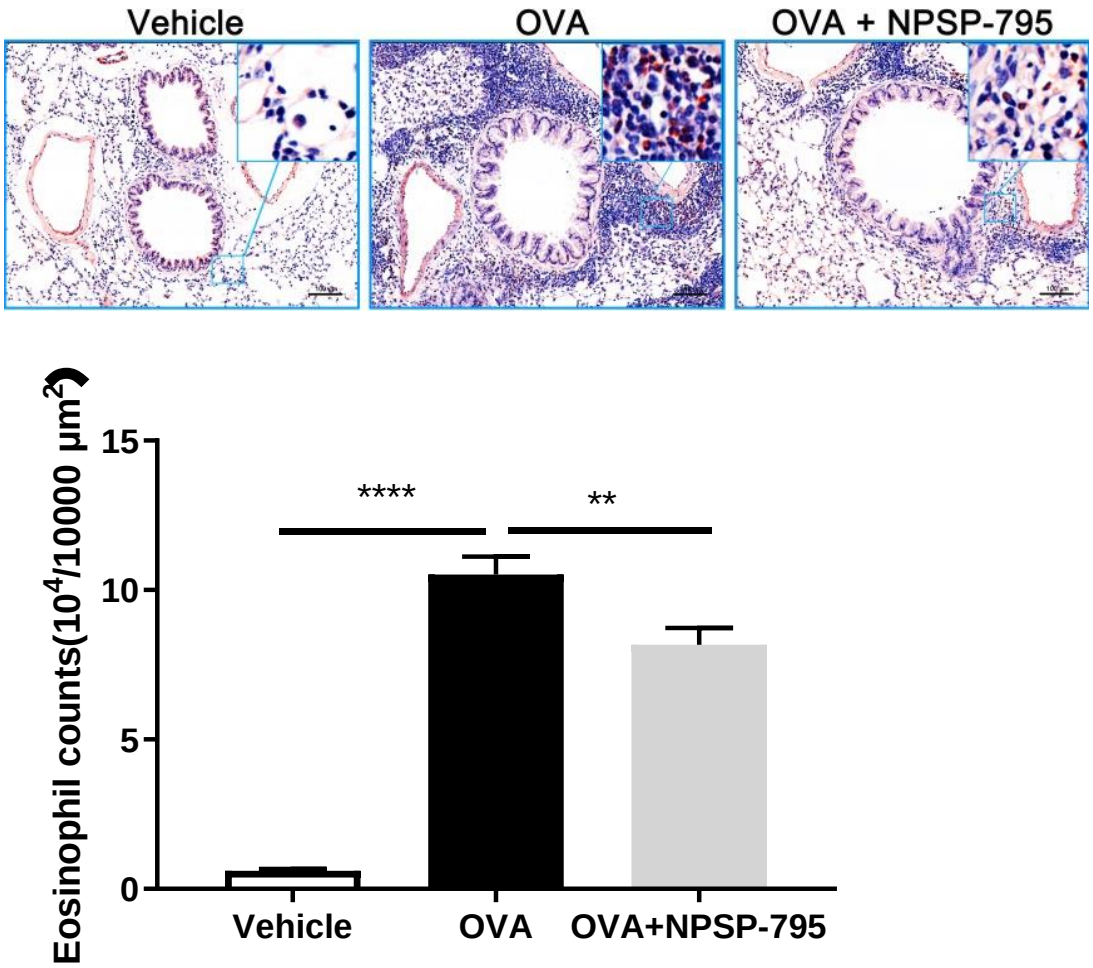

Figure 47. Congo red-stained lung tissue in OVA asthma model.
Female BALB/c mice (6-8 weeks) were sensitized by intraperitoneal injection of 100 µg OVA (OVA group and OVA + NPSP-795 group) or saline (Vehicle group) in $Al(OH)_3$ in 200 µL on days -17 and -5. After sensitisation, animals were intranasally given OVA (50 µg/mouse in 50 µL saline, OVA group and OVA + NPSP-795 group) or saline (Vehicle group) from day 1 to day 6 for 6 days. From day 2, NPSP-795 (200 µg/mouse in 50 µL vehicle, OVA + NPSP-795 group) or vehicle (0.6% DMSO in saline, OVA group and Vehicle group) were given twice daily, with the evening dosing was given 2h before OVA administration. On day 7, the left lung tissues were collected. Congo red-staining was conducted after the lung tissues were fixed and paraffin-embedded. The number of eosinophils around the airway area per 10000 μm^2 area was calculated using the TissueFAXS image analysis software StrataQuest on the scanned Congo red-stained slides. Briefly, the airways were identified by drawing the airway lumen with yellow and the airway

epithelium with green. The number of Congo red-positive cells around the peribronchial region per 10000 μm^2 area tissue was automatically calculated by the software. The top panel is the representative photograph of Congo red staining, and the lower panel is quantitative data quantified using the TissueFAXS image analysis software StrataQuest. NPSP-795 significantly reduced the eosinophil infiltration around the airway and perivascular area in lung tissue in the OVA-induced asthma model. Data are expressed as the cell counts in 10000 μm^2 lung tissue. N = 36-42 slides per experimental group. Data are presented as Mean ± SEM. P values are from one-way ANOVA with Bonferroni's *post-hoc* test. ns: not-significant, **: $p < 0.01$, ****: $p < 0.0001$. Scale bar: 100 µm.

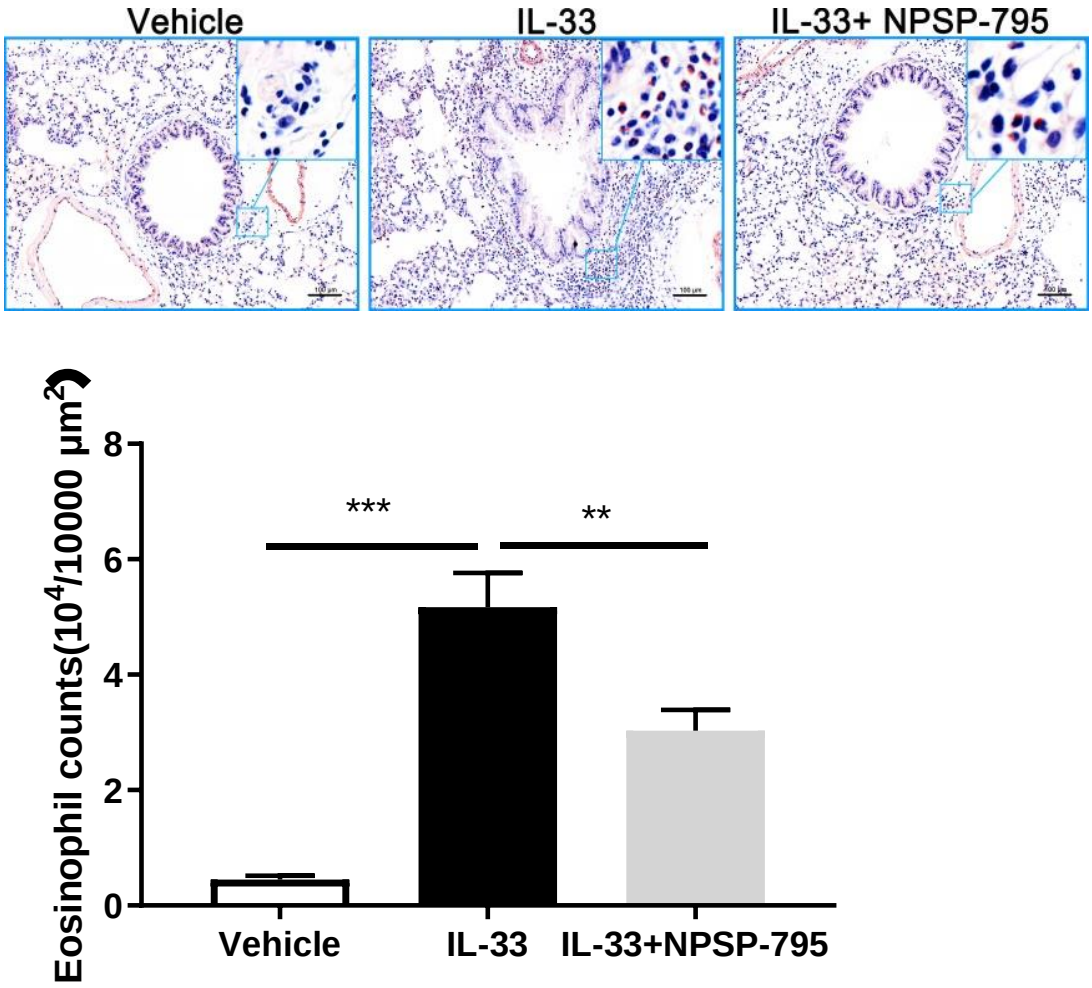

Figure 48. Congo red-stained lung tissue in IL-33 asthma model.
Female BALB/c mice (6-8 weeks) were given IL-33 intranasally (30 ng/mouse in 50 µL saline, IL-33 group and IL-33+ NPSP-795 group) or saline (Vehicle group) from day 1 to day 6 for 6 days. From day 2, NPSP-795 (200 µg/mouse in 50 µL vehicle, IL-33 + NPSP-795 group) or vehicle (0.6% DMSO in saline, IL-33 group and Vehicle group) were given twice daily, with the evening dosing was given 2h before IL-33 administration. On day 7, the left lung tissues were collected. Congo red-staining was conducted after the lung tissues were fixed and paraffin-embedded. As described above, the number of eosinophils around the airway area per 10000 µm^2 area was calculated using the TissueFAXS image analysis software StrataQuest on the scanned Congo red-stained slides. The top panel is a representative photograph of Congo red staining, and the lower panel is quantitative data quantified using the TissueFAXS image analysis software StrataQuest. NPSP-795 significantly reduced the eosinophil infiltration around the airway and perivascular area in

lung tissue in the IL-33-induced asthma model. Data are expressed as the cell counts in 10000 μm^2 lung tissue. N = 48-54 slides per experimental group. Data are presented as Mean ± SEM. P values are from one-way ANOVA with Bonferroni's *post-hoc* test. ns: not-significant, **: $p < 0.01$, ***: $p < 0.001$. Scale bar: 100 µm.

5.4.6 Effect of inhaled NPSP-795 on mucus production in Th2/IgE- and alarmin-driven asthma models

Airway goblet cell hyperplasia and the resulting excessive mucus and phlegm production is another common aspect of asthma. I also investigated the effect of inhaled NPSP-795 on mucus production using Periodic acid-Schiff (PAS) staining. I used the TissueFAXS software StrataQuest (TissueGnostics, Vienna) to count the number of stained cells in the airway and then divided by the area of the airway to quantify the degree of mucus production. Airways were identified by drawing the airway epithelium with green. The number of positively stained cells and the number per 10000 μm^2 area airway were automatically calculated by StataQuest. In both the OVA and IL-33-induced asthma models, there is obvious goblet cell hyperplasia and mucus production in the airway. However, the inhalation of NPSP-795 could not reverse these effects (Figure 49 and Figure 50).

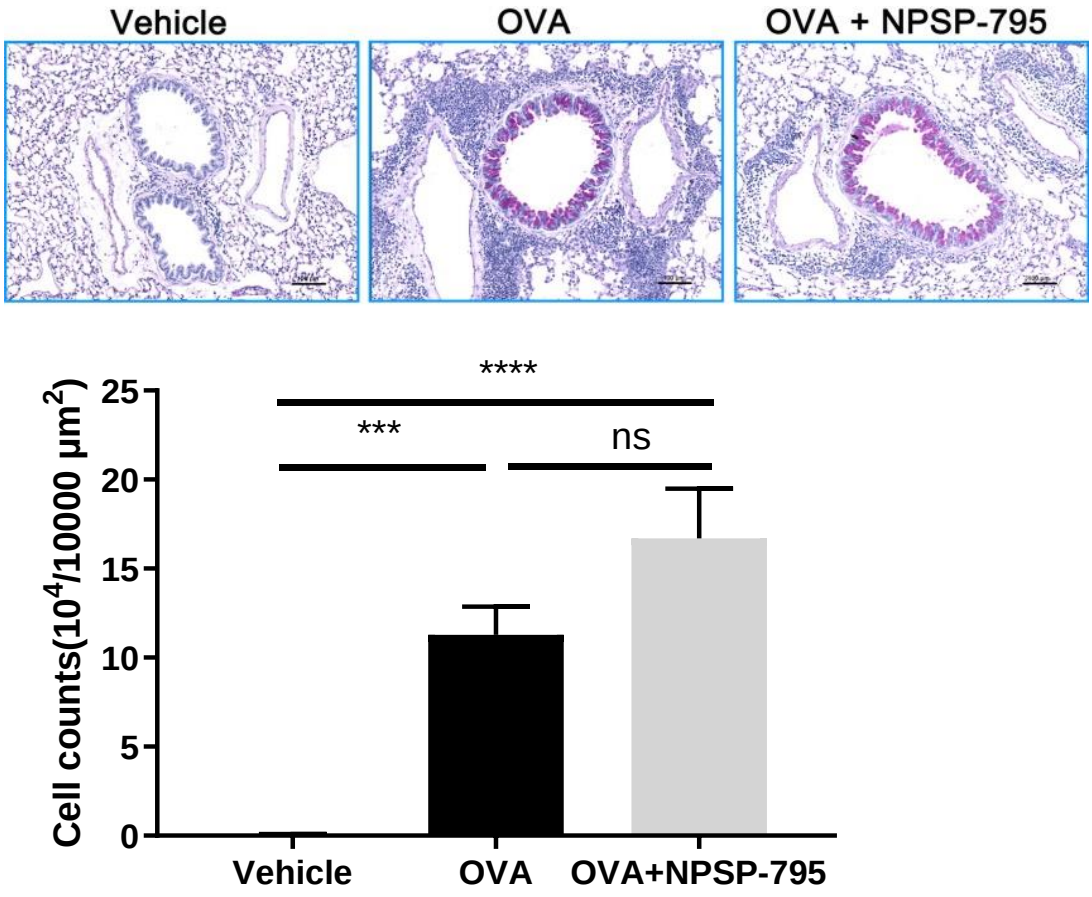

Figure 49. PAS staining in the OVA-induced asthma model.

Female BALB/c mice (6-8 weeks) were sensitized by intraperitoneal injection of 100 μg OVA (OVA group and OVA + NPSP-795 group) or saline (Vehicle group) in $Al(OH)_3$ in 200 μL on days -17 and -5. After sensitisation, animals were intranasally given OVA (50 μg/mouse in 50 μL saline, OVA group and OVA + NPSP-795 group) or saline (Vehicle group) from day 1 to day 6 for 6 days. From day 2, NPSP-795 (200 μg/mouse in 50 μL vehicle, OVA + NPSP-795 group) or vehicle (0.6% DMSO in saline, OVA group and Vehicle group) were given twice daily, with the evening dosing was given 2h before OVA administration. On day 7, the left lung tissues were collected. Periodic acid-Schiff (PAS) staining was conducted after the lung tissues were fixed and paraffin-embedded. The number of stained cells in the airway per 10000 μm^2 area was calculated using the TissueFAXS image analysis software StrataQuest on the scanned PAS-stained slides. Briefly, the airways were identified by drawing the airway lumen with yellow and the airway epithelium with green. The number of PAS-positive cells around the peribronchial region

per 10000 μm^2 area tissue was automatically calculated by the software. The top panel is the representative photograph of PAS staining, and the lower panel is quantitative data quantified using the TissueFAXS image analysis software StrataQuest. NPSP-795 did not significantly reduce mucus secretion in lung tissue in the OVA asthma models. N = 22-31 slides per experimental group. Data are presented as Mean ± SEM. P-values are from one-way ANOVA with Bonferroni's *post hoc* test. ns: non-significant, ***: $p < 0.001$, ****: $p < 0.0001$. Scale bar: 100 μm.

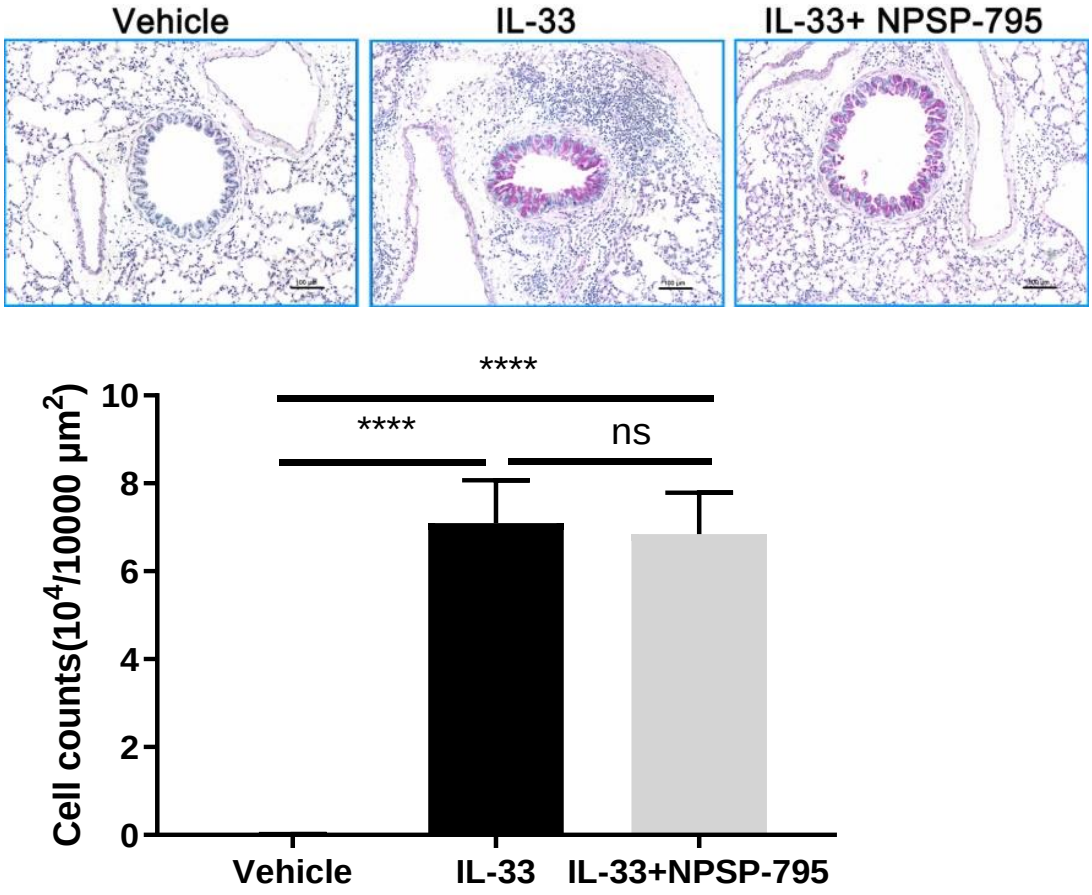

Figure 50. PAS staining in IL-33-induced asthma model.

Female BALB/c mice (6-8 weeks) were given IL-33 intranasally (30 ng/mouse in 50 µL saline, IL-33 group and IL-33+ NPSP-795 group) or saline (Vehicle group) from day 1 to day 6 for 6 days. From day 2, NPSP-795 (200 µg/mouse in 50 µL vehicle, IL-33 + NPSP-795 group) or vehicle (0.6% DMSO in saline, IL-33 group and Vehicle group) were given twice daily, with the evening dosing was given 2h before IL-33 administration. On day 7, the left lung tissues were collected. Periodic acid-Schiff (PAS) staining was conducted after the lung tissues were fixed and paraffin-embedded. As described above, the number of stained cells in the airway per 10000 μm^2 area was calculated using the TissueFAXS image analysis software StrataQuest on the scanned PAS-stained slides. The top panel is the representative photograph of PAS staining, and the lower panel is quantitative data quantified using the TissueFAXS image analysis software StrataQuest. NPSP-795 did not significantly reduce mucus secretion in lung tissue in the asthma model. N = 37-39 slides per experimental group. Data are presented as Mean ± SEM. P-

values are from one-way ANOVA with Bonferroni's *post hoc* test. ns: non-significant, ****: $p < 0.0001$. Scale bar: 100 µm.

5.4.7 Effect of inhaled NPSP-795 on collagen deposition in Th2/IgE- and alarmin-driven asthma models

I next investigated the effect of inhaled NPSP-795 on collagen deposition through Masson's trichrome staining. I quantified the percentage of collagen area around the peribronchial and perivascular regions with an increment of 30 µm to see the degree of collagen deposition in the different parts of the lung tissue. First, Airways were identified by drawing the airway lumen with yellow and the airway epithelium with green. And 7 peribronchial rings extending away from the airway epithelium in increments of 30 µm were also defined to quantify the extent of collagen deposition in different parts of the peribronchial regions. The collagen area in each ring and the percentage of collagen area in the total ring area were automatically calculated by StataQuest. In the OVA-induced asthma model, inhaled NPSP-795 significantly decreased the collagen deposition particularly in the areas closer to the airway lumen and also the total collagen deposition induced by OVA (Figure 51). In the IL-33-induced asthma model, inhaled NPSP-795 significantly decreased collagen deposition in all the analyzed areas of the lung tissue except for the areas closer to the airway lumen and the total collagen deposition induced by IL-33 (Figure 52).

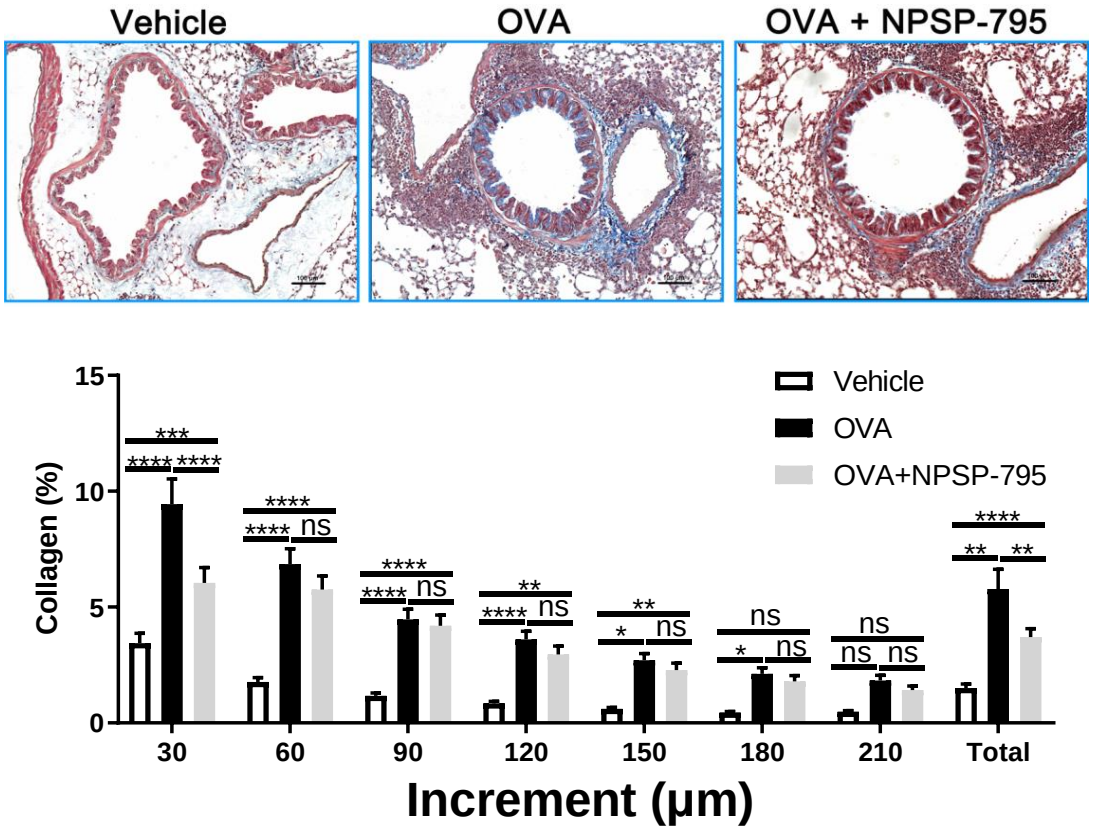

Figure 51. Masson's trichrome staining in the OVA-induced asthma model.

Female BALB/c mice (6-8 weeks) were sensitized by intraperitoneal injection of 100 μg OVA (OVA group and OVA + NPSP-795 group) or saline (Vehicle group) in $Al(OH)_3$ in 200 μL on days -17 and -5. After sensitisation, animals were intranasally given OVA (50 μg/mouse in 50 μL saline, OVA group and OVA + NPSP-795 group) or saline (Vehicle group) from day 1 to day 6 for 6 days. From day 2, NPSP-795 (200 μg/mouse in 50 μL vehicle, OVA + NPSP-795 group) or vehicle (0.6% DMSO in saline, OVA group and Vehicle group) were given twice daily, with the evening dosing was given 2h before OVA administration. On day 7, the left lung tissues were collected. Masson's trichrome stainings were conducted after the lung tissues were fixed and paraffin-embedded. The percentage of collagen area around the peribronchial and perivascular regions with an increment of 30 μm were calculated using the TissueFAXS image analysis software StrataQuest on the scanned Masson-stained slides to see the degree of collagen deposition in the different parts of the lung tissue. Briefly, the airways were identified by drawing the airway lumen with yellow and the airway epithelium with green. 7

peribronchial rings extending away from the airway epithelium in increments of 30 µm were defined. The percentage of collagen area in the total ring area was automatically calculated by the software. The top panel is the representative photograph of Masson's trichrome staining, and the below panel is quantitative data quantified using the TissueFAXS image analysis software StrataQuest. Inhaled calcilytic significantly reduced collagen deposition close to the airway and also the total collagen deposition. N = 30-40 slides per experimental group. Data are presented as Mean ± SEM. P values are from one-way ANOVA with Bonferroni's *post hoc* test. ns: non-significant, *: $p < 0.05$, **: $p < 0.01$, ***: $p < 0.001$, ****: $p < 0.0001$. Scale bar: 100 µm.

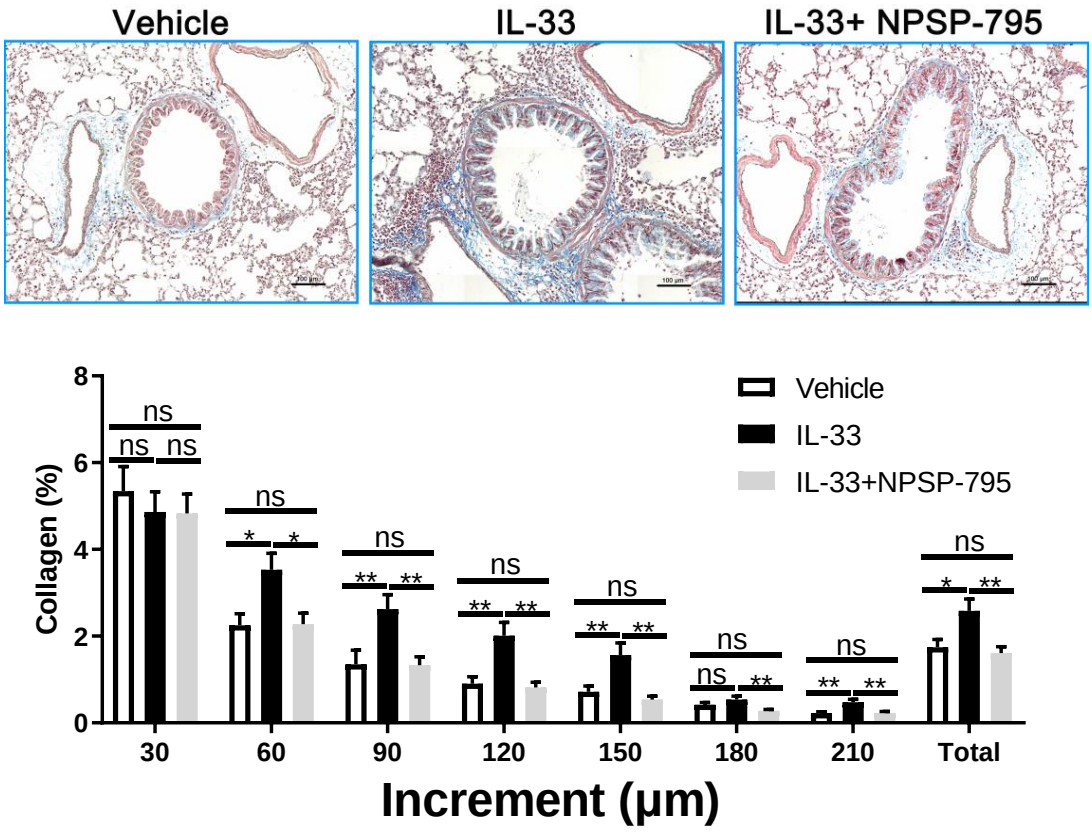

Figure 52. Masson's trichrome staining in IL-33-induced asthma model. Female BALB/c mice (6-8 weeks) were given IL-33 intranasally (30 ng/mouse in 50 μL saline, IL-33 group and IL-33+ NPSP-795 group) or saline (Vehicle group) from day 1 to day 6 for 6 days. From day 2, NPSP-795 (200 μg/mouse in 50 μL vehicle, IL-33 + NPSP-795 group) or vehicle (0.6% DMSO in saline, IL-33 group and Vehicle group) were given twice daily, with the evening dosing was given 2h before IL-33 administration. On day 7, the left lung tissues were collected. Masson's trichrome staining of lung tissues was conducted after the lung tissues were fixed and paraffin-embedded. As described above, the percentage of collagen area around the peribronchial and perivascular regions with an increment of 30 μm were calculated using the TissueFAXS image analysis software StrataQuest on the scanned Masson-stained slides, to see the degree of collagen deposition in the different parts of the lung tissue. The top panel is the representative photograph of Masson's trichrome staining, and the below panel is quantitative data quantified using the TissueFAXS image analysis software StrataQuest. Inhaled calcilytic significantly reduced collagen deposition in all the analysed areas of the lung tissue and the total collagen deposition. N =

36-48 slides per experimental group. Data are presented as Mean ± SEM. P values are from one-way ANOVA with Bonferroni's *post hoc* test. ns: non-significant, *: $p < 0.05$, **: $p < 0.01$. Scale bar: 100 μm.

5.4.8 Effect of topical administration of NPSP-795 on Serum Ca^{2+} levels in Th2/IgE- and alarmin-driven asthma models

Since systemic Ca^{2+} levels are very important to people and CaSR can affect Ca^{2+} levels, I next investigated the effect of topical administration of NPSP-795 on serum Ca^{2+} levels by biochemical analysis to investigate the systemic side effects of topical administration of NPSP-795. My results show that there were no significant differences between vehicle, OVA and OVA + NPSP-795 groups nor between vehicle, IL-33 and IL-33 + NPSP-795 groups, indicating there are no systemic side effects of topical administration of NPSP-795 (Figure 53A and B).

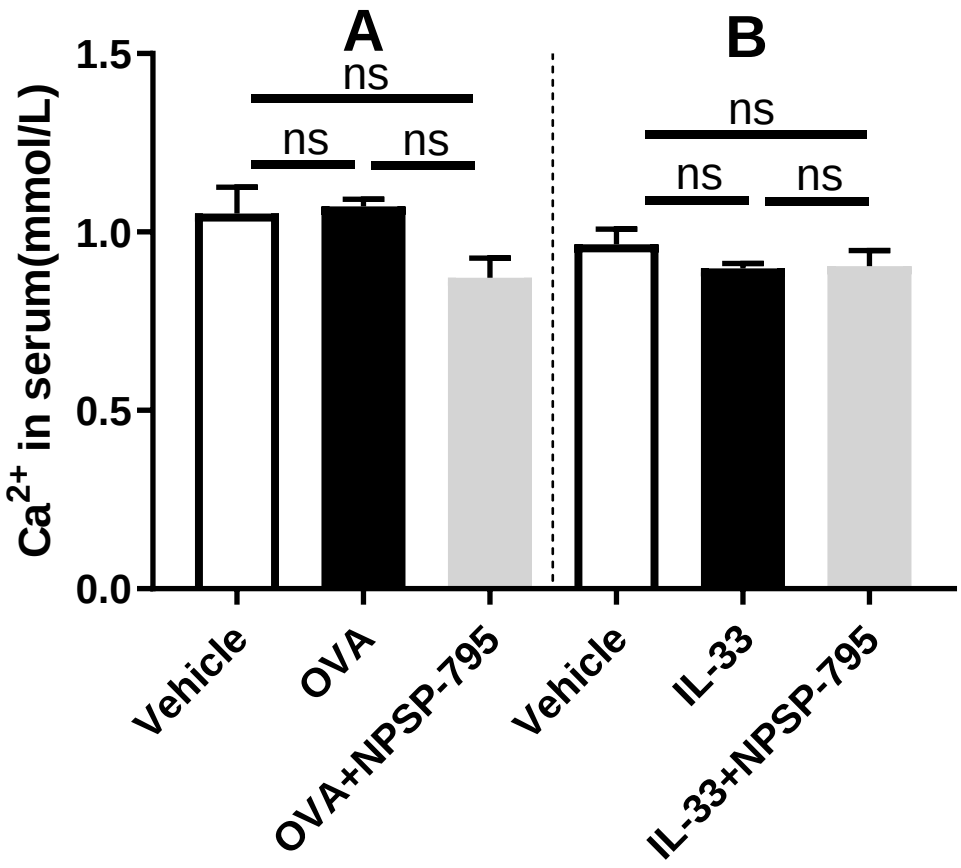

5.5 Discussion

Asthma is a very common chronic pulmonary disease, but its exact causes remain unclear. The traditional theory suggests that asthma is mainly mediated by Th2 type immune response, involving immune cells like mast cells, neutrophil and eosinophils, among which eosinophils play the most important role (Boonpiyathad et al. 2019). Type-2 cytokines such as IL-4, IL-5, and IL-13 are critical in asthma pathogenesis (Lambrecht et al. 2019). IL-4 can promote the differentiation and development of naïve T cells into Th2 cells, and plays an important role in the category conversion of B cells to produce IgE (Barnes 2018). IL-13 can promote the eosinophil infiltration inflammation (Larose et al. 2015) and can also promote increased mucus secretion, airway fibrosis and remodelling, as well as involved in the occurrence of airway hyperresponsiveness (Wills-Karp 2004; Nair and O'Byrne 2019). IL-5 plays a key role in eosinophil infiltration inflammation (Yanagibashi et al. 2017). Recent studies also highlight the role of epithelial-derived cytokines like IL-33, IL-25, and TSLP in the development of asthma

(Abraham et al. 2003). Among these epithelial-derived cytokines, IL-33 is thought to be involved in both type 2 inflammation and non-type 2 inflammation through the activation of ILC2 and Th17 cells, and the latter ones play a major role in attracting and stimulating neutrophils, which was thought to be associated with the neutrophilic inflammation(Israel and Reddel 2017).

Li Yan et al. compared OVA and IL-33-induced asthma models and found that IL-33-induced asthma presents more severe, long-lasting symptoms, including inflammation, airway remodelling, and neutrophil involvement. The OVA model reflects early-phase, allergic asthma, while IL-33 is more representative of later-phase, allergen-independent asthma (Li et al. 2015).Click or tap here to enter text.

In my study, I evaluated the therapeutic effects of inhaled calcilytic on inflammatory cell infiltration in BALF, AHR, cytokines production, inflammatory cell infiltration in lung tissue, lung tissue eosinophilia, mucus production and collagen deposition induced by OVA and IL-33, as well as the change of serum Ca^{2+} levels before and after the inhalation of calcilytic. My results indicate that inhaled calcilytic significantly reverses the symptoms induced by both OVA and IL-33, with the effect being more marked in the IL-33-induced asthma model. These effects were achieved in the absence of significant changes in the serum Ca^{2+} levels, indicating that inhaled calcilytic can be developed as a potential novel treatment for both Th2/IgE and alarmin-driven asthma.

In addition, my result demonstrated that there was no effect on mucus secretion of inhaled calcilytic in the Th2/IgE and alarmin-driven asthma. However, in our short-term OVA model, inhalation of NPSP-795 resulted in a reduction in the mean number of goblet cells in the airways, whereas FP had no effect. This discrepancy may be due to the different stages of mucus secretion in these models. In the acute phase, mucus secretion may not be as pronounced, with gene expression and goblet cell proliferation just beginning. As such, it can be hypothesized that both gene expression and goblet cell

hyperplasia may be suppressed in this early phase. In contrast, our IL-33-induced model may represent a subacute phase, where mucus secretion is heightened, making it more difficult for the current dose of calcilytic to effectively inhibit this stronger mucus production.

This observation is supported by a study from Korea, which demonstrated that the CaSR antagonist NPS2143 can inhibit MUC5AC expression in human airway epithelial cells exposed to cigarette smoke extract (Lee et al. 2017b). MUC5AC and MUC5B are two distinct mucins in the airway, with their production spatially separated. MUC5AC is primarily localized to goblet cells in the tracheobronchial surface epithelium, while MUC5B is mainly localized to mucous cells in submucosal glands (Hovenberg et al. 1996; Groneberg et al. 2002). These mucins have distinct regulatory mechanisms and contribute differently to airway mucus production. MUC5AC plays a key role in mucus gel formation in response to allergens or irritants, while MUC5B is more crucial for maintaining normal mucociliary clearance in healthy airways (Hovenberg et al. 1996; Groneberg et al. 2002). Given the dynamic nature of mucin expression and secretion, the effects of calcilytic may vary across asthma models and stages of disease.

Click or tap here to enter text.Considering the findings from both our study and the study by Lee et al. (Lee et al. 2017b), it may be worthwhile to explore higher doses of calcilytic, particularly in the chronic phase, or adjust the treatment to target the subacute phase more effectively. Future studies should also investigate the dose-response relationship and examine whether increased doses can modulate both MUC5AC and MUC5B expression to inhibit mucus secretion more effectively in these models.

Current asthma treatments like ICS, LABA, and LAMA, while effective for symptom management, cannot reverse long-term airway remodelling, possibly because they don't target IL-33, which is thought to play a role in remodelling (Warner and Knight 2008; Saglani et al. 2013). In contrast, in my alarmin-driven asthma, inhaled calcilytic can inhibit the asthma symptoms as well as airway remodelling, measured from both functional (Flexivent) and immunohistochemical (collagen deposition) standpoints. While biologic therapies have shown promise, limitations such as efficacy in specific asthma

subtypes, poor adherence and high costs limit their use (Busse et al. 2013; Hanania et al. 2013; Bel et al. 2014; Humbert et al. 2014; Ortega et al. 2014; Castro et al. 2015; Bjermer et al. 2016; Corren et al. 2016; *NUCALA® (mepolizumab) prescribing information* 2023; *XOLAIR® (omalizumab) prescribing information* 2024). Given these challenges, our results are significant for their efficacy, route of administration, and side effects.

Another PhD student from our laboratory has demonstrated CaSR expression in ILC2 cells, which may be the downstream of the alarmin signalling (Mansfield et al, unpublished observations). This provides further evidence that inhaled calcilytic could be effective in treating severe asthma, especially since IL-33 is involved in airway remodelling (Olin and Wechsler 2014). However, my study did not investigate the exact underlying disease mechanism, so further studies should explore how IL-33 and CaSR interact, possibly using lung-specific CaSR knock-out (KO) mice to assess asthma symptoms in the absence of CaSR, and examining CaSR expression in isolated mast cells, natural killer (NK) cells involved in the pathogenesis of asthma.

In conclusion, my study indicates that inhaled calcilytic can reduce the asthma symptoms induced by OVA and IL-33. These results, together with the results presented in chapters 3 and 4, suggest that inhaled calcilytic could be developed as a potential novel treatment for asthma.

Chapter VI General discussion, conclusion and future directions

6.1 Discussion

Asthma is a life-threatening disease, affecting more than 300 million people worldwide (Masoli et al. 2004). The main pathological changes in asthma include airway epithelial cell damage, shedding, submucosal oedema, subepithelial fibrosis, smooth muscle hyperplasia, hypertrophy, infiltration of eosinophils, monocytes, mast cells, etc., as well as basement membrane thickening (Global Initiative for Asthma 2023). Histological changes are mainly manifested as airway inflammation and epithelial injury, smooth muscle hyperplasia, submucosal gland hyperplasia, collagen deposition under the basement membrane as well as angiogenesis in the airway; all of these ultimately cause irreversible airway obstruction (Global Initiative for Asthma 2023).

Many mild-to-moderate asthmatic patients can be well controlled with currently available drugs, including inhaled corticosteroids and bronchodilators as well as a combination of these. However, the use of the existing treatments is associated with substantial unwanted effects, such as osteoporosis, hypertension, diabetes, adrenal suppression, and cataracts (Sullivan et al. 2018). In addition, they induce some airway remodelling, which may cause irreversible obstruction in a substantial subgroup of patients, resulting in therapy-resistant chronic morbidity and increased risk of death (Hansbro et al. 2017; O'Byrne et al. 2019). Moreover, there is no asthma therapy which directly targets airway hyperresponsiveness (inhaled bronchodilators temporarily alleviate the symptoms but do not address the underlying problem), or prevents airway remodelling and progressive, irreversible obstruction of the airways (Corrigan 2020). The lack of knowledge about the underlying mechanism and the true molecular triggers for asthma has driven many researchers to identify other drug targets that are involved in the development of airway hyperresponsiveness, airway inflammation and airway remodelling.

On the other hand, the recently approved and developing biologics (monoclonal antibodies) targeting IgE or asthma-related cytokines (IL-13, IL-5, IL-4, IL-25, IL-33 and TSLP) only have effects in a subset of patients and the

degree of effect are varied, and are expensive and are difficult to be self-administered (Walsh 2017).

It was mainly thought that allergens play an important role in asthma pathogenesis since most asthmatics present an allergic phenotype. However, it has been found that many patients present a non-allergic phenotype, which is related to a later onset and more severe disease (Humbert et al. 1999; Novak and Bieber 2003). This evidence raises the question: "*What is the main cause of asthma in non-allergic patients*?". Furthermore, several studies found that the expression of some epithelial-derived cytokines, including IL-33 increased in the serum, sputum and lung tissue of some severe asthmatic patients (Préfontaine et al. 2009; Zhao et al. 2023).

IL-33 was proposed to function as a novel alarmin because it is rapidly released from producing cells upon cell damage or mechanical injury to alert the immune system, thus playing important roles in innate immunity (Moussion et al. 2008; Cayrol and Girard 2009; Lüthi et al. 2009; Pichery et al. 2012; Grotenboer et al. 2013). IL-33 is expressed at high levels in epithelial barrier tissues and lymphoid organs, so it is rapidly released following infection with parasites or viruses, or exposure to allergens to 'alarm' ILC2 cells and other immune cells, including mast cells (Cayrol and Girard 2014). Li Yan et al. used murine surrogates and compared a classical asthma animal model (OVA-induced asthma) with an IL-33-induced asthma model. The authors have found that in the IL-33-induced asthma model, all the asthma symptoms such as inflammatory cellular infiltration, eosinophil infiltration, increased cytokine and chemokine expression, airway goblet cell hyperplasia, extracellular lung matrix protein deposition, airways smooth muscle hypertrophy and angiogenesis seems to appear later, they were more severe as well as persisted longer (Li et al. 2015). These results suggest that IL-33 may be implicated in airway remodelling and severe asthma.

The CaSR is a G-protein coupled receptor which has been found to be involved in asthma pathogenesis in our previous studies. Indeed, we found that eosinophil cationic proteins are CaSR agonists, that bronchial smooth muscle hyperresponsiveness in asthma reflects over-expression of the CaSR and CaSR-mediated signalling is implicated in airway hyperresponsiveness and inflammation (Yarova et al. 2015; Yarova et al. 2016), effects that could

be prevented by prophylactic administration of inhaled calcilytic. In addition, airway inflammation and cytokines production, steroid-resistant neutrophilic inflammation and interstitial wall thickening can be reduced with topical use of the negative allosteric modulators of CaSR, calcilytics (Yarova et al. 2015; Yarova et al. 2016). During the course of my PhD, I aimed to answer the following questions:

Question 1. How well the calcilytics perform against the current standard of care, inhaled corticosteroids?

To achieve this, I have compared the therapeutic effects of inhaled calcilytic with the standard-of-care FP in an OVA-induced asthma animal model *in vivo*. For the short-term and longer-term comparison, since FP is the most common corticosteroid used in the clinic, I selected it as the standard-of-care (positive control). However, it is poorly soluble in common solvents. Since animals were to be dosed in a nebulization chamber, I first detected a suitable vehicle for both calcilytic and FP, which was able to give a good solubility and also had no irritancy for the animals. In my initial studies, I tried 50% ethanol in the presence of 25% DMSO, which was used previously (Lowe et al. 2015) to dissolve the calcilytic in a saline solution. However, FP didn't dissolve completely in this vehicle. Then I tried 30% ethanol without DMSO, which resulted in a good solubility for both calcilytic and FP, however after nebulization, the drugs were left in the nebulizer, mainly due to the evaporation of ethanol during the nebulization process, causing the drugs precipitated in the nebulizer. Finally, I tried polysorbate 80 (Tween 80), a surfactant, which has been widely used as an emulsifier and solubilizer in cosmetics, food and pharmaceutical industry (Ten Tije et al. 2003; Kerwin 2008; Khan et al. 2015). The combination of DMSO and Tween 80 yielded a good solubility for both calcilytic and FP, and no drugs were left in the nebulizer after nebulization. Finally, I selected 0.3% DMSO + 0.01% Tween 80 as the vehicle because these concentrations of DMSO and Tween 80 not only give good solubility for both calcilytic and FP, but also have good tolerance, with low toxicity in mice in vivo. These achievements allowed me to test the effects of inhaled calcilytic against the current standard-of-care in an asthma model using the same vehicle for both drugs. The administration of inhaled calcilytic NPSP-795 to mice sensitized and challenged with OVA

significantly reduced total BALF leucocyte infiltration and eosinophil infiltration, which was comparable to that seen for FP. However, FP and NPSP-795 did not show an additive effect, which was surprising given their different mechanisms of action. This may be because their effects converge onto the same intracellular targets, or their target are at the same pathway. It is known that the main mechanism of action of ICS involves inhibition of mitogen-activated protein kinase (MAPK) signalling pathway (Jaffuel et al. 2000; Barnes 2011), a known downstream of GPCRs (Daub et al. 1996; Natarajan and Berk 2006). Another main mechanism of action of ICS is binding with GR and Galigniana *et al* demonstrated that GR may be nitrosylated by nitric oxide (NO) *in vitro*, indicating NO could reduce glucocorticoid responsiveness, so this may be the reason for steroid resistance in severe asthma patients who have increased expression of inducible NO synthase and large amounts of NO (Galigniana et al. 1999). Therefore, it is reasonable to assume that without function through GR, inhaled calcilytic may be useful in severe asthma. From this point of view, it will be worth investigating the effect of these two drugs in this pathway and the interactions in future. Also, it would be worth testing if there are any additive effects of ICS+ calcilytic to reduce drug exposure while minimizing the side effects of ICS. Overall, these experiments show that inhaled calcilytic can be developed to prevent inhaled corticosteroid side effects and remodelling, and also as a novel potential steroid-independent asthma treatment option.

Question 2. Can we take calcilytics that have been previously tested in the clinic as systemic drugs, and use them as novel asthma treatment, delivered directly to the lung, to bypass systemic drug effects?

Because my plan was to deliver the calcilytics directly to the lung via inhalation, in the first series of experiments, I wanted to test their effects on the airway lumen. To this end, I used wire myography to assess the effects of calcilytics in naïve mouse tracheae half-maximally contracted with ACh *ex vivo* to select the best calcilytic to be used for *in vivo* experiments. Four calcilytics, NPSP-795, Ronacaleret, JTT-305 and AXT 914, were selected as candidate calcilytics to be used *in vivo* because they have been tested in

human phase 1 and 2 clinical trials (Gowen et al. 2000; Ward and Riccardi 2012; Nemeth and Goodman 2016), and were proven safe and well tolerated. In addition, NPS89636 and NPS2143 have been employed in previous studies and were therefore used as positive controls. I investigated the effects of calcilytics on tracheal contraction in both therapeutic and prophylactic settings. My results have demonstrated that calcilytic has effects on tracheal contraction and relaxation. Specifically, in the therapeutic setting, NPS89636, NPSP-795 and Ronacaleret evoked a comparable reduction of the tracheal contraction induced by ACh, which was of larger magnitude compared to NPS2143 and JTT-305. AXT 914 showed no effects on tracheal contraction in this setting. Interestingly, in the prophylactic setting, only NPSP-795 and AXT 914 attenuated ACh-induced tracheal contraction. Ronacaleret, JTT-305 and NPSP-795 are from the same structural class of amino alcohols, with similar structures, so it is not surprising that they all have effects in the therapeutic setting though JTT-305 has a lower effect than the other two. However, only NPSP-795 has an effect in the prophylactic setting, while the other two amino alcohols show no effects. In addition, AXT 914 didn't show an effect in the therapeutic setting, while it did evoke airway relaxation in the prophylactic setting. The reason for these differences is still unclear; but may be related to the distribution of the agent in the tissue, and/or to the affinity to the receptor for the drug. Also, Diao et al. have investigated bronchodilator properties using different NAMs compared with the standard-of-care SABA salbutamol and LABA formoterol (Diao et al. 2023). The authors showed that 1) CaSR NAMs and salbutamol can inhibit MCh-induced airway contraction to a similar extent; 2) the bronchodilator effects of CaSR NAMs still exist when salbutamol has no effect under conditions mimicking a severe asthma attack when β2-adrenergic receptor desensitization; 3). two of the CaSR NAMs they tested (NPS2143 and Pfizer compound 1) demonstrated preventive effect after overnight treatment on MCh-induced airway contraction, while formoterol and one of the CaSR NAMs, BMS compound 1 didn't. Together with their results, CaSR NAMs may have better bronchodilator effects than those of the existing bronchodilators, especially regarding their preventive effects.

Question 3. Which of the existing clinically tested calcilytics is best suited for lung delivery?

Upon the completion of the *ex vivo* work, NPSP-795 was selected as the inhaled calcilytic to be used *in vivo* asthma model since NPSP-795 showed both prophylactic and therapeutic effects in ACh-induced airway contraction in naïve trachea. In addition, studies carried out by my colleague in our laboratory show good PK/PD and formulation characteristics compatible with inhaled drug delivery. Therefore. Next, I further investigated the effects of inhaled NPSP-795 in vivo on airway remodelling by determining its effects on airway hyperresponsiveness, airway inflammation, mucus secretion and collagen deposition.

Question 4. Does therapeutic administration of inhaled calcilytics show efficacy in alarmin-driven asthma, which is associated with steroid resistance?

In the last part of my work, I went to Prof Sun Ying's laboratory in China, to have access to equipment that allowed me to directly measure lung function using an invasive technology, the FlexiVent. There, I have developed parallel animal models of IgE/Th2 and alarmin-driven asthma, in which I have compared the therapeutic effects of the best performing calcilytic, NPSP-795, delivered by inhalation, on airway resistance, inflammation and remodelling. My results showed that inhaled calcilytic have inhibitory effects on airway inflammation, airway hyperresponsiveness and some aspects of remodelling in both IgE- and alarmin-driven asthma models.

The mechanism of asthma mainly involves Th2 cells, IgE, B cells, ILC2, NK cells, basophils, eosinophils, mast cells and their major cytokines, such as IL-4, IL-13, IL-5, IL-33, IL-25, TSLP etc (Boonpiyathad et al. 2019). The start of asthma is characterized by the recruitment of eosinophils and mast cells degranulation in the airway and release of inflammatory mediators to cause airway inflammation, activated by IgE after exposure to allergens, viruses, pollutants and microbes (Lambrecht and Hammad 2015; Israel and Reddel 2017). All asthmatic patients have varying degrees of airway inflammation, mainly including inflammatory cell infiltration and mediator production, which is considered to be the main pathogenetic mechanism and underlying

problem in causing various clinical symptoms of asthma (Hargreave et al. 1986). In my PhD studies, I have shown that inhaled calcilytics do have the ability to reduce inflammatory cell infiltration into the BALF and also lung tissue, including eosinophil, neutrophil and lymphocyte infiltration in both the OVA- and the IL-33-induced models. As mentioned above airway inflammation is a key upstream asthma symptom (Reed 1988). Therefore, the inhibition of airway inflammation by inhaled calcilytic may have benefits to the remaining downstream asthma symptoms, AHR and airway remodelling. AHR is an important pathological feature of asthma and almost all asthmatic patients have increased airway responsiveness, and most importantly, airway responsiveness is life-threatening even in mild patients (Corrigan 2020). AHR not only exists in asthmatic patients, it can also be seen in viral upper respiratory tract infections, acute and chronic bronchitis, allergic rhinitis, gastroesophageal reflux (GRE), bronchiectasis, allergic alveolitis, sarcoidosis, cystic fibrosis, lung transplantation, congestive heart failure and other diseases (Hegele et al. 1995; Thaminy et al. 2000; Ratier et al. 2011). AHR is defined as a premature or too strong contraction response of the airway, stimulated by various factors (such as dust mites, pollen, animal fur, cold air, toluene, sulfur dioxide, etc.), causing airway lumen stenosis and airway resistance significantly increased. There is strong evidence that airway AHR in asthma is associated with increased contractile activity of bronchial smooth muscle, notwithstanding any passive contributions from altered airway geometry (Marsumoto et al. 2007; Léguillette et al. 2009). The precise mechanisms have yet to be determined, but have been linked with alterations in intracellular Ca^{2+} (Ca^{2+}_i) handling and/or sensitivity, the contractile machinery, and cytoskeleton (Triggle 1983; Mahn et al. 2010; Zhang and Gunst 2019). In my studies, inhaled calcilytic also reduces the increased AHR provoked by MCh. This result is consistent with the work conducted by Diao et al. showing CaSR-negative allosteric modulators inhibit chronic airway inflammation, remodelling, and hyperresponsiveness in murine and guinea pig asthma models (Diao et al. 2023). Taken together with my *ex vivo* work showing that certain calcilytics reduce tracheal contraction, these observations may indicate that inhaled calcilytic can be used as a surrogate of bronchodilators. Most importantly, my ex vivo data using wire myography

showed that NPS-P795 have a prophylactic effect on ACh-induced airway contraction, suggesting that NPS-P795 might have the potential to prevent the onset of airway hyperresponsiveness which no existing drugs can do. This is especially important because shortness of breath caused by airway narrowing resulting from airway hyperresponsiveness can be life-threatening even in mild patients (Corrigan 2020).

Increasing mucus production in the airway lumen is one of the possible causes of persistent airflow obstruction, and is the main reason for asthma death (Dunican et al. 2018a; Dunican et al. 2018b). In my OVA and IL-33 comparison study, the result reveals that inhaled calcilytic didn't show any effects on mucus secretion, however, in my other study with a comparison of inhaled calcilytic and FP, quantitative image analysis showed that inhaled NPSP-795 reduced the mean goblet cell number in the airways, while FP did not, indicating inhaled calcilytic may be better in controlling airway remodelling than that of corticosteroids. Since in the inhaled calcilytic and FP comparison study, it has already shown beneficial effects of inhaled calcilytic on goblet cell hyperplasia, in the future, it will also be worth testing the effects of inhaled calcilytic on gene or protein expression of the two different mucins MUC5AC and MUC5B. It is well known that MUC5A and MUC5B are localized to different parts of airway, of which MUC5B protein is mainly localized to mucous cells in submucosal glands, MUC5AC protein is mainly localized to goblet cells in the tracheobronchial surface epithelium and is the most highly induced mucin in the airways of antigen-challenged mice (Hovenberg et al. 1996; Groneberg et al. 2002; Young et al. 2007). Thus, it would be worth to understand whether there might be beneficial effects of inhaled calcilytic on mucus production. Actually, in a study conducted by a Chinese group the authors were able to show by using a HBE16 cell hypoxia model 1). hypoxia can induce increased expression levels of CaSR, MUC5AC protein, and increased expression level of MUC5AC mRNA; 2). transfection with CaSR siRNA can downregulate the above effects induced by hypoxia; 3). pretreatment with CasR signaling pathway Gαq/11 protein inhibitor YM-254890 significantly attenuated the hypoxia-induced MUC5AC hypersecretion (as demonstrated by the decreased expression level of MUC5AC protein and

expression level of MUC5AC mRNA) and $[Ca^{2+}]_i$ (Yang et al. 2014). Another study conducted by Lee et al from Korea also demonstrated that the increased expression of MUC5AC induced by cigarette smoke extract (CSE)-in human airway epithelial cells can be inhibited by CaSR antagonist NPS2143 (Lee et al. 2017b). These studies further demonstrate that calcilytics may have a potential effect on mucus production in asthma. Airway remodelling in asthma refers to hypertrophy of the external smooth muscle layer, is a result of the repeated episodes and repeated repairs of long-lasting airway inflammation, resulting in tissue proliferation and is another mechanism of persistent airflow obstruction (Tagaya and Tamaoki 2007). The mechanism of airway remodelling is related to the smooth muscle cells exposure to pro-inflammatory cytokines and prolonged elevation of intracellular calcium, laydown of structural proteins, hypertrophy of mucus glands, collagen deposition and neovascularisation in the airway's mucosa, any of which may contribute to structural, and consequently irreversible obstruction of the airways (Gosens et al. 2008; Mahn et al. 2010). Airway remodelling caused by inflammatory damage-repair-re-damage-re-repair of airway epithelium may be an important pathophysiological basis for the development of asthma into refractory asthma. In my study, I measured the collagen deposition around different parts of peribronchial and perivascular regions of lungs from asthma animal models induced by OVA and IL-33 and have shown that inhaled calcilytic can reduce the collagen deposition in both models, which indicated that inhaled calcilytic may be beneficial in reducing airway remodelling. However, in my studies, I only measured collagen deposition due to the time limit, in the future, we can further measure other fibrosis parameters, such as the expression of matrix metalloproteinases (MMPs) and of tissue inhibitors of metalloproteinases (TIMPs), and also of other parameters regarding angiogenesis to give an overall view of the effects of inhaled calcilytic on airway remodelling. Actually, in the same paper mentioned above conducted by Lee et al, the authors also showed that NPS2143 reduced the expression of MMP-9 in CSE-stimulated H292 cells (Lee et al. 2017b), which emphasizes the potential effects of calcilytic on airway remodelling and it is worth to further test in future in asthma.

Lastly, because the CaSR can affect systemic Ca^{2+} concentrations and will result in hypercalcaemia with the “overspill” of calcilytic into the systemic circulation, I also measured the systemic side effects of inhaled calcilytic by quantifying serum Ca^{2+} levels. The results revealed no effect of inhaled calcilytic on serum Ca^{2+} levels, suggesting that local application of inhaled calcilytic does not result in significant systemic “overspill”.

Currently, the most common treatment strategy for asthma patients is the chronic use of inhaled corticosteroids to control inflammation and with add-on use of bronchodilators to relieve airway contraction. However, these drugs do not always have effects in all patients, especially patients with severe symptoms, and are associated with side effects with long-term use, which leads the researcher to find new treatments for asthma. Omalizumab, a humanised monoclonal antibody (mAb) against IgE, was the first biologic therapy approved for asthma, and has been used for several years (Buhl 2005; Gennaro et al. 2007; Catley et al. 2011). Studies have shown its efficacy in reducing the rates of asthma exacerbations, improving lung function, reducing the doses of ICS required and hospitalisations in severe allergic asthmatic patients (Holgate et al. 2004; Humbert et al. 2005; Hanania et al. 2011; Alhossan et al. 2017; Mansur et al. 2017). IL-4, IL-5 and IL-13 are very important cytokines responsible for B cell maturation, activation, eosinophil recruitment, mucus secretion, ultimately leading to airway remodelling and permanent airflow limitation over time (Wills-Karp 2004; Kay 2015; Larose et al. 2015; Barnes 2018; Boonpiyathad et al. 2019; Lambrecht et al. 2019; Nair and O’Byrne 2019), thus biologics targeting these cytokines (Mepolizumab, Reslizumab, Benralizumab and Dupilumab) have been developed and shown efficacy in a subset of patients with severe eosinophilic asthma in reducing asthma exacerbations and improvement of quality of life scores and lung function improvement (Pavord et al. 2012; Haldar et al. 2014; Bleecker et al. 2016; FitzGerald et al. 2016; Chupp et al. 2017; Nair et al. 2017; Castro et al. 2018; Rabe et al. 2018). Recently, therapies targeting IL-5 (Mepolizumab, Reslizumab, and Benralizumab), IL-4/IL-13 (Dupilumab) and TSLP (Tezepelumab) are approved to treat some subsets of patients with severe asthma. However, there is also a lack of biomarkers to guide the selection of biologics, for example, some patients with severe asthma have

both high blood eosinophil and IgE levels, so it is difficult to know which is the optimal choice of therapy with omalizumab and anti-cytokines therapies for such patients. There are other biologics targeting epithelial-derived cytokines, IL-25 and IL-33, which are under development since their vital role in inducing activation of Th2 and ILC2, promoting IL-4, IL-5 and IL-13 Th2-immune response in asthma after epithelial damage due to the environmental exposures (Lambrecht and Hammad 2012; Christianson et al. 2015). Clinical studies have shown that REGN3500 (anti-IL-33 mAb) significantly reduce exacerbation rate and improve asthma control (Corren et al. 2017; Gauvreau et al. 2020b), which provide treatment opportunities for asthma in the future. However, there are some limitations of biologics in asthma therapy, one is, as mentioned above, the difficulties in selection of biologics to be used due to the lack of biomarkers to distinguish between patients of different subtypes depending on the heterogeneity of patients. On the other hand, the subcutaneous injection route causes poor patient compliance, so optimization of airway delivery of biological agents needs to be addressed in future development (Eyerich et al. 2020). Another challenge is the expense of biologics, which will limit their use in low- and middle-income settings. Compared to the significant side effects of corticosteroids and bronchodilators as well as the limitations of the recently approved and the underdevelopment of biologics, our results showed that inhaled calcilytics have effects on almost all asthma symptoms including airway inflammation, cytokine production and collagen deposition, suggesting CaSR may be involve in all these processes. Thus, in the future, it may be worth to directly investigate the interaction between CaSR and mediators involved in asthma, such as to investigate the change of expression of CaSR in different cells after they are exposed to asthma triggers as well as to see the effect on asthma symptoms after CaSR ablation. In addition, it would be worth to test if inhaled calcilytics could be easy to be self-administered with a suitable inhalation formulation compared to the biologics and if inhaled calcilytics may function as fast bronchodilators in reducing the acute symptoms, as I saw from my ex vivo wire myography experiment that calcilytics have an effect on tracheal contraction. Actually, Diao et al. (Diao et al. 2023) demonstrated that CaSR NAMs reverse MCh-induced airway contraction using mouse precision-cut lung slices, with

maximal relaxation similar to the standard treatment, salbutamol. In addition, they demonstrated CaSR NAMs caused airway relaxation even when salbutamol was ineffective under conditions of β_2-adrenergic receptor desensitization. These findings further support that CaSR NAMs have the repurposing potential as alternative or adjunct bronchodilators in asthma, especially since their preventive effects are unparalleled by other drugs.

6.2 Conclusions and future work

Together with the therapeutic potential targeting inflammatory cell infiltration, airway hyperresponsiveness, cytokines production and collagen deposition in both the OVA and IL-33 models, inhaled calcilytic might represent a novel therapeutic for the treatment of asthma, including difficult-to-treat, steroid-resistant asthma.

It remains to be determined the exact underlying mechanism and the true molecular triggers for asthma, and additional experiments are required to understand how CaSR interact with different cells and mediators in asthma. In any event, my PhD studies have demonstrated that CaSR is involved in asthma pathogenesis and its negative allosteric modulators, calcilytics, have the potential to act upstream in the asthma signalling cascade, rather than intervening in downstream signalling. Another PhD student from our laboratory has demonstrated that the CaSR is expressed in ILC2 cells, another cell type implicated in the mechanism of non-allergic and severe asthma (Boonpiyathad et al. 2019), and that urban particulate matter directly activates the CaSR. So, our study gives new insights into the mechanism by which asthma develops, and proposes the CaSR as a novel treatment target. Such a target is different from other molecular mechanisms that have long been investigated in clinical research area and by the pharmaceutical industry.

In the future, exploring other key asthma-related markers across various asthma models, including acute asthma, chronic asthma, and steroid-resistant asthma, may provide valuable insights, such as collagen deposition for airway remodeling, as well as fibronectin, transforming growth factor-beta (TGF-β), and connective tissue growth factor (CTGF) for fibrosis and other markers to better understand their potential roles in asthma pathophysiology.

Chapter VII References

Abraham, B. et al. 2003. The ENFUMOSA cross-sectional European multicentre study of the clinical phenotype of chronic severe asthma. European Network for Understanding Mechanisms of Severe Asthma. *The European Respiratory Journal* 22(3), pp. 470–477. doi: 10.1183/09031936.03.00261903.

Adinoff, A.D. and Hollister, J.R. 1983. Steroid-induced fractures and bone loss in patients with asthma. *The New England Journal of Medicine* 309(5), pp. 265–268. doi: 10.1056/NEJM198308043090502.

Agache, I. et al. 2020. Efficacy and safety of treatment with biologicals (benralizumab, dupilumab and omalizumab) for severe allergic asthma: A systematic review for the EAACI Guidelines - recommendations on the use of biologicals in severe asthma. *Allergy* 75(5), pp. 1043–1057. doi: 10.1111/all.14235.

Ahookhosh, K., Vanoirbeek, J. and Vande Velde, G. 2023. Lung function measurements in preclinical research: What has been done and where is it headed? *Frontiers in Physiology* 14, p. 1130096. doi: 10.3389/fphys.2023.1130096.

Akizawa, T., Ikejiri, K., Kondo, Y., Endo, Y. and Fukagawa, M. 2020. Evocalcet: A New Oral Calcimimetic for Dialysis Patients With Secondary Hyperparathyroidism. *Therapeutic Apheresis and Dialysis* 24(3), pp. 248–257. doi: 10.1111/1744-9987.13434.

Akizawa, T., Shimazaki, R. and Fukagawa, M. 2018. Phase 2b study of evocalcet (KHK7580), a novel calcimimetic, in Japanese patients with secondary hyperparathyroidism undergoing hemodialysis: A randomized, double-blind, placebo-controlled, dose-finding study. *PLoS ONE* 13(10), p. e0204896. doi: 10.1371/journal.pone.0204896.

Alam, R., Good, J., Rollins, D., Verma, M., Chu, H.W., Pham, T.H. and Martin, R.J. 2017. Airway and serum biochemical correlates of refractory neutrophilic asthma. *The Journal of Allergy and Clinical Immunology* 140(4), pp. 1004-1014.e13. doi: 10.1016/j.jaci.2016.12.963.

Alhossan, A., Lee, C.S., MacDonald, K. and Abraham, I. 2017. 'Real-life' Effectiveness Studies of Omalizumab in Adult Patients with Severe Allergic Asthma: Meta-analysis. *The Journal of Allergy and Clinical Immunology: In Practice* 5(5), pp. 1362-1370.e2. doi: 10.1016/j.jaip.2017.02.002.

Amelink, M. et al. 2013. Severe adult-onset asthma: A distinct phenotype. *The Journal of Allergy and Clinical Immunology* 132(2), pp. 336–341. doi: 10.1016/j.jaci.2013.04.052.

American Thoracic Society. 2000. Proceedings of the ATS workshop on refractory asthma: current understanding, recommendations, and unanswered questions. American Thoracic Society. *American Journal of Respiratory and Critical Care Medicine* 162(6), pp. 2341–2351. doi: 10.1164/ajrccm.162.6.ats9-00.

Anderson, H.R. et al. 2004. Trends in prevalence of symptoms of asthma, hay fever, and eczema in 12-14 year olds in the British Isles, 1995-2002: questionnaire survey. *BMJ* 328(7447), pp. 1052–1053. doi: 10.1136/bmj.38057.583727.47.

Anderson, H.R., Gupta, R., Strachan, D.P. and Limb, E.S. 2007. 50 Years of asthma: UK trends from 1955 to 2004. *Thorax* 62(1), pp. 85–90. doi: 10.1136/thx.2006.066407.

Antonsen, J.E., Sherrard, D.J. and Andress, D.L. 1998. A calcimimetic agent acutely suppresses parathyroid hormone levels in patients with chronic renal failure. Rapid communication. *Kidney International* 53(1), pp. 223–227. doi: 10.1046/j.1523-1755.1998.00735.x.

Arifin, W.N. and Zahiruddin, W.M. 2017. Sample Size Calculation in Animal Studies Using Resource Equation Approach. *The Malaysian journal of medical sciences* 24(5), pp. 101–105. doi: 10.21315/MJMS2017.24.5.11.

Ba, J. and Friedman, P.A. 2004. Calcium-sensing receptor regulation of renal mineral ion transport. *Cell Calcium* 35(3), pp. 229–237. doi: 10.1016/j.ceca.2003.10.016.

Barnes, P.J. 1999. Effect of beta-agonists on inflammatory cells. *The Journal of Allergy and Clinical Immunology* 104(2 Pt 2), pp. S10-17. doi: 10.1016/S0091-6749(99)70269-1.

Barnes, P.J. 2010a. Inhaled Corticosteroids. *Pharmaceuticals (Basel)* 3(3), pp. 514–540. doi: 10.3390/ph3030514.

Barnes, P.J. 2010b. Mechanisms and resistance in glucocorticoid control of inflammation. *The Journal of Steroid Biochemistry and Molecular Biology* 120(2–3), pp. 76–85. doi: 10.1016/j.jsbmb.2010.02.018.

Barnes, P.J. 2010c. New therapies for asthma: is there any progress? *Trends in Pharmacological Sciences* 31(7), pp. 335–343. doi: 10.1016/j.tips.2010.04.009.

Barnes, P.J. 2011. Glucocorticosteroids: current and future directions. *British Journal of Pharmacology* 163(1), pp. 29–43. doi: 10.1111/j.1476-5381.2010.01199.x.

Barnes, P.J. 2018. Targeting cytokines to treat asthma and chronic obstructive pulmonary disease. *Nature Reviews Immunology* 18(7), pp. 454–466. doi: 10.1038/s41577-018-0006-6.

Barnes, P.J. and Woolcock, A.J. 1998. Difficult asthma. *The European Respiratory Journal* 12(5), pp. 1209–1218. doi: 10.1183/09031936.98.12051209.

Bates, J.H.T., Poynter, M.E., Frodella, C.M., Peters, U., Dixon, A.E. and Suratt, B.T. 2017. Pathophysiology to Phenotype in the Asthma of Obesity. *Annals of the American Thoracic Society* 14(Supplement_5), pp. S395–S398. doi: 10.1513/AnnalsATS.201702-122AW.

Bauer, B.A., Reed, C.E., Yunginger, J.W., Wollan, P.C. and Silverstein, M.D. 1997. Incidence and outcomes of asthma in the elderly. A population-based study in Rochester, Minnesota. *Chest* 111(2), pp. 303–310. doi: 10.1378/chest.111.2.303.

Bel, E.H. 2004. Clinical phenotypes of asthma. *Current Opinion in Pulmonary Medicine* 10(1), pp. 44–50. doi: 10.1097/00063198-200401000-00008.

Bel, E.H. et al. 2014. Oral glucocorticoid-sparing effect of mepolizumab in eosinophilic asthma. *The New England Journal of Medicine* 371(13), pp. 1189–1197. doi: 10.1056/NEJMoa1403291.

Billington, C.K. and Hall, I.P. 2012. Novel cAMP signalling paradigms: therapeutic implications for airway disease. *British Journal of Pharmacology* 166(2), pp. 401–410. doi: 10.1111/j.1476-5381.2011.01719.x.

Billington, C.K., Ojo, O.O., Penn, R.B. and Ito, S. 2013. cAMP regulation of airway smooth muscle function. *Pulmonary Pharmacology and Therapeutics* 26(1), pp. 112–120. doi: 10.1016/j.pupt.2012.05.007.

Billington, C.K. and Penn, R.B. 2003. Signaling and regulation of G protein-coupled receptors in airway smooth muscle. *Respiratory Research* 4(1), p. 2. doi: 10.1186/1465-9921-4-2.

Bjermer, L., Lemiere, C., Maspero, J., Weiss, S., Zangrilli, J. and Germinaro, M. 2016. Reslizumab for Inadequately Controlled Asthma With Elevated Blood Eosinophil Levels: A Randomized Phase 3 Study. *Chest* 150(4), pp. 789–798. doi: 10.1016/j.chest.2016.03.032.

Bleecker, E.R. et al. 2016. Efficacy and safety of benralizumab for patients with severe asthma uncontrolled with high-dosage inhaled corticosteroids and long-acting β2-agonists (SIROCCO): a randomised, multicentre, placebo-controlled phase 3 trial. *The Lancet* 388(10056), pp. 2115–2127. doi: 10.1016/S0140-6736(16)31324-1.

Block, G.A. et al. 2004. Cinacalcet for secondary hyperparathyroidism in patients receiving hemodialysis. *The New England Journal of Medicine* 350(15), pp. 1516–1525. doi: 10.1056/NEJMoa031633.

Block, G.A. et al. 2017. Effect of etelcalcetide vs placebo on serum parathyroid hormone in patients receiving hemodialysis with secondary hyperparathyroidism: Two randomized clinical trials. *Journal of the American Medical Association* 317(2), pp. 146–155. doi: 10.1001/jama.2016.19456.

Bloemen, K., Verstraelen, S., Van Den Heuvel, R., Witters, H., Nelissen, I. and Schoeters, G. 2007. The allergic cascade: Review of the most important molecules in the asthmatic lung. *Immunology Letters* 113(1), pp. 6–18. doi: 10.1016/j.imlet.2007.07.010.

Boonpiyathad, T., Sözener, Z.C., Satitsuksanoa, P. and Akdis, C.A. 2019. Immunologic mechanisms in asthma. *Seminars in Immunology* 46, p. 101333. doi: 10.1016/j.smim.2019.101333.

Boulet, L.P. et al. 1997. Inhibitory effects of an anti-IgE antibody E25 on allergen-induced early asthmatic response. *American Journal of Respiratory and Critical Care Medicine* 155(6), pp. 1835–1840. doi: 10.1164/ajrccm.155.6.9196083.

Brannan, J.D. and Lougheed, M.D. 2012. Airway hyperresponsiveness in asthma: mechanisms, clinical significance, and treatment. *Frontiers in Physiology* 3, p. 460. doi: 10.3389/fphys.2012.00460.

Braun-Fahrländer, C. et al. 2004. No further increase in asthma, hay fever and atopic sensitisation in adolescents living in Switzerland. *The European Respiratory Journal* 23(3), pp. 407–413. doi: 10.1183/09031936.04.00074004.

Brightling, C.E. et al. 2015. Efficacy and safety of tralokinumab in patients with severe uncontrolled asthma: a randomised, double-blind, placebo-controlled, phase 2b trial. *The Lancet Respiratory Medicine* 3(9), pp. 692–701. doi: 10.1016/S2213-2600(15)00197-6.

Brown, E.M. et al. 1993. Cloning and characterization of an extracellular Ca(2+)-sensing receptor from bovine parathyroid. *Nature* 366(6455), pp. 575–580. doi: 10.1038/366575A0.

Brown, E.M. 2007. Clinical lessons from the calcium-sensing receptor. *Nature Clinical Practice Endocrinology & Metabolism* 3(2), pp. 122–133. doi: 10.1038/ncpendmet0388.

Brown, E.M. and Macleod, R.J. 2001. Extracellular calcium sensing and extracellular calcium signaling. *Physiological Reviews* 81(1), pp. 239–297. doi: 10.1152/physrev.2001.81.1.239.

Brown, E.M., Pollak, M., Seidman, C.E., Seidman, J.G., Chou, Y.-H.W., Riccardi, D. and Hebert, S.C. 1995. Calcium-ion-sensing cell-surface receptors. *The New England Journal of Medicine* 333(4), pp. 234–240. doi: 10.1056/NEJM199507273330407.

Buhl, R. 2005. Anti-IgE antibodies for the treatment of asthma. *Current Opinion in Pulmonary Medicine* 11(1), pp. 27–34. doi: 10.1097/01.mcp.0000147860.83639.30.

Busse, W., Corren, J., Lanier, B.Q., McAlary, M., Fowler-Taylor, A., Cioppa, G. Della and Gupta, N. 2001. Omalizumab, anti-IgE recombinant humanized monoclonal antibody, for the treatment of severe allergic asthma. *The Journal of Allergy and Clinical Immunology* 108(2), pp. 184–190. doi: 10.1067/mai.2001.117880.

Busse, W., Spector, S., Rosén, K., Wang, Y. and Alpan, O. 2013. High eosinophil count: A potential biomarker for assessing successful omalizumab treatment effects. *The Journal of Allergy and Clinical Immunology* 132(2), pp. 485-486.e11. doi: 10.1016/j.jaci.2013.02.032.

Busse, W.W. et al. 2010. Safety profile, pharmacokinetics, and biologic activity of MEDI-563, an anti-IL-5 receptor α antibody, in a phase I study of subjects with mild asthma. *The Journal of Allergy and Clinical Immunology* 125(6), pp. 1237-1244.e2. doi: 10.1016/j.jaci.2010.04.005.

Busse, W.W. et al. 2011. Randomized trial of omalizumab (anti-IgE) for asthma in inner-city children. *The New England Journal of Medicine* 364(11), pp. 1005–1015. doi: 10.1056/NEJMoa1009705.

Calhoun, W.J. and Chupp, G.L. 2022. The new era of add-on asthma treatments: where do we stand? *Allergy, Asthma, and Clinical Immunology* 18(1), p. 42. doi: 10.1186/S13223-022-00676-0.

Caltabiano, S. et al. 2013. Characterization of the effect of chronic administration of a calcium-sensing receptor antagonist, ronacaleret, on renal calcium excretion and serum calcium in postmenopausal women. *Bone* 56(1), pp. 154–162. doi: 10.1016/j.bone.2013.05.021.

Camoretti-Mercado, B. and Lockey, R.F. 2021. Airway smooth muscle pathophysiology in asthma. *The Journal of Allergy and Clinical Immunology* 147(6), pp. 1983–1995. doi: 10.1016/j.jaci.2021.03.035.

Castro, M. et al. 2011. Reslizumab for poorly controlled, eosinophilic asthma: A randomized, placebo-controlled study. *American Journal of Respiratory and Critical Care Medicine* 184(10), pp. 1125–1132. doi: 10.1164/rccm.201103-0396OC.

Castro, M. et al. 2014. Benralizumab, an anti-interleukin 5 receptor α monoclonal antibody, versus placebo for uncontrolled eosinophilic asthma: a phase 2b randomised dose-ranging study. *The Lancet Respiratory Medicine* 2(11), pp. 879–890. doi: 10.1016/S2213-2600(14)70201-2.

Castro, M. et al. 2015. Reslizumab for inadequately controlled asthma with elevated blood eosinophil counts: results from two multicentre, parallel, double-blind, randomised, placebo-controlled, phase 3 trials. *The Lancet Respiratory Medicine* 3(5), pp. 355–366. doi: 10.1016/S2213-2600(15)00042-9.

Castro, M. et al. 2018. Dupilumab Efficacy and Safety in Moderate-to-Severe Uncontrolled Asthma. *The New England Journal of Medicine* 378(26), pp. 2486–2496. doi: 10.1056/NEJMoa1804092.

Catley, M.C., Coote, J., Bari, M. and Tomlinson, K.L. 2011. Monoclonal antibodies for the treatment of asthma. *Pharmacology & Therapeutics* 132(3), pp. 333–351. doi: 10.1016/j.pharmthera.2011.09.005.

Cayrol, C. and Girard, J.P. 2009. The IL-1-like cytokine IL-33 is inactivated after maturation by caspase-1. *Proceedings of the National Academy of Sciences of the United States of America* 106(22), pp. 9021–9026. doi: 10.1073/pnas.0812690106.

Cayrol, C. and Girard, J.P. 2014. IL-33: an alarmin cytokine with crucial roles in innate immunity, inflammation and allergy. *Current Opinion in Immunology* 31, pp. 31–37. doi: 10.1016/j.coi.2014.09.004.

Chalitsios, C. V., Shaw, D.E. and Mckeever, T.M. 2021. Risk of osteoporosis and fragility fractures in asthma due to oral and inhaled corticosteroids: Two population-based nested case-control studies. *Thorax* 76(1), pp. 21–28. doi: 10.1136/thoraxjnl-2020-215664.

Chang, W., Pratt, S., Chen, T.H., Nemeth, E., Huang, Z. and Shoback, D. 1998. Coupling of calcium receptors to inositol phosphate and cyclic AMP generation in mammalian cells and Xenopus laevis oocytes and immunodetection of receptor protein by region-specific antipeptide antisera. *Journal of bone and mineral research* 13(4), pp. 570–580. doi: 10.1359/JBMR.1998.13.4.570.

Cheng, I. et al. 1999. Expression of an extracellular calcium-sensing receptor in rat stomach. *Gastroenterology* 116(1), pp. 118–126. doi: 10.1016/S0016-5085(99)70235-0.

Cheng, I., Klingensmith, M.E., Chattopadhyay, N., Kifor, O., Butters, R.R., Soybel, D.I. and Brown, E.M. 1998. Identification and localization of the extracellular calcium-sensing receptor in human breast. *The Journal of*

Clinical Endocrinology and Metabolism 83(2), pp. 703–707. doi: 10.1210/jcem.83.2.4558.

Chibana, K. et al. 2008. IL-13 induced increases in nitrite levels are primarily driven by increases in inducible nitric oxide synthase as compared with effects on arginases in human primary bronchial epithelial cells. *Clinical and Experimental Allergy* 38(6), pp. 936–946. doi: 10.1111/j.1365-2222.2008.02969.x.

Chikatsu, N. et al. 2003. A family of autosomal dominant hypocalcemia with an activating mutation of calcium-sensing receptor gene. *Endocrine Journal* 50(1), pp. 91–96. doi: 10.1507/endocrj.50.91.

Chini, L., Monteferrario, E., Graziani, S. and Moschese, V. 2014. Novel treatments of asthma and allergic diseases. *Paediatric Respiratory Reviews* 15(4), pp. 355–362. doi: 10.1016/j.prrv.2013.10.007.

Chipps, B. et al. 2020. Relative efficacy and safety of inhaled corticosteroids in patients with asthma: Systematic review and network meta-analysis. *Annals of Allergy, Asthma and Immunology* 125(2), pp. 163-170.e3. doi: 10.1016/j.anai.2020.04.006.

Chowdhury, N.U., Guntur, V.P., Newcomb, D.C. and Wechsler, M.E. 2021. Sex and gender in asthma. *European Respiratory Review* 30(162), p. 210067. doi: 10.1183/16000617.0067-2021.

Christianson, C.A. et al. 2015. Persistence of asthma requires multiple feedback circuits involving type 2 innate lymphoid cells and IL-33. *The Journal of Allergy and Clinical Immunology* 136(1), pp. 59-68.e14. doi: 10.1016/j.jaci.2014.11.037.

Chung, K.F. et al. 2014. International ERS/ATS guidelines on definition, evaluation and treatment of severe asthma. *The European Respiratory Journal* 43(2), pp. 343–373. doi: 10.1183/09031936.00202013.

Chupp, G.L. et al. 2017. Efficacy of mepolizumab add-on therapy on health-related quality of life and markers of asthma control in severe eosinophilic asthma (MUSCA): a randomised, double-blind, placebo-controlled, parallel-group, multicentre, phase 3b trial. *The Lancet Respiratory Medicine* 5(5), pp. 390–400. doi: 10.1016/S2213-2600(17)30125-X.

CINQAIR® (reslizumab) Injection – About CINQAIR. 2020. Available at: https://www.cinqair.com/about-cinqair/ [Accessed: 26 March 2024].

Cockcroft, D.W. 2010. Direct challenge tests: Airway hyperresponsiveness in asthma: its measurement and clinical significance. *Chest* 138(2 Suppl), pp. 18S-24S. doi: 10.1378/chest.10-0088.

Cohn, L., Tepper, J.S. and Bottomly, K. 1998. Cutting Edge: IL-4-Independent Induction of Airway Hyperresponsiveness by Th2, But Not Th1, Cells. *The Journal of Immunology* 161(8), pp. 3813–3816. doi: 10.4049/jimmunol.161.8.3813.

Comeau, M.R. and Ziegler, S.F. 2010. The influence of TSLP on the allergic response. *Mucosal Immunology* 3(2), pp. 138–147. doi: 10.1038/mi.2009.134.

Conigrave, A.D. 2016. The Calcium-Sensing Receptor and the Parathyroid: Past, Present, Future. *Frontiers in physiology* 7, p. 563. doi: 10.3389/FPHYS.2016.00563.

Conigrave, A.D. and Ward, D.T. 2013. Calcium-sensing receptor (CaSR): pharmacological properties and signaling pathways. *Best practice & research. Clinical endocrinology & metabolism* 27(3), pp. 315–331. doi: 10.1016/J.BEEM.2013.05.010.

Contoli, M. et al. 2010. Fixed airflow obstruction due to asthma or chronic obstructive pulmonary disease: 5-year follow-up. *The Journal of Allergy and Clinical Immunology* 125(4), pp. 830–837. doi: 10.1016/j.jaci.2010.01.003.

Corren, J. et al. 2009. Efficacy and Safety of AMG 317, an IL-4Ra Antagonist, in Atopic Asthmatic Subjects: A Randomized, Double-blind, Placebo-controlled Study. *The Journal of Allergy and Clinical Immunology* 123(3), p. 732. doi: 10.1016/j.jaci.2009.01.037.

Corren, J. et al. 2010. A randomized, controlled, phase 2 study of AMG 317, an IL-4Ralpha antagonist, in patients with asthma. *American Journal of Respiratory and Critical Care Medicine* 181(8), pp. 788–796. doi: 10.1164/rccm.200909-1448OC.

Corren, J. et al. 2011a. Lebrikizumab Treatment in Adults with Asthma. *The New England Journal of Medicine* 365(12), p. 2433. doi: 10.1056/NEJMoa1106469.

Corren, J., Parnes, J.R., Wang, L., Mo, M., Roseti, S.L., Griffiths, J.M. and van der Merwe, R. 2017. Tezepelumab in Adults with Uncontrolled Asthma. *The New England Journal of Medicine* 377(10), pp. 936–946. doi: 10.1056/NEJMoa1704064.

Corren, J., Weinstein, S., Janka, L., Zangrilli, J. and Garin, M. 2016. Phase 3 Study of Reslizumab in Patients With Poorly Controlled Asthma: Effects Across a Broad Range of Eosinophil Counts. *Chest* 150(4), pp. 799–810. doi: 10.1016/j.chest.2016.03.018.

Corren, J., Wood, R.A., Patel, D., Zhu, J., Yegin, A., Dhillon, G. and Fish, J.E. 2011b. Effects of omalizumab on changes in pulmonary function induced by

controlled cat room challenge. *The Journal of Allergy and Clinical Immunology* 127(2), pp. 398–405. doi: 10.1016/j.jaci.2010.09.043.

Corrigan, C.J. 2020. Calcilytics: a non-steroidal replacement for inhaled steroid and SABA/LABA therapy of human asthma? *Expert Review of Respiratory Medicine* 14(8), pp. 807–816. doi: 10.1080/17476348.2020.1756779.

Cosman, F. et al. 2016. A phase 2 study of MK-5442, a calcium-sensing receptor antagonist, in postmenopausal women with osteoporosis after long-term use of oral bisphosphonates. *Osteoporosis International* 27(1), pp. 377–386. doi: 10.1007/S00198-015-3392-7.

Das, S., Clézardin, P., Kamel, S., Brazier, M. and Mentaverri, R. 2020. The CaSR in Pathogenesis of Breast Cancer: A New Target for Early Stage Bone Metastases. *Frontiers in Oncology* 10, p. 69. doi: 10.3389/fonc.2020.00069.

Daub, H., Weiss, F.U., Wallasch, C. and Ullrich, A. 1996. Role of transactivation of the EGF receptor in signalling by G-protein-coupled receptors. *Nature* 379(6565), pp. 557–560. doi: 10.1038/379557A0.

Devenny, A., Wassall, H., Ninan, T., Omran, M., Khan, S.D. and Russell, G. 2004. Respiratory symptoms and atopy in children in Aberdeen: questionnaire studies of a defined school population repeated over 35 years. *BMJ* 329(7464), pp. 489–490. doi: 10.1136/bmj.38139.666447.F7.

Diao, J., Lam, M., Gregory, K.J., Leach, K. and Bourke, J.E. 2023. Calcium-Sensing Receptor Negative Allosteric Modulators Oppose Contraction of Mouse Airways. *American Journal of Respiratory Cell and Molecular Biology* 69(2), pp. 182–196. doi: 10.1165/rcmb.2021-0544OC.

Dixon, A.E. et al. 2011. Effects of obesity and bariatric surgery on airway hyperresponsiveness, asthma control, and inflammation. *The Journal of Allergy and Clinical Immunology* 128(3), pp. 508-515.e2. doi: 10.1016/j.jaci.2011.06.009.

Doublier, A., Farlay, D., Jaurand, X., Vera, R. and Boivin, G. 2013. Effects of strontium on the quality of bone apatite crystals: a paired biopsy study in postmenopausal osteoporotic women. *Osteoporosis International* 24(3), pp. 1079–1087. doi: 10.1007/S00198-012-2181-9.

Dunican, E.M. et al. 2018a. Mucus plugs in patients with asthma linked to eosinophilia and airflow obstruction. *The Journal of Clinical Investigation* 128(3), pp. 997–1009. doi: 10.1172/JCI95693.

Dunican, E.M., Watchorn, D.C. and Fahy, J. V. 2018b. Autopsy and Imaging Studies of Mucus in Asthma. Lessons Learned about Disease Mechanisms

and the Role of Mucus in Airflow Obstruction. *Annals of the American Thoracic Society* 15(Suppl 3), pp. S184–S191. doi: 10.1513/AnnalsATS.201807-485AW.

Dvorak, M.M., Siddiqua, A., Ward, D.T., Carter, D.H., Dallas, S.L., Nemeth, E.F. and Riccardi, D. 2004. Physiological changes in extracellular calcium concentration directly control osteoblast function in the absence of calciotropic hormones. *Proceedings of the National Academy of Sciences of the United States of America* 101(14), pp. 5140–5145. doi: 10.1073/pnas.0306141101.

Dykman, T.R., Gluck, O.S., Murphy, W.A., Hahn, T.J. and Hahn, B.H. 1985. Evaluation of factors associated with glucocorticoid-induced osteopenia in patients with rheumatic diseases. *Arthritis and Rheumatism* 28(4), pp. 361–368. doi: 10.1002/art.1780280402.

E, R., GB, A., JH, B., ME, P., M, W., S, A. and LK, L. 2012. The Temporal Evolution of Airways Hyperresponsiveness and Inflammation. *Journal of Allergy & Therapy* 1(5), pp. 1–7. doi: 10.4172/2155-6121.S1-005.

Endou, K. et al. 2004. 8-Bromo-cAMP decreases the Ca2+ sensitivity of airway smooth muscle contraction through a mechanism distinct from inhibition of Rho-kinase. *American Journal of Physiology - Lung Cellular and Molecular Physiology* 287(4), pp. L641–L648. doi: 10.1152/ajplung.00287.2003.

Engvall, E. and Perlmann, P. 1971. Enzyme-linked immunosorbent assay (ELISA) quantitative assay of immunoglobulin G. *Immunochemistry* 8(9), pp. 871–874. doi: 10.1016/0019-2791(71)90454-X.

Escotte, S. et al. 2002. Fluticasone propionate inhibits lipopolysaccharide-induced proinflammatory response in human cystic fibrosis airway grafts. *Journal of Pharmacology and Experimental Therapeutics* 302(3), pp. 1151–1157. doi: 10.1124/jpet.102.033407.

Evans, R.L., Nials, A.T., Knowles, R.G., Kidd, E.J., Ford, W.R. and Broadley, K.J. 2012. A comparison of antiasthma drugs between acute and chronic ovalbumin-challenged guinea-pig models of asthma. *Pulmonary Pharmacology and Therapeutics* 25(6), pp. 453–464. doi: 10.1016/j.pupt.2012.08.004.

Eyerich, S., Metz, M., Bossios, A. and Eyerich, K. 2020. New biological treatments for asthma and skin allergies. *Allergy* 75(3), pp. 546–560. doi: 10.1111/all.14027.

Fahy, J. V. et al. 1997. The effect of an anti-IgE monoclonal antibody on the early- and late-phase responses to allergen inhalation in asthmatic subjects.

American Journal of Respiratory and Critical Care Medicine 155(6), pp. 1828–1834. doi: 10.1164/ajrccm.155.6.9196082.

Fahy, J. V. et al. 1999. Effect of aerosolized anti-IgE (E25) on airway responses to inhaled allergen in asthmatic subjects. *American Journal of Respiratory and Critical Care Medicine* 160(3), pp. 1023–1027. doi: 10.1164/ajrccm.160.3.9810012.

Fajt, M.L. and Wenzel, S.E. 2014. Biologic therapy in asthma: Entering the new age of personalized medicine. *Journal of Asthma* 51(7), pp. 669–676. doi: 10.3109/02770903.2014.910221.

Farne, H.A., Wilson, A., Powell, C., Bax, L. and Milan, S.J. 2017. Anti-IL5 therapies for asthma. *The Cochrane Database of Systematic Reviews* 9(9), p. CD010834. doi: 10.1002/14651858.CD010834.pub3.

Fasciani, I. et al. 2022. GPCRs in Intracellular Compartments: New Targets for Drug Discovery. *Biomolecules* 12(10), p. 1343. doi: 10.3390/biom12101343.

Festing, M.F.W. 2006. Design and statistical methods in studies using animal models of development. *ILAR journal* 47(1), pp. 5–14. doi: 10.1093/ilar.47.1.5.

Festing, M.F.W. and Altman, D.G. 2002. Guidelines for the design and statistical analysis of experiments using laboratory animals. *ILAR journal* 43(4), pp. 244–257. doi: 10.1093/ilar.43.4.244.

FitzGerald, J.M. et al. 2016. Benralizumab, an anti-interleukin-5 receptor α monoclonal antibody, as add-on treatment for patients with severe, uncontrolled, eosinophilic asthma (CALIMA): a randomised, double-blind, placebo-controlled phase 3 trial. *The Lancet* 388(10056), pp. 2128–2141. doi: 10.1016/S0140-6736(16)31322-8.

Fitzpatrick, A.M., Chipps, B.E., Holguin, F. and Woodruff, P.G. 2020. T2-"Low" Asthma: Overview and Management Strategies. *The Journal of Allergy and Clinical Immunology: In Practice* 8(2), pp. 452–463. doi: 10.1016/j.jaip.2019.11.006.

Flood-Page, P. et al. 2007. A study to evaluate safety and efficacy of mepolizumab in patients with moderate persistent asthma. *American Journal of Respiratory and Critical Care Medicine* 176(11), pp. 1062–1071. doi: 10.1164/rccm.200701-085OC.

Flood-Page, P.T., Menzies-Gow, A.N., Kay, A.B. and Robinson, D.S. 2003. Eosinophil's role remains uncertain as anti-interleukin-5 only partially depletes numbers in asthmatic airway. *American Journal of Respiratory and Critical Care Medicine* 167(2), pp. 199–204. doi: 10.1164/rccm.200208-789OC.

Fujita, J. et al. 2012. Interleukin-33 induces interleukin-17F in bronchial epithelial cells. *Allergy* 67(6), pp. 744–750. doi: 10.1111/j.1398-9995.2012.02825.x.

Fukagawa, M., Shimazaki, R. and Akizawa, T. 2018. Head-to-head comparison of the new calcimimetic agent evocalcet with cinacalcet in Japanese hemodialysis patients with secondary hyperparathyroidism. *Kidney International* 94(4), pp. 818–825. doi: 10.1016/j.kint.2018.05.013.

Fuseini, H. and Newcomb, D.C. 2017. Mechanisms Driving Gender Differences in Asthma. *Current Allergy and Asthma Reports* 17(3), p. 19. doi: 10.1007/s11882-017-0686-1.

Gacasan, S.B., Baker, D.L. and Parrill, A.L. 2017. G protein-coupled receptors: The evolution of structural insight. *AIMS Biophysics* 4(3), pp. 491–527. doi: 10.3934/biophy.2017.3.491.

Gafni, R.I. et al. 2023. Efficacy and Safety of Encaleret in Autosomal Dominant Hypocalcemia Type 1. *The New England Journal of Medicine* 389(13), pp. 1245–1247. doi: 10.1056/nejmc2302708.

Galigniana, M.D., Piwien-Pilipuk, G. and Assreuy, J. 1999. Inhibition of glucocorticoid receptor binding by nitric oxide. *Molecular Pharmacology* 55(2), pp. 317–323. doi: 10.1124/mol.55.2.317.

Garrettt, J.E. et al. 1995. Molecular cloning and functional expression of human parathyroid calcium receptor cDNAs. *The Journal of Biological Chemistry* 270(21), pp. 12919–12925. doi: 10.1074/jbc.270.21.12919.

Gauvreau, G.M. et al. 2011. Effects of interleukin-13 blockade on allergen-induced airway responses in mild atopic asthma. *American Journal of Respiratory and Critical Care Medicine* 183(8), pp. 1007–1014. doi: 10.1164/rccm.201008-1210OC.

Gauvreau, G.M. et al. 2014. Effects of an anti-TSLP antibody on allergen-induced asthmatic responses. *The New England Journal of Medicine* 370(22), pp. 2102–2110. doi: 10.1056/NEJMoa1402895.

Gauvreau, G.M., Sehmi, R., Ambrose, C.S. and Griffiths, J.M. 2020a. Thymic stromal lymphopoietin: its role and potential as a therapeutic target in asthma. *Expert Opinion on Therapeutic Targets* 24(8), pp. 777–792. doi: 10.1080/14728222.2020.1783242.

Gauvreau, G.M., White, L. and Davis, B.E. 2020b. Anti-alarmin approaches entering clinical trials. *Current Opinion in Pulmonary Medicine* 26(1), pp. 69–76. doi: 10.1097/MCP.0000000000000615.

Gennaro, D., Amedeo, P., Antonello, S., Paolo, N., Maria, D. and Gennaro, L. 2007. A recombinant humanized anti-IgE monoclonal antibody (omalizumab) in the therapy of moderate-to-severe allergic asthma. *Recent Patents on Inflammation & Allergy Drug Discovery* 1(3), pp. 225–231. doi: 10.2174/187221307782418900.

Global Initiative for Asthma. 2023. *2023 GINA Main Report - Global Initiative for Asthma - GINA*. Available at: https://ginasthma.org/2023-gina-main-report/ [Accessed: 26 March 2024].

Gonzalez-Uribe, V., Romero-Tapia, S.J. and Castro-Rodriguez, J.A. 2023. Clinical Medicine Asthma Phenotypes in the Era of Personalized Medicine. *Journal of Clinical Medicine* 12(19), p. 6207. doi: 10.3390/jcm12196207.

Goodman, W.G. 2001. Calcimimetic agents for the treatment of hyperparathyroidism. *Current Opinion in Nephrology and Hypertension* 10(5), pp. 575–580. doi: 10.1097/00041552-200109000-00005.

Goodman, W.G. et al. 2002. The Calcimimetic agent AMG 073 lowers plasma parathyroid hormone levels in hemodialysis patients with secondary hyperparathyroidism. *Journal of the American Society of Nephrology* 13(4), pp. 1017–1024. doi: 10.1681/ASN.V1341017.

Gosens, R. et al. 2008. Pharmacology of airway smooth muscle proliferation. *European Journal of Pharmacology* 585(2–3), pp. 385–397. doi: 10.1016/j.ejphar.2008.01.055.

Gowen, M. et al. 2000. Antagonizing the parathyroid calcium receptor stimulates parathyroid hormone secretion and bone formation in osteopenic rats. *The Journal of Clinical Investigation* 105(11), pp. 1595–1604. doi: 10.1172/JCI9038.

Groneberg, D.A. et al. 2002. Expression of respiratory mucins in fatal status asthmaticus and mild asthma. *Histopathology* 40(4), pp. 367–373. doi: 10.1046/J.1365-2559.2002.01378.X.

Grotenboer, N.S., Ketelaar, M.E., Koppelman, G.H. and Nawijn, M.C. 2013. Decoding asthma: translating genetic variation in IL33 and IL1RL1 into disease pathophysiology. *The Journal of Allergy and Clinical Immunology* 131(3), pp. 856–865. doi: 10.1016/j.jaci.2012.11.028.

Grünig, G. et al. 1998. Requirement for IL-13 independently of IL-4 in experimental asthma. *Science* 282(5397), pp. 2261–2263. doi: 10.1126/science.282.5397.2261.

Gude, W.D., Cosgrove, G.E. and Hirsch, G.P. 1982. *Histological Atlas of the Laboratory Mouse*. New York: Springer. doi: 10.1007/978-1-4615-1743-6.

Haldar, P. et al. 2009. Mepolizumab and exacerbations of refractory eosinophilic asthma. *The New England Journal of Medicine* 360(10), pp. 973–984. doi: 10.1056/NEJMoa0808991.

Haldar, P. et al. 2014. Outcomes after cessation of mepolizumab therapy in severe eosinophilic asthma: a 12-month follow-up analysis. *The Journal of Allergy and Clinical Immunology* 133(3), pp. 921–923. doi: 10.1016/j.jaci.2013.11.026.

Halim, T.Y.F., Krauß, R.H., Sun, A.C. and Takei, F. 2012. Lung natural helper cells are a critical source of Th2 cell-type cytokines in protease allergen-induced airway inflammation. *Immunity* 36(3), pp. 451–463. doi: 10.1016/j.immuni.2011.12.020.

Hamelmann, E., Schwarze, J., Takeda, K., Oshiba, A., Larsen, G.L., Irvin, C.G. and Gelfand, E.W. 1997. Noninvasive measurement of airway responsiveness in allergic mice using barometric plethysmography. *American Journal of Respiratory and Critical Care Medicine* 156((3 Pt 1)), pp. 766–775. doi: 10.1164/ajrccm.156.3.9606031.

Hamid, Q., Tulic', M.K., Liu, M.C., Moqbel, R., Peters-Golden, M., Holgate, S. and Pizzichini, E. 2003. Inflammatory cells in asthma: Mechanisms and implications for therapy. *The Journal of Allergy and Clinical Immunology* 111(1 SUPPL), pp. S5–S17. doi: 10.1067/mai.2003.22.

Hanania, N.A. et al. 2011. Omalizumab in severe allergic asthma inadequately controlled with standard therapy: a randomized trial. *Annals of Internal Medicine* 154(9), pp. 573–582. doi: 10.7326/0003-4819-154-9-201105030-00002.

Hanania, N.A. et al. 2013. Exploring the effects of omalizumab in allergic asthma: An analysis of biomarkers in the EXTRA study. *American Journal of Respiratory and Critical Care Medicine* 187(8), pp. 804–811. doi: 10.1164/rccm.201208-1414OC.

Hannan, F.M., Kallay, E., Chang, W., Brandi, M.L. and Thakker, R. V. 2018. The calcium-sensing receptor in physiology and in calcitropic and noncalcitropic diseases. *Nature reviews. Endocrinology* 15(1), pp. 33–51. doi: 10.1038/S41574-018-0115-0.

Hansbro, P.M. et al. 2017. Mechanisms and treatments for severe, steroid-resistant allergic airway disease and asthma. *Immunological Reviews* 278(1), pp. 41–62. doi: 10.1111/imr.12543.

Hansel, T.T. 2004. How do we measure the effectiveness of inhaled corticosteroids in clinical studies? *Respiratory Medicine* 98(Suppl B), pp. S9–S15. doi: 10.1016/j.rmed.2004.07.010.

Hansen, E.F., Phanareth, K., Laursen, L.C., Kok-Jensen, A. and Dirksen, A. 1999. Reversible and irreversible airflow obstruction as predictor of overall mortality in asthma and chronic obstructive pulmonary disease. *American Journal of Respiratory and Critical Care Medicine* 159(4 Pt 1), pp. 1267–1271. doi: 10.1164/ajrccm.159.4.9807121.

Hargreave, F.E., Ramsdale, E.H., Kirby, J.G. and O'Byrne, P.M. 1986. Asthma and the role of inflammation. *European Journal of Respiratory Diseases. Supplement* 147, pp. 16–21.

Hayrapetyan, H., Tran, T., Tellez-Corrales, E. and Madiraju, C. 2023. Enzyme-Linked Immunosorbent Assay: Types and Applications. In: Robert S. Matson ed. *ELISA. Methods in Molecular Biology*. New York: Humana, pp. 1–17. doi: 10.1007/978-1-0716-2903-1_1.

Hegele, R.G., Hayashi, S., Hogg, J.C. and Paré, P.D. 1995. Mechanisms of airway narrowing and hyperresponsiveness in viral respiratory tract infections. *American Journal of Respiratory and Critical Care Medicine* 151(5), pp. 1659–1664. doi: 10.1164/ajrccm.151.5.7735630.

Hekking, P.P.W., Wener, R.R., Amelink, M., Zwinderman, A.H., Bouvy, M.L. and Bel, E.H. 2015. The prevalence of severe refractory asthma. *The Journal of Allergy and Clinical Immunology* 135(4), pp. 896–902. doi: 10.1016/j.jaci.2014.08.042.

Hirano, T. and Matsunaga, K. 2018. Late-onset asthma: current perspectives. *Journal of Asthma and Allergy* 11, pp. 19–27. doi: 10.2147/JAA.S125948.

Holgate, S.T. et al. 2004. Efficacy and safety of a recombinant anti-immunoglobulin E antibody (omalizumab) in severe allergic asthma. *Clinical and Experimental Allergy* 34(4), pp. 632–638. doi: 10.1111/j.1365-2222.2004.1916.x.

Hovenberg, H.W., Davies, J.R. and Carlstedt, I. 1996. Different mucins are produced by the surface epithelium and the submucosa in human trachea: identification of MUC5AC as a major mucin from the goblet cells. *The Biochemical Journal* 318(Pt 1), pp. 319–324. doi: 10.1042/bj3180319.

Huang, C., Hujer, K.M., Wu, Z. and Miller, R.T. 2004. The Ca2+-sensing receptor couples to Galpha12/13 to activate phospholipase D in Madin-Darby canine kidney cells. *American journal of physiology. Cell physiology* 286(1). doi: 10.1152/AJPCELL.00229.2003.

Humbert, M. et al. 1996a. High-affinity IgE receptor (FcepsilonRI)-bearing cells in bronchial biopsies from atopic and nonatopic asthma. *American Journal of Respiratory and Critical Care Medicine* 153(6 Pt 1), pp. 1931–1937. doi: 10.1164/ajrccm.153.6.8665058.

Humbert, M. et al. 1996b. IL-4 and IL-5 mRNA and protein in bronchial biopsies from patients with atopic and nonatopic asthma: evidence against 'intrinsic' asthma being a distinct immunopathologic entity. *American Journal of Respiratory and Critical Care Medicine* 154(5), pp. 1497–1504. doi: 10.1164/ajrccm.154.5.8912771.

Humbert, M. et al. 2005. Benefits of omalizumab as add-on therapy in patients with severe persistent asthma who are inadequately controlled despite best available therapy (GINA 2002 step 4 treatment): INNOVATE. *Allergy* 60(3), pp. 309–316. doi: 10.1111/j.1398-9995.2004.00772.x.

Humbert, M., Busse, W., Hanania, N.A., Lowe, P.J., Canvin, J., Erpenbeck, V.J. and Holgate, S. 2014. Omalizumab in Asthma: An Update on Recent Developments. *The Journal of Allergy and Clinical Immunology: In Practice* 2(5), pp. 525-536.e1. doi: 10.1016/j.jaip.2014.03.010.

Humbert, M., Menz, G., Ying, S., Corrigan, C.J., Robinson, D.S., Durham, S.R. and Kay, A.B. 1999. The immunopathology of extrinsic (atopic) and intrinsic (non-atopic) asthma: more similarities than differences. *Immunology Today* 20(11), pp. 528–533. doi: 10.1016/S0167-5699(99)01535-2.

Huscher, D. et al. 2009. Dose-related patterns of glucocorticoid-induced side effects. *Annals of the Rheumatic Diseases* 68(7), pp. 1119–1124. doi: 10.1136/ard.2008.092163.

Ilmarinen, P., Tuomisto, L.E., Niemelä, O., Danielsson, J., Haanpää, J., Kankaanranta, T. and Kankaanranta, H. 2016. Comorbidities and elevated IL-6 associate with negative outcome in adult-onset asthma. *The European Respiratory Journal* 48(4), pp. 1052–1062. doi: 10.1183/13993003.02198-2015.

Israel, E., Banerjee, T.R., Fitzmaurice, G.M., Kotlov, T. V., LaHive, K. and LeBoff, M.S. 2001. Effects of inhaled glucocorticoids on bone density in premenopausal women. *The New England journal of medicine* 345(13), pp. 941–947. doi: 10.1056/NEJMOA002304.

Israel, E. and Reddel, H.K. 2017. Severe and Difficult-to-Treat Asthma in Adults. *The New England Journal of Medicine* 377(10), pp. 965–976. doi: 10.1056/NEJMra1608969.

Izuhara, K., Arima, K. and Yasunaga, S. 2002. IL-4 and IL-13: their pathological roles in allergic diseases and their potential in developing new therapies. *Current Drug Targets Inflammation and Allergy* 1(3), pp. 263–269. doi: 10.2174/1568010023344661.

Jaffuel, D. et al. 2000. Transcriptional potencies of inhaled glucocorticoids. *American Journal of Respiratory and Critical Care Medicine* 162(1), pp. 57–63. doi: 10.1164/ajrccm.162.1.9901006.

James, A.L. and Wenzel, S. 2007. Clinical relevance of airway remodelling in airway diseases. *The European Respiratory Journal* 30(1), pp. 134–155. doi: 10.1183/09031936.00146905.

Jawaid, I. and Rajesh, S. 2020. Hyperparathyroidism (primary) NICE guideline: diagnosis, assessment, and initial management. *The British Journal of General Practice* 70(696), pp. 362–363. doi: 10.3399/bjgp20X710717.

Jena Patel and Mary Barna Bridgeman. 2018. Etelcalcetide (Parsabiv) for Secondary Hyperparathyroidism in Adults With Chronic Kidney Disease on Hemodialysis. *Pharmacy and Therapeutics* 43(7), pp. 396–399.

John, M.R. et al. 2011. ATF936, a novel oral calcilytic, increases bone mineral density in rats and transiently releases parathyroid hormone in humans. *Bone* 49(2), pp. 233–241. doi: 10.1016/j.bone.2011.04.007.

John, M.R. et al. 2014. AXT914 a novel, orally-active parathyroid hormone-releasing drug in two early studies of healthy volunteers and postmenopausal women. *Bone* 64, pp. 204–210. doi: 10.1016/j.bone.2014.04.015.

Kanani, A.S., Broder, I., Greene, J.M. and Tarlo, S.M. 2005. Correlation between nasal symptoms and asthma severity in patients with atopic and nonatopic asthma. *Annals of Allergy, Asthma & Immunology* 94(3), pp. 341–347. doi: 10.1016/S1081-1206(10)60985-4.

Katritch, V., Cherezov, V. and Stevens, R.C. 2013. Structure-function of the G protein-coupled receptor superfamily. *The Annual Review of Pharmacology and Toxicology* 53, pp. 531–556. doi: 10.1146/annurev-pharmtox-032112-135923.

Kay, A.B. 2015. The early history of the eosinophil. *Clinical and Experimental Allergy* 45(3), pp. 575–582. doi: 10.1111/cea.12480.

Kerwin, B.A. 2008. Polysorbates 20 and 80 used in the formulation of protein biotherapeutics: structure and degradation pathways. *Journal of Pharmaceutical Sciences* 97(8), pp. 2924–2935. doi: 10.1002/jps.21190.

Khan, T.A., Mahler, H.C. and Kishore, R.S.K. 2015. Key interactions of surfactants in therapeutic protein formulations: A review. *European Journal of Pharmaceutics and Biopharmaceutics* 97(Pt A), pp. 60–67. doi: 10.1016/j.ejpb.2015.09.016.

Kifor, O. et al. 2001. Regulation of MAP kinase by calcium-sensing receptor in bovine parathyroid and CaR-transfected HEK293 cells. *American journal of*

physiology. Renal physiology 280(2). doi: 10.1152/AJPRENAL.2001.280.2.F291.

Kim, S.H. 2019. Risk of pneumonia associated with the use of inhaled corticosteroids in asthma. *Allergy, Asthma and Immunology Research* 11(6), pp. 760–762. doi: 10.4168/aair.2019.11.6.760.

Kim, T.B., Park, C.S., Bae, Y.J., Cho, Y.S. and Moon, H.B. 2009. Factors associated with severity and exacerbation of asthma: a baseline analysis of the cohort for reality and evolution of adult asthma in Korea (COREA). *Annals of Allergy, Asthma & Immunology* 103(4), pp. 311–317. doi: 10.1016/S1081-1206(10)60530-3.

Kimura, G. et al. 2013. Toll-like receptor 3 stimulation causes corticosteroid-refractory airway neutrophilia and hyperresponsiveness in mice. *Chest* 144(1), pp. 99–105. doi: 10.1378/chest.12-2610.

Kitajima, M., Lee, H.C., Nakayama, T. and Ziegler, S.F. 2011. TSLP enhances the function of helper type 2 cells. *European Journal of Immunology* 41(7), pp. 1862–1871. doi: 10.1002/eji.201041195.

Kitch, B.T., Levy, B.D. and Fanta, C.H. 2000. Late onset asthma: epidemiology, diagnosis and treatment. *Drugs & Aging* 17(5), pp. 385–397. doi: 10.2165/00002512-200017050-00005.

Krebs, H.A. and Henseleit, K. 1932. Untersuchungen über die Harnstoffbildung im Tierkörper. *Klinische Wochenschrift* 11(18), pp. 757–759. doi: 10.1007/BF01757657.

Krug, N. et al. 2015. Allergen-induced asthmatic responses modified by a GATA3-specific DNAzyme. *The New England Journal of Medicine* 372(21), pp. 1987–1995. doi: 10.1056/NEJMoa1411776.

Kumar, S. et al. 2010. An orally active calcium-sensing receptor antagonist that transiently increases plasma concentrations of PTH and stimulates bone formation. *Bone* 46(2), pp. 534–542. doi: 10.1016/j.bone.2009.09.028.

Kuo, C.H.S. et al. 2017. T-helper cell type 2 (Th2) and non-Th2 molecular phenotypes of asthma using sputum transcriptomics in U-BIOPRED. *The European Respiratory Journal* 49(2), p. 1602135. doi: 10.1183/13993003.02135-2016.

Kurosawa, M., Shimizu, Y., Tsukagoshi, H. and Ueki, M. 1992. Elevated levels of peripheral-blood, naturally occurring aliphatic polyamines in bronchial asthmatic patients with active symptoms. *Allergy* 47(6), pp. 638–643. doi: 10.1111/j.1398-9995.1992.tb02388.x.

Kuruvilla, M.E., Lee, F.E.H. and Lee, G.B. 2019. Understanding Asthma Phenotypes, Endotypes, and Mechanisms of Disease. *Clinical Reviews in Allergy & Immunology* 56(2), pp. 219–233. doi: 10.1007/S12016-018-8712-1.

Kwong, G.N.M. et al. 2001. Increasing prevalence of asthma diagnosis and symptoms in children is confined to mild symptoms. *Thorax* 56(4), pp. 312–314. doi: 10.1136/thorax.56.4.312.

Lambrecht, B.N. and Hammad, H. 2012. The airway epithelium in asthma. *Nature medicine* 18(5), pp. 684–692. doi: 10.1038/nm.2737.

Lambrecht, B.N. and Hammad, H. 2015. The immunology of asthma. *Nature Immunology* 16(1), pp. 45–56. doi: 10.1038/ni.3049.

Lambrecht, B.N., Hammad, H. and Fahy, J. V. 2019. The Cytokines of Asthma. *Immunity* 50(4), pp. 975–991. doi: 10.1016/j.immuni.2019.03.018.

Larose, M.C., Chakir, J., Archambault, A.S., Joubert, P., Provost, V., Laviolette, M. and Flamand, N. 2015. Correlation between CCL26 production by human bronchial epithelial cells and airway eosinophils: Involvement in patients with severe eosinophilic asthma. *The Journal of Allergy and Clinical Immunology* 136(4), pp. 904–913. doi: 10.1016/j.jaci.2015.02.039.

Leach, C.L. 1998. Improved delivery of inhaled steroids to the large and small airways. *Respiratory Medicine* 92(SUPPL. A), pp. 3–8. doi: 10.1016/S0954-6111(98)90211-6.

Leckie, M.J. et al. 2000. Effects of an interleukin-5 blocking monoclonal antibody on eosinophils, airway hyper-responsiveness, and the late asthmatic response. *The Lancet* 356(9248), pp. 2144–2148. doi: 10.1016/S0140-6736(00)03496-6.

Lee, J.W. et al. 2017a. NPS2143 Inhibits MUC5AC and Proinflammatory Mediators in Cigarette Smoke Extract (CSE)-Stimulated Human Airway Epithelial Cells. *Inflammation* 40(1), pp. 184–194. doi: 10.1007/S10753-016-0468-2.

Lee, J.W. et al. 2017b. NPS2143 Inhibits MUC5AC and Proinflammatory Mediators in Cigarette Smoke Extract (CSE)-Stimulated Human Airway Epithelial Cells. *Inflammation* 40(1), pp. 184–194. doi: 10.1007/S10753-016-0468-2.

Léguillette, R. et al. 2009. Myosin, transgelin, and myosin light chain kinase: expression and function in asthma. *American Journal of Respiratory and Critical Care Medicine* 179(3), pp. 194–204. doi: 10.1164/rccm.200609-1367OC.

Lexmond, A.J., Singh, D., Frijlink, H.W., Clarke, G.W., Page, C.P., Forbes, B. and van den Berge, M. 2018. Realising the potential of various inhaled airway challenge agents through improved delivery to the lungs. *Pulmonary Pharmacology & Therapeutics* 49, pp. 27–35. doi: 10.1016/j.pupt.2018.01.004.

Leynaert, B., Sunyer, J., Garcia-Esteban, R., Zureik, M., Burney, P.G.J., Anto, J.M. and Neukirch, F. 2012. Gender differences in prevalence, diagnosis and incidence of allergic and non-allergic asthma: a population-based cohort. *Thorax* 67(7), pp. 625–631. doi: 10.1136/thoraxjnl-2011-201249.

Li, Y. et al. 2015. Distinct sustained structural and functional effects of interleukin-33 and interleukin-25 on the airways in a murine asthma surrogate. *Immunology* 145(4), pp. 508–518. doi: 10.1111/imm.12465.

Liew, F.Y., Pitman, N.I. and McInnes, I.B. 2010. Disease-associated functions of IL-33: the new kid in the IL-1 family. *Nature reviews Immunology* 10(2), pp. 103–110. doi: 10.1038/nri2692.

Lin, K.I. et al. 1998. Elevated extracellular calcium can prevent apoptosis via the calcium-sensing receptor. *Biochemical and Biophysical Research Communications* 249(2), pp. 325–331. doi: 10.1006/bbrc.1998.9124.

Lloyd, C.M. 2010. IL-33 family members and asthma - bridging innate and adaptive immune responses. *Current Opinion in Immunology* 22(6), pp. 800–806. doi: 10.1016/j.coi.2010.10.006.

Lomask, M. 2006. Further exploration of the Penh parameter. *Experimental and Toxicologic Pathology* 57(SUPPL 2), pp. 13–20. doi: 10.1016/j.etp.2006.02.014.

Lowe, A.P.P., Thomas, R.S., Nials, A.T., Kidd, E.J., Broadley, K.J. and Ford, W.R. 2015. LPS exacerbates functional and inflammatory responses to ovalbumin and decreases sensitivity to inhaled fluticasone propionate in a guinea pig model of asthma. *British Journal of Pharmacology* 172(10), pp. 2588–2603. doi: 10.1111/bph.13080.

Lulich, K.M., Goldie, R.G., Ryan, G. and Paterson, J.W. 1986. Adverse reactions to beta 2-agonist bronchodilators. *Medical Toxicology* 1(4), pp. 286–299. doi: 10.1007/BF03259844.

Lund, S., Walford, H. and Doherty, T. 2013. Type 2 Innate Lymphoid Cells in Allergic Disease. *Current Immunology Reviews* 9(4), pp. 214–221. doi: 10.2174/15733955106661403042359 16.

Lundbäck, B. 1998. Epidemiology of rhinitis and asthma. *Clinical and Experimental Allergy* 28(Suppl 2), pp. 3–10.

Luo, J. et al. 2024. IL-5 antagonism reverses priming and activation of eosinophils in severe eosinophilic asthma. *Mucosal immunology* 17(4), pp. 524–536. doi: 10.1016/J.MUCIMM.2024.03.005.

Lüthi, A.U. et al. 2009. Suppression of interleukin-33 bioactivity through proteolysis by apoptotic caspases. *Immunity* 31(1), pp. 84–98. doi: 10.1016/j.immuni.2009.05.007.

Ma, Y., Zhao, J., Han, Z.R., Chen, Y., Leung, T.F. and Wong, G.W.K. 2009. Very low prevalence of asthma and allergies in schoolchildren from rural Beijing, China. *Pediatric Pulmonology* 44(8), pp. 793–799. doi: 10.1002/ppul.21061.

Maarsingh, H., Zaagsma, J. and Meurs, H. 2008. Arginine homeostasis in allergic asthma. *European Journal of Pharmacology* 585(2–3), pp. 375–384. doi: 10.1016/j.ejphar.2008.02.096.

Mahn, K., Ojo, O.O., Chadwick, G., Aaronson, P.I., Ward, J.P.T. and Lee, T.H. 2010. Ca(2+) homeostasis and structural and functional remodelling of airway smooth muscle in asthma. *Thorax* 65(6), pp. 547–552. doi: 10.1136/thx.2009.129296.

Mamillapalli, R., VanHouten, J., Zawalich, W. and Wysolmerski, J. 2008. Switching of G-protein usage by the calcium-sensing receptor reverses its effect on parathyroid hormone-related protein secretion in normal versus malignant breast cells. *The Journal of biological chemistry* 283(36), pp. 24435–24447. doi: 10.1074/JBC.M801738200.

Mamillapalli, R. and Wysolmerski, J. 2010. The calcium-sensing receptor couples to Galpha(s) and regulates PTHrP and ACTH secretion in pituitary cells. *The Journal of endocrinology* 204(3), pp. 287–297. doi: 10.1677/JOE-09-0183.

Mansur, A.H., Srivastava, S., Mitchell, V., Sullivan, J. and Kasujee, I. 2017. Longterm clinical outcomes of omalizumab therapy in severe allergic asthma: Study of efficacy and safety. *Respiratory Medicine* 124, pp. 36–43. doi: 10.1016/j.rmed.2017.01.008.

Marsumoto, H., Moir, L.M., Oliver, B.G.G., Burgess, J.K., Roth, M., Black, J.L. and McParland, B.E. 2007. Comparison of gel contraction mediated by airway smooth muscle cells from patients with and without asthma. *Thorax* 62(10), pp. 848–854. doi: 10.1136/thx.2006.070474.

Masoli, M., Fabian, D., Holt, S. and Beasley, R. 2004. The global burden of asthma: Executive summary of the GINA Dissemination Committee Report. *Allergy* 59(5), pp. 469–478. doi: 10.1111/j.1398-9995.2004.00526.x.

Matera, M.G., Calzetta, L., Rogliani, P. and Cazzola, M. 2019. Monoclonal antibodies for severe asthma: Pharmacokinetic profiles. *Respiratory Medicine* 153, pp. 3–13. doi: 10.1016/j.rmed.2019.05.005.

McGregor, M.C., Krings, J.G., Nair, P. and Castro, M. 2019. Role of biologics in asthma. *American Journal of Respiratory and Critical Care Medicine* 199(4), pp. 433–445. doi: 10.1164/rccm.201810-1944CI.

McIntyre, A.P. and Viswanathan, R.K. 2023. Phenotypes and Endotypes in Asthma. *Advances in Experimental Medicine and Biology* 1426, pp. 119–142. doi: 10.1007/978-3-031-32259-4_6.

Mead, R., Gilmour, S.G. and Mead, A. 2009. *Statistical principles for the design of experiments*. Cambridge: Cambridge University Press. doi: 10.1017/CBO9781139020879.

Mentaverri, R. et al. 2006. The calcium sensing receptor is directly involved in both osteoclast differentiation and apoptosis. *FASEB Journal* 20(14), pp. 2562–2564. doi: 10.1096/fj.06-6304fje.

Menzies-Gow, A. et al. 2021. Tezepelumab in Adults and Adolescents with Severe, Uncontrolled Asthma. *The New England Journal of Medicine* 384(19), pp. 1800–1809. doi: 10.1056/NEJMoa2034975.

Meurs, H., Gosens, R. and Zaagsma, J. 2008. Airway hyperresponsiveness in asthma: lessons from in vitro model systems and animal models. *The European Respiratory Journal* 32(2), pp. 487–502. doi: 10.1183/09031936.00023608.

Miethe, S., Karsonova, A., Karaulov, A., Renz, H. and Marburg, à. 2020. Obesity and asthma. *Journal of Allergy and Clinical Immunology* 146(4), pp. 685–693. doi: 10.1016/j.jaci.2020.08.011.

Milgrom, H. et al. 2001. Treatment of childhood asthma with anti-immunoglobulin E antibody (omalizumab). *Pediatrics* 108(2), p. E36. doi: 10.1542/peds.108.2.e36.

Milgrom, H., Fick, R.B., Su, J.Q., Reimann, J.D., Bush, R.K., Watrous, M.L. and Metzger, W.J. 1999. Treatment of allergic asthma with monoclonal anti-IgE antibody. rhuMAb-E25 Study Group. *The New England Journal of Medicine* 341(26), pp. 1966–1973. doi: 10.1056/NEJM199912233412603.

Miranda, C., Busacker, A., Balzar, S., Trudeau, J. and Wenzel, S.E. 2004. Distinguishing severe asthma phenotypes: Role of age at onset and eosinophilic inflammation. *The Journal of Allergy and Clinical Immunology* 113(1), pp. 101–108. doi: 10.1016/j.jaci.2003.10.041.

Miyashiro, K., Kunii, I., Della Manna, T., De Menezes Filho, H.C., Damiani, D., Setian, N. and Hauache, O.M. 2004. Severe hypercalcemia in a 9-year-old Brazilian girl due to a novel inactivating mutation of the calcium-sensing receptor. *The Journal of Clinical Endocrinology and Metabolism* 89(12), pp. 5936–5941. doi: 10.1210/jc.2004-1046.

Moon, H.B., Severinson, E., Heusser, C., Johansson, S.G.O., Möller, G. and Persson, U. 1989. Regulation of IgG1 and IgE synthesis by interleukin 4 in mouse B cells. *Scandinavian Journal of Immunology* 30(3), pp. 355–361. doi: 10.1111/J.1365-3083.1989.TB01221.X.

Moore, W.C. et al. 2010. Identification of asthma phenotypes using cluster analysis in the Severe Asthma Research Program. *American Journal of Respiratory and Critical Care Medicine* 181(4), pp. 315–323. doi: 10.1164/rccm.200906-0896OC.

Moorman, J.E. et al. 2007. National surveillance for asthma--United States, 1980-2004. *MMWR Surveillance Summaries* 56(8), pp. 1–54.

Morosco, G. and Kiley, J. 2007. Expert Panel Report 3 (EPR-3): Guidelines for the Diagnosis and Management of Asthma-Summary Report 2007. *The Journal of Allergy and Clinical Immunology* 120(5 Suppl), pp. S94–S138. doi: 10.1016/j.jaci.2007.09.043.

Moussion, C., Ortega, N. and Girard, J.P. 2008. The IL-1-like cytokine IL-33 is constitutively expressed in the nucleus of endothelial cells and epithelial cells in vivo: a novel ‘alarmin’? *PloS One* 3(10), p. e3331. doi: 10.1371/journal.pone.0003331.

Mullane, K. 2011. The increasing challenge of discovering asthma drugs. *Biochemical Pharmacology* 82(6), pp. 586–599. doi: 10.1016/j.bcp.2011.06.033.

Nabe, T. 2014. Interleukin (IL)-33: new therapeutic target for atopic diseases. *Journal of Pharmacological Sciences* 126(2), pp. 85–91. doi: 10.1254/jphs.14r12cp.

Nair, P. et al. 2017. Oral Glucocorticoid-Sparing Effect of Benralizumab in Severe Asthma. *The New England Journal of Medicine* 376(25), pp. 2448–2458. doi: 10.1056/NEJMoa1703501.

Nair, P. and O’Byrne, P.M. 2019. The interleukin-13 paradox in asthma: effective biology, ineffective biologicals. *The European Respiratory Journal* 53(2), p. 1802250. doi: 10.1183/13993003.02250-2018.

Natarajan, K. and Berk, B.C. 2006. Crosstalk coregulation mechanisms of G protein-coupled receptors and receptor tyrosine kinases. *Methods in Molecular Biology* 332, pp. 51–77. doi: 10.1385/1-59745-048-0:51.

Nave, R. 2009. Clinical pharmacokinetic and pharmacodynamic profile of inhaled ciclesonide. *Clinical Pharmacokinetics* 48(4), pp. 243–252. doi: 10.2165/00003088-200948040-00002.

Nemeth, E.F. and Goodman, W.G. 2016. Calcimimetic and Calcilytic Drugs: Feats, Flops, and Futures. *Calcified Tissue International* 98(4), pp. 341–358. doi: 10.1007/s00223-015-0052-z.

Nemeth, E.F., Steffey, M.E., Hammerland, L.G., Hung, B.C.P., Van Wagenen, B.C., DelMar, E.G. and Balandrin, M.F. 1998. Calcimimetics with potent and selective activity on the parathyroid calcium receptor. *Proceedings of the National Academy of Sciences of the United States of America* 95(7), pp. 4040–4045. doi: 10.1073/pnas.95.7.4040.

NICE. 2023. *Prevalence | Background information | Asthma | CKS | NICE*. Available at: https://cks.nice.org.uk/topics/asthma/background-information/prevalence/ [Accessed: 26 March 2024].

Normansell, R., Walker, S., Milan, S.J., Walters, E.H. and Nair, P. 2014. Omalizumab for asthma in adults and children. *Cochrane Database of Systematic Reviews* 2014(1), p. CD003559. doi: 10.1002/14651858.CD003559.pub4.

Novak, N. and Bieber, T. 2003. Allergic and nonallergic forms of atopic diseases. *The Journal of Allergy and Clinical Immunology* 112(2), pp. 252–262. doi: 10.1067/mai.2003.1595.

NUCALA® (mepolizumab) prescribing information. 2023. Available at: https://www.nucala.com/ [Accessed: 26 March 2024].

Nunes, C., Pereira, A.M. and Morais-Almeida, M. 2017. Asthma costs and social impact. *Asthma Research and Practice* 3, p. 1. doi: 10.1186/s40733-016-0029-3.

O'Byrne, P., Fabbri, L.M., Pavord, I.D., Papi, A., Petruzzelli, S. and Lange, P. 2019. Asthma progression and mortality: the role of inhaled corticosteroids. *The European Respiratory Journal* 54(1), p. 1900491. doi: 10.1183/13993003.00491-2019.

Oguma, T. et al. 2006. Involvement of reduced sensitivity to Ca2+ in β-adrenergic action on airway smooth muscle. *Clinical and Experimental Allergy* 36(2), pp. 183–191. doi: 10.1111/j.1365-2222.2006.02412.x.

Ohashi, N. et al. 2004. The calcimimetic agent KRN 1493 lowers plasma parathyroid hormone and ionized calcium concentrations in patients with chronic renal failure on haemodialysis both on the day of haemodialysis and on the day without haemodialysis. *British Journal of Clinical Pharmacology* 57(6), pp. 726–734. doi: 10.1111/j.1365-2125.2004.02088.x.

Olin, J.T. and Wechsler, M.E. 2014. Asthma: pathogenesis and novel drugs for treatment. *BMJ* 349, p. g5517. doi: 10.1136/bmj.G5517.

O'Neill, S. et al. 2015. The cost of treating severe refractory asthma in the UK: an economic analysis from the British Thoracic Society Difficult Asthma Registry. *Thorax* 70(4), pp. 376–378. doi: 10.1136/thoraxjnl-2013-204114.

Ortega, H.G. et al. 2014. Mepolizumab treatment in patients with severe eosinophilic asthma. *The New England Journal of Medicine* 371(13), pp. 1198–1207. doi: 10.1056/NEJMoa1403290.

Paganin, F., Séneterre, E., Chanez, P., Daurés, J.P., Bruel, J.M., Michel, F.B. and Bousquet, J. 1996. Computed tomography of the lungs in asthma: influence of disease severity and etiology. *American Journal of Respiratory and Critical Care Medicine* 153(1), pp. 110–114. doi: 10.1164/ajrccm.153.1.8542102.

Page, C. and Cazzola, M. 2014. Bifunctional drugs for the treatment of asthma and chronic obstructive pulmonary disease. *The European Respiratory Journal* 44(2), pp. 475–482. doi: 10.1183/09031936.00003814.

Paggiaro, P. and Bacci, E. 2011. Montelukast in asthma: a review of its efficacy and place in therapy. *Therapeutic Advances in Chronic Disease* 2(1), pp. 47–58. doi: 10.1177/2040622310383343.

Panizza, J.A., James, A.L., Ryan, G., De Klerk, N. and Finucane, K.E. 2006. Mortality and airflow obstruction in asthma: a 17-year follow-up study. *Internal Medicine Journal* 36(12), pp. 773–780. doi: 10.1111/j.1445-5994.2006.01214.x.

Patel, B.S., Ravix, J., Pabelick, C. and Prakash, Y.S. 2020. Class C GPCRs in the airway. *Current Opinion in Pharmacology* 51, pp. 19–28. doi: 10.1016/j.coph.2020.04.002.

Patterson, C.M., Morrison, R.L., D'Souza, A., Teng, X.S. and Happel, K.I. 2012. Inhaled fluticasone propionate impairs pulmonary clearance of Klebsiella Pneumoniae in mice. *Respiratory Research* 13(1), p. 40. doi: 10.1186/1465-9921-13-40.

Pavord, I.D. et al. 2012. Mepolizumab for severe eosinophilic asthma (DREAM): a multicentre, double-blind, placebo-controlled trial. *The Lancet* 380(9842), pp. 651–659. doi: 10.1016/S0140-6736(12)60988-X.

Payne, D.N.R. and Adcock, I.M. 2001. Molecular mechanisms of corticosteroid actions. *Paediatric Respiratory Reviews* 2(2), pp. 145–150. doi: 10.1053/prrv.2000.0122.

Peacock, M., Bilezikian, J.P., Klassen, P.S., Guo, M.D., Turner, S.A. and Shoback, D. 2005. Cinacalcet hydrochloride maintains long-term normocalcemia in patients with primary hyperparathyroidism. *The Journal of Clinical Endocrinology and Metabolism* 90(1), pp. 135–141. doi: 10.1210/jc.2004-0842.

Pearce, S.H.S. et al. 1995. Calcium-sensing receptor mutations in familial benign hypercalcemia and neonatal hyperparathyroidism. *The Journal of Clinical Investigation* 96(6), pp. 2683–2692. doi: 10.1172/JCI118335.

Pelaia, C., Paoletti, G., Puggioni, F., Racca, F., Pelaia, G., Canonica, G.W. and Heffler, E. 2019. Interleukin-5 in the Pathophysiology of Severe Asthma. *Frontiers in Physiology* 10, p. 1514. doi: 10.3389/fphys.2019.01514.

Pereira, L., Meng, C., Marques, D. and Frazão, J.M. 2018. Old and new calcimimetics for treatment of secondary hyperparathyroidism: Impact on biochemical and relevant clinical outcomes. *Clinical Kidney Journal* 11(1), pp. 80–88. doi: 10.1093/ckj/sfx125.

Peters, S.P. 2014. Asthma phenotypes: nonallergic (intrinsic) asthma. *The Journal of Allergy and Clinical Immunology: In Practice* 2(6), pp. 650–652. doi: 10.1016/j.jaip.2014.09.006.

Pichery, M., Mirey, E., Mercier, P., Lefrancais, E., Dujardin, A., Ortega, N. and Girard, J.-P. 2012. Endogenous IL-33 is highly expressed in mouse epithelial barrier tissues, lymphoid organs, brain, embryos, and inflamed tissues: in situ analysis using a novel Il-33-LacZ gene trap reporter strain. *The Journal of Immunology* 188(7), pp. 3488–3495. doi: 10.4049/jimmunol.1101977.

Piper, E. et al. 2013. A phase II placebo-controlled study of tralokinumab in moderate-to-severe asthma. *The European Respiratory Journal* 41(2), pp. 330–338. doi: 10.1183/09031936.00223411.

Pirinase Allergy 0.05% Nasal Spray - Summary of Product Characteristics (SmPC). 2023. Available at: https://www.medicines.org.uk/emc/product/4502/smpc [Accessed: 26 March 2024].

Pollak, M.R. et al. 1993. Mutations in the human Ca(2+)-sensing receptor gene cause familial hypocalciuric hypercalcemia and neonatal severe hyperparathyroidism. *Cell* 75(7), pp. 1297–1303. doi: 10.1016/0092-8674(93)90617-Y.

Pollak, M.R. et al. 1994a. Autosomal dominant hypocalcaemia caused by a Ca(2+)-sensing receptor gene mutation. *Nature Genetics* 8(3), pp. 303–307. doi: 10.1038/ng1194-303.

Pollak, M.R. et al. 1994b. Familial hypocalciuric hypercalcemia and neonatal severe hyperparathyroidism. Effects of mutant gene dosage on phenotype. *The Journal of Clinical Investigation* 93(3), pp. 1108–1112. doi: 10.1172/JCI117062.

Préfontaine, D. et al. 2009. Increased expression of IL-33 in severe asthma: evidence of expression by airway smooth muscle cells. *The Journal of Immunology* 183(8), pp. 5094–5103. doi: 10.4049/jimmunol.0802387.

Préfontaine, D. et al. 2010. Increased IL-33 expression by epithelial cells in bronchial asthma. *The Journal of Allergy and Clinical Immunology* 125(3), pp. 752–754. doi: 10.1016/j.jaci.2009.12.935.

Quinto, K.B., Zuraw, B.L., Poon, K.Y.T., Chen, W., Schatz, M. and Christiansen, S.C. 2011. The association of obesity and asthma severity and control in children. *The Journal of Allergy and Clinical Immunology* 128(5), pp. 964–969. doi: 10.1016/j.jaci.2011.06.031.

Rabe, K.F. et al. 2018. Efficacy and Safety of Dupilumab in Glucocorticoid-Dependent Severe Asthma. *The New England Journal of Medicine* 378(26), pp. 2475–2485. doi: 10.1056/NEJMoa1804093.

Rackemann, F.M. 1940. Intrinsic asthma. *Journal of Allergy* 11(2), pp. 147–162. doi: 10.1016/S0021-8707(40)90829-2.

Rackemann, F.M. 1947. A working classification of asthma. *The American Journal of Medicine* 3(5), pp. 601–606. doi: 10.1016/0002-9343(47)90204-0.

Ranieri, M., Schepelmann, M., Valenti, G., Kallay, E. and Riccardi, D. 2023. Editorial: The calcium-sensing receptor: from physiology to pharmacology. *Frontiers in Physiology* 14, p. 1225074. doi: 10.3389/fphys.2023.1225074.

Ratier, J.C. de A., Pizzichini, E. and Pizzichini, M. 2011. Gastroesophageal reflux disease and airway hyperresponsiveness: concomitance beyond the realm of chance? *The Brazilian Journal of Pulmonology* 37(5), pp. 680–688. doi: 10.1590/S1806-37132011000500017.

Ravanetti, L. et al. 2017. An early innate response underlies severe influenza-induced exacerbations of asthma in a novel steroid-insensitive and anti-IL-5-responsive mouse model. *Allergy* 72(5), pp. 737–753. doi: 10.1111/all.13057.

Ray, A. and Kolls, J.K. 2017. Neutrophilic Inflammation in Asthma and Association with Disease Severity. *Trends in Immunology* 38(12), pp. 942–954. doi: 10.1016/j.it.2017.07.003.

Reed, C.E. 1988. Basic mechanisms of asthma. Role of inflammation. *Chest* 94(1), pp. 175–177. doi: 10.1378/chest.94.1.175.

Renauld, J.C. 2001. New insights into the role of cytokines in asthma. *Journal of Clinical Pathology* 54(8), pp. 577–589. doi: 10.1136/jcp.54.8.577.

Van Rensen, E.L.J. et al. 2009. Eosinophils in bronchial mucosa of asthmatics after allergen challenge: effect of anti-IgE treatment. *Allergy* 64(1), pp. 72–80. doi: 10.1111/j.1398-9995.2008.01881.x.

Rhen, T. and Cidlowski, J.A. 2005. Antiinflammatory action of glucocorticoids--new mechanisms for old drugs. *The New England Journal of Medicine* 353(16), pp. 1711–1723. doi: 10.1056/NEJMra050541.

Riccardi, D. and Brown, E.M. 2010. Physiology and pathophysiology of the calcium-sensing receptor in the kidney. *American Journal of Physiology-Renal Physiology* 298(3), pp. F485-499. doi: 10.1152/ajprenal.00608.2009.

Riccardi, D., Park, J., Lee, W. Sen, Gamba, G., Brown, E.M. and Hebert, S.C. 1995. Cloning and functional expression of a rat kidney extracellular calcium/polyvalent cation-sensing receptor. *Proceedings of the National Academy of Sciences of the United States of America* 92(1), pp. 131–135. doi: 10.1073/pnas.92.1.131.

Riccardi, D., Ward, J.P.T., Yarova, P.L., Janssen, L.J., Lee, T.H., Ying, S. and Corrigan, C.J. 2022. Topical therapy with negative allosteric modulators of the calcium-sensing receptor (calcilytics) for the management of asthma: The beginning of a new era? *The European Respiratory Journal* 60(2), p. 2102103. doi: 10.1183/13993003.02103-2021.

Ricciardolo, F.L.M., Bertolini, F. and Carriero, V. 2021. The role of dupilumab in severe asthma. *Biomedicines* 9(9), p. 1096. doi: 10.3390/biomedicines9091096.

Roberts, M.S. et al. 2019. Treatment of Autosomal Dominant Hypocalcemia Type 1 With the Calcilytic NPSP795 (SHP635). *Journal of Bone and Mineral Research* 34(9), pp. 1609–1618. doi: 10.1002/jbmr.3747.

Robertson, C.F., Roberts, M.F. and Kappers, J.H. 2004. Asthma prevalence in Melbourne schoolchildren: have we reached the peak? *The Medical Journal of Australia* 180(6), pp. 273–276. doi: 10.5694/j.1326-5377.2004.tb05924.x.

Romanet-Manent, S., Charpin, D., Magnan, A., Lanteaume, A. and Vervloet, D. 2002. Allergic vs nonallergic asthma: what makes the difference? *Allergy* 57(7), pp. 607–613. doi: 10.1034/J.1398-9995.2002.23504.X.

Rosenbaum, D.M., Rasmussen, S.G.F. and Kobilka, B.K. 2009. The structure and function of G-protein-coupled receptors. *Nature* 459(7245), pp. 356–363. doi: 10.1038/nature08144.

RV, T. 2012. Calcium-sensing receptor: Role in health and disease. *Indian Journal of Endocrinology and Metabolism* 16(Suppl 2), pp. 213–216. doi: 10.4103/2230-8210.104041.

Saco, T.V., Pepper, A.N. and Lockey, R.F. 2017. Benralizumab for the treatment of asthma. *Expert Review of Clinical Immunology* 13(5), pp. 405–413. doi: 10.1080/1744666X.2017.1316194.

Sadatsafavi, M., Lynd, L., Marra, C., Carleton, B., Tan, W.C., Sullivan, S. and FitzGerald, J.M. 2010. Direct health care costs associated with asthma in British Columbia. *Canadian Respiratory Journal* 17(2), pp. 74–80. doi: 10.1155/2010/361071.

Saglani, S. et al. 2013. IL-33 promotes airway remodeling in pediatric patients with severe steroid-resistant asthma. *The Journal of Allergy and Clinical Immunology* 132(3), pp. 676-685.e13. doi: 10.1016/j.jaci.2013.04.012.

Saikumar Jayalatha, A.K., Hesse, L., Ketelaar, M.E., Koppelman, G.H. and Nawijn, M.C. 2021. The central role of IL-33/IL-1RL1 pathway in asthma: From pathogenesis to intervention. *Pharmacology & Therapeutics* 225, p. 107847. doi: 10.1016/j.pharmthera.2021.107847.

Schatz, M. and Rosenwasser, L. 2014. The allergic asthma phenotype. *The Journal of Allergy and Clinical Immunology: In Practice* 2(6), pp. 645–648. doi: 10.1016/j.jaip.2014.09.004.

Schmitz, J. et al. 2005. IL-33, an interleukin-1-like cytokine that signals via the IL-1 receptor-related protein ST2 and induces T helper type 2-associated cytokines. *Immunity* 23(5), pp. 479–490. doi: 10.1016/j.immuni.2005.09.015.

SCIREQ. 2024. *Preclinical Respiratory Research Equipment*. Available at: https://www.scireq.com/ [Accessed: 26 March 2024].

Serra-Batlles, J., Plaza, V., Morejón, E., Comella, A. and Brugués, J. 1998. Costs of asthma according to the degree of severity. *The European*

Respiratory Journal 12(6), pp. 1322–1326. doi: 10.1183/09031936.98.12061322.

Shaw, D.E. et al. 2007. Association between neutrophilic airway inflammation and airflow limitation in adults with asthma. *Chest* 132(6), pp. 1871–1875. doi: 10.1378/chest.07-1047.

Shaw, D.E. et al. 2015. Clinical and inflammatory characteristics of the European U-BIOPRED adult severe asthma cohort. *The European Respiratory Journal* 46(5), pp. 1308–1321. doi: 10.1183/13993003.00779-2015.

Sibila, O., Suarez-Cuartin, G., Rodrigo-Troyano, A. and Anzueto, A. 2015. Corticosteroids and Pneumonia in COPD: A Dual Effect? *Barcelona Respiratory Network* 1(2), pp. 105–115. doi: 10.23866/brnrev:2015-m0010.

Slager, R.E. et al. 2012. IL-4 receptor polymorphisms predict reduction in asthma exacerbations during response to an anti-IL-4 receptor α antagonist. *The Journal of Allergy and Clinical Immunology* 130(2), pp. 516-522.e4. doi: 10.1016/j.jaci.2012.03.030.

Solèr, M. et al. 2001. The anti-IgE antibody omalizumab reduces exacerbations and steroid requirement in allergic asthmatics. *The European Respiratory Journal* 18(2), pp. 254–261. doi: 10.1183/09031936.01.00092101.

Spiers, A. and Padmanabhan, N. 2005. A guide to wire myography. In: Jérôme P. FennellAndrew H. Baker ed. *Hypertension. Methods In Molecular Medicine*. New York: Humana, pp. 91–104. doi: 10.1385/1-59259-850-1:091.

Van Staa, T.P., Leufkens, H.G.M. and Cooper, C. 2002. The epidemiology of corticosteroid-induced osteoporosis: a meta-analysis. *Osteoporosis International* 13(10), pp. 777–787. doi: 10.1007/S001980200108.

Sterk, P.J. et al. 1993. Airway responsiveness. Standardized challenge testing with pharmacological, physical and sensitizing stimuli in adults. *The European Respiratory Journal, Supplement* 6(16), pp. 53–83.

Sullivan, P.W., Ghushchyan, V.H., Globe, G. and Schatz, M. 2018. Oral corticosteroid exposure and adverse effects in asthmatic patients. *The Journal of Allergy and Clinical Immunology* 141(1), pp. 110-116.e7. doi: 10.1016/j.jaci.2017.04.009.

Susan Mayor. 2016. *Adult onset asthma may increase risk of heart disease and stroke*. Available at: https://www.bmj.com/content/354/bmj.i4685 [Accessed: 26 March 2024].

Tagaya, E. and Tamaoki, J. 2007. Mechanisms of airway remodeling in asthma. *Allergology International* 56(4), pp. 331–340. doi: 10.2332/allergolint.R-07-152.

Tattersall, M.C., Barnet, J.H., Korcarz, C.E., Hagen, E.W., Peppard, P.E. and Stein, J.H. 2016. Late-Onset Asthma Predicts Cardiovascular Disease Events: The Wisconsin Sleep Cohort. *Journal of the American Heart Association* 5(9), p. e003448. doi: 10.1161/JAHA.116.003448.

Tennakoon, S., Aggarwal, A. and Kállay, E. 2016. The calcium-sensing receptor and the hallmarks of cancer. *Biochimica et biophysica acta* 1863, pp. 1398–1407. doi: 10.1016/J.BBAMCR.2015.11.017.

Thakker, R. V. 2004. Diseases associated with the extracellular calcium-sensing receptor. *Cell Calcium* 35(3), pp. 275–282. doi: 10.1016/j.ceca.2003.10.010.

Thaminy, A., Lamblin, C., Perez, T., Bergoin, C., Tonnel, A.B. and Wallaert, B. 2000. Increased frequency of asymptomatic bronchial hyperresponsiveness in nonasthmatic patients with food allergy. *The European Respiratory Journal* 16(6), pp. 1091–1094. doi: 10.1034/J.1399-3003.2000.16F12.X.

Thomson, N.C. and Chaudhuri, R. 2011. Omalizumab: Clinical use for the management of asthma. *Clinical Medicine Insights: Circulatory, Respiratory and Pulmonary Medicine* 6(1), pp. 27–40. doi: 10.4137/CCRPM.S7793.

Ten Tije, A.J., Verweij, J., Loos, W.J. and Sparreboom, A. 2003. Pharmacological effects of formulation vehicles : implications for cancer chemotherapy. *Clinical Pharmacokinetics* 42(7), pp. 665–685. doi: 10.2165/00003088-200342070-00005.

Toelle, B.G., Ng, K., Belousova, E., Salome, C.M., Peat, J.K. and Marks, G.B. 2004. Prevalence of asthma and allergy in schoolchildren in Belmont, Australia: three cross sectional surveys over 20 years. *BMJ* 328(7436), pp. 386–387. doi: 10.1136/bmj.328.7436.386.

Triggle, D.J. 1983. Calcium, the control of smooth muscle function and bronchial hyperreactivity. *Allergy* 38(1), pp. 1–9. doi: 10.1111/j.1398-9995.1983.tb00849.x.

Tuteja, N. 2009. Signaling through G protein coupled receptors. *Plant Signaling and Behavior* 4(10), pp. 942–947. doi: 10.4161/psb.4.10.9530.

Vignola, A.M. et al. 2004. Efficacy and tolerability of anti-immunoglobulin E therapy with omalizumab in patients with concomitant allergic asthma and persistent allergic rhinitis: SOLAR. *Allergy* 59(7), pp. 709–717. doi: 10.1111/J.1398-9995.2004.00550.X.

Virchow, J.C. 2000. Intrinsic Asthma. In: Stephen T. Holgate and William W. Busse eds. *Asthma and Rhinitis*. 2nd ed. Oxford: Blackwell Science, pp. 1355–1378. doi: 10.1002/9780470694923.ch19.

Wakahara, K. et al. 2008. Repeated instillations of Dermatophagoides farinae into the airways can induce Th2-dependent airway hyperresponsiveness, eosinophilia and remodeling in mice. Effect of intratracheal treatment of fluticasone propionate. *European Journal of Pharmacology* 578(1), pp. 87–96. doi: 10.1016/j.ejphar.2007.09.005.

Waller, S. et al. 2004. Neonatal severe hyperparathyroidism: genotype/phenotype correlation and the use of pamidronate as rescue therapy. *European Journal of Pediatrics* 163(10), pp. 589–594. doi: 10.1007/S00431-004-1491-0.

Walsh, G.M. 2017. Biologics for asthma and allergy. *Current Opinion in Otolaryngology & Head and Neck Surgery* 25(3), pp. 231–234. doi: 10.1097/MOO.0000000000000352.

Ward, D.T. and Riccardi, D. 2012. New concepts in calcium-sensing receptor pharmacology and signalling. *British Journal of Pharmacology* 165(1), pp. 35–48. doi: 10.1111/j.1476-5381.2011.01511.x.

Warner, S.M. and Knight, D.A. 2008. Airway modeling and remodeling in the pathogenesis of asthma. *Current Opinion in Allergy and Clinical Immunology* 8(1), pp. 44–48. doi: 10.1097/ACI.0b013e3282f3b5cb.

Webb, D.C., McKenzie, A.N.J., Koskinen, A.M.L., Yang, M., Mattes, J. and Foster, P.S. 2000. Integrated Signals Between IL-13, IL-4, and IL-5 Regulate Airways Hyperreactivity. *The Journal of Immunology* 165(1), pp. 108–113. doi: 10.4049/jimmunol.165.1.108.

Wendell, S.G., Fan, H. and Zhang, C. 2020. G protein–coupled receptors in asthma therapy: Pharmacology and drug actions. *Pharmacological Reviews* 72(1), pp. 1–49. doi: 10.1124/pr.118.016899.

Wennergren, G. 2011. The prevalence of asthma has reached a plateau. *Acta Paediatrica* 100(7), pp. 938–939. doi: 10.1111/j.1651-2227.2011.02307.x.

Wenzel, S. et al. 2013. Dupilumab in Persistent Asthma with Elevated Eosinophil Levels. *The New England Journal of Medicine* 368(26), pp. 2455–2466. doi: 10.1056/NEJMoa1304048.

Wenzel, S. et al. 2016. Dupilumab efficacy and safety in adults with uncontrolled persistent asthma despite use of medium-to-high-dose inhaled corticosteroids plus a long-acting β2 agonist: a randomised double-blind

placebo-controlled pivotal phase 2b dose-ranging trial. *The Lancet* 388(10039), pp. 31–44. doi: 10.1016/S0140-6736(16)30307-5.

Wenzel, S.E. and Busse, W.W. 2007. Severe asthma: lessons from the Severe Asthma Research Program. *The Journal of Allergy and Clinical Immunology* 119(1), pp. 14–21. doi: 10.1016/j.jaci.2006.10.025.

Wenzel, S.E., Schwartz, L.B., Langmack, E.L., Halliday, J.L., Trudeau, J.B., Gibbs, R.L. and Chu, H.W. 1999. Evidence That Severe Asthma Can Be Divided Pathologically into Two Inflammatory Subtypes with Distinct Physiologic and Clinical Characteristics. *American Journal of Respiratory and Critical Care Medicine* 160(3), pp. 1001–1008. doi: 10.1164/ajrccm.160.3.9812110.

WHO. 2024. *Asthma*. Available at: https://www.who.int/news-room/fact-sheets/detail/asthma [Accessed: 26 March 2024].

Widler, L. 2011. Calcilytics: antagonists of the calcium-sensing receptor for the treatment of osteoporosis. *Future Medicinal Chemistry* 3(5), pp. 535–547. doi: 10.4155/fmc.11.17.

Williamson, I.J., Matusiewicz, S.P., Brown, P.H., Greening, A.P. and Crompton, G.K. 1995. Frequency of voice problems and cough in patients using pressurized aerosol inhaled steroid preparations. *The European Respiratory Journal* 8(4), pp. 590–592. doi: 10.1183/09031936.95.08040590.

Wills-Karp, M. 2004. Interleukin-13 in asthma pathogenesis. *Immunological Reviews* 202, pp. 175–190. doi: 10.1111/j.0105-2896.2004.00215.x.

Wills-Karp, M., Luyimbazi, J., Xu, X., Schofield, B., Neben, T.Y., Karp, C.L. and Donaldson, D.D. 1998. Interleukin-13: Central mediator of allergic asthma. *Science* 282(5397), pp. 2258–2261. doi: 10.1126/science.282.5397.2258.

Wonneberger, K., Scofield, M.A. and Wangemann, P. 2000. Evidence for a calcium-sensing receptor in the vascular smooth muscle cells of the spiral modiolar artery. *The Journal of Membrane Biology* 175(3), pp. 203–212. doi: 10.1007/S00232001068.

XOLAIR® (omalizumab) prescribing information. 2024. Available at: https://www.xolair.com/ [Accessed: 26 March 2024].

Yagami, A. et al. 2010. IL-33 Mediates Inflammatory Responses in Human Lung Tissue Cells. *The Journal of Immunology* 185(10), pp. 5743–5750. doi: 10.4049/jimmunol.0903818.

Yamaguchi, T. and Sugimoto, T. 2007. Impaired bone mineralization in calcium-sensing receptor (CaSR) knockout mice: the physiological action of CaSR in bone microenvironments. *Clinical Calcium* 17(10), pp. 1567–1573.

Yanagibashi, T., Satoh, M., Nagai, Y., Koike, M. and Takatsu, K. 2017. Allergic diseases: From bench to clinic - Contribution of the discovery of interleukin-5. *Cytokine* 98, pp. 59–70. doi: 10.1016/j.cyto.2016.11.011.

Yang, H., Perelman, J.M., Kolosov, V.P. and Zhou, X. 2014. Role of calcium-sensing receptor in hypoxia-induced airway mucous hypersecretion. *National Medical Journal of China* 94(12), pp. 944–947. doi: 10.3760/cma.j.issn.0376-2491.2014.12.017.

Yarova, P.L. et al. 2015. Calcium-sensing receptor antagonists abrogate airway hyperresponsiveness and inflammation in allergic asthma. *Science Translational Medicine* 7(284), p. 284ra58. doi: 10.1126/scitranslmed.aaa0282.

Yarova, P.L. et al. 2016. Inhaled calcilytics: effects on airway inflammation and remodeling. *Respiratory Drug Delivery* 1(1), pp. 1–12.

Yarova, P.L. et al. 2021. Characterization of Negative Allosteric Modulators of the Calcium-Sensing Receptor for Repurposing as a Treatment of Asthma. *The Journal of Pharmacology and Experimental Therapeutics* 376(1), pp. 51–63. doi: 10.1124/jpet.120.000281.

Yim, R.P. and Koumbourlis, A.C. 2012. Steroid-resistant asthma. *Paediatric Respiratory Reviews* 13(3), pp. 172–177. doi: 10.1016/j.prrv.2011.05.002.

Young, H.W.J. et al. 2007. Central role of Muc5ac expression in mucous metaplasia and its regulation by conserved 5' elements. *American Journal of Respiratory Cell and Molecular Biology* 37(3), pp. 273–290. doi: 10.1165/rcmb.2005-0460OC.

Yu, Q.L. and Chen, Z. 2018. Establishment of different experimental asthma models in mice. *Experimental and Therapeutic Medicine* 15(3), pp. 2492–2498. doi: 10.3892/etm.2018.5721.

Zein, J.G. and Erzurum, S.C. 2015. Asthma is Different in Women. *Current Allergy and Asthma Reports* 15(6), p. 28. doi: 10.1007/s11882-015-0528-y.

Zemp, E., Schikowski, T., Dratva, J., Schindler, C. and Probst-Hensch, N. 2012. Asthma and the menopause: A systematic review and meta-analysis. *Maturitas* 73(3), pp. 212–217. doi: 10.1016/j.maturitas.2012.08.010.

Zhang, W. and Gunst, S.J. 2019. Molecular Mechanisms for the Mechanical Modulation of Airway Responsiveness. *Journal of Engineering and Science in*

Medical Siagnostics and Therapy 2(1), pp. 0108051–0108058. doi: 10.1115/1.4042775.

Zhao, R., Shi, Y., Liu, N. and Li, B. 2023. Elevated levels of interleukin-33 are associated with asthma: A meta-analysis. *Immunity, Inflammation and Disease* 11(4), p. e842. doi: 10.1002/iid3.842.

Zöllner, I.K. et al. 2005. No increase in the prevalence of asthma, allergies, and atopic sensitisation among children in Germany: 1992-2001. *Thorax* 60(7), pp. 545–548. doi: 10.1136/thx.2004.029561.

Zoratti, E. et al. 2014. Differentiating asthma phenotypes in young adults through polyclonal cytokine profiles. *Annals of Allergy, Asthma & Immunology* 113(1), pp. 25–30. doi: 10.1016/j.anai.2014.04.013.